# Epigenetic regulation mediated nanotherapy for inhibition of Parkinson's disease

**Mohammed Nadim Sardoiwala**

*A thesis submitted for the partial fulfillment of the*
*Degree of Doctor of Philosophy*


Institute of Nano Science and Technology
Knowledge City, Sector 81, SAS Nagar 140306, Punjab, India.

Indian Institute of Science Education and Research Mohali
Knowledge City, Sector 81, SAS Nagar, Manauli PO, Mohali 140306, Punjab, India.

**December 2022**

*“Dedicated to little Princess...]*

# Declaration

The work presented in this thesis has been carried out by me under the guidance of Dr. Subhasree Roy Choudhury at the Institute of Nano Science and Technology (INST), Mohali. This work has not been submitted in part or in full for a degree, a diploma, or a fellowship to any other university or institute. Whenever contributions of others are involved, every effort is made to indicate this clearly, with due acknowledgment of collaborative research and discussions. This thesis is a bonafide record of my original work done by me and all sources listed within have been detailed in the bibliography.

Place:
Date:

**Mohammed Nadim Sardoiwala**

In my capacity as the supervisor of the candidate's thesis work, I certify that the above statements by the candidate are true to the best of my knowledge.

Place:
Date:

**Dr. Subhasree Roy Choudhury**
Scientist D
Institute of Nano Science and Technology, Mohali

## Acknowledgments

*First and foremost, I praise the **Almighty God**, **the Merciful and most Beneficent**, the best creator and scientist of the Universe, for showering me with limitless blessing by providing patience, courage, and enthusiasm to accomplish my Ph.D. thesis work.*

*The Journey made me by shaping my career, and personality and providing me the platform and exposure that is very much hard to acquire for the benefit of the individual to develop the skill, talent, and cleverness in almost every aspect of career and life. It is a very much fruitful and worthy time to provide an investment to get a return throughout life.*

*At this magnificent moment, I would like to express my heartfelt gratitude to my great mentor **Dr. Subhasree Roy Choudhury**, for her constant supervision, patience, guidance, perceptive suggestions, constant support, and motivation which gave me enormous enthusiasm to complete the challenging tasks successfully. I am grateful to her for teaching me how to conduct research, think about the problems for their solutions, and have a vision for the upcoming time. She has not only been an excellent mentor, but also a valuable moral supporter on personal grounds. It is indeed a rare privilege to work under her supervision and mentorship. Indeed, the scientific and moral support of **Prof. Surajit Karmakar** has made the journey very much passionate and delightful to acquire the vision to shape and build the career, obtain maturity to tackle the tough time, and how to gather the strength to overcome worrying situations. It is privileged to have the blooming and fruitful atmosphere to get shine as one of the beautiful flowers of the garden.*

*I would like to extend my gratitude towards my Ph.D. monitoring committee members **Prof. Prakash P. Neelakandan** and **Prof. Md Ehsan Ali**, for their constant monitoring of my work, their valuable time, and insightful comments.*

*I am very thankful to **Prof. Amitava Patra**, Director INST, for providing excellent infrastructure, and all necessary things under one roof to carry out our research work. I wish to express my special thanks to the founder Director of INST, **Prof. A. K. Ganguli**, and ex-officiating Director, **Prof. H. N. Ghosh**. I also extend my acknowledgments for the financial*

*support from the CSIR, New Delhi for awarding me the Junior Research Fellowship (JRF) and Senior Research Fellowship (SRF) fellowship throughout my Ph.D. tenure.*

*I would like to thank all my collaborators,* ***Prof. S. S. Sharma (NIPER, Mohali)****,* ***Dr. Presnjit Gucchait (RCB, Faridabad), Dr. Nitin Singhal (NABI, Mohali), and Dr. Chandra Shekhar (IISER, Mohali)*** *for providing me the exposure and platform to complete my work. I also want to thank all the members of our group, both alumni and present,* ***Dr. Pankaj K. Singh****,* ***Dr. Arpit Bhargawa****,* ***Dr. Iqbal****,* ***Dr. Ankur Sood****,* ***Dr. Anup K. Srivastava, Dr. Atul Dev, Dr. Babita Kaundal, Mr. Aviansh C. Kushwaha, Mr. Jignesh M. Soni, Ms. Babita Bhatt, Mr. Liku Biswal, Ms. Mrunalini Boddu, Mrs. Angela Sharma, Ms. Shushmita Sena, Ms. Devangi, Mr. Ayoub Choudhury, Mr. Apurba Gouri, Mr. Devraj Sarkar, and Mr. Shymantak*** *for showering their friendliness nature, critical perception, knowledge, and motivation to work with them during the tenure.*

*Account of my journey in INST would be incomplete without the support of* ***Dr. Rohit Varsheny, Dr. JoJo****,* ***Dr. Anjana****,* ***Dr. Vijay Pal, Dr. Kalpesh, Dr. Ankush Garg, Mr. Bhupesh Vaidya (NIPER, Mohali), Mr. Rehan (NIPER, Mohali) and Mr. Shakeel (NIPER, Mohali)****. I also want to thank all the technical and non-technical staff members of INST for their enormous support, especially* ***Mr. Rohit Sharma****. Special warm regards to* ***Dr.Naimat K. Bari****,* ***Dr. Bilal Massodi****,* ***Dr. Hasan****,* ***Dr. Tariq Aziz****,* ***Dr. Anas Ahemad****,* ***Dr. Arif Dar****,* ***Dr. Zubair****,* ***Dr. Riyaj****,* ***Dr. Rejaul****,* ***Dr. Selim****,* ***Dr. Atikur Raheman****,* ***Mr. Mujeeb****,* ***Mr. Farhan****,* ***Mr. Raihan****,* ***Mr. Naushad****,* ***Mr. Kashif****,* ***Mr. Firdaus****,* ***Mr. Khizr****,* ***Mr. Aquib****,* ***Mr. Aneesh****,* ***Mr. Afshan****,* ***Mr. Shumile****,* ***Mr. Ahmad****,* ***Mr. Zubair****,* ***Mr. Imran*** *and* ***Mr. S.M. Rose*** *for providing me their love, care, and selflessness. Thanks to Almighty we had some of the most memorable times that we will never forget for the rest of our lives.*

*I am fortunate to have a family that might be a rare privilege, my lovely little princess,* ***Ms. Maryam Fatimah****, my soulmate* ***Mrs. Mahera****, my elder brother cum personal coach,* ***Mr. Khalid Ibn Aziz*** *and sister–in–law,* ***Mrs. Humaira****, who always provided moral support and my entire friend circles, My cousins, My family elders, especially my grandfather,* ***Mr. Abdullah Sheth*** *and my uncles, especially* ***Mr. Aziz*** *and* ***Er. Gulammoyddin****, who provided me with the dream that I have pursued.*

*I would also like to thank everyone else who I may not be able to name here, but I deeply appreciate their love, care, and motivation during the ups and downs of life.*

*Last but not the least, I am indebted to my parents,* ***Mr. Aziz*** *and* ***Mrs. Sirdar Banu*** *for their endless love, care, humbleness, patience, motivation, courage, and aggressive thought behind making educate their children and enlightening the community about the worthiness of the education. My simple expression of gratitude to my parents does not seem adequate, as their contributions are more than enough to make me indebted forever. I would also extend my gratitude to the spiritual mentor,* ***Mr. Muhammad Umar Qureshi Naqshbandi Usmani,*** *and* ***Khawajgan e Naqshbandiya,*** *who changed my thought on life by changing my perspective to look towards it. They made me understand that the existence of the world is with the power of love, mercy, and justice. They nurture me to find my inner power and inner self. You all are the sacred stars and guardians in my life.*

*Finally, in all humility, I thank Almighty God, the most merciful for showering me with an enormous blessing by providing lovely people, caretakers, career builders, moral supporters, and so on...*

*Mohammed Nadim Sardoiwala*

# Contents

# List of Abbreviations

Parkinson's disease (PD)

Substantia Nigra pars compacta (SNpc)

Adenosine triphosphate (ATP)

Polycomb repressor complexes 1 and 2 (PRC1/2)

Enhancer of zeste homolog 2 (EZH2)

O-GlcNacyltransferase (OGT)

Blood-brain barrier (BBB)

Monoamine oxidase B inhibitors (MAO-B)

Catechol-O-methyltransferase (COMT) inhibitors

Deep brain stimulation (DBS)

3-[4,5-dimethylthiazol-2-yl]-2,5-diphenyltetrazolium bromide (MTT)

Sodium hydroxide (NaOH)

Fingolimod (FTY720) hydrochloride

2′,7′-dichlorodihydrofluorescin diacetate (DCFH-DA)

Dulbecco's modified Eagle's medium (DMEM)

Phosphate-buffered saline (PBS)

Hank's balanced salt solution (HBSS)

Sodium tripolyphosphate (STPP)

Dynamic light scattering (DLS)

Transmission Electron Microscopy (TEM)

Scanning Electron Microscopy (SEM)

Fourier-transformed infrared spectroscopy (FTIR)

X-ray diffraction pattern analysis (XRD)

Fluorescein isothiocyanate (FITC)

Phycoerythrin (PE)

Room temperature (RT)

Real-time quantitative polymerase chain reaction (qPCR)

Polyvinylidene fluoride (PVDF)

Radioimmunoprecipitation assay (RIPA)

Horse redox peroxidase (HRP)

Electrochemiluminescent (ECL)

Chromatin Immunoprecipitation (ChIP)

# List of Figures

# List of Tables

## ABSTRACT

Parkinson's disease (PD) is the second most common progressive neurodegenerative infirmity. The recent pharmacological and innovative surgical approaches are effective but have multiple side effects. Therefore, it is imperative to introduce new anti-PD agents. In this regard, the present thesis enlightens the nanotherapeutic applications and underlying neuroprotective mechanisms by overcoming the existing limitations of promising neurotherapeutic agents including metformin, Hytrin, and FTY720. The nature-inspired polydopamine nanoparticles, polydopamine-serotonin nanohybrids, chitosan nanoparticles, and FTY720 nanoparticles have shown endowment in the therapeutic efficacy of metformin, Hytrin, and FTY720 *in vitro*, *ex vivo*,and *in vivo* experimental PD models, respectively. The presented biocompatible nanostructures exhibited brain retention, anti-inflammatory activity, and a slower drug release profile leading to neuroprotection against PD deficits. The known molecular therapeutic target of PD, alpha-synuclein has been focused on the exploration of epigenetic regulation to understand the neuroprotective mechanisms of presented nanocomposites. The thesis has predominantly explored epigenetic regulation in the nanotherapeutic intervention of PD by understanding the camouflaged role of EZH2, the epigenetic master regulator, and targeting H3K27ac in the reduction of synucleinopathy to retard PD. Cumulatively, the nanostructures have shown EZH2- mediated endowment in ubiquitination/proteasomal degradation of phosphorylated alpha-synuclein. The non-canonical role of PP2A was also revealed in the EZH2-mediated degradation of phosphorylated alpha-synuclein. The thesis also emphasized and explored the nanocomposites-mediated deacetylation of H3K27ac to halt synuclein gene (SNCA) expression in PD retardation. Thus, the thesis divulges nature-inspired nanocomposites-mediated neuroprotective actions by highlighting epigenetic regulation in PD treatment as an emerging and promising therapeutic target. The thesis has presented work has the promising significance due to utilization of widely known biocompatible and utrastable nanocarriers with already FDA approved drugs. Hence, repurposing of these FDA approved drugs with presented nanoformulations may lead to provide breakthrough in PD treatment if they will further investigated in the clinical setup. The major limitation of presented work is that the long-term toxicity and chronic dose toxicity of nanoformulation has not investigated with comparison of commercially available PD drugs.

# SYNOPSIS

# Epigenetic regulation mediated nanotherapy for inhibition of Parkinson's disease

Parkinson's disease (PD) is a progressive neurodegenerative disorder, affecting developing countries including India (1). In the last decades, the progression of medical pharmacologic therapies and innovative surgical approaches like deep brain stimulation (DBS) seems to be effective against PD(2). However, definitive disease-controlling therapy is still lacking due to the multiple side effects of therapeutic agents (3). An understanding of PD etiology is necessary to solve the puzzle of PD pathology. Several active pathological processes entangled with each other are implicated in Parkinson's disease, but the core cause of chronic and progressive neuronal damage is not well understood (4-7). The PD signature molecule, alpha-synuclein is encoded by the SNCA gene having an immense physiological role in the neurotransmitter release, neuronal maintenance, and regulation of neurochemicals. (8, 9) However, the post-translation modifications and misfolding of alpha-synuclein, defective proteasomal pathway, and upregulated SNCA gene result in synucleinopathy associated with PD.(5-7) Alpha-synucleinopathy, neuroinflammation, and mitochondrial dysfunction are the major causative factors involved in the pathological cycle of Parkinson's disease. Besides, investigating the post-translational modification of alpha-synuclein, transcriptional regulation, and epigenetic modifications are found to be causative factors in PD progression. (4) Indeed, epigenetic intervention is an emerging mechanism gaining attention in PD onset management and progression. The histone hyperacetylation of synuclein is well characterized in the PD progression having a higher association with H3K27ac. (10-12) Indeed, the master epigenetic regulator, Enhancer of zeste homolog 2 (EZH2) is required for the maintenance of neuronal function which reduction leads to a progression of neurogenerative diseases. (13) Hence, designing the strategy to reduce histone acetylation and restoration of EZH2 paves the way for the development of PD treatment. Several neurotherapeutic agents have the potency to control epigenetic events in PD regulation. (2) However, the limitations of lower solubility, blood-brain-barrier hindrance; poor drug release kinetics hamper the therapeutic efficacy of anti-PD drugs. (3)

Therefore, it is imperative to find a new antiparkinsonian agent. The emerging nano-drug delivery platform has immense potential to overcome the existing limitations of potent anti-PD drugs. Hence, the first and second chapter describes and discusses the PD etiology, epigenetic regulation, and methodology applied to develop and evaluate the neurotherapeutic potential of presented nanoformulations.

The present thesis focused to explore epigenetic regulation in the nanotherapeutic intervention of PD by understanding the camouflaged role of EZH2 and targeting H3K27ac in the management of synucleinopathy. The third chapter started with the demonstration of the neuroprotective effect of metformin-loaded polydopamine nanoparticles, and the camouflaged role of EZH2, the modulator of H3K27me3 in the reduction of alpha-synuclein has been revealed. (14) Recently, metformin emerges as a potential therapeutic agent in various diseases like aging disorders and reduces the risk of PD in diabetes patients is supported by a clinical trial study in the diabetes mellitus population of Taiwan. (15) The neuroprotective response of metformin is mediated by anti-inflammatory action, histone deacetylase SIRT1 activation, and reduction of phosphorylated proteins involved in Lewy body formation. Despite having prodigious therapeutic potential, metformin, possess absorption limited kinetics with less bioavailability and a risk of lactic acidosis. The study evaluates the neurotherapeutic efficacy of nature-inspired polydopamine nanoparticles in the metformin delivery in *vitro*, 3D, and *in vivo* experimental PD models. The neuroprotective potential was arbitrated by EZH2-mediated ubiquitination and degradation of phospho-serine 129 (pSer129) α-Syn and histone deacetylation of SNCA. The study divulges the neuroprotective role of Met-loaded PDANPs by reversing the neurochemical deficits by confirming an epigenetic-mediated nanotherapeutic approach for PD prevention.

In the fourth chapter, we have elaborated on the promising therapeutic potential of the PP2A activator, FTY720 to retard PD. However, the less bio-availability and risk of severe infection limits its therapeutic efficiency. Therefore, we have demonstrated FTY720 loaded chitosan nanoparticles to improve their bioavailability and release kinetics in the study. Hence, FTY720 loaded chitosan nanoformulation has been evaluated *in vitro*, *ex vivo, and in vivo* experimental PD models. (16) In the exploration of EZH2-mediated synuclein degradation, the study uncovered the role of PP2A in the polycomb group of protein Enhancer of zeste homolog 2 to regulate ubiquitination-mediated degradation of agglomerated pSer129 α-Syn.

Indeed, this study establishes the neuroprotective potential of chitosan-based FTY720 nanoformulations by PP2A-mediated epigenetic regulation for PD prevention. The study also elaborated on the role of PP2A in the regulation of O-GlcNacyl transferase (OGT) responsible for O-GlcNacylation of synuclein which reduces during PD conditions. Thus, the study confirms the FTY720 nanoformulation mediated PP2A activation and its direct physical interaction with OGT leads to OGT activation and O-GlcNacylation of synuclein to alleviate the synucleinopathy.

In the fifth chapter, Hytrin has been employed to understand its effect on IDH2 expression due to its consideration as a novel suppressor of alpha-synuclein-mediated toxicity. Therefore, we are keen to understand IDH2-mediated hytrin's neurotherapeutic effect on the reduction of synucleinopathy. Despite potential therapeutic effects, the FDA-approved drug, Hytrin has some limitations like burst drug release kinetic with rapid absorption. Thus, a strategy is warranted to improve the therapeutic efficiency of Hytrin. Therefore, we aimed to improve Hytrin release kinetics through nanocarrier-mediated delivery and replenish dopamine and serotonin by formulating a Hytrin-loaded polydopamine serotonin nanohybrid for PD treatment. Nanoformulation has shown effective neurotherapeutic potential in the reduction of PD symptoms *in vitro*, *ex vivo, and in vivo PD models*. The study demonstrates that the restorative effect of our nanoformulation significantly retards the PD deficits by inducing IDH2-mediated alpha-synuclein ubiquitination and proteasomal degradation pathway. (17) Further investigation of neurotherapeutic action divulges the reduction of nitrated synuclein through chaperon-mediated autophagy.

Overall, the presented thesis demonstrates the development of novel nano-drug delivery systems for PD treatment. Nanotherapeutic intervention by epigenetic regulation showed promising therapeutic strategies for the treatment of Parkinson’s disease.

**References**


1. U. Muthane, M. Ragothaman, G. J. J. Gururaj, Epidemiology of Parkinson's disease and movement disorders in India: problems and possibilities. **55**, 719-724 (2007).
2. P. Hickey, M. J. D. d. Stacy, development, therapy, Available and emerging treatments for Parkinson’s disease: a review. **5**, 241 (2011).

3. B. D. Li *et al.*, Adverse effects produced by different drugs used in the treatment of Parkinson's disease: a mixed treatment comparison. **23**, 827-842 (2017).
4. C. Labbé, O. Lorenzo-Betancor, O. A. Ross, Epigenetic regulation in Parkinson's disease. *Acta neuropathologica* **132**, 515-530 (2016).
5. B. Thomas, M. F. Beal, Parkinson's disease. *Human molecular genetics* **16 Spec No. 2**, R183-194 (2007).
6. M. H. Polymeropoulos *et al.*, Mutation in the alpha-synuclein gene identified in families with Parkinson's disease. *Science* **276**, 2045-2047 (1997).
7. W. Poewe *et al.*, Parkinson disease. **3**, 1-21 (2017).
8. I. J. Siddiqui, N. Pervaiz, A. A. Abbasi, The Parkinson Disease gene SNCA: Evolutionary and structural insights with pathological implication. *Scientific reports* **6**, 24475-24475 (2016).
9. L. Stefanis, α-Synuclein in Parkinson's disease. *Cold Spring Harb Perspect Med* **2**, a009399-a009399 (2012).
10. M. Huang *et al.*, Mitochondrial dysfunction–induced H3K27 hyperacetylation perturbs enhancers in Parkinson's disease. *JCI Insight* **6** (2021).
11. S. Guhathakurta, E. Bok, B. A. Evangelista, Y.-S. Kim, Deregulation of α-synuclein in Parkinson's disease: Insight from epigenetic structure and transcriptional regulation of SNCA. *Prog Neurobiol* **154**, 21-36 (2017).
12. S. Guhathakurta *et al.*, Targeted attenuation of elevated histone marks at SNCA alleviates α-synuclein in Parkinson's disease. *EMBO Mol Med* **13**, e12188-e12188 (2021).
13. E. Sodersten *et al.*, others. 2014. Dopamine signaling leads to loss of Polycomb repression and aberrant gene activation in experimental parkinsonism. **10**, e1004574.
14. M. N. Sardoiwala, A. K. Srivastava, B. Kaundal, S. Karmakar, S. R. Choudhury, Recuperative effect of metformin loaded polydopamine nanoformulation promoting EZH2 mediated proteasomal degradation of phospho-α-synuclein in Parkinson's disease model. *Nanomedicine: Nanotechnology, Biology and Medicine* **24**, 102088 (2020).
15. M. L. Wahlqvist *et al.*, Metformin-inclusive sulfonylurea therapy reduces the risk of Parkinson's disease occurring with Type 2 diabetes in a Taiwanese population cohort. **18**, 753-758 (2012).

16. M. N. Sardoiwala, S. Karmakar, S. R. Choudhury, Chitosan nanocarrier for FTY720 enhanced delivery retards Parkinson's disease via PP2A-EzH2 signaling in vitro and ex vivo. *Carbohydrate Polymers* https://doi.org/10.1016/j.carbpol.2020.117435, 117435 (2020).
17. M. N. Sardoiwala, S. J. Mohanbhai, S. Karmakar, S. R. Choudhury, Hytrin loaded polydopamine-serotonin nanohybrid induces IDH2 mediated neuroprotective effect to alleviate Parkinson's disease. *Materials Science and Engineering: C* https://doi.org/10.1016/j.msec.2021.112602, 112602 (2021).

# Chapter 1

---

# Introduction

## 1.1. Neurodegeneration

Neurodegenerative diseases lead to cumulative atrophy of neurons. Mainly ataxia, dementia, and muscular regression are consequences of neurodegenerative diseases. So many research efforts have been devoted to curing these fatal diseases. Despite that, there is no prominent strategy to overcome most of these diseases. The common pathological cause is the protein aggregation due to several environmental factors. The post-translational modifications of protein like phosphorylation of synuclein leads to its aggregation results in the Parkinson's disease (PD) progression.(1) In fact, the neurodegenerative disease are caused by selective neuronal loss in the specific area of the brain like in case of PD, there is loss of dopaminergic neurons in the Substantia Nigra pars compacta (SNpc).(2) There are distinct etiology and pathophysiological process involved behind the development of various neurodegenerative infirmities. Major recognized factors are oxidative stress, exposure of pesticides, impaired protein degradation machinery, impaired mitochondrial homeostasis, ATP depletion, post translational modification and aggregation of involved key proteins.(2, 3)

## 1.2. Parkinson's disease

PD is the second most neurodegenerative disease firstly introduced by Dr. James Parkinson, before that it is called as shaking palsy. It impacts many of the brain regions due to loss of dopaminergic neurons.(4) The major characteristic symptoms are rigidity, tremor, abnormal movements, motor dysfunctions, and muscle stiffness. PD is affecting the major population of North America and Europe as well as developing regions such as India (5).The recent survey has shown that from 1999 to 2017, age-adjusted death rates for Parkinson's disease among adults aged ≥65 years increased from 41.7 to 65.3 per 100,000 population.(6) Among men, the age-adjusted death rate increased from 65.2 per 100,000 in 1999 to 97.9 in 2017. Among women, the rate increased from 28.4 per 100,000 in 1999 to 43.0 in 2017. Throughout 1999–2017, the death rates for Parkinson's disease for men were higher than those for women at globe.(6) Similarly, the PD foundation has also shown that nearly 1 million people live with PD in the US only and it is predicted to be 1.2 million by 2030.(7) PD foundation also noticed that 60,000 Americans are diagnosed with PD every year and more than 10 million people are suffering from PD at a globe. In India, according to a survey of 2010 of the Kolkata population, the age-adjusted prevalence

rate (PR) and average annual incidence rate were 52.85/100,000 and 5.71/100,000 per year, respectively.(8) The adjusted average annual mortality rate was 2.89/100,000 per year. The relative risk of death was 8.98. It is predicted that the disease burden might be doubled by 2030. The major cause of the PD pathogenesis is the degeneration of dopaminergic neurons that resides in the SNpc, the region controls body movements. PD-associated risk factors include aging, family history, pesticide exposure, and environmental factors. However, molecular pathophysiology and signalling is very complex and still not resolved.

The lewy body formation is the major pathological process happens during the PD progression. The lewy body formation is the accumulation of defective, post-translated protein due to impaired proteasomal degradation and impaired bioenergetics with dysfunctional mitochondria. (2, 3) In that, misfolded and post-translated alpha synuclein is the majorly accumulated protein that leads to form cytoplasmic inclusions called as lewybody or lewy neurites.(9, 10) Besides the hall mark of PD, alpha synuclein, lewy body contains parkin, lipid content, proteasomal components, lysosomal components, tubulin, neurofilaments and ubiquitin.(11)A century ago, Tretiakoff demonstrated neuropathological changes, lewy body formation and loss of the dark pigmented neuromelanin containing neurons in the SNpc region of PD patient's brain.(12, 13)That's how, the dopaminergic neuronal loss in SNpc and lewy body formations (abnormal cytoplasmic accumulations) considers as pathological hallmark of PD.Major of the PD cases (~90%) are under the classification of spontaneously occurring PD condition (idiopathic and sporadic) that makes difficult to understand this multifactorial disease with its complex pathological events.(10) Hence, the causative factors and regulatory conditions are entangled with each other due to interplay of environmental (life styles) conditions and genetic or molecular changes. Among the causative environmental factors, there are the pesticides exposure, heave metal exposure, rural area life, agriculture occupation, higher dairy product consumption, type 2 diabetes, brain injury and etc.(14, 15)Thus, the exploration of interplay of environmental factors and their molecular targets may reveal the new pathological mechanisms that might help in early PD diagnosis or to improve PD conditions. An understanding of PD etiology is necessary to solve the puzzle of PD pathology. Several active pathological processes entangled with each other are implicated in Parkinson's disease, but the core cause of chronic and progressive neuronal damage is not well understood (3, 16-18). The PD signature molecule, alpha-synuclein is encoded by the SNCA gene having an immense physiological role in the

neurotransmitter release, neuronal maintenance, and regulation of neurochemicals.(19, 20) However, the post-translation modifications and misfolding of alpha-synuclein, defective proteasomal pathway, and upregulated SNCA gene result in synucleinopathy associated with PD.(3, 17, 18) Alpha-synucleinopathy, neuroinflammation, and mitochondrial dysfunction are the major causative factors involved in the pathological cycle of Parkinson's disease. Besides, investigating the post-translational modification of alpha-synuclein, transcriptional regulation, and epigenetic modifications are found to be causative factors in PD progression.(16)

### 1.3 Epigenetic regulations in PD

Recent research gain attention to understand the epigenetic regulation in the PD regulation. At the results of these efforts shed the light on vital role of epigenetic regulators and changes in gene expression associated with PD pathogenesis. In fact, the epigenetic mechanisms involved in maintaining the homeostasis of any gene expression by tightly regulating its gene expressing by turning gene off and on according to the stimuli or condition. Hence, the same DNA sequence has the differential mRNA and protein expression profiles. Therefore, the understanding of the epigenetic phenomena is necessary to untangle the environmental factors mediated epigenetic changes and their possible modulation in the development of PD treatment.

Epigenetic modulation is an emerging mechanism gaining attention in the research of PD onset and progression. Epigenetic regulation with lower DNA methylation leads to aggregation of α-Syn in PD progression is widely studied(21). Indeed, the involvement of polycomb groups of proteins, including polycomb repressor complex 1 and 2 (PRC1/2) is under investigation for implications in PD. PRC2 member, Enhancer of zeste homolog 2 (EZH2) trimethylates H3K27 for maintenance of neuronal function was reported(22).They have also demonstrated that transcriptionaldysregulation in PRC2 deficient mice leads to progression of neurogenerative diseases. Alterations in EZH2 and H3K27 levels have been implicated with Parkinsonism (23). In a similar way, downregulation of B cell-specific Moloney murine leukemia virus integration site 1 (BMI1), a PRC1 member is associated with apoptosis of neurons and its overexpression has immense potentialfor the treatment of neurodegenerative diseases (24). Although, the underlying mechanism of PRC 1/2 mediated prevention of Parkinson's disease is not well understood. A recent study shows acute treatment of rotenone (PD inducing pesticide) declines

ubiquitinated proteins level and E1A activity that requires in activation of ubiquitin for the functioning of Ubiquitin proteosomal pathway (25). In the ubiquitin mediated proteasomal pathway, ubiquitin binds to aggregated proteins and directs them to the proteasomal degradation machinery. The reports that have shown human polycomb protein 2, a PRC1 member induced SUMOylation of α-Syn which promotes aggregation of α-Syn and SUMO modification works antagonistically to ubiquitination (26, 27). Recently, the study has also shown that SUMOylation and ubiquitination in the regulation of α-Syn are reciprocal events (27).

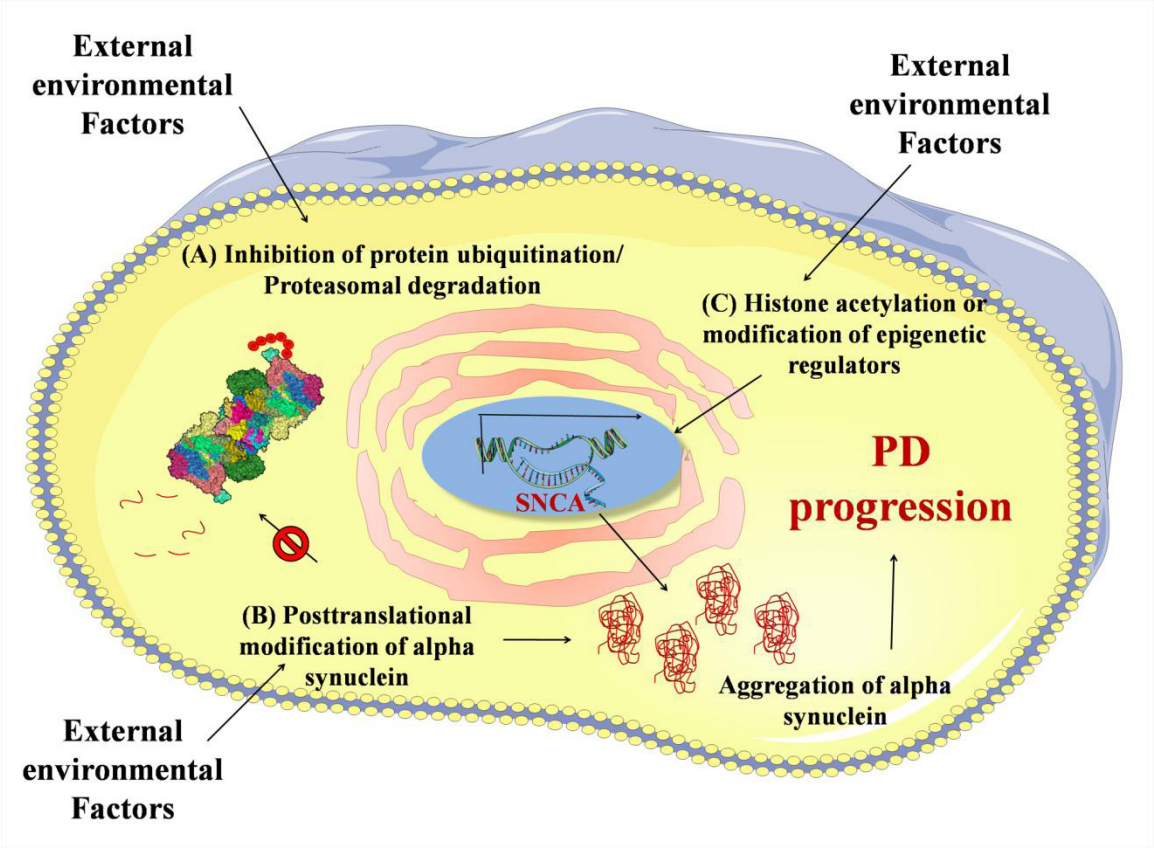


Figure.1 Epigenetic regulations in the PD progression.

In other epigenetic regulations, histone modifications and post translational modifications of synuclein are also considered. Post-translational modification of histone like histone acetylation and methylation alters the chromatin structures and accessibility of DNA transcript. In general, Histone acetylation endows transcriptional activation of gene and histone methylation inhibits the transcription of associated gene. The study has shown that histone acetylation is higher in the SNpc region of the PD patients compare to healthy controls.(28)Indeed, the histone

hyperacetylation of synuclein is well characterized in the PD progression having a higher association of H3K27ac.(29-31)Association of post translational modification of synuclein in PD etiology has great influence on PD management.(32) In that, the phosphorylation, majorly serine 129 phosphorylated alpha synuclein and nitration of synucleinare major hallmarks that leads to synuclein aggregation and PD progression, while O-GlcNacylation of synucelin reduces synucelinopathy that has been well demonstrated. Indeed, the enzyme, O-GlcNacyltransferase (OGT) responsible for O-GlcNacylation of synuclein is also reported to be reduced during the PD conditions.(33) The schematic has been illustrated to visualize the epigenetic regulation in the PD condition (Fig.1). The knowledge of PD pathogenesis leads to pave the way for the development of PD treatment. The existing treatments are majorly based on replenishing the dopamine level but are comprising of major limitations. While epigenetic based drug are under study to explore their preclinical and clinical efficacy overcoming major limitations of existing therapeutics.

## 1.4 PD treatments and limitations

Current therapeutic drugs can only able to slow down the PD conditions. Various anti-PD therapeutic agents are available for the treatment. However, the blood brain barrier (BBB) restricts them due to their incompetency to cross the BBB. Hence, carrying drug to the brain is always the problem for the researchers.(34) In the mechanism of anti-PD drug, majorly dopamine endowment or stimulation of dopamine receptors are involved. However, the death of the dopaminergic neurons still continues. Levodopa has been considered as the gold standard treatment for the PD.(35) However, it only provides the temporary relief and long term side effects of levodopa or unresponsiveness of patient to the drug limits the drug efficacy.(35)In recent decades, the progression of medical pharmacologic therapies has been done by using carbidopa-levodopa, a dopamine agonist, monoamine oxidase B inhibitors (MAO-B) inhibitors, **catechol-O-methyltransferase (COMT) inhibitors, anticholinergics,** amantadine as a therapeutic agent, and innovative surgical approach like deep brain stimulation (DBS)(36, 37). However, definitive disease-controlling therapy is still lacking due to multiple side effects of therapeutic agents like low blood pressure, vomiting, loss of appetite, etc. (38). Hence the new therapeutic approach that leads toward PD inhibition will be a breakthrough. Several

neurotherapeutic agents have the potency to control epigenetic events in PD regulation.(2) However, the limitations of lower solubility, blood-brain-barrier hindrance; poor drug release kinetics hamper the therapeutic efficacy of anti-PD drugs.(39) Therefore, it is imperative to find a new antiparkinsonian agent. The emerging nano-drug delivery platform has immense potential to overcome the existing limitations of potent anti-PD drugs.

## 1.5 Nanotechnology in PD management

The researchers are still in progress to find the conclusive treatment for the PD including exploring the antioxidant agents, vaccines and different surgical approaches.(40) Recently, the nanotechnology emerged as the one of the promising and potent strategy to endow the therapeutic efficacy of the potent drugs. Therefore, the applications of nanotechnology may able to retard the neurodegenerative disease conditions by making potent drug to cross BBB hindrance. (41-45) The nanoformulation of different drug exhibited advantage over the bare drug mediated treatments.(46) The nano-drug delivery system provides many advantages besides making the drug to cross BBB like improving drug solubility, drug release profile, stability, bioavailability, drug targeting and safety of the drug.(47) There are various nanodrug delivery systems utilized to carry the drugs to the brain like solid-lipid nanoparticles, polymeric nanoparticles and nanoliposomes.(48) Hence, nanomedicine is emerging as excellent tools for the development of the brain related infirmities. The surface modification of the nanoparticles makes the drug to target disease site for location specific drug release and facilitate the way to minimize the therapeutic dose of the drug. The variety of drugs like curcumin, quercetin, resveratrol, catechin and ginsenosides that are incompatible to cross the BBB has been successfully demonstrated to accumulate inside the brain and improving its solubility and availability by utilizing nano-drug delivery approaches.(48)

There are various approaches and strategies have been utilized to address limitations of therapeutic agent by using nanoplatforms. In the recent development about nanodrug delivery system by considering repositioning strategies, ligand or peptides modified nanocarrier systems and magnetically assisted nanoparticle accumulation have been applied to improve BBB penetration in PD management. Various metal based nanoformulations called as nanozymes have been developed to mimic the anti-oxidative enzymes to alleviate oxidation stress in the PD

treatment. In that, cerium oxide nanoparticles have been demonstrated to reduce synuclein toxicity, copper based nanoparticles reported to eliminate ROS generated in MPTP induced PD model, and PtCu nanozymes having mimicking ability of peroxidise, catalase and SOD shown prevention to prion like alpha synuclein spreading in PD.(49) The second strategy utilized to targeting alpha synuclein aggregation with utilization of nanoparticles. In the second strategy, grapheme quantum dots and cerium oxide nanoparticles shown to inhibit fibrillation of alpha synuclein and rabies virus glycoprotein peptide modified exosome demonstrated to inhibit synuclein gene expression by delivering synuclein siRNA.(49) The ligand or peptide modification to the nanoparticles also utilized to improve BBB permeation. In these aspects, researchers have developed various docosahexaenoic acid modified plasmid DNA loaded nanocarriers and shown their BBB crossing ability with improvement in PD condition.(50) In addition, vascular adhesion cell molecule-1 modified liposomes, angiopep-2 tagged red blood cell membrane coated nanoparticles and RVG peptide attached exosomes have also been reported to retard PD by improving BBB penetration.(50) The repositioning of potent drug is also widely considered pharmaceutical nanotechnology inspired approaches in PD treatment. In that, Ginkgolide loaded polyetheleneglycol (PEG)–polycaprolactone (PCL) nanoparticles, dopamine loaded liposome nanoparticles, levo dopamine loaded polylactic-co-glycolic acid (PLGA) nanoparticles, bromocriptine loaded chitosan nanoparticles, coumarin loaded PLGA-PEG nanoparticles, nalbuphine loaded solid-lipid nanoparticles, and dopamine loaded exosome reported in recent time that have shown PD retardation by improving drug efficacy.(50, 51) Besides that magnetic assisted and photothermal effect driven nanoparticles also reported to enhance drug or nanoparticles accumulation in brain. In this, iron oxide nanoparticles conjugated with PEG and polyethylamine has shown enhanced accumulation of nanoforulation in presence of magnetic field and iron oxide nanoparticle caged transferrin also demonstrated to show enhanced BBB penetration in PD retardation.(51, 52) Thus, the nanotherapeutic approaches are the best promising modality for the development of PD treatment by improving therapeutic efficacy and overcoming its associated limitations.(53) Hence, the present thesis work also aimed to evaluate the anti-PD therapeutic efficiency of the various nanoformulations that are discussed in details.

## 1.6 Objectives of the thesis

The present thesis focused to explore epigenetic regulation in the nanotherapeutic intervention of PD by understanding the camouflaged role of EZH2 and targeting H3K27ac in the management of synucleinopathy. In the last decades, metformin, FTY720 and hytrin emerged as the wonder therapeutic molecule in the management of several infirmities including neurodegenerative diseases (54-59). Besides having a potential therapeutic effect, these drugs have limitations like lower bioavailability due to absorption limited drug kinetics, poor solubility and burst drug release, respectively (60-63). By considering the emerging advantage of a nano-drug delivery system in the advancement and improvement of drug efficacy, present work demonstrated polydopamine, chitosan and polydopamine-serotonin nanoparticles to overcome the limitation of the metformin, FTY720 and Hytrin drug *in vitro* and *in vivo* PD model, respectively (1, 64, 65). The demonstration of the neuroprotective effect of metformin-loaded polydopamine nanoparticles, and the camouflaged role of EZH2, PP2A-EZH2 signalling and IDH2 role in the ubiquitination/proteasomal degradation of alpha-synuclein has been revealedin *in vitro* PD model.(1, 64, 65) Indeed, the metformin nanoformulation induced SIRT1 mediated histone deacetyaltion to inhibit SNCA gene expression, FTY720 nanocomposition induced Glc-N-acylation of synuclein to restrict the synuclein aggregation and Hytrin nanohybrid assisted chaperone mediated autophagy in degradation of synuclein are also explored *in vivo* PD model. Overall thesis majorly comprises eight objectives as follow:

Objective 1: Review of the literature to find potent drug and nanocarriers by considering the following criteria:

i) Drug should be FDA approved and it neuroprotective potential should be reported. So, its long term effect and safety standard should be well understood to repurpose the drug for PD treatment.

ii) Drug molecule should have potential to target alpha synucleinopathy as direct or indirect epigenetically driven therapeutic action.

iii) Nanocarrier should be nature inspired, biocompatible, and biodegradable having the neuroprotective or anti-oxidative properties. So, the biocompatibility, safety standard and stability could be better.

Objective 2: Review of the literature to design the methodology to synthesize, characterize and evaluate therapeutic efficacy of the nanoformulations.

Objective 3: To evaluate neuroprotective effect and molecular action of metformin loaded polydopamine nanoformulation *in vitro* and *ex vivo* Parkinson's disease (PD) model.

Objective 4: To investigate neuroprotective potential and molecular pathway of metformin loaded polydopamine nanoformulation *in vivo* Parkinson's disease (PD) model.

Objective 5: To evaluate neuroprotective efficacy of FTY720 loaded chitosan nanoparticles with exploring it's the molecular insight *in vitro* and *ex vivo* Parkinson's disease (PD) model.

Objective 6: To investigate neuroprotective efficacy and molecular pathway of FTY720 loaded chitosan nanoparticles *in vivo* Parkinson's disease (PD) model.

Objective 7: To examine neuroprotective caliber of hytrin loaded polydopamine-serotonin nanohybrid and exploration of it molecular pathway *in vitro* and *ex vivo* PD model.

Objective 8: To study the neuroprotecive efficiency and molecular insight of hytrin loaded polydopmaine-serotonin nanohybrid *in vivo* PD model.

Herein, the FDA approved drugs, metformin, FTY720 and hytrin have the limitation of rapid absorption with off targeting, low solubility with compromised bioavailability, and burst release kinetics, respectively. Therefore, the promising nanocarriers system should be employed to overcome the limitations of the drug and improve their therapeutic efficacy. Hence, the nature inspired nanocarriers polydopamine, chitosan and polydopamine-serotonin nanoparticles considered to improve delivery and efficacy of metformin, FTY720 and hytrin drug. As mentioned in the earlier section, epigenetic regulation in the PD is gaining attention to address the problems related to PD therapy. So, all selected nanoformulation has been tested to explore role of epigenetic factors in molecular neuroprotective action of nanoformulation. Despite of having numerous researches on PD, the ideal solution for PD therapy has not been demonstrated. In other means, there is no curative PD therapy available. The available therapy has ability to retard the disease progression. Therefore, new dimension of the research and more potent therapeutic candidates or strategies to improve efficacy of existing PD therapeutic agents are warranted. Thus, the presented thesis discusses the development, evaluation of therapeutic

efficacy and neuroprotective mechanisms of novel nano-drug delivery systems for PD treatment. The results of nanotherapeutic intervention in the epigenetic regulation of the PD divulged the promising calibre of our nanoformulationsas novel therapeutic candidate for PD.

Finally, the structure and research design of thesis has been represented below by comprising all objectives and thesis chapters.

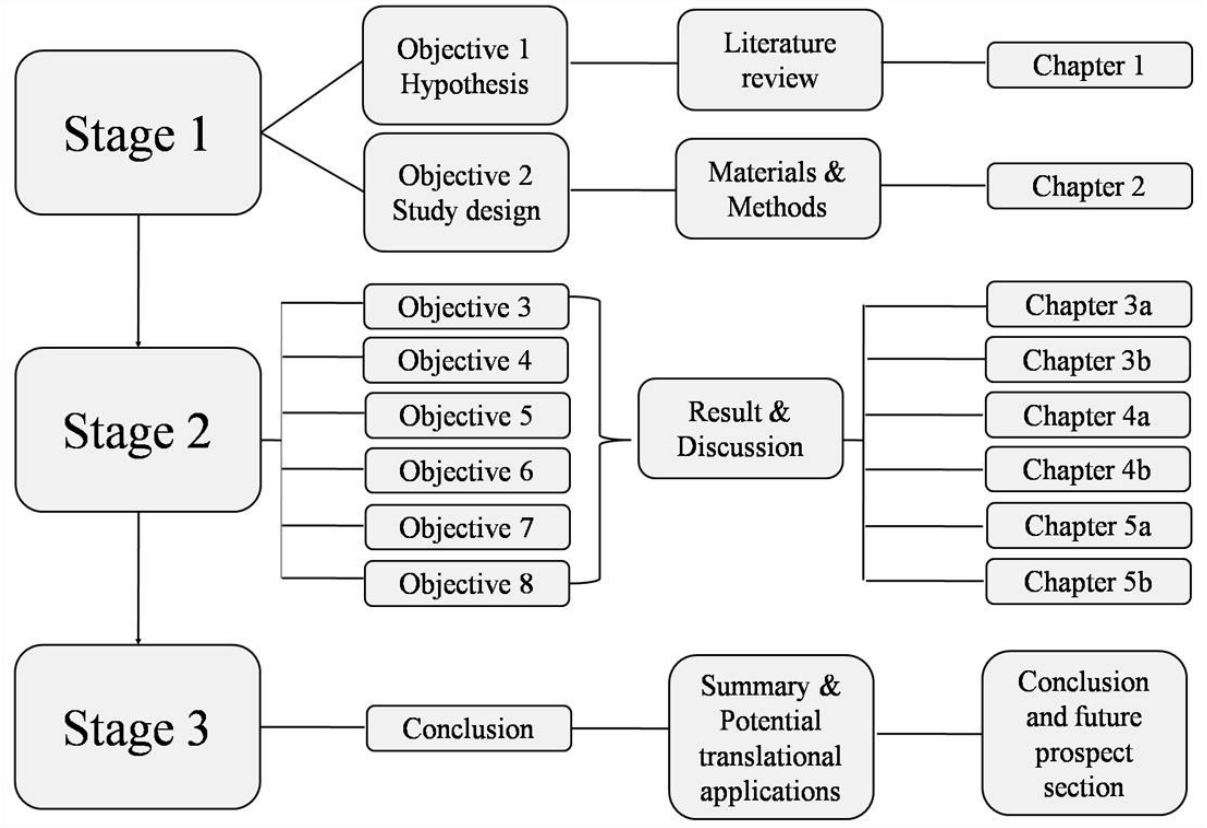


Scheme 1: Research design of the thesis.

## 1.7 References

1. M. N. Sardoiwala, A. K. Srivastava, B. Kaundal, S. Karmakar, S. R. Choudhury, Recuperative effect of metformin loaded polydopamine nanoformulation promoting EZH2 mediated proteasomal degradation of phospho-α-synuclein in Parkinson's disease model. *Nanomedicine: Nanotechnology, Biology and Medicine* **24**, 102088 (2020).

2. P. Hickey, M. J. D. d. Stacy, development, therapy, Available and emerging treatments for Parkinson's disease: a review. **5**, 241 (2011).
3. B. Thomas, M. F. Beal, Parkinson's disease. *Hum Mol Genet* **16 Spec No. 2**, R183-194 (2007).
4. B. Newland, S. B. Dunnett, E. Dowd, Targeting delivery in Parkinson's disease. *Drug Discov Today* **21**, 1313-1320 (2016).
5. P. Surathi, K. Jhunjhunwala, R. Yadav, P. K. Pal, Research in Parkinson's disease in India: A review. *Annals of Indian Academy of Neurology* **19**, 9-20 (2016).
6. Anonymous, QuickStats: Age-Adjusted Death Rates* for Parkinson Disease(dagger) Among Adults Aged >/=65 Years - National Vital Statistics System, United States, 1999-2017. *MMWR Morb Mortal Wkly Rep* **68**, 773 (2019).
7. C. Marras *et al.*, Prevalence of Parkinson's disease across North America. *npj Parkinson's Disease* **4**, 21 (2018).
8. S. K. Das *et al.*, Epidemiology of Parkinson disease in the city of Kolkata, India: a community-based study. *Neurology* **75**, 1362-1369 (2010).
9. M. Ozansoy, A. N. Başak, The central theme of Parkinson's disease: α-synuclein. *Molecular neurobiology* **47**, 460-465 (2013).
10. A. Kouli, K. M. Torsney, W. L. Kuan, "Parkinson's Disease: Etiology, Neuropathology, and Pathogenesis" in Parkinson's Disease: Pathogenesis and Clinical Aspects, T. B. Stoker, J. C. Greenland, Eds. (Codon Publications Copyright: The Authors., Brisbane (AU), 2018), 10.15586/codonpublications.parkinsonsdisease.2018.ch1.
11. Q. Xia *et al.*, Proteomic identification of novel proteins associated with Lewy bodies. *Frontiers in bioscience : a journal and virtual library* **13**, 3850-3856 (2008).
12. A. J. Lees, M. Selikhova, L. A. Andrade, C. Duyckaerts, The black stuff and Konstantin Nikolaevich Tretiakoff. *Movement disorders : official journal of the Movement Disorder Society* **23**, 777-783 (2008).
13. N. L.-G. Del Rey *et al.*, Advances in Parkinson's Disease: 200 Years Later. **12** (2018).
14. D. K. Simon, C. M. Tanner, P. Brundin, Parkinson Disease Epidemiology, Pathology, Genetics, and Pathophysiology. *Clinics in geriatric medicine* **36**, 1-12 (2020).
15. A. Ascherio, M. A. Schwarzschild, The epidemiology of Parkinson's disease: risk factors and prevention. *The Lancet. Neurology* **15**, 1257-1272 (2016).

16. C. Labbé, O. Lorenzo-Betancor, O. A. Ross, Epigenetic regulation in Parkinson's disease. *Acta neuropathologica* **132**, 515-530 (2016).
17. M. H. Polymeropoulos *et al.*, Mutation in the alpha-synuclein gene identified in families with Parkinson's disease. *Science* **276**, 2045-2047 (1997).
18. W. Poewe *et al.*, Parkinson disease. **3**, 1-21 (2017).
19. I. J. Siddiqui, N. Pervaiz, A. A. Abbasi, The Parkinson Disease gene SNCA: Evolutionary and structural insights with pathological implication. *Scientific reports* **6**, 24475-24475 (2016).
20. L. Stefanis, α-Synuclein in Parkinson's disease. *Cold Spring Harb Perspect Med* **2**, a009399-a009399 (2012).
21. I. A. Qureshi, M. F. Mehler, Advances in epigenetics and epigenomics for neurodegenerative diseases. *Curr Neurol Neurosci Rep* **11**, 464-473 (2011).
22. M. von Schimmelmann *et al.*, Polycomb repressive complex 2 (PRC2) silences genes responsible for neurodegeneration. *Nature neuroscience* **19**, 1321-1330 (2016).
23. E. Sodersten *et al.*, Dopamine signaling leads to loss of Polycomb repression and aberrant gene activation in experimental parkinsonism. *PLoS genetics* **10**, e1004574 (2014).
24. M. Abdouh *et al.*, Bmi1 is down-regulated in the aging brain and displays antioxidant and protective activities in neurons. *PloS one* **7**, e31870 (2012).
25. Q. Huang, H. Wang, S. W. Perry, M. E. Figueiredo-Pereira, Negative regulation of 26S proteasome stability via calpain-mediated cleavage of Rpn10 subunit upon mitochondrial dysfunction in neurons. *J Biol Chem* **288**, 12161-12174 (2013).
26. Y. Oh, Y. M. Kim, M. M. Mouradian, K. C. Chung, Human Polycomb protein 2 promotes alpha-synuclein aggregate formation through covalent SUMOylation. *Brain research* **1381**, 78-89 (2011).
27. R. Rott *et al.*, SUMOylation and ubiquitination reciprocally regulate alpha-synuclein degradation and pathological aggregation. *Proceedings of the National Academy of Sciences of the United States of America* **114**, 13176-13181 (2017).
28. G. Park *et al.*, Regulation of Histone Acetylation by Autophagy in Parkinson Disease. *The Journal of biological chemistry* **291**, 3531-3540 (2016).
29. M. Huang *et al.*, Mitochondrial dysfunction–induced H3K27 hyperacetylation perturbs enhancers in Parkinson's disease. *JCI Insight* **6** (2021).

30. S. Guhathakurta, E. Bok, B. A. Evangelista, Y.-S. Kim, Deregulation of α-synuclein in Parkinson's disease: Insight from epigenetic structure and transcriptional regulation of SNCA. *Prog Neurobiol* **154**, 21-36 (2017).
31. S. Guhathakurta *et al.*, Targeted attenuation of elevated histone marks at SNCA alleviates α-synuclein in Parkinson's disease. *EMBO Mol Med* **13**, e12188-e12188 (2021).
32. J. Zhang, X. Li, J. D. Li, The Roles of Post-translational Modifications on α-Synuclein in the Pathogenesis of Parkinson's Diseases. *Frontiers in neuroscience* **13**, 381 (2019).
33. B. E. Lee *et al.*, O-GlcNAcylation regulates dopamine neuron function, survival and degeneration in Parkinson disease. *Brain* **143**, 3699-3716 (2020).
34. K. Pathak, N. Akhtar, Nose to Brain Delivery of Nanoformulations for Neurotherapeutics in Parkinson`s disease: Defining the Preclinical, Clinical and toxicity issues. *Current drug delivery* (2016).
35. L. V. Kalia, A. E. Lang, Parkinson's disease. *The Lancet* **386**, 896-912 (2015).
36. B. S. Connolly, A. E. Lang, Pharmacological treatment of Parkinson disease: a review. *Jama* **311**, 1670-1683 (2014).
37. P. Hickey, M. Stacy, Available and emerging treatments for Parkinson's disease: a review. *Drug design, development and therapy* **5**, 241-254 (2011).
38. B. D. Li *et al.*, Adverse effects produced by different drugs used in the treatment of Parkinson's disease: A mixed treatment comparison. *CNS neuroscience & therapeutics* **23**, 827-842 (2017).
39. B. D. Li *et al.*, Adverse effects produced by different drugs used in the treatment of Parkinson's disease: a mixed treatment comparison. **23**, 827-842 (2017).
40. N. Singh, V. Pillay, Y. E. Choonara, Advances in the treatment of Parkinson's disease. *Prog Neurobiol* **81**, 29-44 (2007).
41. C. Giordano *et al.*, Nanocomposites for neurodegenerative diseases: hydrogel-nanoparticle combinations for a challenging drug delivery. *The International journal of artificial organs* **34**, 1115-1127 (2011).
42. G. Linazasoro, Potential applications of nanotechnologies to Parkinson's disease therapy. *Parkinsonism & Related Disorders* **14**, 383-392 (2008).
43. M. Mazza *et al.*, Nanofiber-Based Delivery of Therapeutic Peptides to the Brain. *ACS Nano* **7**, 1016-1026 (2013).

44. G. Modi *et al.*, Nanotechnological applications for the treatment of neurodegenerative disorders. *Prog Neurobiol* **88**, 272-285 (2009).
45. G. Soursou *et al.*, Applications of Nanotechnology in Diagnostics and Therapeutics of Alzheimer's and Parkinson's Disease. *Current Drug Metabolism* **16**, 705-712 (2015).
46. G. Leyva-Gómez *et al.*, Nanoparticle technology for treatment of Parkinson's disease: the role of surface phenomena in reaching the brain. *Drug Discovery Today* **20**, 824-837 (2015).
47. E. Garbayo, E.-H. d. A. Mendoza, J. M. Blanco-Prieto, Diagnostic and Therapeutic Uses of Nanomaterials in the Brain. *Current Medicinal Chemistry* **21**, 4100-4131 (2014).
48. P. Ganesan, H. M. Ko, I. S. Kim, D. K. Choi, Recent trends in the development of nanophytobioactive compounds and delivery systems for their possible role in reducing oxidative stress in Parkinson's disease models. *Int J Nanomedicine* **10**, 6757-6772 (2015).
49. A. Li *et al.*, Emerging Nanotechnology for Treatment of Alzheimer's and Parkinson's Disease. **9** (2021).
50. G. Cheng *et al.*, Anti-Parkinsonian Therapy: Strategies for Crossing the Blood–Brain Barrier and Nano-Biological Effects of Nanomaterials. *Nano-Micro Letters* **14**, 105 (2022).
51. H. Hernández-Parra *et al.*, Repositioning of drugs for Parkinson's disease and pharmaceutical nanotechnology tools for their optimization. *Journal of Nanobiotechnology* **20**, 413 (2022).
52. M. N. Sardoiwala, A. Sood, L. Biswal, S. Roy Choudhury, S. Karmakar, Reconstituted Super Paramagnetic Protein "Magnetotransferrin" for Brain Targeting to Attenuate Parkinsonism. *ACS Applied Materials & Interfaces* **15**, 12708-12718 (2023).
53. A. D. Kulkarni *et al.*, Nanotechnology-mediated nose to brain drug delivery for Parkinson's disease: a mini review. *Journal of drug targeting* **23**, 775-788 (2015).
54. R. Cai *et al.*, Enhancing glycolysis attenuates Parkinson's disease progression in models and clinical databases. *The Journal of clinical investigation* **129**, 4539-4549 (2019).
55. P. Zhao *et al.*, Neuroprotective effects of fingolimod in mouse models of Parkinson's disease. **31**, 172-179 (2017).
56. G. Vidal-Martinez *et al.*, FTY720/Fingolimod Reduces Synucleinopathy and Improves Gut Motility in A53T Mice: CONTRIBUTIONS OF PRO-BRAIN-DERIVED

NEUROTROPHIC FACTOR (PRO-BDNF) AND MATURE BDNF. *J Biol Chem* **291**, 20811-20821 (2016).

57. P. Joshi *et al.*, Fingolimod Limits Acute Aβ Neurotoxicity and Promotes Synaptic Versus Extrasynaptic NMDA Receptor Functionality in Hippocampal Neurons. *Scientific Reports* **7**, 41734 (2017).
58. M. Foretz, B. J. N. R. E. Viollet, Metformin takes a new route to clinical efficacy. **11**, 390-392 (2015).
59. M. Clyne, Metformin—the new wonder drug? *Nature Reviews Urology* **11**, 366-366 (2014).
60. T. Takasaki, K. Hagihara, R. Satoh, R. Sugiura, More than Just an Immunosuppressant: The Emerging Role of FTY720 as a Novel Inducer of ROS and Apoptosis. *Oxid Med Cell Longev* **2018**, 4397159 (2018).
61. M. Kinaan, H. Ding, C. R. J. M. p. Triggle, practice, Metformin: an old drug for the treatment of diabetes but a new drug for the protection of the endothelium. **24**, 401-415 (2015).
62. M. K. Kumar, K. Nagaraju, S. Bhanja, M. J. I. J. o. P. S. Sudhakar, Research, Formulation and evaluation of sublingual tablets of terazosin hydro-chloride. **5**, 417 (2014).
63. S. Bhattacharjee, Understanding the burst release phenomenon: toward designing effective nanoparticulate drug-delivery systems. **12**, 21-36 (2021).
64. M. N. Sardoiwala, S. J. Mohanbhai, S. Karmakar, S. R. Choudhury, Hytrin loaded polydopamine-serotonin nanohybrid induces IDH2 mediated neuroprotective effect to alleviate Parkinson's disease. *Materials Science and Engineering: C* https://doi.org/10.1016/j.msec.2021.112602, 112602 (2021).
65. M. N. Sardoiwala, S. Karmakar, S. R. Choudhury, Chitosan nanocarrier for FTY720 enhanced delivery retards Parkinson's disease via PP2A-EzH2 signaling in vitro and ex vivo. *Carbohydrate Polymers* **254**, 117435 (2021).

# Chapter 2

---

# Materials and Methods

## 2.1. Reagents

Dopamine hydrochloride, Sodium hydroxide (NaOH), 5-Hydroxytryptamine hydrochloride (serotonin), rotenone, Terazosin hydrochloride dihydrate (Hytrin), 3-[4,5-dimethylthiazol-2-yl]-2,5-diphenyltetrazolium bromide (MTT), paraformaldehyde, isopropanolalcohol (IPA), Hydrochloric acid (HCl), 2′,7′-dichlorodihydrofluorescin diacetate (DCFH-DA), DAPI, HEPES, Rhodamine B, Fingolimod (FTY720) hydrochloride, Chitosan, Sodium Tri PolyPhosphate, Indocyanine green, Tris-base, NaCl, glycine, were acquired from sigma. Anti-α-Syn (p-ser129), anti-β-actin, anti-DRD3, anti-CASPASE3, anti-EZH2, anti-BMI1, anti-H3K27me3, anti-TH, anti-PP2A, IDH1/2 antibody, ubiquitin antibody and secondary antibodies conjugated to HRP/FITC/TRITC were procured from Santa Cruz Biotechnology (CA, USA). Fetal bovine serum (FBS), HiGlutaXL$^{TM}$ high glucose Dulbecco's modified Eagle's medium (DMEM), phosphate-buffered saline (PBS), Trypsin-EDTA, antimycotic antibiotic solution, and Hank's balanced salt solution (HBSS) were procured from Himedia (USA). Halt protease/phosphatase inhibitor cocktail (Sigma) and ECL Western blotting substrate purchased from Bio-Rad (California, USA), and culture consumables from Nunc (Denmark). The rest of the chemicals used in the study were of Analytical Reagent grade and procured from Indian companies.

The methodological study design presented to understand aim of synthesis, characterization and therapeutic evaluation of nanoformulation and align the methodology to each chapter for better understanding of chapter 2 and thesis work.

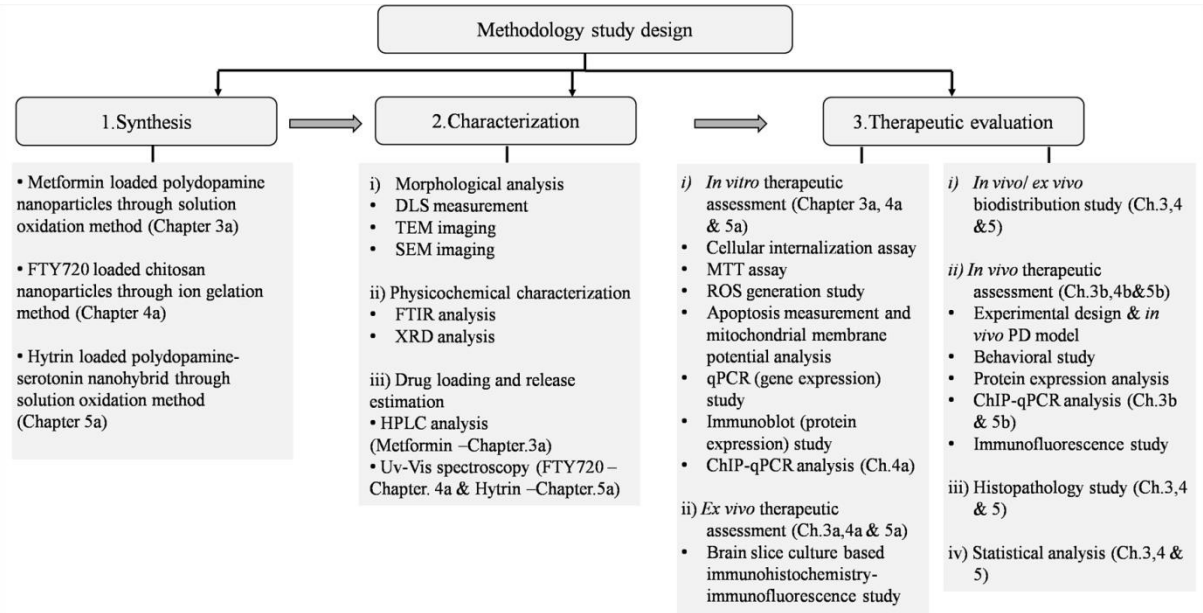

Scheme 2: Study design represents methodology and common aims of each chapter of thesis.

## 2.2. Synthesis of nanoparticles

### 2.2.1. Synthesis of polydopamine nanoparticles (PDANPs) and Metformin-loaded PDANPS

Met-loaded PDANPs synthesized through the solution oxidation method (1, 2). In a typical synthesis of PDANPs, 1mg/ml dopamine solution prepared in Milli-Q water and NaOH added in a molar ratio of dopamine to NaOH (1:0.8). For Met loaded PDANPs, metformin added to the dopamine solution in a molar ratio of metformin to dopamine (1:5, 1:10 and 1:20). Generally, in this mild alkaline condition, oxidation leads to self-polymerization of dopamine monomers with the encapsulation of metformin for 24 hours at 29.5 °C. Centrifugation carried out to remove NaOH and washing of PDANPs was performed at 16000 rpm for 30 minutes. The smaller size particles separated through centrifugation of washed PDANPs at 4000 rpm for 10 minutes and the supernatant further pellet down at 16000 rpm for 30 minutes. Final PDANPs resuspended in Milli-Q water and lyophilized.

### 2.2.2. Synthesis of chitosan nanoparticles and FTY720 loaded Chitosan Nanoparticles

CsNPs synthesized through the ion gelation method following previously described protocols (3). Chitosan (1mg/ml) and sodium tripolyphosphate (STPP-1mg/ml) solubilized in 1% acetic acid and Milli-Q water, respectively. Here, the pH of the solution was 4 during the synthesis. The stability of FTY720 in the acidic solution studied for four hours due to its little exposure required to the acidic environment during synthesis. Varying concentrations of FTY720 according to the w/w ratio of chitosan and FTY720 dissolved in ethanol and added to the chitosan solution. STPP solution added dropwise at the rate of 0.15 ml/min in chitosan solution under continuous stirring (700 rpm) with incubation for 1 hour at room temperature (20-25 °C). The ratio of chitosan and STTP (2:1, 4:1, 6:1, 10:1, and 15:1) utilized against mean particle size, polydispersity index, and zeta potential to finalize the nanoparticles. Final prepared CsNPs and FCsNPs resuspended in Milli-Q water and lyophilized. In the process of lyophilization, the samples have been frozen at -80°C overnight, and the next day, the samples have been kept in a lyophilizer (Lyodry benchtop freeze dryer, UK). The samples had nanoparticles dispersed in water. Hence, it has required 5-

pascal Vaccum pressure and -5 °C to sublime. The sublimation process happened to convert ice crystals into gaseous vapor and dried the samples.

### 2.2.3. Synthesis of polydopamine-serotonin nanohybrids and Hytrin loaded polydopamine-serotonin nanoformulations

Hytrin-loaded polydopamine-serotonin nanoparticles (H@PSNPs) synthesized through the solution oxidation method(1, 2, 4). In a typical synthesis of Polydopamine-serotonin nanoparticles (PSNPs), 1mg/ml dopamine and serotonin solution prepared in Milli-Q water and NaOH added in various a molar ratio of dopamine/serotonin to NaOH (1:0.4, 1:0.8, and 1:1.2) to optimize the molar ratio for the synthesis of H@PSNPs. For that, Hytrin added to the dopamine solution in a 1:5 molar ratio of Hytrin to dopamine. In this mild alkaline condition, oxidation leads to self-polymerization of dopamine/serotonin monomers with the encapsulation of Hytrin for 24 hours at room temperature with stirring at 300 rpm. NaOH removal and washing have been performed by centrifugation at 16000 rpm for 30 minutes. Then, the smaller-sized nanoparticles have been separated by centrifugation at 4000 rpm for 10 minutes and the supernatant pellet down at 16000 rpm for 30 minutes. Final nanoformulations lyophilized for further use.

## 2.3. Morphological and physicochemical characterization of nanoformulations

### 2.3.1. Dynamic light scattering analysis

Dynamic light scattering (DLS) used to measure the mean hydrodynamic diameter of nanoparticles. The developed nanoformulations subjected to hydrodynamic size, PDI, and surface zeta potential measurement by using Malvern Zeta Sizer (Nano ZS, Malvern instrument, UK). 100-fold diluted samples measured for 120 sec on the base of the electrophoretic mobility of nanoparticles by considering samples in triplicate.

2.3.2. Transmission Electron Microscopy (TEM) and Scanning Electron Microscopy (SEM) analysis

Morphological characterization performed by SEM/TEM analysis. For that, diluted samples and negative staining dyes (in the case of TEM) dropped cast on a clean silicon wafer/carbon-coated TEM grid (300 meshes). The excess entities cleared out using filter papers and kept under a vacuum. TEM imaging performed with JEOL TEM 2100 at 120 kV. SEM images obtained with JEOL SEM (IT 200).

2.3.3. Physicochemical and spectroscopy analysis

Precursors of nanocarrier and drug compatibility examined by Fourier-transformed infrared spectroscopy (FTIR System, Cary Agilent 660 IR spectrophotometer), X-ray diffraction pattern analysis (XRD), and Raman confocal spectrophotometer. The assessment of any physicochemical interaction measured via scanning in the IR range from 400 to 4000 $cm^{-1}$. The physical nature and structural compatibility of samples observed by the XRD pattern obtained with Bruker/D8 Advanced X-ray Diffractometer. Moreover, Raman spectroscopy also performed to know the interactions between dopamine and metformin. Raman confocal spectroscopic analyses performed at room temperature using a WITec Raman spectrometer (Germany, UK) with an unpolarised Nd-YAG laser. 532 nm Nd-YAG laser with 75 mW power focused on the samples with 1 mm spot size through 20X magnification. The Raman spectrums acquired at 600 lines/mm grating by the Peltier-cooled (-60 °C) charge-coupled detector.

2.4. Drug loading and encapsulation efficiency measurement

Metformin estimated from Metformin (Met) loaded PDANPs using HPLC analysis at 233nm. The C-18 column utilized to separate metformin at the isocratic flow of acetonitrile: methanol-35:65. The HPLC peak area analyzed to estimate metformin.

The presence of FTY720 evaluated from FCsNPs using UV-Vis spectroscopy at 220nm by following an existing study for estimation of FTY720 drug loading with UV-Vis spectroscopy. (5) Here, we prepared FCsNPs by adding an optimized concentration of FTY720 (1.7 mg) to 10 mg/ml chitosan solution. After 1 hour, prepared nanoparticles centrifuged at 10,000 rpm for 20

minutes. The supernatant has been collected and analyzed under the UV-Vis spectrometer to know the drug concentration in nanoformulation by subtracting the amount of detected drug in the supernatant from the initially applied drug concentration. A similar process also applied to placebo nanoparticles without FTY720. The supernatant solution of placebo nanoparticles without FTY720 has been utilized to create a baseline before measuring for FTY720 to estimate loading frequency. Hence, it helps to nullify the interferences of solvent and nanoparticles during estimation.

Hytrin was estimated from H@PSNPs using fluorimetry analysis at 376 nm at an excitation of 330 nm by following the existing study that has shown the sensitive determination of Hytrin by spectrofluorimetry. (6) The fluorescence intensity analyzed to detect Hytrin. Here, we synthesized H@PSNPs by adding an optimized concentration of Hytrin (2 mg) to 1mg/ml dopamine/serotonin solution (10 ml). After 24 hours, prepared nanoformulations centrifuged and washed. The supernatant has been collected and analyzed under the UV-Vis spectrofluorimeter to estimate the concentration of Hytrin in H@PSNPs by subtracting the amount of detected Hytrin in the supernatant from the initially applied drug concentration. A similar process also applied to blank nanoparticles without Hytrin. The supernatant solution of blank nanoparticles without Hytrin has also been analyzed to nullify the interferences of solvent and nanoparticles during estimation before measuring for Hytrin to estimate loading content.

Drug loading content and encapsulation efficiency calculated by the following equations.

Drug loading content =

(Concentration of the drug obtained in nanoformulation ÷ Concentration of nanoformulation)×100

Drug encapsulation efficiency =

(Concentration of the drug obtained in nanoformulation ÷ Concentration of the drug added)×100

2.5. *In vitro* drug release and kinetic analysis from nanoformulation

The dialysis membrane method utilized to estimate the drug release profile (7). Bare drug (1mg/ml) solution and equalized drug containing nanoformulation solutions prepared in 1 ml PBS (pH 7.4). 12 kDa molecular weight cutoff dialysis bag filled with solutions and deep in a 40 mL sink of PBS + 0.5% (Sodium dodecyl sulfate) SDS pH 7.4 at 37 ± 0.5 °C. 1 ml of the sample has been collected for respective time points. Sink volume maintained by adding an equal volume of PBS + 0.5% SDS that was drawn during sample collection. The released drug quantified as mentioned in the methodology previous section of drug loading and encapsulation efficiency. Mathematical modeling performed to understand the release kinetic of nanoformulations. DDSolver software has been utilized to predict drug release kinetic mechanisms. DDSolver is a freely available add-in program useful to facilitate the modeling of dissolution data using nonlinear optimization methods based on a built-in model library. It is very much helpful software to speed up the calculation and provide a convenient way to report dissolution data quickly with reduced errors. It is easy to use to select the model and input the experimental data of time and % release to run the program to show the fitted model for the same.

2.6. Cell culture and 3D multilayer culture

Undifferentiated SH-SY5Y Cells used to access the impact of nanoparticles on cell viability. Undifferentiated cells were shown as more susceptible to oxidative stress in comparison to differentiated cells and more preferred *in vitro* model of PD (8,9). SH-SY5Y cells were cultured in HiGlutaXL™ DMEM media comprising 10% FBS and 1% antimycotic antibiotic solution (100 U penicillin, 100 µg streptomycin, and 250 ng amphoterin) at 37°C in an incubator (Thermo Fisher, USA) providing 5% $CO_2$ and 90% humidity. Cells were grown and sub-cultured after trypsinization using 0.25% trypsin or seeded for cellular treatments.

3D cell culturing gains interest with time. 3D spheroids and multilayered cell culturing mimic *in vivo* conditions and are useful to develop model studies. A recent study has shown that insert-based rapid *in vitro* system support 3D cell culturing (10). Following protocol with some modifications, $10^5$ cells were grown on 12 well plates with 3 µm pore size millicell hanging cell insert, made up of polyethylene terephthalate (Merck Millipore, USA). The insert hung that created an outer chamber below the insert matrix and an inner chamber upper the insert matrix.

Cells seeded in the inner chambers with 200 µl 20% FBS enriched growth media/well and further 1 ml media/well provided from the outer chamber. Media was replaced every 48 hours. Cells grown for 12-15 days until they acquired a 3D multilayer structure, morphology called a 3D raft that used for further experiments.

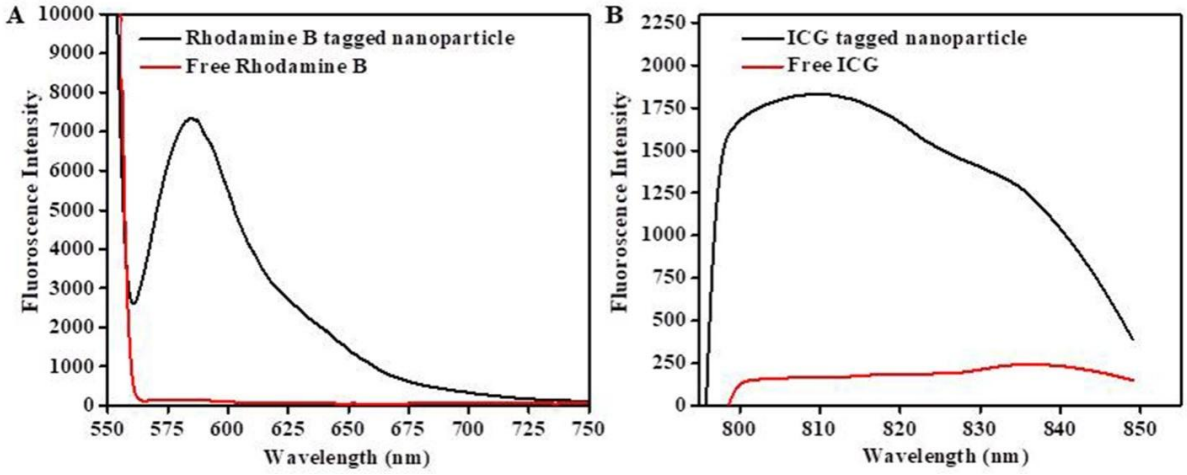


Figure 2.1. Fluorescence spectroscopy analysis; (A) Emission spectrum of Rhodamine B nanoparticles and free rhodamine B after purification (dialysis) represented (Excitation=535nm, Emission=583nm), (B) in similar way emission spectra for ICG tagged nanoparticles and free ICG shown (Excitation=760nm, Emission=810nm). This has shown a negligible amount of released dye after 24 hours period.

2.6.1. Cellular internalization of nanoformulations

Cells differentiated with the treatment of 10 µM retinoic acid for 6 days before performing a cellular uptake study(11). Retinoic acid activates PI3K/Akt signaling pathways in the differentiation of SH-SY5Y cells (12). Cells grown on the coverslip inside 6 well plates with cell densities of 10,000 cells/well in 1 ml growth media. On the next day, cells incubated with Rhodamine B (50 nM / 1mg NPs) tagged nanoformulations for 6 hours. In preparation of Rhodamine B tagged nanoparticles by the following method with some modification (13), Rhodamine B interacted with nanoformulations on a rotary shaker for one day. To remove excess or unbound Rhodamine B, the solution has been washed out with repeated centrifugation at 15,000 rpm for 10 minutes until the supernatant gets cleared. Further, nanoparticles dialyzed

with a 10kDa filter (Amicon, Millipore) five times to get tagged nanoparticles. Incubated cells with Rhodamine B tagged nanoformulations washed with 1X PBS and fixed with chilled 4% paraformaldehyde for 30 minutes and further washed with 1X PBS. Fixed cells incubated with 10µl of 100nM DAPI to stain nuclei for 10 minutes and mounted with 80% glycerol. Confocal Laser Scanning Microscopy performed with ZEISS 880, Germany. Imaging performed under 60X magnification with a dye-specific excitation laser line, 405 nm for DAPI (blue channel) and 565 nm for Rhodamine B (red channel). Excitation and emission λm of Rhodamine tagged nanoparticles are 535nm and 583nm, respectively. The spectrum of nanoparticles and their purity after extensive dialysis evaluated (Fig.2.1) To mimic the tissue condition and monitor the internalization of nanoparticles at the tissue level, the rhodamine B tagged H@PSNPs has been incubated with a 3D raft for 12 hours, and 3D raft washed thrice before staining with DAPI. The mounting media has been used to prepare a permanent slide that has been imaged under a Zeiss confocal microscope (ZEISS 880, Germany).

2.6.2. Cellular viability (MTT) assay, *in vitro* PD model, and neuroprotection assay

To determine the effect of rotenone and nanoformulations, 10,000/well SH-SY5Y cells seeded in 96 well plates. To determine the IC50 dose of rotenone, cells treated with rotenone (0.01 to 10 µM ) for 24 and 48 hours. For neuroprotection evaluation of nanoformulations, cells exposed to metformin (25 to 250 nM) and an equivalent concentration of metformin bearing PDANPs, FTY720 (0.1 to 2µM), equal 0.1 to 2µM FTY720 carrying FCsNPs concentration, Hytrin (0.1 to 100 µM), equal Hytrin carrying H@PSNPs (0.1 to 100 µM) and rotenone (500-750 nM) concentration was given for 24-48 hours. This co-treatment method of rotenone and the proposed neuroprotectant was followed for further experiments also. On completion of treatment, cell viability analyzed by MTT reduction assay. Estimation of Cell viability was based on the cleavage of MTT tetrazolium salt and the formation of formazan crystal on exposure to mitochondrial dehydrogenase of live cells. In this assay, 10µl/well of MTT (5mg/ml) added to the media and incubated for 4 hours at 37°C in a$CO_2$ incubator. Formozan crystals solubilized in slight acidic isopropanol and quantified absorbance at 595 nm in a microplate reader(14) (SYNERGY H1, Bio-Tek Instrument, USA). The results have been analyzed concerning untreated control SH-SY5Y cells.

Effective doses of AG-221, EPZ011989 selected as per the recommendation of the manufacturer (Adooq bioscience, USA) and the MG132 dose has been opted by following existing reports. (4, 15, 16) (4)

2.6.3. Reactive oxygen species (ROS) generation assay

DCFH-DA dye employed to estimate the ROS generation by following the reported method (17). Fluorescently inactive DCFH-DA dye transforms into fluorescent 2', 7'-dichlorofluorescein on the exposure of cellular ROS. In brief, $10^3$ cells/well seeded in 96 wells plate for overnight. On the next day, cells incubated with 10 μM DCFH-DA dye for 45 min in a $CO_2$ incubator. Cells washed with PBS to remove excess dye and treated as previously described for this study. Then, ROS generation measured with a microplate reader (infinite 200 PRO, Tecan Group Ltd, Switzerland) at 485 nm/ 527 nm (excitation/emission).

2.6.4. Apoptosis measurement and mitochondrial membrane potential study

PE/Annexin V apoptosis kit I (BD bioscience, USA) used to quantitatively evaluate apoptotic cells. $10^6$ Cells seeded in a 6-well plate and treated similarly as mentioned earlier, excluding stained and unstained controls. On completion of treatment, cells collected and washed twice with cold 1X PBS and resuspended in 1X Annexin-binding buffer. 5μl PE/Annexin and 7AAD added to a 100μl suspension of cells and incubated for 15 minutes in the dark. Finally, cells resuspended in 1X Annexin-binding buffer and analyzed under a flow cytometer (Aria system, BD Bioscience). Results were analyzed with flow jo software.

$10^5$ cells seeded in 70mm plates and treated as mentioned in the earlier methodology section. On completion of treatment, cells washed with 1X phosphate buffer saline (PBS) and harvested. Cells incubated with Jc1 dye (1:500 dilutions of 1mg/ml stock solution) at RT for 30 minutes. Cells washed with 1X PBS to remove excess Jc1 dye. The Jc1-based mitochondrial analysis has been performed by using a flow cytometer (BDFACSAria™, BD, USA) at the green (FITC) and red emission (PE) laser lines.

3D rafts of SH-SY5Y grown and treatment of metformin, Met loaded PDANPs, and rotenone given for 96 hours excluding untreated control as mentioned earlier. On completion of treatment,

matrix-adhered 3D rafts of SH-SY5Y removed and placed on a clear slide. 3D rafts washed with 1x PBS and incubated with Jc1 (1:500 dilutions) at room temperature (RT) for 30 minutes. Washed again with 1x PBS before fixation in 1ml of 4% paraformaldehyde at RT for 30 minutes. 3D rafts washed thrice and made permeable with methanol for 30 minutes at 0°C. Then, 3D rafts again washed and incubated with 2% BSA incubation buffer for 2 hours at RT. Further, incubated with mouse-raised anti-CASPASE3 antibody (1:500 dilutions) for 1 hour at RT and washed twice with incubation buffer. The incubation buffer used to block the non-specific binding sites of the antibody. Finally, 3D rafts incubated with FITC conjugated anti-mouse secondary antibody (1:1000 dilutions) for 1 hour at RT and washed with incubation buffer before staining with DAPI (20ul of 100nM). 80% glycerol used as mounting media and prepared slides imaged under a Zeiss confocal microscope (ZEISS 880, Germany). The results analyzed in comparison to untreated control 3D rafts and quantified through Fiji software.

2.6.5. Real-time quantitative polymerase chain reaction (qPCR) study

$10^6$ cells seeded in 6 well plates and treated excluding the control group as mentioned in the earlier protocol. On completion of treatment, cells washed with 1X PBS, and mRNAs isolated using an mRNA isolation kit (PureLink RNA Mini Kit, life technologies) as per the manufacturer's instructions. Quantification of mRNA performed by NanoDrop (2000/2000c, Thermo Fisher Scientific, USA) to normalize mRNA concentration. Reverse transcription from 1 µg of total RNA /groups, including the control group executed by using the High-Capacity cDNA Archive Kit (Applied Biosystems) as per the manufacturer's protocol. Diluted cDNA with 15 µl of ultrapure water (Applied Biosystems) used for gene expression analysis. Quantitative real-time PCR (qRT-PCR) executed on the Quantstudio 3 RT-PCR system (Thermo Fisher Scientific, USA) using Power SYBR Green PCR master mix (Applied Biosystems, Thermo Fisher, USA) according to manufacturer recommended procedure. Primers were procured from Integrated DNA Technologies, USA. An experiment performed with triplets of samples. For verification of amplified PCR products, melting curves checked. GAPDH gene expression used to normalize presented relative gene expressions. Fold change of expression was calculated and analyzed using the comparative CT method ($2^{-\Delta\Delta CT}$) with Quant studio 3 software.

2.6.6. Immunoblot analysis and immunoprecipitation study

$1 \times 10^6$ cells seeded in 100mm culture Petri plates and treated as already described in the above section. 2.5 µM neurotherapeutic doses of Hytrin and H@PSNPs have been utilized. In the protein isolation, cell lysis has been performed by Radioimmunoprecipitation assay (RIPA) buffer for 20 minutes at 4°C. The cell scraper has been utilized to collect cell lysate and probe sonicated at 5% amplitude with 5 sec on/off impulse for 60 seconds. The processed cell lysates centrifuged at 13,500 rcf for 5 minutes at 4°C. Supernatants had been collected and estimated for protein concentration using Bradford reagent (Sigma, USA). An equal amount of protein samples run on Tris-Glycine gel electrophoresis. The protein has been transferred to the Immuno-Blot®polyvinylidene fluoride (PVDF)membrane (Bio-Rad, USA) by using the Trans-Blot®Turbo™ transfer system (Bio-Rad, USA) as per the manufacturer's instructions. Then, the blocking of protein membranes performed by incubating it with 3% BSA buffer for 2 hours at RT. After that, blots incubated with primary antibodies at 4 °C. These immunoblots washed and further horse redox peroxidase (HRP) conjugated 2°antibody incubation performed for 2 hours at RT. After washing, Clarity™ Western electrochemiluminescent (ECL) substrate (Bio-Rad, USA) was utilized to develop immunoblots, and imaging carried out by the Gel Doc system (LAS 500, GE Healthcare, USA). Results analyzed with Quantity One software (Bio-Rad, USA).

100-µg protein samples prepared in lysis buffer and incubated for 1 hour at 4°C on the rocker after the addition of 2 µl primary antibody of 1mg/ml solution. After incubation added 20 µl of A/G plus agarose beads and further incubated overnight at 4°C on the rocker. Then, Immunoprecipitates collected by centrifugation at 3000 pm for 6 minutes at 4°C. Pellets washed three times with 1X PBS. Finally, supernatants aspirated and resuspended pellets to 40 µl of 1X SDS gel-loading buffer to perform a western blot. Here, IgG controls for each sample also prepared separately by adding IgG to each sample.

2.6.7. Chromatin Immunoprecipitation (ChIP)- qPCR analysis

ChIP qPCR assay executed on a quant studio 3 qPCR system with three primer sets of EZH2 promoter-specific regions. Here, sample groups of control, rotenone, FCsNPs, and FCsNPs with OKA examined in triplicates. 2µl ChIP DNA per sample was considered as input. Three primer sets for the EZH2 promoter region were (forward:5′GACACGTGCTTAGAACTACGAACAG 3′,

reverse: 5′ AAGCTCGGCCAGCCAAA 3′ for region 1, from −1107 to -1002), (forward: 5′ AGACCAGCCTGACCAAGACC 3′, reverse: 5′ GGACAACCAGAGCGAAACT 3′, for region 2, from −862 to -678) and (forward: 5′ GAACTGGTTCAAACTTGGCTTC 3′, reverse: 5′ ATAAAAGCGATGGCGATTGG 3′, for region 2, from −436 to + 48). Primer sequences obtained by following the published reports (18-20). RT-PCR study conducted and data analyzed by following the percentage input method(21). Percentage input normalized to the input DNA samples (1%) for each region.

2.7. *Ex vivo* PD model (Brain Slice culture)

Brain slice culture executed as per earlier published reports with some modifications (22, 23). Brains from mice bisected to two hemi-brains. Basal ganglia collected by chopping with a McIlwain tissue chopper (Stoelting Europe, Ireland). Washed with saline, 1X PBS, and readily transferred to Millicell culture inserts (Merck Millipore, USA). 1 ml of growth media/insert (50% HiGlutaXL™ DMEM/HEPES, 25% heat-inactivated FBS, 1% antimycotic antibiotic solution having 100 U penicillin, 100 µg streptomycin and 250 ng amphoterin, 25% HBSS with maintained pH 7.2) used. The media replaced after 3 hours and incubated at 37°C in a $CO_2$ incubator. Growth media changed after every 48 hours and cultured for 14 days to be ready for treatment and further experiment.

2.8. Immunohistochemistry-immunofluorescence study

IHC expression study of pSer129 α-Syn, CASPASE3, TH, DRD3, BMI1, and EZH2 for Metformin nanoformulations, pSer129 α-Syn, PP2A, and EzH2 for FTY720 nanoformulations and pSer129 alpha-synuclein, IDH2 for Hytrin nanoformulations performed in cultured brain slices by following published protocol(24) with modification. Rotenone-induced brain slice PD model adopted from an earlier report(25) that used 10 µM rotenone in the induction of PD. 1 µM metformin, equivalent metformin carrying PDANPs, and equivalent PDANPs, 1 µM FTY720, equivalent 1 µM FTY720 carrying FCsNPs and equivalent CsNPs, 25 µM Hytrin, equivalent Hytrin carrying H@PSNPs, and equivalent H@PSNPs employed in the treatment of rotenone-induced brain slice *ex vivo* PD model. In the brief of the IHC procedure, on completion of treatment, slices washed with cold 1X PBS and fixed in cold 4% paraformaldehyde for 45

minutes at RT. Washed thrice with cold 1X PBS and each group of brain slices sectioned (20 µm thickness) with HM525 NX Cryostat (Thermo Fisher Scientific, USA) by following manufacturer instructions. Brain slice sections collected on gelatin plus poly L-lysin coated slides. 1X PBS washed each slice section incubated with 20% methyl alcohol prepared in 1X PBS for initial permeabilization for 5 minutes and again washed with cold 1X PBS. For complete permeabilization, they incubated with a permeabilization solution (0.5% Triton X-100 in PBS) for at least 12 hours at 4°C. After 12 hours, the permeabilization solution replaced with a blocking solution (20% BSA in PBS) and kept overnight at 4°C. Primary antibody solutions of rabbit raised anti-α-Syn (p-ser129) + mouse-raised anti-CASPASE3, rabbit-raised anti-DRD3 + mouse-raised anti-EZH2 and rabbit-raised anti-TH + mouse-raised anti-BMI1 were prepared with 1:1 ratio in 5% BSA/PBS solution for dual staining purpose. Each section incubated with 50 µl of primary antibody overnight at 4°C. Washed them thrice with 5% BSA/PBS solution and incubated with 50µl FITC conjugated anti-rabbit + TRITC conjugated anti-mouse secondary antibodies for 4 hours at RT. 1:500 dilutions of primary antibodies and 1:1000 dilutions of secondary antibodies were used. After incubation, each section washed with 5% BSA/PBS solution followed by 1X PBS. 20µl of 100nM DAPI solution used to stain nuclei. Further, they washed with 1X PBS and mounted with 90% glycerol mounting media. CLSM imaging conducted with a Zeiss confocal microscope (ZEISS 880, Germany) and analyzed by Fiji software. 3D surface plot analysis performed for a better representation of protein expression.

### 2.9. Animals

Experiments involving the animals performed following the standard institutional animal ethical committee. The BALB/c mice (n=3 per group) housed under pathogen-free conditions, cared and used according to laboratory protocols. The animals housed and cared and the biodistribution experiment. All animal work also conducted by following the guidelines of the Committee for Control and Supervision of Experiments on Animals (CPCSEA) and approved by the Institutional Animal Ethical Committee (IAEC). Sprague-Dawley (SD) rats (200-250gm, N=8) have been employed for the animal study for PD model and therapy. All animals utilized for the behavioral study allowed for acclimatizing before experimenting.

2.9.1. *In vivo* and *ex vivo* bio-distribution study of nanoformulations

BALB/c mice used to perform *in vivo* bio-distribution study. Mice anesthetized with isoflurane and ICG-tagged nanoformulation was injected through the intravenous route, intraperitoneal and oral route as per the requirement of the study. ICG-tagged nanoparticles prepared by following the earlier discussed method for the preparation of Rhodamine B-tagged nanoparticles(13). ICG amount analyzed in the sink of the dialysis system with time to ensure the purity of ICG tagged nanoparticles (Fig.5B). Bio-distribution of nanoformulation observed at 0, 1/2, 1, 2, 6, and 24 hours then mice have been sacrificed. *In vivo* and *ex vivo* imaging performed with IVIS® Spectrum *In Vivo* Imaging System (PerkinElmer, USA).

In detail, three groups of mice (n=4) allowed to acclimatize. The animals given intravenous injections of 1 mg/ml ICG as a reference control and 5mg/ml ICG-tagged nanoparticles. PBS injected into the control group. ICG alone considered to analyze tagging effect on bio-distribution. Animals shaved and anesthetized in a vaporizer chamber with the provision of 1.5 % isoflurane and oxygen. Then, animals translocated to the chamber of IVIS Spectrum 200. 1.5% isoflurane also supplied to this chamber. The whole body of the animal imaged at 0, 1/2, 1, 2, 6, and 24 h after I.V. injection. The illumination parameters were auto exposure time, high lamp voltage, f/stop = 2; field of view = B and 800nm emission filter, 745nm excitation filter, and 8 binning. Living Image software v4.0 used to acquire images. Excitation of ICG-tagged nanoparticles was at 750nm and emission was at 830nm. Further, the *ex-vivo* imaging of the organs obtained by imaging the ICG-tagged nanoparticles treated mice tissues (kidney, liver, lung, spleen, and brain) including the same tissues from PBS-injected mice as control.

2.9.2. Experimental design and *In vivo* PD model

The SD rats (250-300 g) randomized to perform grouping. The PD model established by following administration of intraperitoneal injection of rotenone 0.5 mg/kg/day in a divided manner (0.25 mg/kg in morning and 0.25 mg/kg in evening) in the equal ratio of PEG400:PBS for 35 days (n=8).(26)The grouping performed as following: Control (100 ul PBS, i.p.), Rotenone (0.5mg/kg/day, i.p.), Rotenone + Metformin (0.5mg/kg/day, i.p. + 50 mg/kg/day, p.o.), Rotenone + Polydopamine nanoparticles (0.5mg/kg/day, i.p. + 100mg/kg/day, i.p.), Rotenone + Metformin loaded Polydopamine nanoparticles (0.5mg/kg/day, i.p. + 100mg/kg/day, i.p.), Rotenone + FTY720 (0.5 mg/kg/day rotenone, i.p + 1 mg/kg/day FTY720), Rotenone + FCsnps

(0.5 mg/kg/day rotenone, i.p. + 5.7 mg/kg/day FCsnps), Rotenone + Csnps (0.5 mg/kg/day rotenone, i.p. + 5.7 mg/kg/day Csnps), Rotenone + Hytrin (0.5 mg/kg/day, + 10 μg/kg/day), Rotenone + HPSnps (0.5 mg/kg/day, i.p. + 5.7 mg/kg/day equivalent hytrin by considering 15% drug loading of nanoparticle from our previous study(27), and Rotenone + PSnps (0.5 mg/kg/day, i.p. + 5.7 mg/kg/day equivalent dose to HPSnps). The behavioral study performed after 28 days and the necropsy conducted for 35 days. Five brain samples from each group fixed with 4% formaldehyde and processed for immunohistochemistry. The rest of the brain samples stored at -80°C and processed for immunoblot study. Herein, the metformin-loaded polydopamine nanoformulation (MPdanps) and polydopamine nanoparticles (Pdanps) adopted from the previous study and are well-characterized nanoformulation (4). The 1 mg/kg/day dose of FTY720 has been selected by following the previous study for the neuroprotective dose of FTY720. (28) The dose of FCsnps (5.7mg) has been considered by equalized loaded drug concentration of FTY720 (1mg) according to the reported loading percentage (17.52%) of our previous study for FTY720 loaded chitosan nanoparticles. (29) The 10 μg/kg/day dose of Hytrin has been considered by following the reported neurotherapeutic dose of Hytrin. (30)

2.9.3. Behavioural studies

Rotarod test for the evaluation of locomotory activity

All animals have been acclimatized before the experiment. Rotarod study performed by using apparatus having a 3 cm radius and rough surface. The rod height was 25 cm from the base and 5 disks used to divide them into the four chambers. Each animal trained at 15 rotations per minute (rpm) for 60 sec for constitutive three days before final testing. In the final trial, the fall latency measured as a function of time, rotational speed and distance traveled after exposure of animals to a ramp of 4 rpm to 40 rpm for 300 seconds. The distance traveled, and fall latency analyzed to analyze the impairment of locomotor activity. (31)

Open field test for locomotor activity assessment

An open-field test performed to analyze gross locomotor activity and anxiety. All animals acclimatized before the start of the experiment with assuring light conditions. The camera and apparatus setup performed to track the movement of the animals with the help of ANY-maze

software. The peripheral zone and central zone assigned by following software instructions. Animals allowed to move in the apparatus freely after keeping them in the central zone at the start of the experiment. The apparatus cleaned with 70% ethanol after the completion of the testing of each animal. Herein, more time spent or movement in the central zone defines anxiety-free behavior. (32)

Y-maze test – spontaneous alternation for observation of cognitive impairment

In the behavioral study, the Y-maze alternative spontaneous alteration test conducted to analyze cognitive and motor neuron impairment. In that, a Y-shaped apparatus having three arms at a 120-degree angle to each other utilized by marking the zone, central zone, A-zone, B-zone, and C-zone. All animals allowed to move freely in the apparatus for 5 minutes after completion of the experimental set-up. The apparatus was continuously wiped with 70% ethanol after every test. The percentage of spontaneous alteration calculated with the following reported formula (33)

(no. of alterations)/ (total no. of arm entries – 2)*100

Passive avoidance task for evaluation of memory function

The two compartments instruments containing a dark and light-emitting chamber with a guillotine door and grid floor utilized to deliver foot shock to the animal. Three trials performed; habituation, acquisition, and retention. In the habituation trial, animals kept in a light-emitting chamber. The animals allowed to go into the dark chamber after 15 sec while opening the door and it closed after the entry of the animals into the dark chamber. The acquisition trial performed after 1 hour of habituation task. In that, the animal kept in the illuminated chamber and allowed to go into the dark chamber, where 0.6 mA current foot shock given to them. Finally, the retention trial performed 24 hours after the acquisition trial to measure the transfer latency from the illuminated to the dark chamber by following the existing report (33).

Catalepsy

The grid and bar tests carried out to examine the neuromuscular and motor dysfunction. To observe the grip strength, each animal hung in the middle of the vertical grid. The score provided by examining the listed parameters: 0 – fall; 1- hangs by two forepaws; 2 - climb attempt by two

forepaws; 3- hangs by two forepaws and one of the hind paws; 4- hangs by two forepaws, two hind paws and warped tail and 5 – escape from the apparatus. The stopwatch utilized to note descent latency. Similarly, a bar test also performed and the animal's forepaws have been fixed on the bar by keeping the half-rearing posture. The decent latency examined by observing the removal of one forepaw on the bar with time. The three trials performed for a 180-sec cut-off time and both experiments conducted by following the reported procedure of behavior assay. (34, 35)

2.9.4. Protein expression analysis

The frozen substantia nigra (50 mg) homogenized in the 1 ml radioimmunoprecipitation assay (RIPA) lysis buffer at 4°C. The solution probe sonicated for 1 minute at 10 Hz amplitude before centrifuging at 13600 rcf for 25 minutes at 4°C. The protein sample estimated and normalized by the Bradford protein estimation method. SDS-PAGE performed and transferred the protein to the Immuno-Blot® PVDF membrane by following the instruction of the manufacturer using the Trans-Blot® Turbo™ transfer system (Bio-Rad, USA). Immunoblot blocked for 1 hour incubating in 5% BSA solution. The immunoblot incubated with the primary antibody overnight at 4°C and washed with TBST three times before incubating with the secondary antibody at RT for 1 and half hours. The blot developed with ECL chemiluminescence substrate and imaged under the Gel Doc system (LAS 500, GE Healthcare, USA). The quantification performed by Image J software.

100ug protein has been collected for all samples and the protein samples incubated with IgG antibody for 1 hour at 4°C. Then, the samples allowed to interact with A/G beads (SCBT, USA) which leads to the end with IgG clear protein samples (pre-clear samples). The pre-clear protein samples allowed interaction with 2 ul primary antibody at 4°C for 1 hour and then 20 ul A/G beads added to the immunocomplex to incubate them overnight at 4°C. Immunoprecipitate collected after centrifuge samples at 2500 rpm for 5 minutes at 4°C. The immunoprecipitate resuspended in 2X sample loading buffer and run the SDS-PAGE to perform western blot study obtained after centrifuging at 2500 rpm for 5 minutes and run the SDS PAGE to perform a western blot study for the desired protein marker. IgG controls for each sample also considered during the study.

2.9.5. Chromatin Immunoprecipitation (ChIP)- qPCR analysis

The ChIP assay performed by following the reported protocols of the DNA-protein binding study. (36)The protein lysate processed with a probe sonicator by applying 15 pulsed of 20 amplitude power for 30 seconds. 40 ul A/G beads incubated with samples to clear the chromatin. Then, the chromatin samples incubated with primary antibody at 4°C for 1 hour and immunocomplex further incubated with 40ul A/G beads overnight at 4°C. Antibody-negative control (without antibody) and anti-mouse IgG control were also considered. On the next day, the immunocomplex has been thoroughly washed with low salt, high salt, and $LiCl_2$ buffer by following our previous report. (37) Then, the sample has been eluted and DNA was isolated by using the phenol: chloroform extraction method and stored at -80°C.

the qPCR study performed with isolated ChIP samples using quant studio 3 (Applied biosystem, Thermo). The two different primer sets utilized for the synuclein promoter-specific region. Herein, samples of control, rotenone, and MPdanps were investigated. Control input for each sample also considered during the experiment. The synuclein promoter primer set is as follows:

primer set-1 (forward: 5′TCCCCGGGAAACGCGAGGAT3′,

reverse: 5′CCCCGCGCCAGCACTTGTTA3′ for region 1, from +668 to +846).

Primer set-2 (forward: 5′ TGCCTTTGCATCAGATAATGGC3′,

reverse: 5′ ATGATGAGCAGGCAGTCCG3′, for region 2, from +79746 to +79860).

Three different primer sets of the LAMP2a promoter utilized to evaluate the hsc70 binding to LAMP2a. Input and treated samples for control, rotenone, and HPSnps employed in the study. Quantstudio3 system (Applied biosystem, Thermo) utilized for the analysis and performance of the qPCR study. The % input method followed to analyze the expression.(21, 29, 37)

2.9.6. Immunofluorescence study

The fixed brain utilized for coronal sectioning using the cryostat (HM525, Thermo). In that, the tissue incubated in a gradient sucrose solution until it sinks. Then, an optimal cutting temperature (OCT) solution applied to freeze the tissue. The cryostat set to -30 degree temperature and the soft tissue cutter blade adjusted. The 30-micron sections have been obtained and kept in TBST solution by following the tissue processing. (38)

The immunofluorescence study performed by following the existing reported method with slight modifications. (39) In that, Heat-induced antigen retrieval performed by incubating sections in the antigen retrieval solution (citric acid, pH 6 in TBST) for 30 minutes at 95°C in water bath steam. After that, the solution kept at room temperature (RT) for 30 minutes and processed for the blocking with 2.5 % horse serum albumin for 2 hours at RT. The sections washed with TBST for 10 minutes and incubated with primary antibody solution prepared in TBST overnight at 4°C. Washing with TBST performed thrice for 10 minutes before incubating with fluorescence-conjugated secondary antibody at RT for 2 hours. Again, sections washed thrice with TBST and mounted on the slide. The mounted sections processed for permanent slide preparation with an anti-fed solution and air sealed. The sections tile imaged to confirm the *in vivo* PD model by observing Tyrosine Hydroxylase expression at 10X resolution (Fig.2.2). After that, the degenerating region of Substantial Nigra imaged with the fluorescence microscope at 20X resolution.

### 2.9.7. Histopathology study

Haematoxylin and Eosin (H&E) staining utilized to observe the morphological changes. The brain sectioned utilizing a microtome (RM2235, Leica) and obtained tissue sections of thickness 10μm. Poly-l-lysine coated slides used to mount sections on the slide and stained using a standard protocol of Haematoxylin and Eosin (H&E). Sections were stained with Haematoxylin solution for 10 minutes after washing with distilled water. Then, the sections stained with Eosin solution for 30 seconds. The sections were dehydrated using gradient alcohol and xylene. The slides mounted with DPX mounting media, air-dried, and observed under a microscope for any pathological demarcation.

## 2.10. Statistical analysis

Statistical analysis performed by using OriginLab software (Washington, MA, USA). One-way and two-way variance analysis (ANOVA) was calculated following the Bonferroni and Tukey comparison test. A p-Values $\leq 0.05$ has been considered statistically significant.

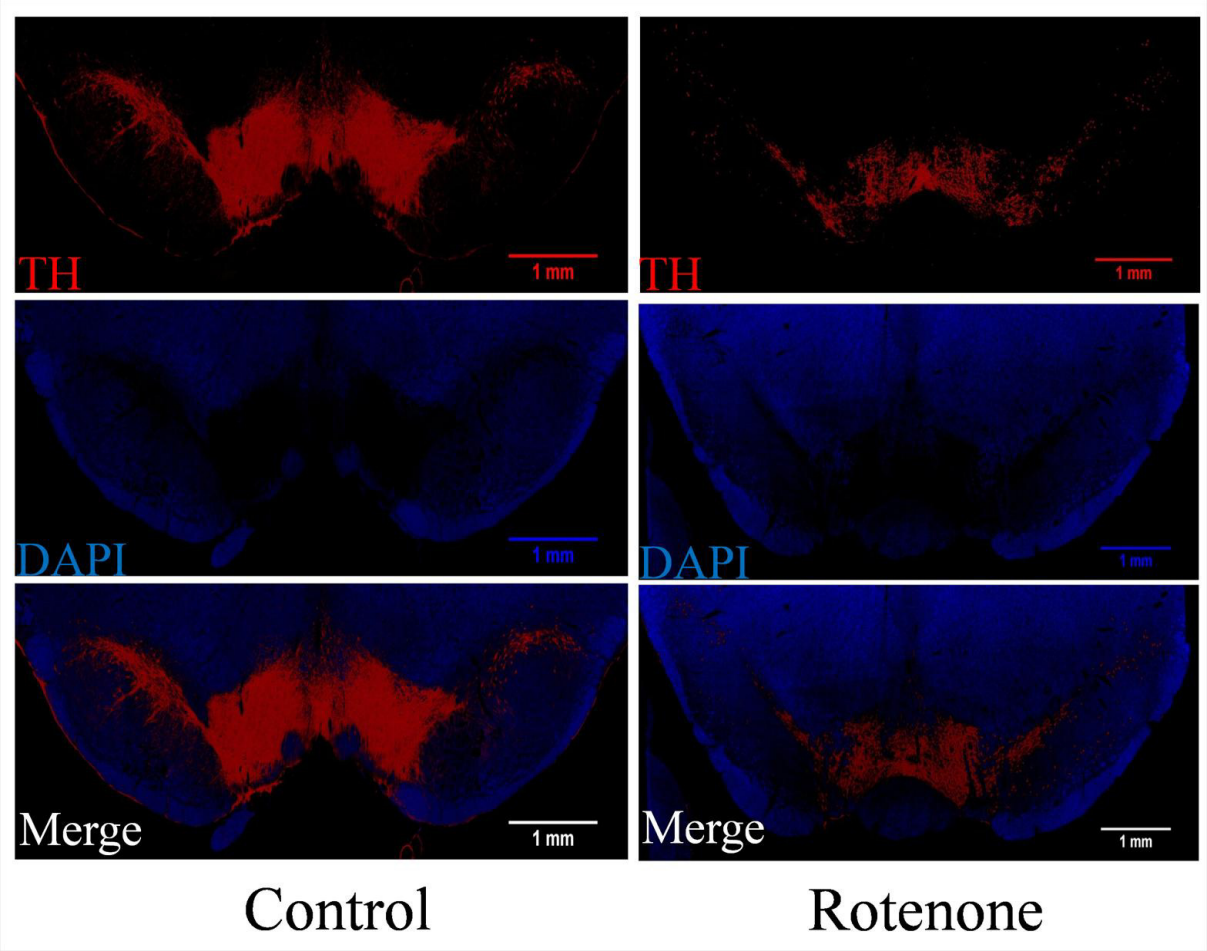


Fig.2.2. The in vivo PD model was confirmed by evaluating TH expression analysis in SNpc and VTA area.

## 2.11. References

1. K. Y. Ju, Y. Lee, S. Lee, S. B. Park, J. K. Lee, Bioinspired polymerization of dopamine to generate melanin-like nanoparticles having an excellent free-radical-scavenging property. *Biomacromolecules* **12**, 625-632 (2011).
2. Y. Liu, K. Ai, L. Lu, Polydopamine and its derivative materials: synthesis and promising applications in energy, environmental, and biomedical fields. *Chemical reviews* **114**, 5057-5115 (2014).
3. S. H. Hussein-Al-Ali, A. Kura, M. Z. Hussein, S. Fakurazi, Preparation of chitosan nanoparticles as a drug delivery system for perindopril erbumine. **39**, 544-552 (2018).

4. M. N. Sardoiwala, A. K. Srivastava, B. Kaundal, S. Karmakar, S. R. Choudhury, Recuperative effect of metformin loaded polydopamine nanoformulation promoting EZH2 mediated proteasomal degradation of phospho-α-synuclein in Parkinson's disease model. *Nanomedicine: Nanotechnology, Biology and Medicine* **24**, 102088 (2020).
5. J.-Y. Wu *et al.*, Targeted co-delivery of Beclin 1 siRNA and FTY720 to hepatocellular carcinoma by calcium phosphate nanoparticles for enhanced anticancer efficacy. *International journal of nanomedicine* **13**, 1265-1280 (2018).
6. M. Zeeb, M. Sadeghi, Sensitive determination of terazosin in pharmaceutical formulations and biological samples by ionic-liquid microextraction prior to spectrofluorimetry. *Int J Anal Chem* **2012**, 546282-546282 (2012).
7. J. Q. Hudson, T. J. Comstock, G. M. Feldman, Evaluation of an in vitro dialysis system to predict drug removal. *Nephrol Dial Transplant* **19**, 400-405 (2004).
8. F. Wang, R. Franco, M. Skotak, G. Hu, N. Chandra, Mechanical stretch exacerbates the cell death in SH-SY5Y cells exposed to paraquat: mitochondrial dysfunction and oxidative stress. *Neurotoxicology* **41**, 54-63 (2014).
9. H. Xicoy, B. Wieringa, G. J. M. Martens, The SH-SY5Y cell line in Parkinson's disease research: a systematic review. *Molecular Neurodegeneration* **12**, 10 (2017).
10. M. Innala *et al.*, 3D culturing and differentiation of SH-SY5Y neuroblastoma cells on bacterial nanocellulose scaffolds. *Artificial cells, nanomedicine, and biotechnology* **42**, 302-308 (2014).
11. H. Ammer, R. Schulz, Retinoic acid-induced differentiation of human neuroblastoma SH-SY5Y cells is associated with changes in the abundance of G proteins. *Journal of neurochemistry* **62**, 1310-1318 (1994).
12. G. Lopez-Carballo, L. Moreno, S. Masia, P. Perez, D. Barettino, Activation of the phosphatidylinositol 3-kinase/Akt signaling pathway by retinoic acid is required for neural differentiation of SH-SY5Y human neuroblastoma cells. *The Journal of biological chemistry* **277**, 25297-25304 (2002).
13. D. R. Amin, C. Sugnaux, K. H. A. Lau, P. B. Messersmith, Size Control and Fluorescence Labeling of Polydopamine Melanin-Mimetic Nanoparticles for Intracellular Imaging. *Biomimetics* **2** (2017).

14. T. Mosmann, Rapid colorimetric assay for cellular growth and survival: application to proliferation and cytotoxicity assays. *Journal of immunological methods* **65**, 55-63 (1983).
15. B. Kaundal *et al.*, Nanoformulation of EPZ011989 Attenuates EZH2–c-Myb Epigenetic Interaction by Proteasomal Degradation in Acute Myeloid Leukemia. *Molecular Pharmaceutics* **17**, 604-621 (2020).
16. A. C. Kushwaha *et al.*, PRT4165 nanocomposite promoting epigenetic retardation through proteasomal depletion of polycomb in acute myeloid leukemia. *Applied Materials Today* **21**, 100847 (2020).
17. A. Aranda *et al.*, Dichloro-dihydro-fluorescein diacetate (DCFH-DA) assay: a quantitative method for oxidative stress assessment of nanoparticle-treated cells. *Toxicology in vitro: an international journal published in association with BIBRA* **27**, 954-963 (2013).
18. Y.-M. Pan *et al.*, STAT3 signaling drives EZH2 transcriptional activation and mediates poor prognosis in gastric cancer. *Molecular Cancer* **15**, 79 (2016).
19. P. Kunderfranco *et al.*, ETS transcription factors control transcription of EZH2 and epigenetic silencing of the tumor suppressor gene Nkx3.1 in prostate cancer. *PLoS One* **5**, e10547 (2010).
20. X. Wu *et al.*, BRD4 Regulates EZH2 Transcription through Upregulation of C-MYC and Represents a Novel Therapeutic Target in Bladder Cancer. *Mol Cancer Ther* **15**, 1029-1042 (2016).
21. E. Lacazette, A laboratory practical illustrating the use of the ChIP-qPCR method in a robust model: Estrogen receptor alpha immunoprecipitation using Mcf-7 culture cells. *Biochemistry and Molecular Biology Education* **45**, 152-160 (2017).
22. B. Hutter-Schmid, K. M. Kniewallner, C. Humpel, Organotypic brain slice cultures as a model to study angiogenesis of brain vessels. *Frontiers in cell and developmental biology* **3**, 52 (2015).
23. L. Stoppini, P. A. Buchs, D. Muller, A simple method for organotypic cultures of nervous tissue. *Journal of neuroscience methods* **37**, 173-182 (1991).
24. N. Gogolla, I. Galimberti, V. DePaola, P. Caroni, Staining protocol for organotypic hippocampal slice cultures. *Nature protocols* **1**, 2452-2456 (2006).

25. C. Ullrich, C. Humpel, Rotenone induces cell death of cholinergic neurons in an organotypic co-culture brain slice model. *Neurochemical research* **34**, 2147-2153 (2009).
26. L. Yu *et al.*, Neurochemical and Behavior Deficits in Rats with Iron and Rotenone Co-treatment: Role of Redox Imbalance and Neuroprotection by Biochanin A. *Front Neurosci* **11**, 657-657 (2017).
27. M. N. Sardoiwala, S. J. Mohanbhai, S. Karmakar, S. R. Choudhury, Hytrin loaded polydopamine-serotonin nanohybrid induces IDH2 mediated neuroprotective effect to alleviate Parkinson's disease. *Materials Science and Engineering: C* https://doi.org/10.1016/j.msec.2021.112602, 112602 (2021).
28. P. Zhao *et al.*, Neuroprotective effects of fingolimod in mouse models of Parkinson's disease. **31**, 172-179 (2017).
29. M. N. Sardoiwala, S. Karmakar, S. R. Choudhury, Chitosan nanocarrier for FTY720 enhanced delivery retards Parkinson's disease via PP2A-EzH2 signaling in vitro and ex vivo. *Carbohydrate Polymers* **254**, 117435 (2021).
30. H. Chaytow *et al.*, Targeting phosphoglycerate kinase 1 with terazosin improves motor neuron phenotypes in multiple models of amyotrophic lateral sclerosis. *eBioMedicine* **83** (2022).
31. A. Jangra, A. K. Datusalia, S. Khandwe, S. S. Sharma, Amelioration of diabetes-induced neurobehavioral and neurochemical changes by melatonin and nicotinamide: Implication of oxidative stress–PARP pathway. *Pharmacology Biochemistry and Behavior* **114-115**, 43-51 (2013).
32. M. L. Seibenhener, M. C. Wooten, Use of the Open Field Maze to measure locomotor and anxiety-like behavior in mice. *J Vis Exp* 10.3791/52434, e52434-e52434 (2015).
33. P. Thapak, M. Bishnoi, S. Sharma, Tranilast, a Transient Receptor Potential Vanilloid 2 Channel (TRPV2) Inhibitor Attenuates Amyloid β-Induced Cognitive Impairment: Possible Mechanisms. *NeuroMolecular Medicine* **24**, 1-12 (2022).
34. V. Bashkatova, M. Alam, A. Vanin, W. J. Schmidt, Chronic administration of rotenone increases levels of nitric oxide and lipid peroxidation products in rat brain. *Experimental neurology* **186**, 235-241 (2004).
35. M. Alam, W. J. Schmidt, Rotenone destroys dopaminergic neurons and induces parkinsonian symptoms in rats. *Behavioural brain research* **136**, 317-324 (2002).

36. T. Waldron *et al.*, c-Myb and its target Bmi1 are required for p190BCR/ABL leukemogenesis in mouse and human cells. *Leukemia* **26**, 644-653 (2012).
37. M. N. Sardoiwala *et al.*, Hypericin-Loaded Transferrin Nanoparticles Induce PP2A-Regulated BMI1 Degradation in Colorectal Cancer-Specific Chemo-Photodynamic Therapy. *ACS Biomaterials Science & Engineering* **6**, 3139-3153 (2020).
38. A. H. Fischer, K. A. Jacobson, J. Rose, R. Zeller, Cryosectioning tissues. *CSH protocols* **2008**, pdb.prot4991 (2008).
39. M. A. Alshammari, T. K. Alshammari, F. Laezza, Improved Methods for Fluorescence Microscopy Detection of Macromolecules at the Axon Initial Segment. *Frontiers in cellular neuroscience* **10**, 5 (2016).

# Chapter 3a

---

# Recuperative effect of metformin-loaded polydopamine nanoparticles in PD retardation

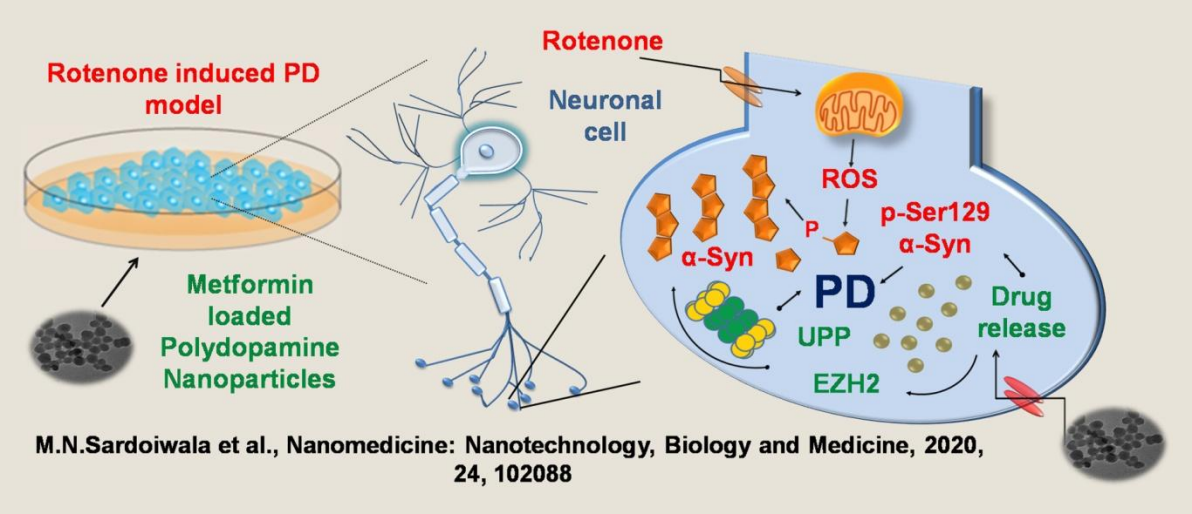

3a.1. Introduction

Parkinson's disease (PD) is a progressive neurodegenerative disorder, affecting developing countries including India(1). It develops by degeneration of dopaminergic neurons with depletion of dopamine levels in the substantia nigra, a midbrain region that controls body movement(2). The major causative factors behind the loss of dopaminergic neurons are still unexplored. Formation of Lewy bodies in the substantial innominate by the aggregation of phosphorylated (ser 129) α-Syn results in synucleinopathy and pathogenesis of PD(3). Mitochondrial oxidative stress augments synuclein aggregation resulting in aggressive PD phenotype rendering phosphorylated α-Syn as a major therapeutic target (4). Epigenetic modulation is an emerging mechanism affecting PD onset and progression. Epigenetic regulation with lower DNA methylation leads to aggregation of α-Syn in PD progression is widely studied(5). Indeed, the involvement of polycomb groups of proteins, including polycomb repressor complexes 1 and 2 (PRC1/2) is under investigation for implications in PD. PRC2 member, Enhancer of zeste homolog 2 (EZH2) trimethylates H3K27 for maintenance of neuronal function was reported(6). They have also demonstrated that transcriptional dysregulation in PRC2-deficient mice leads to a progression of neurogenerative diseases. Alterations in EZH2 and H3K27 levels have been implicated with Parkinsonism (7). Similarly, downregulation of B cell-specific Moloney murine leukemia virus integration site 1 (BMI1), a PRC1 member is associated with apoptosis of neurons, and its overexpression has immense potential for the treatment of neurodegenerative diseases (8). Although, the underlying mechanism of PRC 1/2 mediated prevention of Parkinson’s disease is not well understood. However, a recent report has shown that human polycomb protein 2, a PRC1 member-induced SUMOylation of α-Syn promotes aggregation of α-Syn(9). A recent report also shows SUMOylation and ubiquitination in the regulation of α-Syn are reciprocal events (10). But, there is no current knowledge about the role of EZH2, a PRC2 member in the regulation of α-synucleinopathy.

In the last decades, the progression of medical pharmacologic therapies and innovative surgical approaches like deep brain stimulation (DBS) seems to be effective against PD(11). However, definitive disease-controlling therapy is still lacking due to the multiple side effects of therapeutic agents (12). Recently, metformin emerges as a potential therapeutic agent in various

diseases like aging disorders, periodontitis, and tuberculosis including Central Nervous System (CNS)disorders (13-17). Metformin reduces the risk of PD in diabetes patients is supported by a clinical trial study in the diabetes mellitus population of Taiwan (18). Labuzek et al. (2010) studied oral administration of metformin readily passes the Blood Brain Barrier (BBB) in the rat (19). The neuroprotective response of metformin is mediated by anti-inflammatory action (20), induction of autophagy (21), and reduction of phosphorylated proteins involved in Lewy body formation (22). However, the detailed mechanism of metformin-based neuroprotection is still not well understood. Despite having prodigious therapeutic potential, metformin, possess absorption limited kinetics with less bioavailability and a risk of lactic acidosis (23). An emerging application of nanocarriers as a better drug delivery system is taken into account to overcome metformin limitations(24). For the present study, polydopamine nanoparticle (PDANP) was considered as a metformin-delivering system to replenish dopamine loss which is associated with PD pathology. Few reports have shown polydopamine as a free radical scavenger and its coating for mitigating the cytotoxicity of various nanomaterials(25, 26).

In the present study, a potent nanoformulation of Met-loaded PDANPs was assessed for its novel therapeutic application against PD. The crucial preliminary examinations of enhanced drug loading and a controlled release give superior anti-oxidant and neuroprotective efficacy. The effective encapsulation of metformin in biocompatible polydopamine enhances the availability of the drug at the site of action. The neuroprotection mechanism induced by nanoformulation attributes to upregulated epigenetic marker EZH2 expression. For the first time, the link between the role of EZH2 in the regulation of α-Syn degradation and PD pathogenesis was investigated which could be a regulatory target for the therapeutic intervention of PD. We demonstrated that our nanoformulation regulates α-Syn degradation by the ubiquitin/proteasome pathway, which is crucial for neuronal survival. The project design of the chapter 3a represented hypothesis and rationale of chapter to understand the potential significance of the presented study. The justification of the selected compound and aligned expected outcomes of the aims are also as described in project design below.

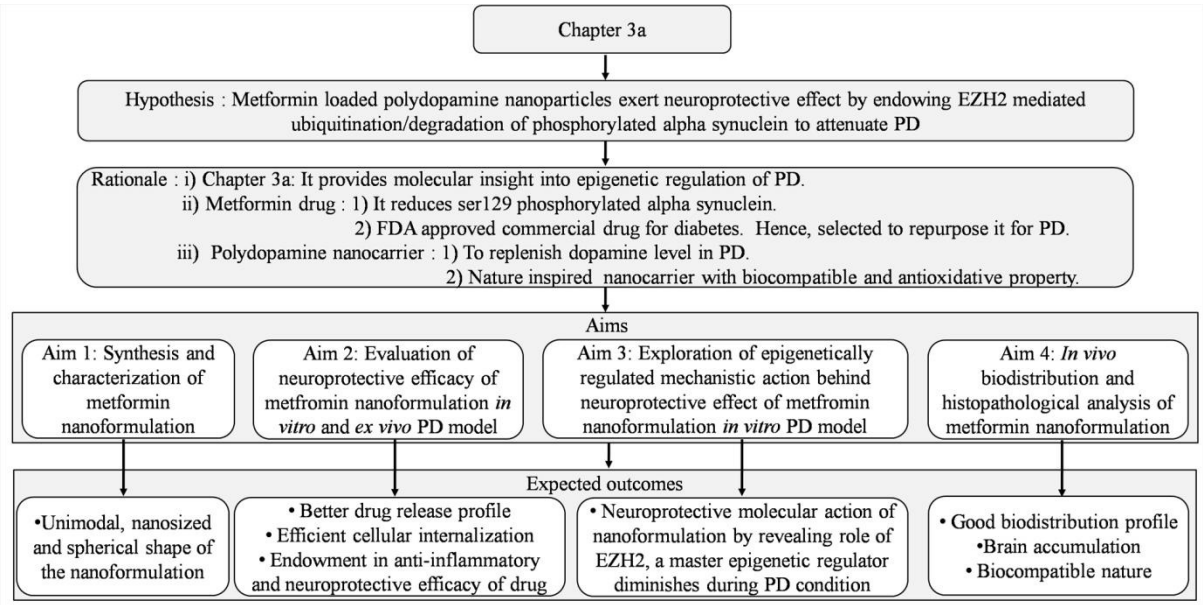


Scheme 3: The project design represents hypothesis, rationale, aims and it's aligned expected outcomes.

3a.2. Results and discussion

New neuroprotective drugs are urgently warranted to prevent and overcome the limitation of present therapy for Parkinsonism. Beyond canonical function, metformin is emerging as a potent neuroprotective agent in PD treatment (22). Rather, metformin possesses crucial limitations of low bio-availability at the disease site and elevates the risk of lactic acidosis (23). Therefore, we prepared Met-loaded PDANPs to enhance bioavailability along with a controlled drug release profile. Earlier, Polydopamine coated nanoparticle systems were also reported for targeting brain glioma in rats (27). Recently, PDANPs was revealed as a potent therapeutic agent for inflammation-induced injuries(28). In our approach, Polydopamine as a nanocarrier was selected to enhance metformin bio-availability, and replenish depleted dopamine levels with enhanced neuroprotective efficiency of both drugs in a single platform. Met-loaded PDANPs exhibited excellent neuroprotection against rotenone-induced oxidative stress, neurotoxicity, and cellular damage in SH-SY5Y monolayer; 3D culture and a mouse brain slice of experimental PD models by effectively crossing the blood-brain barrier (BBB).

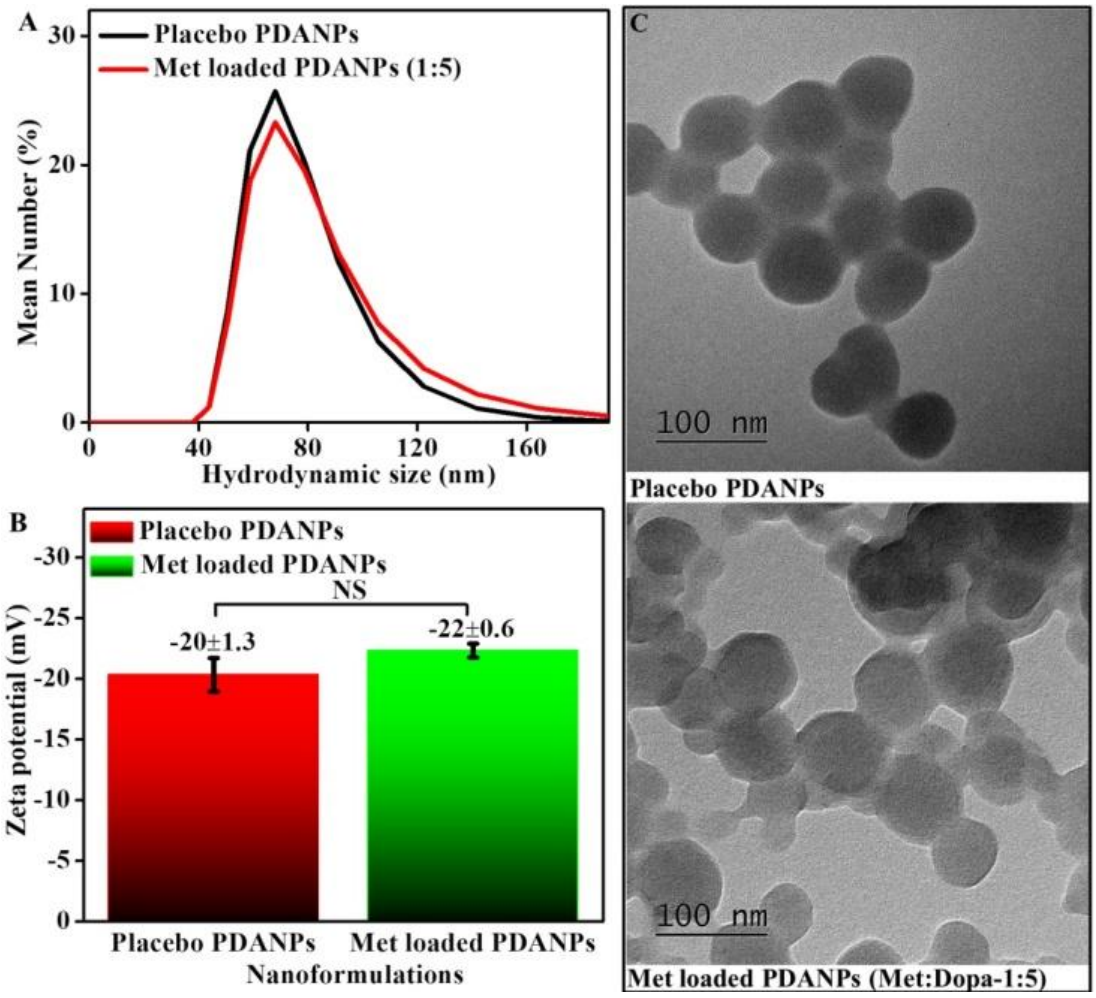


Figure 3.1.Morphological characterization of PDA nanoparticles. The DLS measurement of Placebo and Metformin (Met) loaded PDANPs showing the mean hydrodynamic size (A); and surface zeta potential (B); the transmission electron micrograph (C) showing spherical morphology of placebo PDA nanoformulations and Metformin loaded PDANPs with a ratio of Met: Dopa-1:5.

3a.2.1. Morphological analysis of nanoformulations

PDANPs and Met-loaded PDANPs were synthesized by using the solution oxidation method. (26, 29)Desirably, water-soluble nanoformulations with a ratio of metformin to dopamine 1:5, 1:10, and 1:20 were formed. Morphological and functional characterization of particle size, zeta potential, and shape was determined to validate synthesized Met-loaded PDANPs. The Mean hydrodynamic particle size by Dynamic Light Scattering (DLS) was 73±4 nm for placebo

PDANPs with a polydispersity index (PDI) of 0.079±0.002 and 80±5 nm for Met loaded PDANPs (Met: Dopa-1:5) with PDI 0.205±0.03, respectively (Fig.3.1A). These monodisperse nanoformulation have shown considerable surface zeta potential of -20 mV±1.3 and -22 mV±0.6 for placebo and Met loaded PDANPs, respectively (Fig.3.1B). TEM micrographs of placebo and Met loaded PDANPs (Met: Dopa-1:5) were represented in Fig.1C. TEM imaging represented a particle size range of 65±6 nm for placebo PDANPs and 70±10 nm of Met loaded PDANPs (Met: Dopa-1:5). Results of morphological characterizations for Met loaded PDANPs with a ratio of metformin to dopamine (Met: Dopa) (1:10) and (1:20) have shown in Fig.3.2. In the morphological evaluation, the particle size analysis by DLS and TEM were comparable and confirmed nano range size, uniformity, and spherical shape of our nanoformulations with moderate colloidal stability.

From these, Met-loaded PDANPs (Met: Dopa-1:5) have been considered throughout the study due to the smallest size and the possibility of crossing the BBB efficiently. Drug-nanocarrier compatibility analysis has confirmed the amorphous nature of nanoparticles and the major involvement of the N-H and O-H functional groups in the interaction of dopamine and metformin.

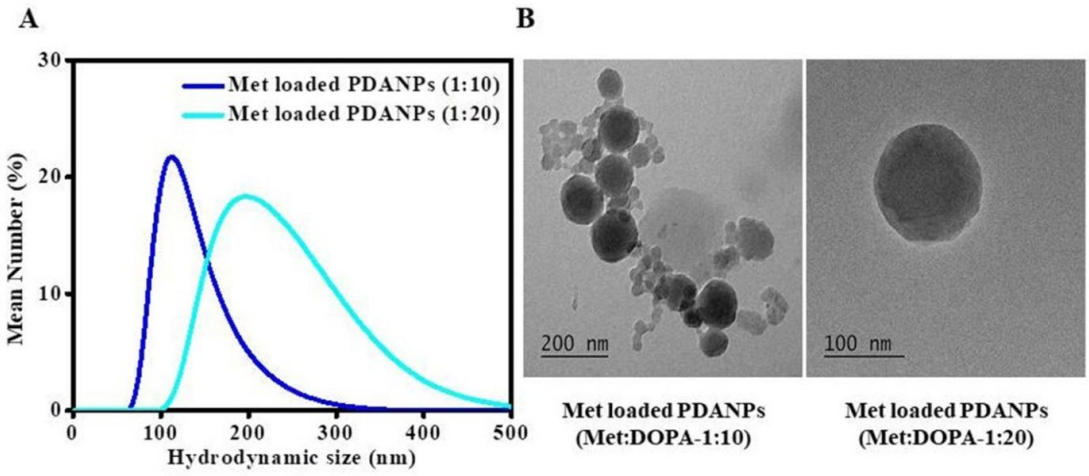


Figure 3.2. (A) The mean hydrodynamic diameter of Metformin-loaded PDANPs showed the size of 123nm (Met: Dopa-1:10) and 210nm (Met: Dopa-1:20), respectively. (B) TEM analysis showing spherical morphology of metformin-loaded PDA nanoformulations.

3a.2.2. Physicochemical analysis of nanoformulations

Drug and nanocarrier compatibility were accessed by the functional characterizations (XRD, FTIR, and RAMAN spectroscopy) of nanoformulation that has been described in Fig.3.3. In a further study, drug loading and encapsulation efficiency of nanoformulation were estimated. Metformin and dopamine both precursors are water soluble and as the outcome of non-covalent polymerization, Met loaded PDANPs are also water-soluble. These conditions indicate higher drug loading and encapsulation capacity of PDANPs. In agreement with the report that PDA serves as a multivalent matrix for higher drug loading(30), we achieved higher drug loading and encapsulation efficiency were 45.2 ± 5% and 90 ± 3%. Placebo PDANPs and Met loaded PDANPs nanoformulation showed a broad XRD (X-Ray Diffraction) peak at 23.3°. Here, the disappearance of pristine metformin XRD diffraction peaks could be due to drug solvation to the amorphous carrier or overlapped of amorphous carrier XRD peaks with the limited crystalline size of the drug. Hence, XRD results show the dispersal of metformin into the PDANPs matrix. PDANPs synthesized after oxidation and self-polymerization of dopamine molecules may be attributed due to the formation of hydrogen bonding. FTIR spectrum of metformin and the PDANPs physical mixture obtained more or less similar to metformin due to the presence of free metformin molecules in the mixture. These reveal the interaction of the drug and nanocarrier.

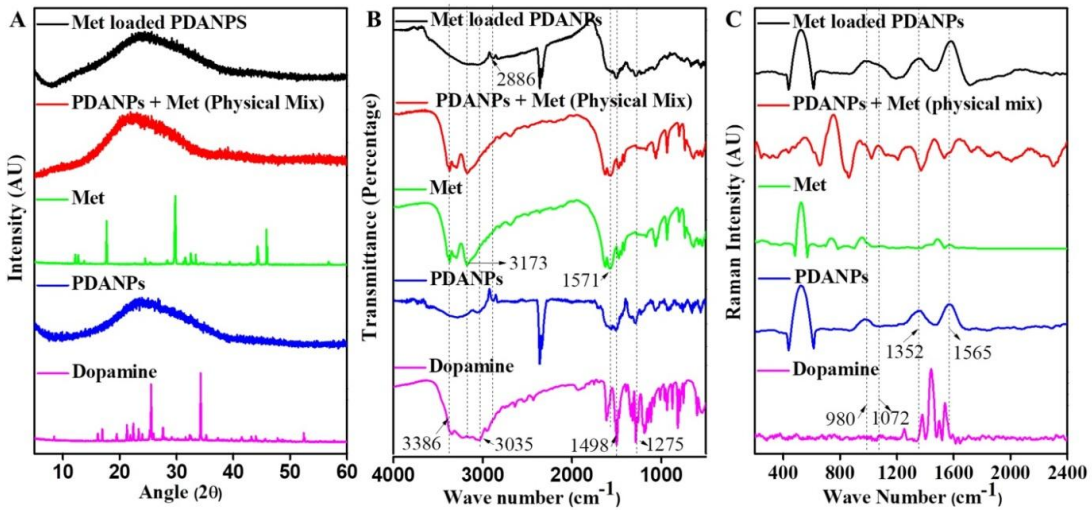


Figure 3.3. Physiochemical characterizations of nanoparticles. The X-Ray Diffraction pattern shows the amorphous nature of nanoparticles (A); the Fourier Transformed Infra-Red

spectroscopy analysis (B); and Raman spectral analysis (C) reveals the interaction of metformin and dopamine to form metformin-loaded PDANPs.

### 3a.2.3. *In vitro* drug release analysis

*In vitro* drug release study was carried out to determine the stability of the drug and its release by mimicking *in-vivo* conditions. *In vitro* drug release profile was acquired for a triplicate of samples by the equilibrium dialysis membrane technique at physiological conditions (Fig.3.4A). The release kinetics of metformin from suspension solution and Met loaded PDANPs were analyzed throughout 96 hours. From the cumulative drug release graph, a burst release of metformin was observed during the initial hours. Metformin suspension has shown consistent burst release after the initial hours and it has achieved saturation after 6 hours. In contrast, the controlled metformin release kinetics of our Met loaded nanoformulation was observed with 70 ± 2% drug release till 96 hours. Further, a significant advantage provided by Met-loaded PDANPs is an enhanced and controlled drug release profile. It is biphasic, initial burst release due to dissolution and diffusion of surface deposited molecules and then controlled drug release with time-dependent degradation of nanocarriers. This release kinetic pattern fulfills our requirement as an initial release for enhanced drug availability at the disease site and later controlled release with time for exhibiting therapeutic efficiency. The biphasic release pattern of drug-encapsulated nanoparticles is reported as beneficiary(31) and a recent study regarding the potential of PDANPs in the enhancement of bio-availability of the drug is also supportive(32). It is believed that the controlled release of any drug might decrease cytotoxicity by controlling premature drug release and eventually ameliorating the drug release profile(33).

### 3a.2.4. *In vitro* therapeutic efficiency evaluation of nanoformulation

To evaluate *in vitro* therapeutic efficiency, cell viability assays were performed. We have processed MTT [3-(4, 5-dimethylthiazol-2-yl)-2, 5-diphenyltetrazolium bromide] assay to verify the effect of our nanomaterials on SH-SY5Y cells. It has shown negligible cytotoxicity of metformin, PDANPs, Met loaded PDANPs, and dopamine with a lower dose (0.01 to 10 μM) than described in Fig.3.5. Significant toxicity has been observed with high doses of dopamine (100 μM and 1000 μM). In contrast, 100 μM dose of PDANPs were founded nontoxic and bio-

compatible. Based on these results the neuroprotective efficiency was evaluated against rotenone-induced neurotoxicity in SH-SY5Y cells. The 2 µM dose of rotenone was significantly determined as IC50 dose (Fig.3.4B). Here, a 500 nM acute dose of rotenone was selected to induce a PD effect at the cellular level by following the previous report (34). The acute exposure of 500 nM rotenone-induced aggregation of α-Syn which is a hallmark of PD pathogenesis. In the evaluation of neuroprotective efficiency, Met loaded PDANPs and metformin with a dose range (25 to 250 nM) against 500 nM rotenone were exposed to SH-SY5Y for 48 hours. In the results, a 100 nM dose of Met-loaded PDANPs has shown a significantly higher recuperative effect than bare equivalent metformin (Fig.3.4C). Interesting dose-independent response phenomena of metformin effects were also observed in agreement with the previous report (22). Extracellular dopamine was reported cytotoxic due to oxidization and ROS generation (35) and metformin also induces cytotoxicity at higher concentrations (36). In contrast, several studies are reported in the agreement with bio-compatibility and radical scavenging potential of PDANPs (25, 26). Neuroprotection efficiency and anti-inflammatory actions of metformin are also reported (20, 22, 37). In our study, we found excellent bio-compatibility of PDANPs, metformin, and Met loaded PDANPs.

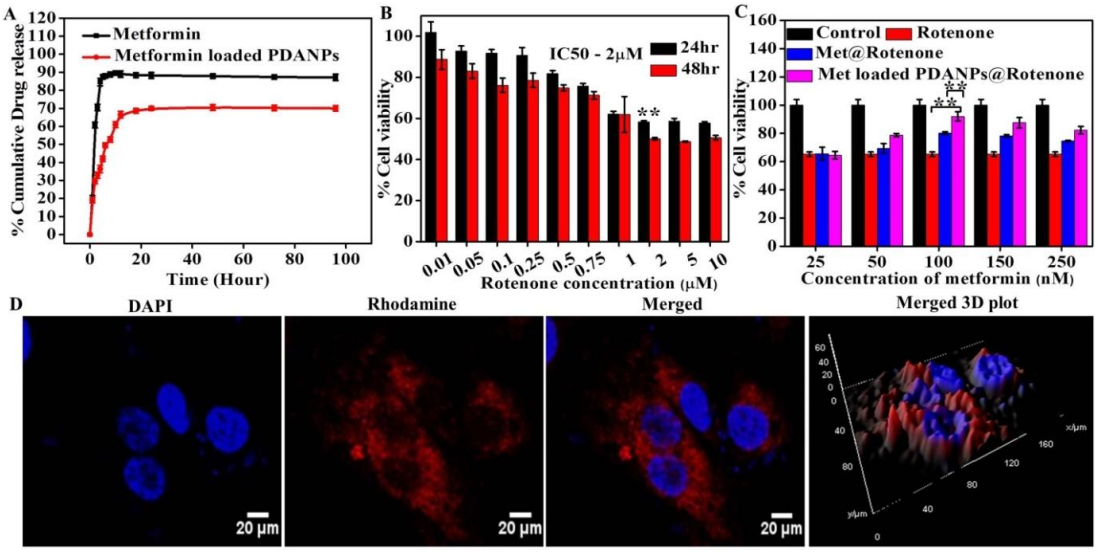


Figure 3.4. *In vitro* therapeutic efficiency of Met loaded PDANP. Drug release profile showing controlled drug release profile of nanoformulation (A); evaluation of cytotoxicity of rotenone (B) has determined 2 µM as IC 50 dose with significance (**p<0.01, one way ANOVA; Turkey and Bonferroni test). The neuroprotective efficacy of Met loaded PDANPs was evaluated to rotenone-induced Parkinson's pathogenic effect (**p<0.01, one way ANOVA; Turkey and

Bonferroni test) (C) Nanoformulations uptake in SH-SY5Y cells were examined by confocal laser scanning microscopy and represented 3D surface plot reflects maximum cytoplasmic uptake (D). The scale bar: 20µm.

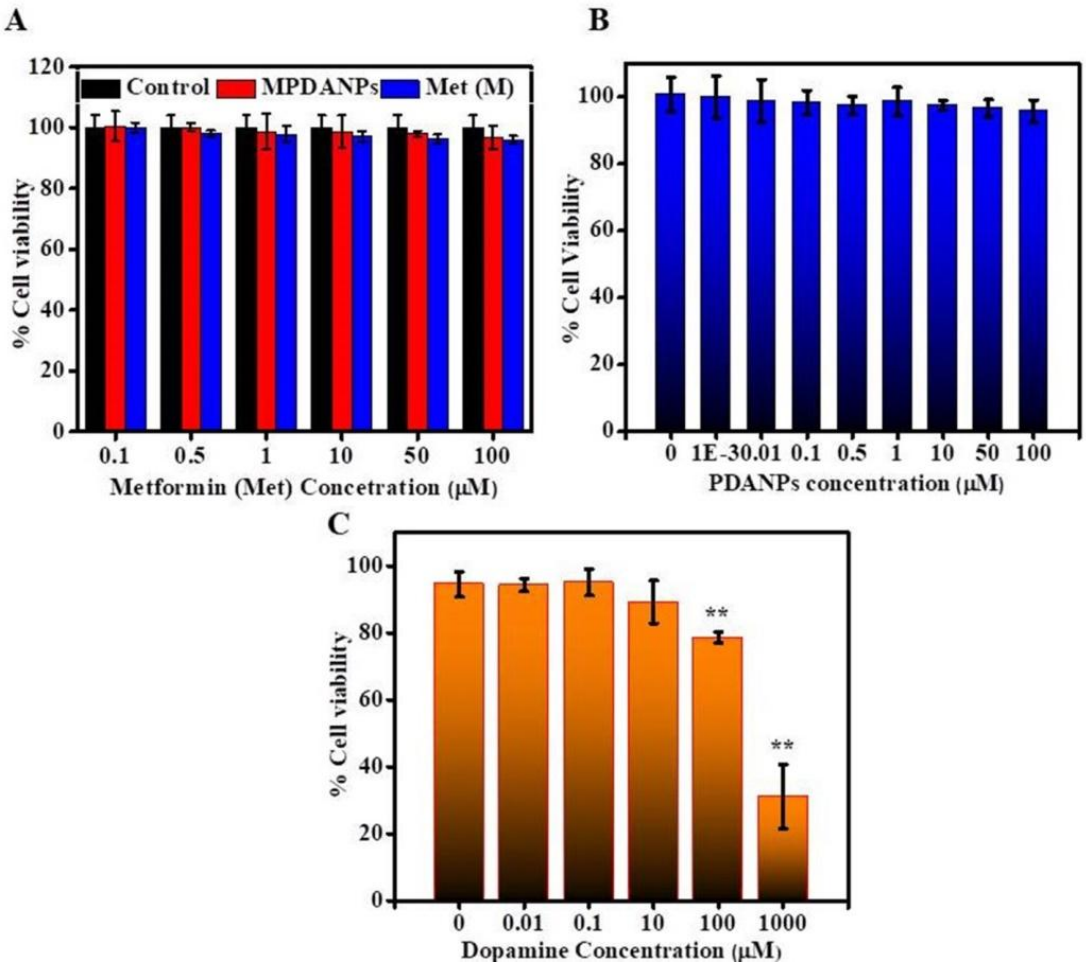


Figure 3.5. Cytotoxicity assessment of metformin and metformin-loaded PDANPs (A), placebo PDANPs (B), and dopamine (C) were presented. Bare PDANPs, Metformin, and Metformin-loaded PDANPs have shown bio-compatible behavior and dopamine has shown toxicity at higher concentrations (**$p<0.01$, one-way ANOVA; Turkey and Bonferroni test).

The potential of nanocarrier to release the drug into target cells is important for the therapeutic efficiency of nanoformulations. Hence, we investigated the uptake of Met-loaded PDANPs to SH-SY5Y neuronal cells, a model of dopaminergic neurons (38). Here, Rhodamine B tagged Met loaded PDANPs were imaged after 6 hours of exposure to SH-SY5Y cells with confocal laser

scanning microscopy. Image shows major uptake of Met loaded PDANPs to the cytoplasm of SH-SY5Y. Confocal imaging confirmed the uptake of our nanoformulation inside the cells (Fig.3.4D). In the brain, dopamine secretion and utilization are a continuous process. Internalization of dopamine to storage vesicles and release from dopaminergic neurons both are transporter-mediated events. Organic cation transporters like plasma monoamine transporters are expressed in the brain and are involved in the transport of dopamine and metformin (39, 40). In the context of this, our nanoformulations easily uptake in SH-SY5Y cells and mouse brains without any deterioration. Uptake of nanoformulation could follow either electrostatic interaction-based cellular internalization or transporter-mediated endocytosis. Both mechanisms are facile to follow for our nanoformulations according to the knowledge of cellular uptake of nanoparticles (25, 40).

Annexin-PE-based anti-apoptosis analysis was performed to authenticate the neuroprotective effect (Fig.3.6A). From the rotenone-treated group, 32.6% of cells underwent late apoptosis, 10.9% in early apoptosis, and only 56.2% of cell populations were remaining viable which is in the agreement with MTT results. In contrast, Met loaded PDANPs have shown significantly higher neuroprotective efficiency with 93.7% cell viability in comparison to metformin (77.6%) and PDANPs (77.3%). These results are also following the cytotoxicity assay. Quantitative estimation of live cells and apoptotic cells by flowjo software were represented in Fig.3.6B.

Growing cells in a multilayer manner are a promising way to study *in vitro* effect of a drug on proliferating cells, mimicking the *in-vivo* tissue model (41). Hence, we have examined the neuroprotective efficacy of our nanoformulation in the 3D culture of SH-SY5Y cells (3D raft) by following the hanging cell insert method(42). In the assessment, Jc1 fluorescence and CASPASE3 expression analysis were performed in the 3D raft PD model. In Fig.3.6C, confocal microscopy images of the 3D raft for untreated control, rotenone treated, metformin, and Met loaded PDANPs supplemented groups with rotenone treatment were shown. Jc1 dye is a probe to analyze the membrane potential of mitochondria. Jc1 molecules agglomerate and give red fluorescence at the hyperpolarized mitochondrial membrane and turn monomer with green fluorescence at depolarization. We further observed, mitochondrial membranes were depolarized on exposure to rotenone and mitochondrial membranes were hyperpolarized by the restorative effect of our nanoformulation. Moreover, immunofluorescence of CASPASE3 was estimated for the expression of CASPASE3, an apoptotic cell death marker. Image J analysis was performed to

significantly quantify the level of Jc1 and CASPASE3 with different formulations mentioned in Fig.3.6D. A higher agglomeration of Jc1 and a lower level of CASPASE3 were found in the control cell raft. Rotenone-treated cell raft has shown lower agglomeration of Jc1 and upregulation of CASPASE3 expression. In comparison to the bare metformin-supplemented group, Met-loaded PDANP has shown significant agglomeration of Jc1 and inhibition of CASPASE3 in the 3D raft PD model. Hence, Met loaded PDANPs have shown better mitochondrial protection and restoration of cell viability.

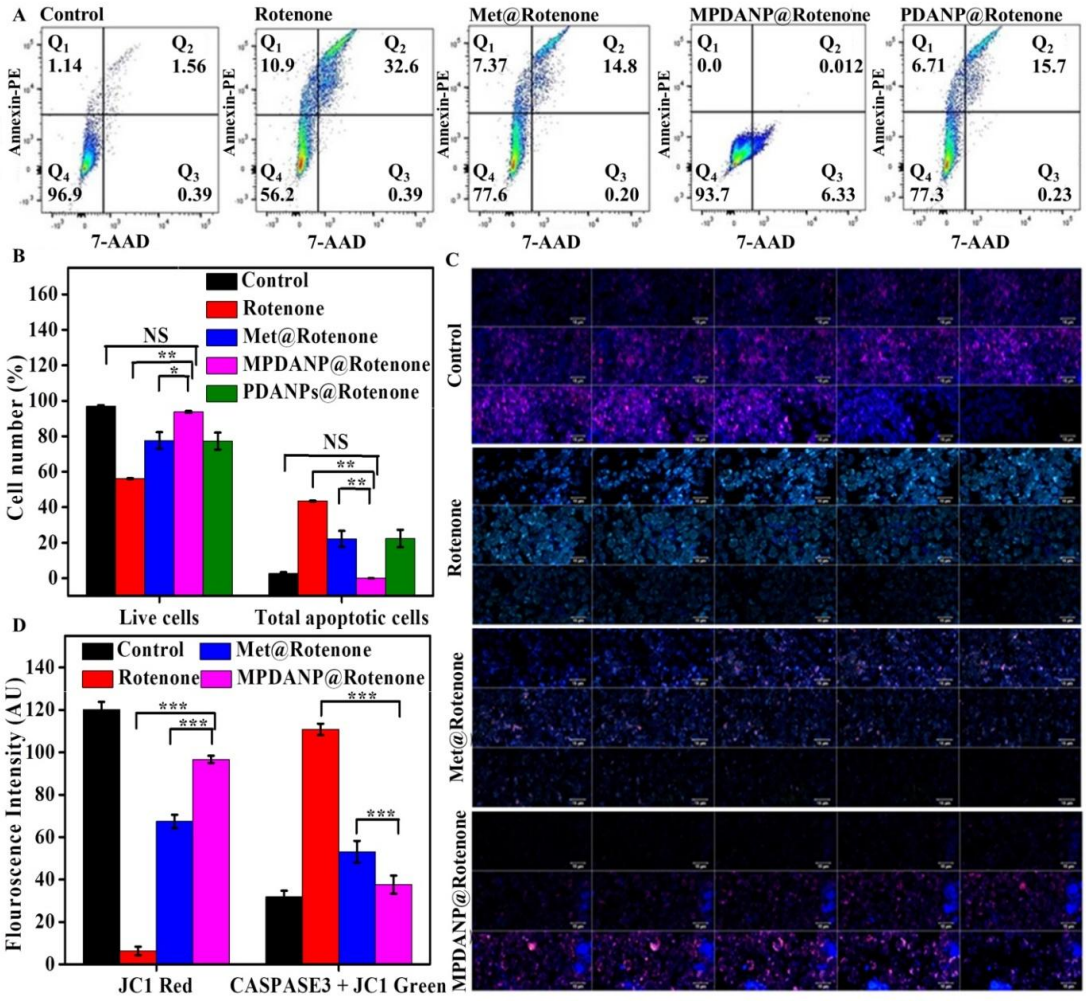


Figure 3.6.Anti-apoptosis analysis in monolayer and 3-D culture of SH-SY5Y. (A) Met-loaded PDANPs show the antiapoptotic effect and protect SH-SY5Y cells from rotenone-induced neuropathy analyzed with flow cytometry. (B) Quantitative data of cell number (%) of live and apoptotic cells by flowjo (**p<0.01,*p<0.05; one-way ANOVA; Turkey and Bonferroni test). (C)

Met-loaded PDANPs show anti-apoptosis effects against rotenone-induced neurotoxicity in Z-stack images of 3D multilayered SH-SY5Y rafts. The scale bar-15µm (D) Expression level of Jc1 red and CASPASE3 + Jc1 green were shown (***p<0.001; one way ANOVA; Turkey and Bonferroni test).

SH-SY5Y cells are used to study the neurotoxicity of rotenone in the experimental PD model *in vitro*. Rotenone, a complex I inhibitor of the electron transport chain inhibits the proteasomal degradation pathway that leads to the aggregation of α-Syn and the progression of PD(43). Herein, we simulated PD in SH-SY5Y monolayer cells, 3D culture, and mouse brain slice by rotenone. The eminent neuroprotection potential of Met-loaded PDANPs against rotenone-induced effects has been confirmed in our study. Results of cell viability assay, PE-Annexin V apoptosis, and Jc1, CASPASE3 based mitochondrial functional analysis are in agreement with each other and confirm higher neuroprotective efficiency of Met loaded PDANPs in comparison to bare drugs.

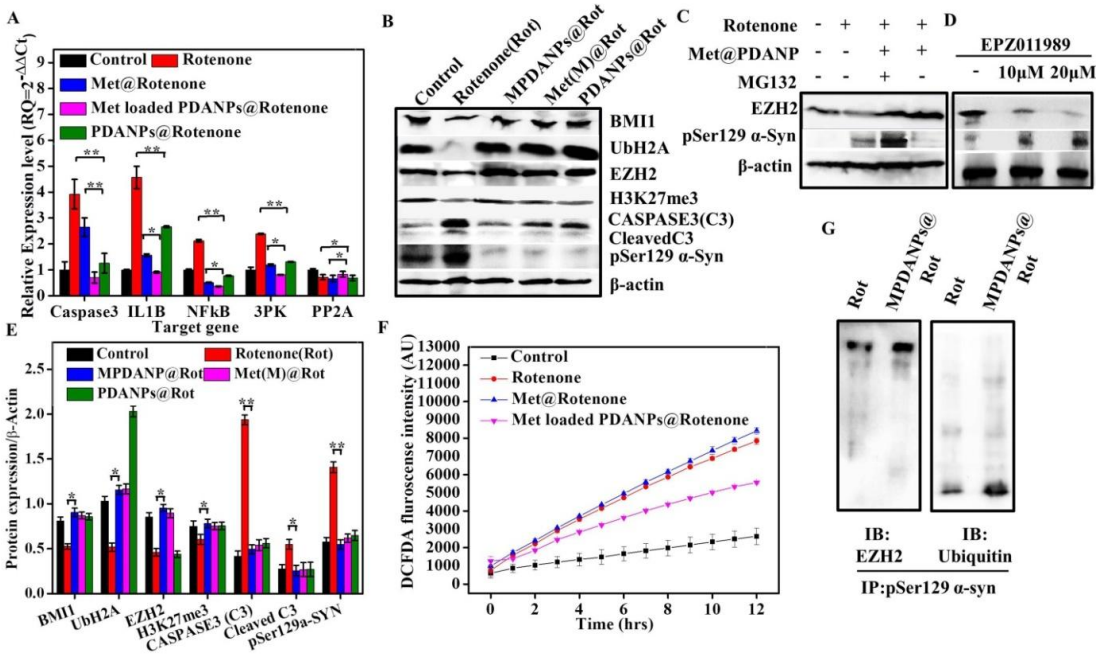


Figure 3.7. Molecular insight into the neuroprotective action of Met loaded PDANPs. (A) Gene expression of CASPASE3, IL1β, NFkB, and PP2A are shown in corresponds to Met loaded PDANPs. Met-loaded PDANPs have shown significant upregulation of PP2A and downregulation of CASPASE3, 3PK, IL1β and NFkB that shows the anti-inflammatory effect (**p<0.01,*p<0.05; one way ANOVA; Turkey and Bonferroni test). (B) Immunoblot is

represented and (E) quantitative analysis of protein expression is shown (*p<0.05; one-way ANOVA; Turkey and Bonferroni test). Significant upregulation of BMI1, EZH2, UbH2A, H3K27me3, and inhibition of CASPASE3 and pSer129 α-Syn reveals a neuroprotective effect. (C, D) EZH2-mediated proteasomal degradation of α-Syn is shown. (F) The anti-inflammatory response of Met-loaded PDANPs has been observed with ROS quenching. (G) Physical interaction of EZH2 and α-Syn has shown epigenetic regulation of α-Syn degradation by ubiquitin proteasomal pathway.

3a.2.5. Molecular insights of neuroprotective mechanism of nanoformulation

Q-PCR analysis was performed to analyze gene expressions of CASPASE3, Mitogen-Activated Protein Kinase-Activated Protein Kinase 3 (MAPKAPK3/3PK), Protein Phosphatase 2 (PP2A), Nuclear Factor kappa-light-chain-enhancer of activated B cells (NFkB) and Interleukin 1 Beta (IL1β) (Fig.3.7A). The analysis indicated significant upregulation of 3PK, CASPASE3, NFkB and IL1β genes expression and downregulation of PP2A in rotenone treated group. The effect of rotenone on neuroinflammation-associated gene expression has been significantly reversed by Met-loaded PDANPs. In the overall gene expression analysis, Met loaded PDANPs show better neuroprotection as compared to bare metformin which has been analyzed statistically. Hence, the downregulation of these potential regulatory targets is achieved with our nanoformulation. PDANPs and metformin both are modulators of inflammatory mechanisms (20, 28). Generally, neuroinflammation is associated with PD progression (44, 45). Hence, we analyze neuroinflammation and PD-associated gene expression. In analysis, upregulated 3PK in rotenone-treated group is due to its stress-mediated p38 signaling (44). Significant downregulation of 3PK was observed in the case of metformin and Met loaded PDANPs indicate a neuroprotective response. 3PK is a protein kinase that is upregulated during α-synucleinopathy to elevate NFkB-mediated death of dopaminergic neurons (45, 46). So by inhibiting 3PK our nanoformulation supports the prevention of neurodegeneration with concomitant downregulation of NFkB signifies anti-inflammatory activities. Further, our formulation has triggered PP2A expression against rotenone insult. This finding is in the agreement with reports that show PP2A upregulation and is indicative of α-Syn dephosphorylation in PD (22, 37). CASPASE3, IL1β, and NFkB were also determined as they have regulatory roles in neuroinflammation-associated PD pathogenesis. Downregulation of CASPASE3, IL-1β, and NFkB with metformin and Met loaded

PDANPs group reflect the neuroprotective effect of nanoformulations against rotenone-induced PD effect.

Epigenetic regulation is emerging as a promising therapeutic approach in the prevention of neurodegenerative diseases. In the present study, protein expression has been studied to confirm the epigenetically regulated recuperative effect of Met-loaded PDANPs. Expression study of CASPASE3, pSer129 α-Syn, EZH2, H3K27me3, BMI1 and Ubiquitylated *H2A (*UbH2A) were performed (Fig.3.7B). In our study, we have observed a significant reduction in the expression level of CASPASE3 and pSer129 α-Syn with Met-loaded PDANPs in contrast to rotenone-induced upregulation of these targets. Further, the PD association of potential epigenetic targets has been assessed. We found significant downregulation of BMI1 and EZH2 with the treatment of rotenone and upregulation with Met-loaded PDANPs. These results gain our interest to know about the downstream targets of both epigenetic markers. In an exploration, Met-loaded PDANPs showed significant upregulation of UbH2A and H3K27me3 by reversing the rotenone effect, confirming the association of epigenetic regulation with PD. The quantification of protein expression has been performed with image J analysis represented in Fig.3.7E. EZH2 is the major player of the PRC2 complex that has been proposed regulatory target in α-synucleinopathy(47). We, therefore, inhibited EZH2 expression by the reported potent EZH2 inhibitor, EPZ011989 (48). We also observed EZH2 inhibitor dose-dependent enhancement in the aggregation of α-Syn (Fig.3.7D).MG132, an inhibitor of the proteasomal pathway was employed to understand the neuroprotective mechanism of our nanoformulation. We found that our formulation follows EZH2-mediated proteasomal degradation of α-Syn (Fig.3.7C). In confirmation of these findings, we have observed novel physical interaction of EZH2 and pSer129 α-Syn proteins (Fig.3.7G). An immunoprecipitation result has confirmed that Met-loaded PDANPs regulate proteasomal degradation and ubiquitination of α-Syn. In PD pathogenesis, the death of dopaminergic neurons is associated with CASPASE3-mediated apoptosis and Lewy body formation with overexpression of pSer129 α-Syn(37). Herein, Met-loaded PDANPs have inhibited CASPASE3 and pSer129 α-Syn protein expression and reversed the neurodegenerative effect of rotenone. To further elucidate the mechanism of pSer129 α-Syn degradation by our nanoformulation it was observed that epigenetic regulation by a polycomb group of proteins plays a crucial role in pSer129 α-Syn's degradation. Reported literature shows PRC1 member, BMI1 is also reported as a potential therapeutic target for neurodegenerative diseases (8). Dysfunction of BMI1 might be

due to impaired DNA damage response pathway with depletion of UbH2A (49). Hence, Met-loaded PDANPs triggered upregulation of BMI1 and UbH2A agreeing with earlier studies that have proposed BMI1 as a potent therapeutic target in the treatment of neurodegenerative infirmities(8). Human polycomb protein 2 is also reported as an inducer of SUMOylation of α-Syn that results in the progression of PD(9). Indeed, repression of PRC2 activity is associated with the progression of PD (6) and deficiency of EZH2 leads to neurodegeneration by an alteration in gene expression is also reported (7). Therefore, we are interested to know the novel interaction of PRC proteins and α-Syn to understand its role in PD. Herein, upregulated EZH2 and H3K27me3 as the neuroprotective effect of Met-loaded PDANPs has shown the camouflaged role of EZH2 in PD prevention. There is no direct correlation of H3K27me3 with PD progression. But, H3K27me3 alteration has been implicated in the study of experimental Parkinsonism (7). In our observation, the direct interaction of EZH2 with Phospho-α-Syn (Ser129) indicates the regulatory role of EZH2 in neuroprotection. A recent study shows acute treatment of rotenone declines ubiquitinated proteins level and E1A activity that requires activation of ubiquitin for the functioning of the Ubiquitin proteasomal pathway (50). In the ubiquitin proteasomal pathway, ubiquitin binds to aggregated proteins and directs them to the proteasomal degradation machinery. Hence, we found that our nanoformulation has the potential to attenuate the effect of rotenone by ubiquitination of aggregated α-Syn and restoration of proteasomal degradation pathways. There are earlier reports that have shown human polycomb protein 2, a PRC1 member induced SUMOylation of α-Syn which promotes aggregation of α-Syn, and SUMO modification works antagonistically to ubiquitination(9, 10). However, there is no such report that showed EZH2-mediated regulation of α-Syn degradation. This is the first report that has shown EZH2, a PRC2 member-induced proteasomal degradation of aggregated α-Syn in PD prevention.

Generally, neurodegeneration has an association with neuroinflammation based on comprehensive studies (44, 45). Therefore, reactive oxygen species (ROS) detection analysis was also performed to analyze the anti-inflammatory response of our nanoformulation. Fig.3.7F is showing a lower level of ROS generation with Met-loaded PDANPs due to the ROS scavenging property of PDANPs(28). Further, the ROS scavenging property of Met-loaded PDANPs reflects excellent neuroprotective potential. Bare metformin is not able to quench ROS against rotenone treatment. This supports an earlier report that has shown metformin-mediated ROS

generation(51). In the present study, our finding is in line with a study that showed PDANPs as potent ROS scavengers (28).

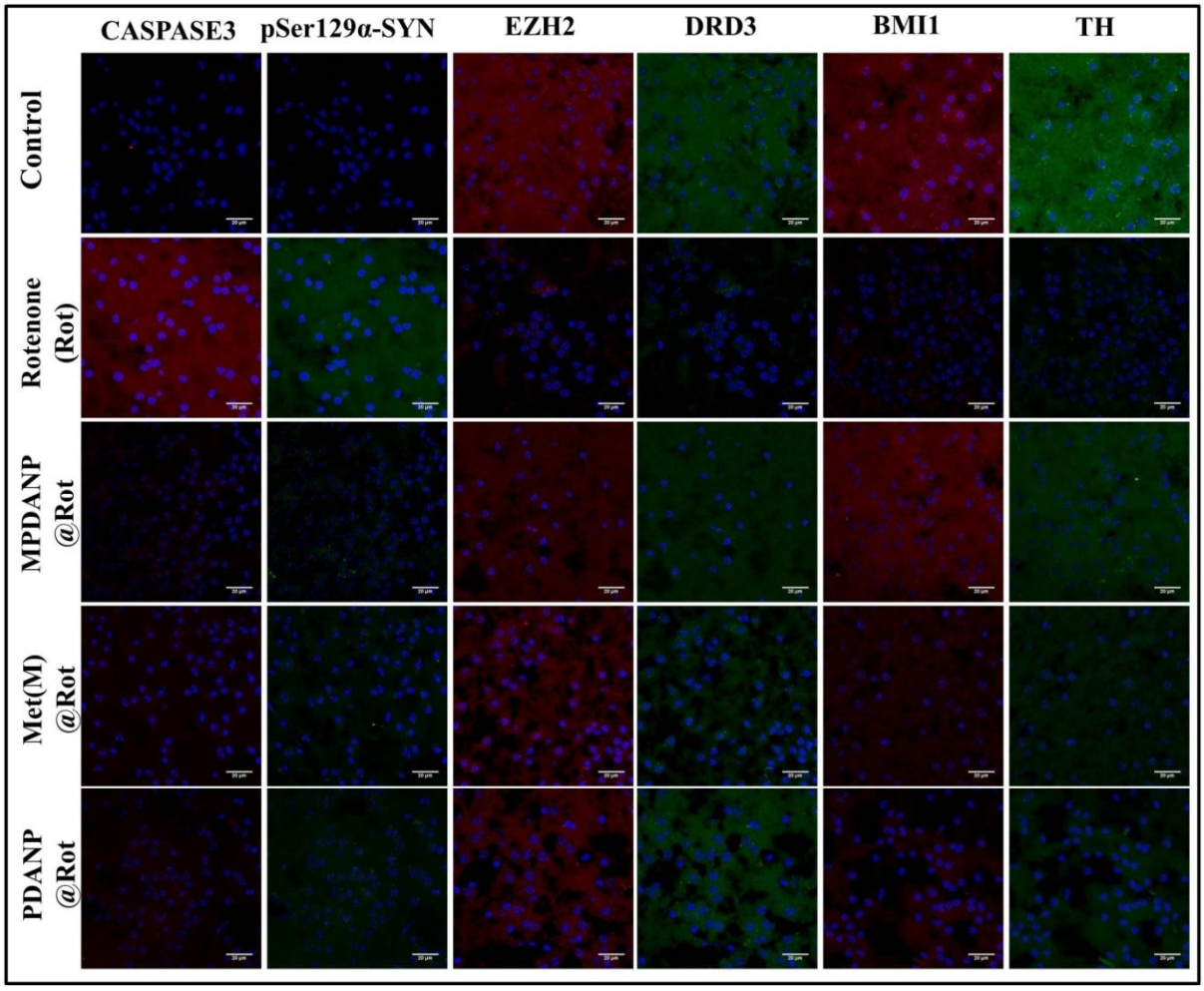


Figure 3.8.Immunohistochemical analysis in brain slice culture. Confocal laser scanning microscopy images as part of IHC analysis of protein expression shows upregulation of TH, DRD3, EZH2, and BMI1. Inhibition of CASPASE3, pSer129 α-Syn as neuroprotective action of Met loaded PDANPs against rotenone-induced neurodegeneration confirming therapeutic intervention of PD pathogenesis. Confocal images are represented as a 3D surface plot. Scale bar-20μm.

3a.2.6. Evaluation of the neuroprotective potential of nanoformulation in *ex vivo* PD model

Nanoformulations have shown potent neuroprotection *in vitro* PD models. To check its response at the tissue level, we have performed an immunohistochemistry (IHC) analysis of potential

therapeutic targets in mice brain slice culture. Tyrosine Hydroxylase (TH), Dopamine Receptor D3 (DRD3), EZH2, BMI1, CASPASE3, and pSer129 α-Syn expressions were analyzed (Fig.3.8). Selection of TH in the study is due to its downregulation leads to depletion of dopamine in case of PD(52). In our observation, TH expression has been upregulated with Met-loaded PDANPs that show dopamine synthesis restoration. DRD3 is also studied as a potential target that reduces α-Syn accumulation in PD [53]. In agreement with these, we also found upregulation of DRD3 with our nanoformulation in contrast to the rotenone effect. Herein, the emerging role of epigenetics in the regulation of neuroprotection has been explored. Upregulated EZH2 and BMI1 have confirmed their unexplored role in neuroprotective action (6, 8). Inhibitions of potential therapeutic targets, pSer129 α-Syn and CASPASE3 have also been determined. The α-syn aggregation reduces TH activity with the reduction of dopamine *in vitro* models was also evident (54). The neuroprotective role of DRD3 in MPTP (1-methyl-4-phenyl-1, 2, 3, 6-tetrahydropyridine) induced PD pathogenesis is also reported (55). Herein, our formulation has reversed the rotenone effect in mouse brain slices by upregulating EZH2, BMI1, TH, and DRD3 and inhibiting CASPASE3 and pSer129 α-Syn. Comprehensive IHC analysis has shown a better recuperative effect of nanoformulation against rotenone-induced neurotoxicity in comparison to metformin and PDANPs. IHC results are also in agreement with our immunoblot analysis.

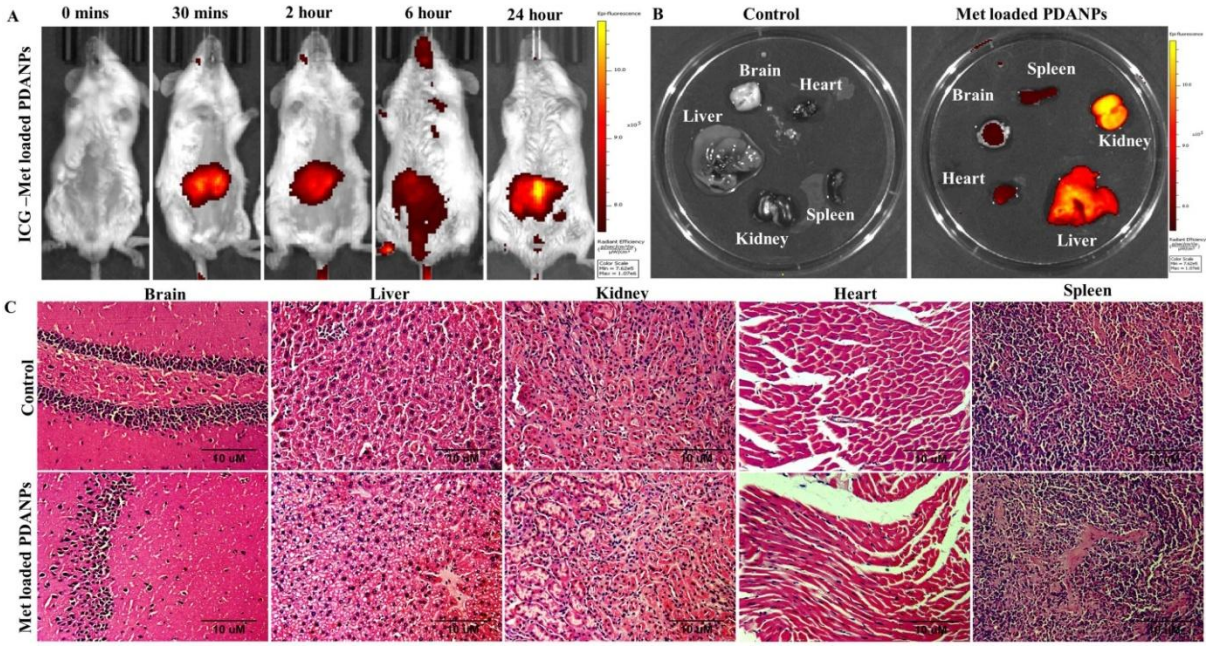


Figure 3.9.*In vivo/ex vivo* bio-distribution and histopathology analysis. *In vivo* bio-distribution study displays a readily higher intake of nanoformulation to the brain, then it distributes to the

heart, spleen, liver, and kidney (A). *Ex vivo* organ reflectance imaging is showing a higher percentage in the liver, kidney, and brain 2 hours of post-injection (B). Histopathology analysis has shown the bio-compatibility of Met-loaded PDANPs with no adverse pathological demarcation. Scale bar-10 μm (C).

3a.2.7. *In vivo/ ex vivo* bio-distribution and histopathological analysis of nanoformulation

*In vivo* bio-distribution of ICG (Indocyanine Green) tagged nanoformulation was performed to evaluate the bio-distribution profile of Met-loaded PDANPs. Post-injection, bio-distribution analysis was performed until 24 hours. In the initial 6 hours, nanoformulations have shown major distribution to the brain and liver. Besides that, it is also distributed to the spleen, heart, and kidney (Fig.3.9A). Further, in confirmation of the existence of nanoformulation, *Ex vivo* imaging of organs was performed 24 hours after post-injection. Results have shown a good distribution of nanoformulations with retention in the brain (Fig.3.9B). In observation of fluorescence intensity, a high accumulation of nanoparticles in the kidney and liver indicate a clearance path of nanoformulations(40). Plasma membrane monoamine transporter highly expressed in the brain may involve in the transportation of dopamine and metformin (39, 40). These results show the efficiency of nanoformulation to cross the BBB. Considering these facts, Met-loaded PDANPs has believed to execute well bio-distribution profile. It has the potential to be a new suitable vector system for metformin in the treatment of PD as well as other neurodegenerative and anti-aging diseases. We have performed histopathological analysis to ensure its bio-compatibility (Fig. 3.9C). In a histopathological analysis to control mice tissues, we found that our nanoformulation is safe having no pathological signature.

Finally, *In vivo/ex vivo* bio-distribution and histopathological analysis have confirmed the internalization and retention of nanoparticles in the brain without any deterioration. This indicates the bio-compatibility of our nanoformulations and reflects its immense therapeutic potential in preclinical PD models.

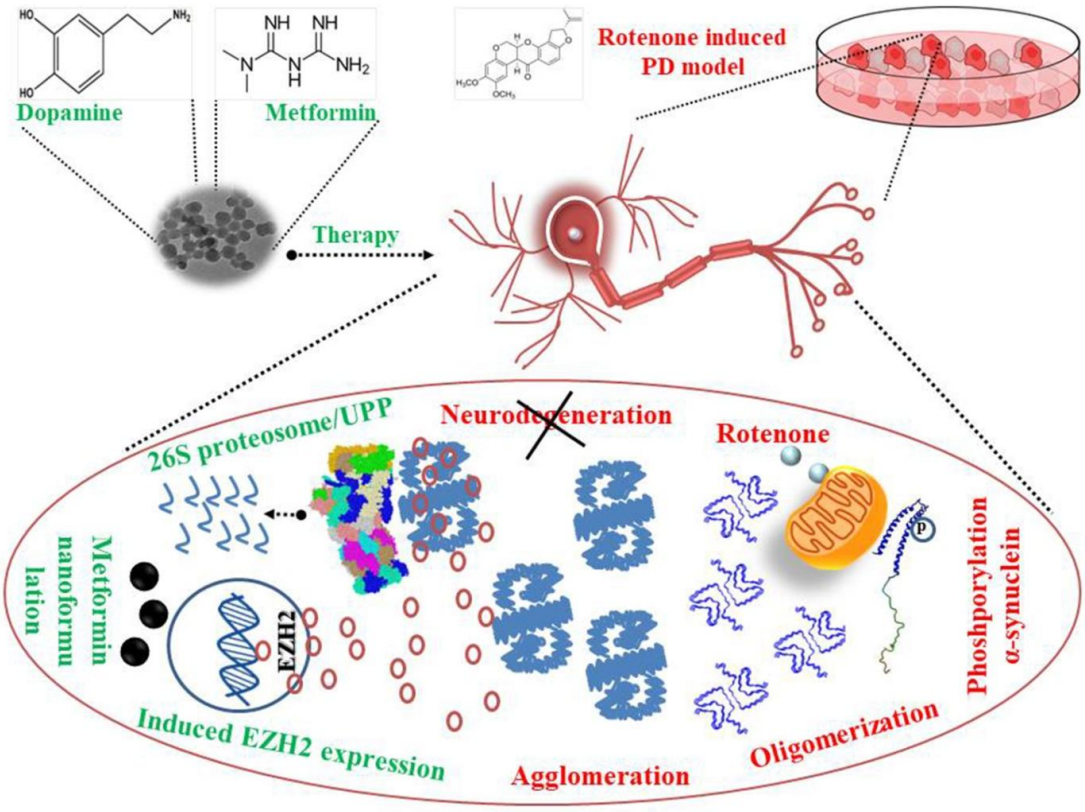


Figure 3.10. The schematic diagram represents a neuroprotective mechanism of nanoformulation. Metformin nanoformulation (Met loaded PDANPs) inhibiting rotenone-induced neurotoxicity by promoting EZH2 mediated α-Synuclein ubiquitination and degradation to prevent PD pathogenesis.

## 3a.3 Conclusion

In the overall finding, we reported the neuroprotective potential and anti-Parkinsonism effect of Met-loaded PDANPs. The major key findings are the nanosized, unnimodal and spherical nanoparticles that exhibited improved metformin release profile. In addition, our present findings show the cumulative therapeutic efficiency of metformin and polydopamine at the single platform by reversing rotenone-induced oxidative stress, mitochondrial damage, and cytotoxicity with the reduction of α-Syn agglomeration. The novel points of presented work are first time metformin conjugated within polydopamine nanoparticles and exploration of epigenetic regulation in PD treatment. In that, the mechanism of neuroprotection highlighted EZH2

mediated phosphor-α-Syn (Ser129) ubiquitination and proteasomal degradation that is illustrated in Fig.3.10. Our finding demonstrates that Met-loaded PDANPs enhance the neuroprotective potential of drugs in rescuing cells from rotenone-induced neurodegenerative effects by inducing EZH2-regulated α-Syn ubiquitination/proteasomal degradation. Thus, the present study suggests the neuroprotective potentiality of our nanoformulation in PD prevention. The major breakthrough and benefit of the present study is to reveal the camouflaged role of EZH2 in the removal of neurodegenerative effect could be considered as a therapeutic target in PD treatment. However, a detailed investigation of the EZH2-mediated prevention of α-Synucleionopathy is warranted in the clinical setup to translate its potential application in therapy. The limitations of the present work are that the commercial drug has not been tested as the positive control and work has shown majorly *in vitro* neuroprotection efficacy. However, Met-loaded PDANPs have considerably shown *ex vivo* neuroprotective efficiency by reversing the neurotoxic effect of rotenone in the mouse brain slice culture. In significance of the presented metformin nanoformulation in comparison to other reported triphenylphosphonium functionalized mito-metformin encapsulated polyanhydride nanoparticle in PD treatment divulges the superior drug release profile and therapeutic efficacy of our metformin nanoformulation. (56) Thus, the metformin nanoformulation has the potential to be new PD therapeutic agent if it will be tested in clinical setup with comparison to commercialized drug like levodopamine in further investigation.

## 3a.4 References


1. U. B. Muthane, M. Ragothaman, G. Gururaj, Epidemiology of Parkinson's disease and movement disorders in India: problems and possibilities. *The Journal of the Association of Physicians of India* **55**, 719-724 (2007).
2. W. Poewe *et al.*, Parkinson disease. *Nature Reviews Disease Primers* **3**, 17013 (2017).
3. N. J. Rutherford, M. Brooks, B. I. Giasson, Novel antibodies to phosphorylated alpha-synuclein serine 129 and NFL serine 473 demonstrate the close molecular homology of these epitopes. *Acta neuropathologica communications* **4**, 80 (2016).
4. L. Devi, V. Raghavendran, B. M. Prabhu, N. G. Avadhani, H. K. Anandatheerthavarada, Mitochondrial import and accumulation of alpha-synuclein impair complex I in human

dopaminergic neuronal cultures and Parkinson disease brain. *The Journal of biological chemistry* **283**, 9089-9100 (2008).

5. I. A. Qureshi, M. F. Mehler, Advances in epigenetics and epigenomics for neurodegenerative diseases. *Curr Neurol Neurosci Rep* **11**, 464-473 (2011).
6. M. von Schimmelmann *et al.*, Polycomb repressive complex 2 (PRC2) silences genes responsible for neurodegeneration. *Nature neuroscience* **19**, 1321-1330 (2016).
7. E. Sodersten *et al.*, Dopamine signaling leads to loss of Polycomb repression and aberrant gene activation in experimental parkinsonism. *PLoS genetics* **10**, e1004574 (2014).
8. M. Abdouh *et al.*, Bmi1 is down-regulated in the aging brain and displays antioxidant and protective activities in neurons. *PloS one* **7**, e31870 (2012).
9. Y. Oh, Y. M. Kim, M. M. Mouradian, K. C. Chung, Human Polycomb protein 2 promotes alpha-synuclein aggregate formation through covalent SUMOylation. *Brain research* **1381**, 78-89 (2011).
10. R. Rott *et al.*, SUMOylation and ubiquitination reciprocally regulate alpha-synuclein degradation and pathological aggregation. *Proceedings of the National Academy of Sciences of the United States of America* **114**, 13176-13181 (2017).
11. P. Hickey, M. Stacy, Available and emerging treatments for Parkinson's disease: a review. *Drug design, development and therapy* **5**, 241-254 (2011).
12. B. D. Li *et al.*, Adverse effects produced by different drugs used in the treatment of Parkinson's disease: A mixed treatment comparison. *CNS neuroscience & therapeutics* **23**, 827-842 (2017).
13. M. Foretz, B. Viollet, Therapy: Metformin takes a new route to clinical efficacy. *Nature reviews. Endocrinology* **11**, 390-392 (2015).
14. N. Nath *et al.*, Metformin attenuated the autoimmune disease of the central nervous system in animal models of multiple sclerosis. *Journal of immunology* **182**, 8005-8014 (2009).
15. M. Markowicz-Piasecka *et al.*, Metformin - a Future Therapy for Neurodegenerative Diseases : Theme: Drug Discovery, Development and Delivery in Alzheimer's Disease Guest Editor: Davide Brambilla. *Pharmaceutical research* **34**, 2614-2627 (2017).
16. D. K. Khajuria, O. N. Patil, D. Karasik, R. Razdan, Development and evaluation of novel biodegradable chitosan based metformin intrapocket dental film for the management of

periodontitis and alveolar bone loss in a rat model. *Archives of oral biology* **85**, 120-129 (2018).

17. E. Lachmandas *et al.*, Metformin Alters Human Host Responses to Mycobacterium tuberculosis in Healthy Subjects. *The Journal of infectious diseases* **220**, 139-150 (2019).
18. M. L. Wahlqvist *et al.*, Metformin-inclusive sulfonylurea therapy reduces the risk of Parkinson's disease occurring with Type 2 diabetes in a Taiwanese population cohort. *Parkinsonism & related disorders* **18**, 753-758 (2012).
19. K. Labuzek *et al.*, Quantification of metformin by the HPLC method in brain regions, cerebrospinal fluid and plasma of rats treated with lipopolysaccharide. *Pharmacological reports : PR* **62**, 956-965 (2010).
20. H. A. Hirsch, D. Iliopoulos, K. Struhl, Metformin inhibits the inflammatory response associated with cellular transformation and cancer stem cell growth. *Proceedings of the National Academy of Sciences of the United States of America* **110**, 972-977 (2013).
21. M. Lu *et al.*, Metformin Prevents Dopaminergic Neuron Death in MPTP/P-Induced Mouse Model of Parkinson's Disease via Autophagy and Mitochondrial ROS Clearance. *The international journal of neuropsychopharmacology* **19** (2016).
22. N. Katila *et al.*, Metformin lowers alpha-synuclein phosphorylation and upregulates neurotrophic factor in the MPTP mouse model of Parkinson's disease. *Neuropharmacology* **125**, 396-407 (2017).
23. M. Kinaan, H. Ding, C. R. Triggle, Metformin: An Old Drug for the Treatment of Diabetes but a New Drug for the Protection of the Endothelium. *Medical principles and practice : international journal of the Kuwait University, Health Science Centre* **24**, 401-415 (2015).
24. T. Gunasekaran, T. Haile, T. Nigusse, M. D. Dhanaraju, Nanotechnology: an effective tool for enhancing bioavailability and bioactivity of phytomedicine. *Asian Pacific journal of tropical biomedicine* **4**, S1-7 (2014).
25. X. Liu *et al.*, Mussel-inspired polydopamine: a biocompatible and ultrastable coating for nanoparticles in vivo. *ACS nano* **7**, 9384-9395 (2013).
26. K. Y. Ju, Y. Lee, S. Lee, S. B. Park, J. K. Lee, Bioinspired polymerization of dopamine to generate melanin-like nanoparticles having an excellent free-radical-scavenging property. *Biomacromolecules* **12**, 625-632 (2011).

27. J. Hu *et al.*, Asn-Gly-Arg-modified polydopamine-coated nanoparticles for dual-targeting therapy of brain glioma in rats. *Oncotarget* **7**, 73681-73696 (2016).
28. H. Zhao *et al.*, Polydopamine nanoparticles for the treatment of acute inflammation-induced injury. *Nanoscale* **10**, 6981-6991 (2018).
29. Y. Huang *et al.*, Mimicking Melanosomes: Polydopamine Nanoparticles as Artificial Microparasols. *ACS central science* **3**, 564-569 (2017).
30. J. Hou *et al.*, A novel high drug loading mussel-inspired polydopamine hybrid nanoparticle as a pH-sensitive vehicle for drug delivery. *International Journal of Pharmaceutics* **533**, 73-83 (2017).
31. P. Jose, K. Sundar, C. H. Anjali, A. Ravindran, Metformin-loaded BSA nanoparticles in cancer therapy: a new perspective for an old antidiabetic drug. *Cell biochemistry and biophysics* **71**, 627-636 (2015).
32. B. Poinard *et al.*, Polydopamine Nanoparticles Enhance Drug Release for Combined Photodynamic and Photothermal Therapy. *ACS applied materials & interfaces* **10**, 21125-21136 (2018).
33. J. H. Lee, Y. Yeo, Controlled Drug Release from Pharmaceutical Nanocarriers. *Chemical engineering science* **125**, 75-84 (2015).
34. S. Dadakhujaev *et al.*, Autophagy protects the rotenone-induced cell death in alpha-synuclein overexpressing SH-SY5Y cells. *Neuroscience letters* **472**, 47-52 (2010).
35. Y. Jiang, L. Pei, S. Li, M. Wang, F. Liu, Extracellular dopamine induces the oxidative toxicity of SH-SY5Y cells. *Synapse* **62**, 797-803 (2008).
36. O. N. Pyaskovskaya, D. L. Kolesnik, A. G. Fedorchuk, G. V. Gorbik, G. I. Solyanik, Cytotoxic activity of metformin in vitro does not correlate with its antitumor action in vivo. *Experimental oncology* **39**, 264-268 (2017).
37. B. I. Perez-Revuelta *et al.*, Metformin lowers Ser-129 phosphorylated alpha-synuclein levels via mTOR-dependent protein phosphatase 2A activation. *Cell death & disease* **5**, e1209 (2014).
38. H. R. Xie, L. S. Hu, G. Y. Li, SH-SY5Y human neuroblastoma cell line: in vitro cell model of dopaminergic neurons in Parkinson's disease. *Chinese medical journal* **123**, 1086-1092 (2010).

39. J. Wang, The plasma membrane monoamine transporter (PMAT): Structure, function, and role in organic cation disposition. *Clinical pharmacology and therapeutics* **100**, 489-499 (2016).
40. L. J. McCreight, C. J. Bailey, E. R. Pearson, Metformin and the gastrointestinal tract. *Diabetologia* **59**, 426-435 (2016).
41. M. Innala *et al.*, 3D culturing and differentiation of SH-SY5Y neuroblastoma cells on bacterial nanocellulose scaffolds. *Artificial cells, nanomedicine, and biotechnology* **42**, 302-308 (2014).
42. L. Au - Tricoli, D. L. Au - Berry, C. Au - Albanese, A Rapid Filter Insert-based 3D Culture System for Primary Prostate Cell Differentiation. *JoVE* doi:10.3791/55279, e55279 (2017).
43. M. Shamoto-Nagai *et al.*, An inhibitor of mitochondrial complex I, rotenone, inactivates proteasome by oxidative modification and induces aggregation of oxidized proteins in SH-SY5Y cells. *Journal of neuroscience research* **74**, 589-597 (2003).
44. S. A. Correa, K. L. Eales, The Role of p38 MAPK and Its Substrates in Neuronal Plasticity and Neurodegenerative Disease. *Journal of signal transduction* **2012**, 649079 (2012).
45. H. J. Lee, C. Kim, S. J. Lee, Alpha-synuclein stimulation of astrocytes: Potential role for neuroinflammation and neuroprotection. *Oxidative medicine and cellular longevity* **3**, 283-287 (2010).
46. E. H. Joe *et al.*, Astrocytes, Microglia, and Parkinson's Disease. *Experimental neurobiology* **27**, 77-87 (2018).
47. Y. Wang *et al.*, HIV-1 Vpr disrupts mitochondria axonal transport and accelerates neuronal aging. *Neuropharmacology* **117**, 364-375 (2017).
48. J. E. Campbell *et al.*, EPZ011989, A Potent, Orally-Available EZH2 Inhibitor with Robust in Vivo Activity. *ACS medicinal chemistry letters* **6**, 491-495 (2015).
49. V. Ginjala *et al.*, BMI1 is recruited to DNA breaks and contributes to DNA damage-induced H2A ubiquitination and repair. *Molecular and cellular biology* **31**, 1972-1982 (2011).

50. Q. Huang, H. Wang, S. W. Perry, M. E. Figueiredo-Pereira, Negative regulation of 26S proteasome stability via calpain-mediated cleavage of Rpn10 subunit upon mitochondrial dysfunction in neurons. *J Biol Chem* **288**, 12161-12174 (2013).
51. Z. Y. Gao *et al.*, Metformin induces apoptosis via a mitochondria-mediated pathway in human breast cancer cells in vitro. *Experimental and therapeutic medicine* **11**, 1700-1706 (2016).
52. Y. Chen *et al.*, The expression and significance of tyrosine hydroxylase in the brain tissue of Parkinsons disease rats. *Experimental and therapeutic medicine* **14**, 4813-4816 (2017).
53. J. D. Wang *et al.*, A pivotal role of FOS-mediated BECN1/Beclin 1 upregulation in dopamine D2 and D3 receptor agonist-induced autophagy activation. *Autophagy* **11**, 2057-2073 (2015).
54. R. G. Perez *et al.*, A role for alpha-synuclein in the regulation of dopamine biosynthesis. *The Journal of neuroscience : the official journal of the Society for Neuroscience* **22**, 3090-3099 (2002).
55. S. R. Cote, E. V. Kuzhikandathil, Chronic levodopa treatment alters expression and function of dopamine D3 receptor in the MPTP/p mouse model of Parkinson's disease. *Neuroscience letters* **585**, 33-37 (2015).
56. B. W. Schlichtmann *et al.*, Functionalized polyanhydride nanoparticles for improved treatment of mitochondrial dysfunction. **110**, 450-459 (2022).

# Chapter 3b

---

# Metformin-loaded polydopamine nanoparticles inhibit rotenone-induced PD deficits in the rat model

3b.1. Introduction

Parkinson's disease (PD) is the second most neurodegenerative disease with a developing burden in the Asian populations (1). There are enormous causative factors involved in PD progression and considerable studies are underway to understand poor PD etiology. However, the accumulation of synuclein called synucleinopathy is one of the major causes that lead to the death of the dopaminergic neuron resulting in involuntary body movement (2). The PD signature molecule, alpha-synuclein is encoded by the SNCA gene having an immense physiological role in the neurotransmitter release, neuronal maintenance, and regulation of neurochemicals (3, 4). However, the post-translation modifications and misfolding of alpha-synuclein, defective proteasomal pathway, and mutation of the SNCA gene result in synucleinopathy associated with PD(5, 6). Besides, investigating the post-translational modification of alpha-synuclein, transcriptional regulation, and epigenetic modifications are found to be causative factors in PD progression (7). Indeed, the histone hyperacetylation of synuclein is well characterized in the PD progression having a higher association of H3K27ac (8-10). Hence, designing the strategy to reduce histone acetylation paves the way for the development of PD treatment. In the epigenetic regulation of PD, a reduced level of H3K27me3 and downregulated master epigenetic regulator polycomb repressor complex 2 protein, EZH2 has been demonstrated in PD progression (11). The restoration of EZH2 and H3K27me3 has been reported as one of the potential therapeutic targets for PD treatment (12, 13). In our previous study with the demonstration of the neuroprotective effect of metformin-loaded polydopamine nanoparticles, the camouflaged role of EZH2, the modulator of H3K27me3 in the reduction of alpha-synuclein has been revealed (14). Thus, we hypothesize that the reduction of hyperacetylated H3K27ac of SNCA reduces the synuclein expression and aggregation by considering the evidence of SNCA repression with H3K27me3 restoration in the development of PD therapy.

In the era of PD investigation, pharmacological neuroprotective agents and deep brain stimulation (DBS) have been recognized as effective therapy (15). However, existing therapy is still not preventing PD, and has major limitations with immense side effects (16). Therefore, definitive PD-controlling treatment is warranted. In the last decades, metformin emerged as the wonder therapeutic molecule in the management of several infirmities including neurodegenerative diseases (17, 18). The clinical survey of the Taiwanese population on diabetic medication has divulged that metformin reduces PD risk (19). There are growing shreds of

evidence highlighting the neuroprotective effect of metformin that can pass the blood-brain barrier (20, 21). Metformin's therapeutic actions have been reported as an anti-inflammatory, autophagy inducer, epigenetic regulator, and reducing agent of synucleinopathy(14, 22). However, the detailed mechanistic approach of metformin in the transcriptional regulation of SNCA has been not explored. Besides having a potential therapeutic effect, metformin has limitations like lower bioavailability due to absorption limited drug kinetics, and lactic acidosis (23). By considering the emerging advantage of a nano-drug delivery system in the advancement and improvement of drug efficacy, we have previously reported metformin-loaded polydopamine nanoparticles to overcome the limitation of the metformin in vitro PD model (14). Herein, we have investigated the neurotherapeutic effect of our developed nanoformulation in vivo PD model. The project design of the chapter 3b represented for better understanding of hypothesis, rationale of chapter with justification of the selected compound aligned to expected outcomes of the aims as below.

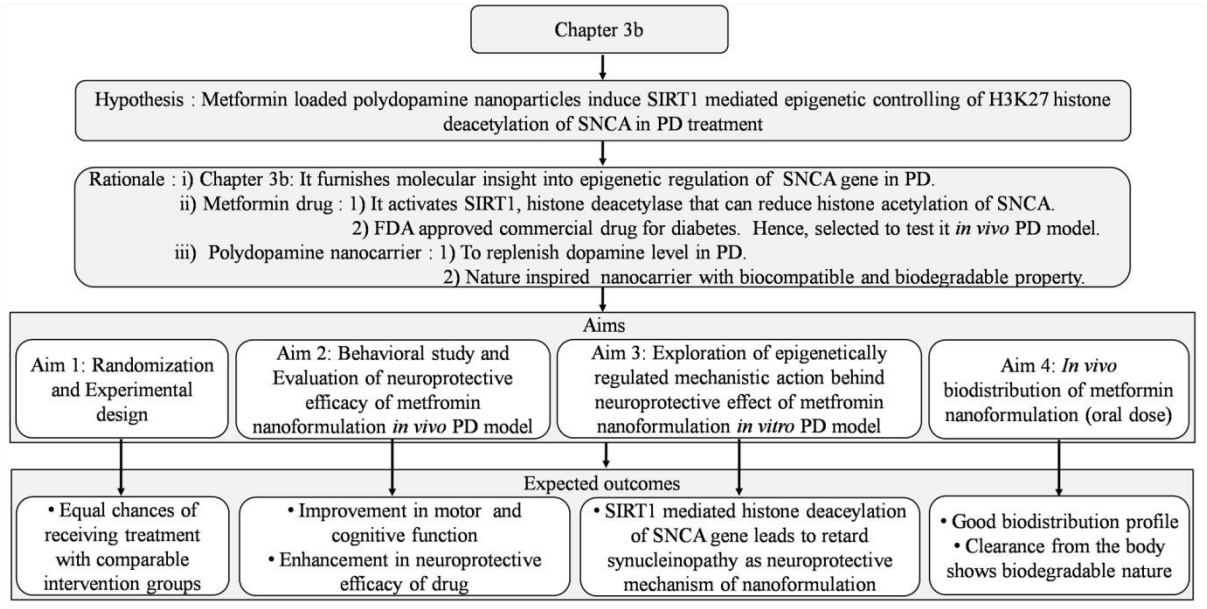


Scheme 4: The project design represents hypothesis, rationale, aims and it's aligned expected outcomes.

In the exploration of the neurotherapeutic action of our reported nanoformulation, we aimed to understand the efficiency of our metformin nanoformulation to control the epigenetic regulator and histone acetylation of SNCA. Metformin is widely reported to induce SIRT1, the histone deacetylase and it is also well documented that reduction of SIRT1 is one of the key factors in

the PD progression. (24-31) However, there is not much evidence that how SIRT1 can modulate the SNCA expression. Therefore, we have for the first time explored the neurotherapeuticefficacy of our developed nanoformulation in vivo. In that, we have first time revealed the metformin nanoformulation induced SIRT1 mediated epigenetic controlling of H3K27 histone deacetylation of SNCA in PD treatment. Thus, the metformin nanoformulation-induced SIRT1-mediated SNCA transcription repression leads to a reduction of synucleinopathy and retardation of PD.

3b.2. Results and discussion

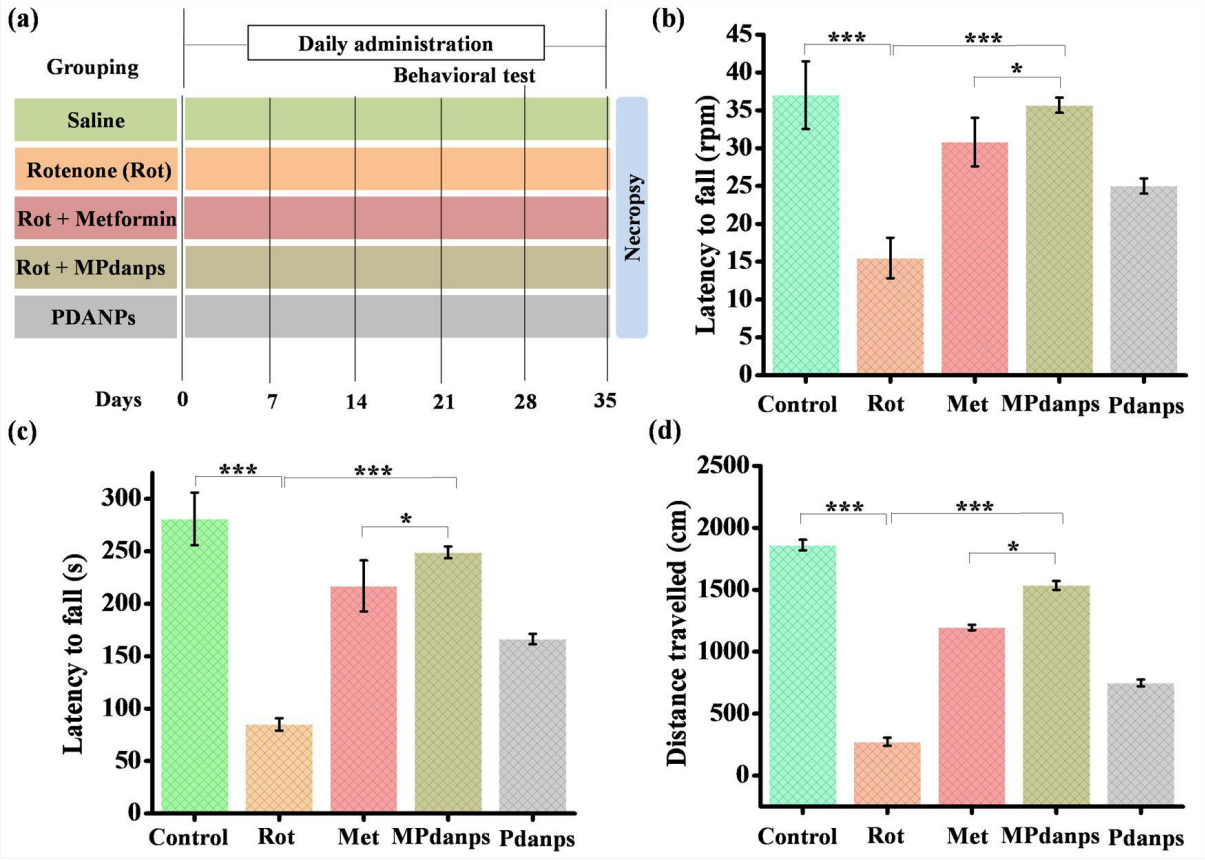


Fig.3.11 Experimental design of the *in vivo* study has shown (a), the rotarod test parameters latency of fall-rpm (b), the latency of fall-sec, and traveled distance (c) reflect the protective effect of our nanoformulation.

3b.2.1. Motor performance signifies the protective effect of Metformin-loaded polydopamine nanoparticles

In the rotarod test, the rats walking on a rotating rod were utilized to examine the motor status in the laboratory setup. All animals were trained before the test and allowed to learn to walk on the rotating rod. Control reached Tmax 300 sec (40rpm) within 2 or 3 trials, whereas the rotenone-treated group has been trained for 7-8 trials to achieve the Tmax 200±30 sec (25±5rpm) during the training. The rats of other treatment groups including MPdanps were also able to learn the walking without any support after 2 or 3 trials with Tmax 280±20 sec (36±4rpm). After making them learn for constitutive four days with at least 4 trials per animal, the test has been performed on the fifth day. The latency to fall has been measured by considering three different parameters to confirm motor dysfunction and recovery. In figure.3.11b, the rotenone-treated group has shown a significant reduction in the motor ability of the animal with latency to fall at 15.5±2.7 rpm.

In contrast, the polydopamine nanoparticles (Pdanps), Metformin (Met), and metformin-loaded polydopamine nanoparticles have exhibited recovery by restoring locomotor activity with latency to fall at 25±1 rpm, 30±3 rpm, and 36±1 rpm, respectively. In support of it, the results of time duration (sec) and traveled distance (cm) with rotation remained by animals on the rotating rod have also suggested a protective effect of our MPdanps. (Fig.3.11c,d) The rotenone effect has diminished the motor activity that has been observed at 85±6 sec and 273±32 cm. In contrast, a significant recovery has been observed with MPdanps treated group that has reverted the rotenone effect by exhibiting 249±6 sec and 1536±35 cm. The result of the rotarod test also divulges that MPdanps has recovered locomotor activity of animals against the rotenone effect in comparison to bare metformin drug and Pdanps. Herein, the rotarod test behavioral test has been performed to indicate the dopaminergic loss and motor neuron dysfunction and the results are in line with the reports that have shown rotenone-induced loss of motor activity and recovery by neuroprotective agents. (32, 33) The results of the rotarod test have shown better neuroprotection efficiency by endowing permanence time (fall of animal) by ~ 3 folds against rotenone-induced damage. The MPdanps exhibited superior protection efficacy in comparison to existing reports of the metformin formulations with ~ 2 folds restoration of locomotory activity in PD treatment. (34, 35)

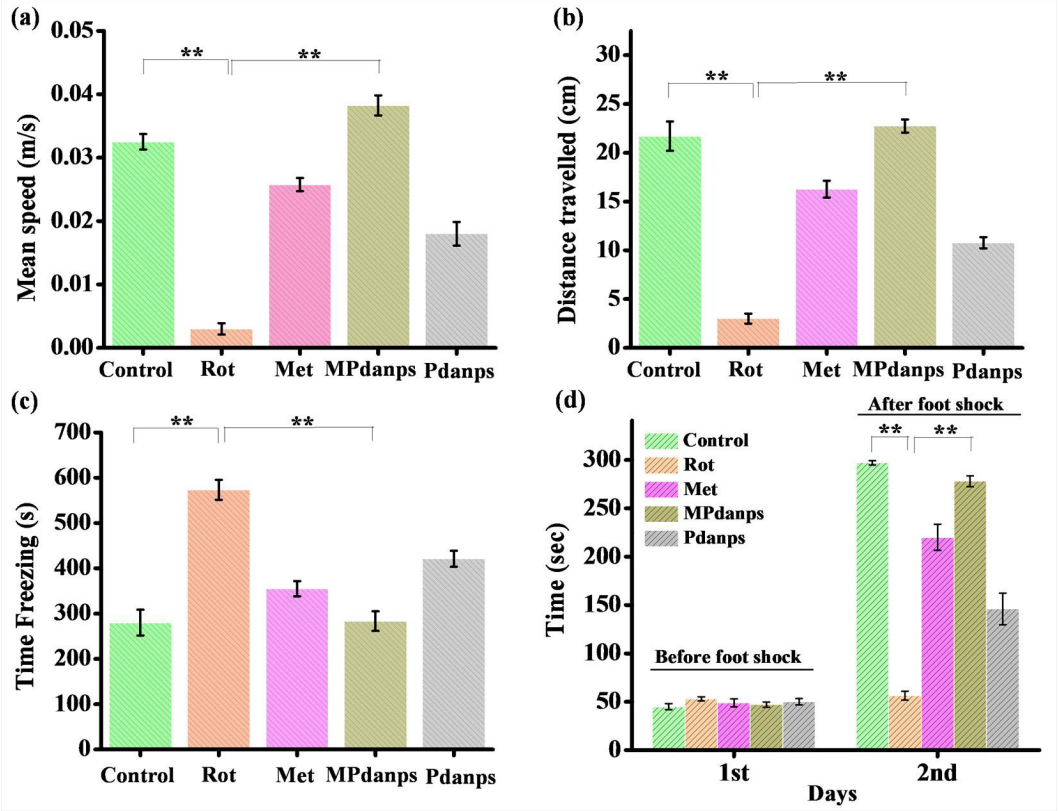


Fig.3.12. Open field test results have been represented with mean speed (a), distance traveled (b), and freezing time (c) showing the recuperative effect of MPdanps against rotenone-induced insults. The cognitive impairment has also been improved with the treatment of nanoformulation that has been tested through passive avoidance test (d).

3b.2.2. Exploratory activity and locomotory activity exhibit neuroprotective effects of nanoformulation

The open field test was also performed to understand the exploratory and locomotor activity. The exploratory activity has been assessed by the distance traveled by the animals which shows how it has been explored. It also indicates its locomotory activity by examining its mean speed of travel. The freeing or immobilized time indicates signs of depression. The rotenone has imposed fatigue and unhealthy situation therefore the locomotory action and exploratory activity have been hampered compared to controlling healthy animal activity. In fig.3.12a, the mean speed of rotenone-treated animals has been obtained at 0.003 m/s, in contrast, recovery against the rotenone effect has been analyzed as a mean speed of 0.025 m/s, 0.038 m/s, and 0.018 m/s for

Met, MPdanps and Pdanps groups, respectively. Similarly, significant restored exploratory activity has been observed with traveled distances of 16 cm, 22 cm, and 10 cm against the rotenone effect showing only 3 cm locomotor activity. (Fig.3.12b) The depression-like behavior has been analyzed by assessing the freezing or immobilized time. The rotenone has shown more immobilized episodes with 573 sec and the reversal action has been noted by the treatment of Met, Pdanps, and MPdanps with lesser freezing times of 375 sec, 283 sec, and 421 sec, respectively. (Fig.3.12c) The representative tracking plot for all treated groups has been also shown in fig.3.13. Herein, the open field test has been employed to reveal the neuroprotective effect of our MPdanps that signifies improved locomotor activity of animals against the rotenone-induced effect. The results have been in line with the existing literature that has demonstrated rotenone-induced damage in the PD condition by behavioral open field test study. Herein, the MPdanps have exhibited better neuroprotective potential by showing similar fold (~2 folds) recovery in mobility with a minimized therapeutic dose of metformin (100mg/kg) in comparison to the existing reported metformin formulations (500 mg/kg). (34, 36) The results of recovered exploratory and depression behavior are also in support of rotarod results that indicate the better neuroprotective effect of MPdanps in comparison to Met and Pdanps.

### 3b.2.3. Metformin loaded Polydopamine nanoparticles alleviate Anxiety like behavior

The anxiety behavior has been observed during the open field test. The field has been differentiated into the peripheral zone and central zone. The time percentage has been spent in the peripheral zone has been accounted which signifies the anxiety level. The rotenone-treated animals have spent a higher time in the immobilized and peripheral zone, while MPdanps have shown a significantly higher percentage of time spent in the central zone. The results show a reduction in anxiety with the treatment of our nanoformulation that has been imposed by rotenone. The graph of time spent in the peripheral zone has been shown in fig.3.13f. The track plot of the open field test also supports the anxiety behavioral analysis. Similar results have been shown by open-field behavioral tests that are in line with the fact that the rotenone-induced effect caused anxiety and depression. (37, 38) The MPdanps exhibited superior improvement (~10 folds) in anxiety behavior in comparison to the existing reported metformin formulation shown ~2 folds recovery from anxiety behavior. (39) Herein, the captured videos for all represented

animals corresponding to their represented track plots of each treatment group have been provided as supporting information.

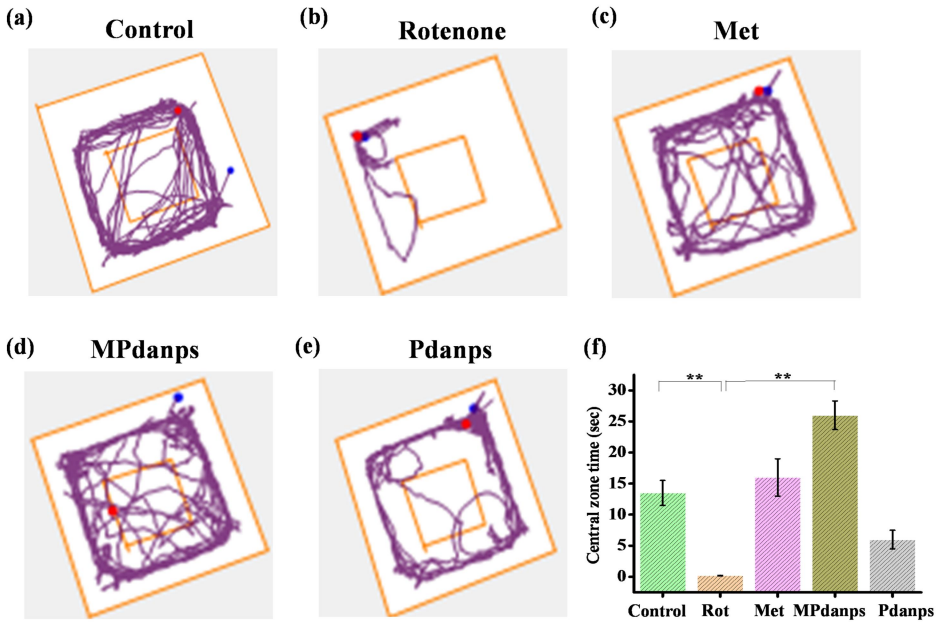


Fig.3.13. The track plot of each represented animal of the treatment group has been shown (a) and the time spent in the central zone of the open field (b) is indicating the anti-anxiety potential of our treatment.

3b.2.4. Metformin loaded Polydopamine nanoparticles improve cognitive impairment

The passive avoidance test is performed to confirm the cognitive impairment caused by rotenone and the neuroprotective effect of our nanoformulation. On a 24-hour retention trial, using a maximum cut-off of 300 sec, the step-through latency (sec) has been marked. The hampered step-through latency has been noted with rotenone-induced damages and that has been recovered through the treatment of our nanoformulations. The rotenone-treated animals have not been able to retain the memory of foot shock and step in the dark chamber within 56 sec. In contrast, a significant improvement has been observed with MPdanps (278 sec), Met (220 sec), and Pdanps (146 sec), respectively. (Fig. 3.12d)

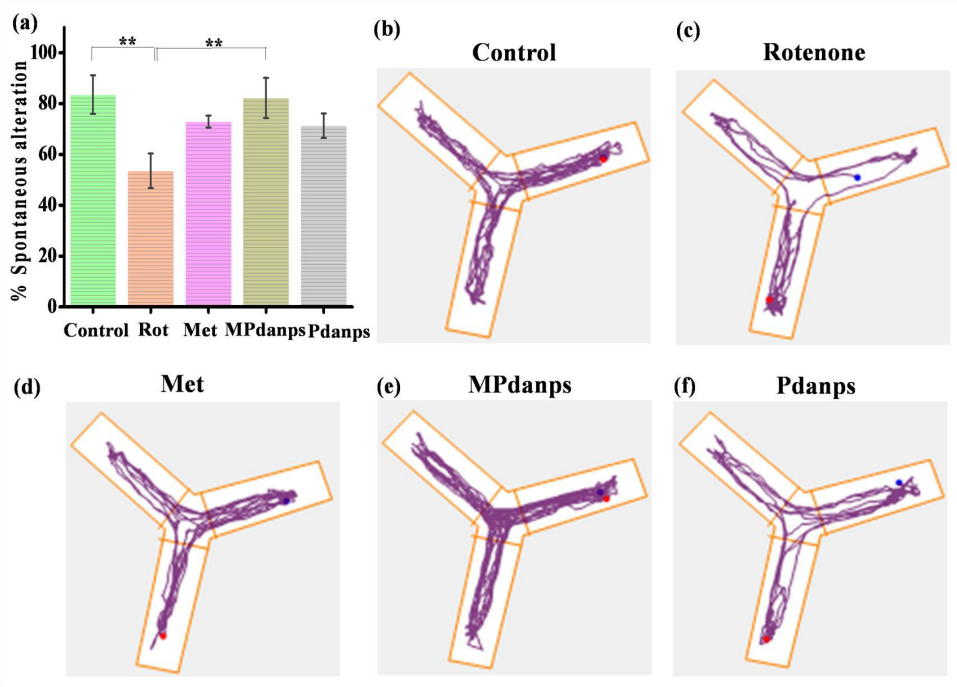


Fig.3.14. Spontaneous alteration test has confirmed the potency of our nanoformulation to improve cognitive impairment (a) and track plots of the representative candidate per group have been shown (b).

The spontaneous alternation has been also assessed through the Y-maze test to understand the cognitive impairment. Rotenone has been widely reported that induced cognitive impairment associated with PD condition. (40, 41) We also found similar results that showed a 53.56% alteration from the A-B-C arm. However, the recovery in the alteration percentage has been noted for the Met, MPdanps, and Pdanps with 73%, 83%, and 71%, respectively. (Fig.3.14a) Here also the neuroprotective effect of MPdanps has been observed better in comparison to Met and Pdanps. The results indicate the neuroprotective effect of our nanoformulation that can improve cognitive impairment also. The representative track plot for each treated group has been shown in Fig.3.14.

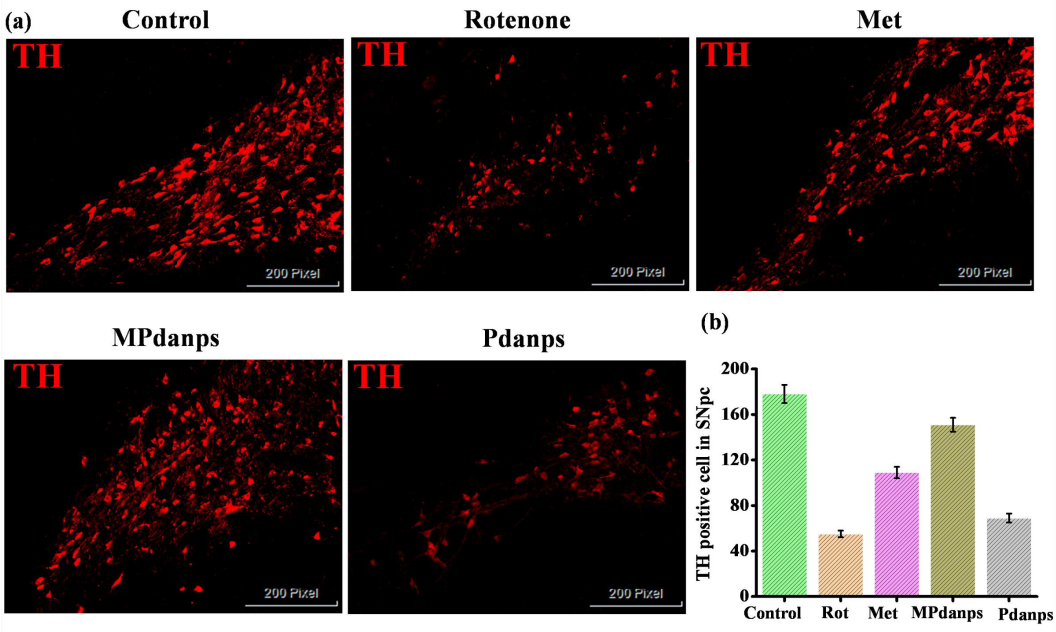


Fig.3.15. The neurotherapeutic effect of MPdanps has been confirmed by analyzing TH expression in SNpc (a) and the TH positive neuron quantification has been also illustrated (b).

### 3b.2.5. Metformin loaded Polydopamine nanoparticles restore $TH^+$ neurons

TH is the rate-limiting enzyme in the process of dopamine synthesis and the hallmark of dopaminergic neurons. Immunofluorescence imaging of substantial nigra has been conducted to analyze the rotenone effect and confirm the PD model. The $TH^+$ neurons and fibers have been stained and quantified based on fluorescence intensity. The loss of dopaminergic neurons leads to the loss of the neurotransmitter dopamine resulting in PD conditions. The higher loss of dopaminergic neurons has been analyzed with rotenone-treated groups and the recovery has been observed with the treatment of MPdanps. (Fig.3.15) Herein, the MPdanps has exhibited the highest recovery of $TH^+$ neurons to Pdanps and Met. Hence, it is proved that MPdanps recuperate the rotenone-induced PD deficits in the rat model. The *in vivo* study results are also supported by our previously reported neuroprotective effects of metformin-loaded polydopamine nanoparticles *in vitro* and *ex vivo* experimental PD models. (14) The results are also in line with the reports that have shown the depletion of $TH^+$ neurons as a sign of PD and its restoration by metformin as a neuroprotective agent. Our nanoformulation has shown superior restoration of dopaminergic neuron cells against the effect of PD-inducing agent in comparison to existing reported

metformin formulation. (34, 35) The plausible reason for better neuroprotective efficiency is that our formulation has shown endowment in the efficacy of metformin by improving its drug kinetics which is reported previously. (14)

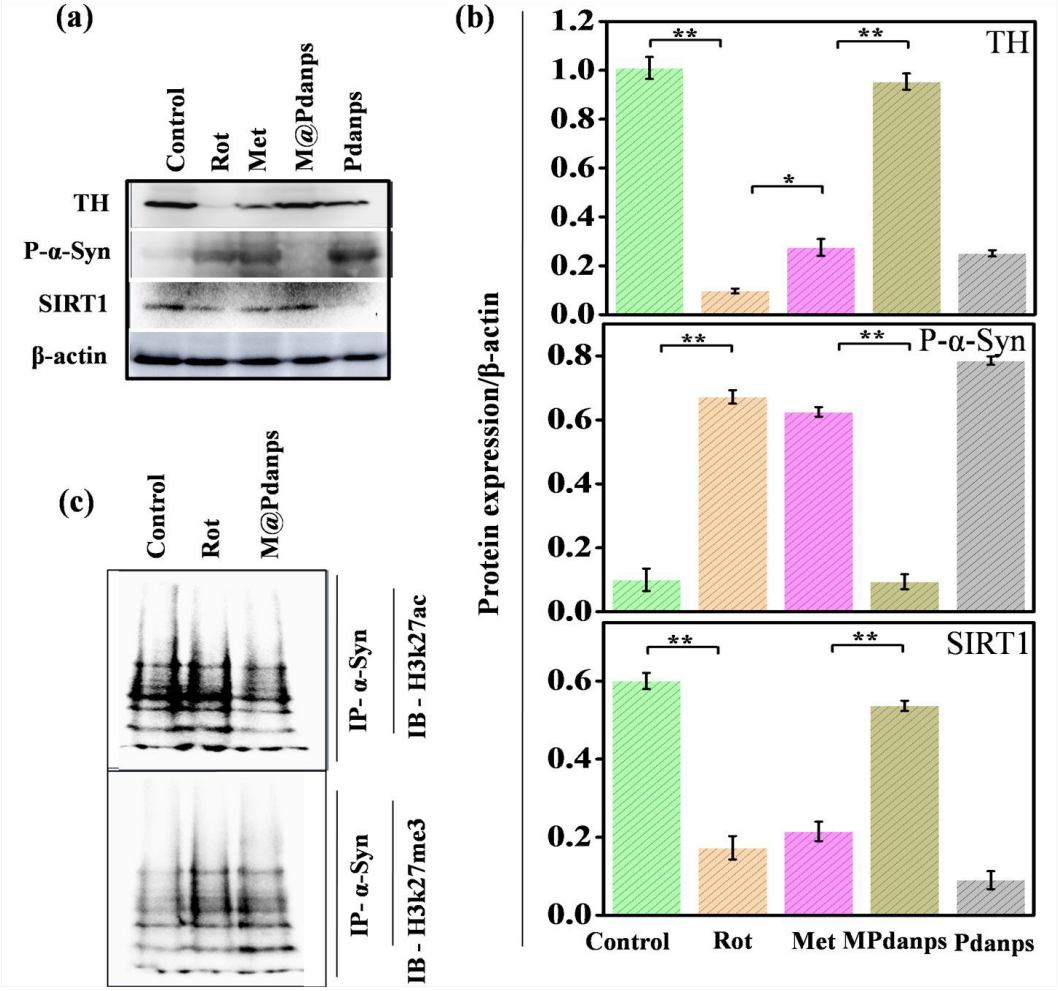


Fig.3.16. Protein expression analysis has validated the neurotherapeutic efficacy of MPdanps (a) and the quantified protein expression has been represented (b). The immunoprecipitation study is also showing the effect of MPdanps that induced SIRT1 and due to that histone deacetylation in the treatment group has been observed. (c)

3b.2.6. Mechanistic Insight into Neuroprotective action of Metformin loaded Polydopamine nanoparticles

The rotenone effect for PD induction and restoration of rotenone-induced damages by our nanoformulation has been confirmed by investigating PD molecular hallmarks, TH, and p-alpha synuclein. The upregulation of alpha-synuclein and reduction of TH has been widely reported in PD pathogenesis and its reversal effect leads the way toward PD treatment. (42, 43) In fig.3.16a, the results of protein expression analysis confirmed the PD model by estimating the expression of TH and p-alpha-synuclein, the PD signature molecular markers. The TH expression has been found ~10 folds reduced by rotenone that has been restored with the MPdanps treatment. Our metformin nanoformulation has shown impressive results by restoring ~10 folds of TH expression in comparison to the reported literature that shows nearly ~ 2 folds restoration of TH with their metformin formulation. (44) Similarly, p-alpha-synuclein also found ~ 6-folds elevated due to the rotenone effect, and the recuperative effect of MPdanps has been observed by downregulating p-alpha-synuclein expression by 6 folds. This result reflects the superior neuroprotective effect of our nanoformulation in comparison to an existing report of metformin that shows ~ 2 folds reduction in alpha-synuclein expression. (22). The quantification of protein expression analysis has been represented in fig.3.16b. Herein, TH is the rate-limiting enzyme required in dopamine synthesis and its depletion leads to scarcity of dopamine and ends in PD deficits. (42) Similarly, post-translational modification of alpha-synuclein also contributes to the formation of the Lewy body in PD progression, especially phosphorylated alpha-synuclein has been found in higher content in the Lewy body formation. Hence, it is the hallmark of PD. (43) Therefore, TH depletion and phosphorylated alpha-synuclein upregulation in the case of rotenone validate *in vivo* PD model of the present study. The restoration of TH and downregulation of phosphorylated alpha-synuclein also proved the neurotherapeutic effect of MPdanps. Herein, MPdanps have shown better protection against rotenone in comparison to Met and Pdanps also in line with the results of the behavioral study and IHC study.

In the exploration of epigenetic intervention in the neuroprotective mechanism of our nanoformulation, SIRT1 has been analyzed due to metformin's potential to induce SIRT1 expression. (24) Herein, epigenetic regulation in PD intervention is a promising therapeutic way to investigate PD etiology and treatment. The histone modifications and their mediated

transcriptional regulation are gaining more and more attention recently. The hyperacetylation of histone is widely reported in PD conditions. (8, 29, 30, 45, 46) Indeed, the histone hyperacetylation of the SNCA gene is also well demonstrated. (9, 10, 30, 47) That's how the strategy to deacetylate histone of SNCA paves the way for PD treatment has been developed by the present study. Recently, metformin has emerged as a promising neurotherapeutic agent having the potential to activate SIRT1. (48-50) SIRT1 is the well-studied class III histone deacetylase that is majorly involved in the deacetylation of histone H3.(51, 52) The SIRT1-mediated neuroprotective action that induces autophagy to treat PD has also been reported. (53) However, there is no well-understood mechanism discovered whether SIRT1 regulates the transcription of SNCA or not. Therefore, we explored the metformin nanoformulation-mediated SIRT1 activation and its effect on the transcription repression of SNCA that leads to alleviating synucleinopathy. The depletion of the SIRT1 level also supports the reports that have demonstrated that SIRT1 reduction is also involved in PD progression. (27) The rotenone has ~3-fold reduced SIRT1 that has been restored by the neuroprotective effect of MPdanps. The question is whether SIRT1 depletion affects histone acetylation, especially H3k27ac which is majorly involved in SNCA transcription activation. (26, 30) Therefore, an immunoprecipitation assay has been performed to reveal the expression level of H3k27ac and H3k27me3 associated with alpha-synuclein. Interestingly, the results have shown that higher histone acetylation (H3k27ac) and reduced histone methylation, H3k27me3 level that associated with synuclein in the rotenone-treated group (Fig.3.16c). The H3K27ac upregulation and H3K27me3 reduction involved in SNCA transcription activation and inhibition of H3k27ac and upregulation of H3k27me3 of SNCA gene lead to repression of SNCA gene expression. (7, 54) Therefore, the reported literature about hyperacetylation of H3k27 in PD conditions supports our finding that a higher H3k27ac level is associated with synuclein. (9, 10, 30, 47) To validate the effect of MPdanps-mediated SIRT1 activation and its effect on SNCA transcription regulation, a chromatin immunoprecipitation assay has been performed (Fig.3.17). The results have proved that a higher association or binding of H3k27ac has been analyzed with the SNCA promoter region in the case of rotenone treatment. In contrast, MPdanps-mediated SIRT1-induced histone deacetylation leads to a reduction in H3k27ac-assisted SNCA transcription activation and synuclein expression. Therefore, several pieces of evidence divulge that MPdanps shows neuroprotection action by SIRT1-mediated deacetylation of H3k27 of SNCA. Thus, the

reduction in the synuclein expression through transcription regulation paves the way for PD treatment. Herein, as per our best knowledge, the present study has first time revealed the epigenetic effect of metformin nanoformulation that induced SIRT1 mediated H3K27 deacetylation in the repression of SNCA gene to alleviate the PD condition.

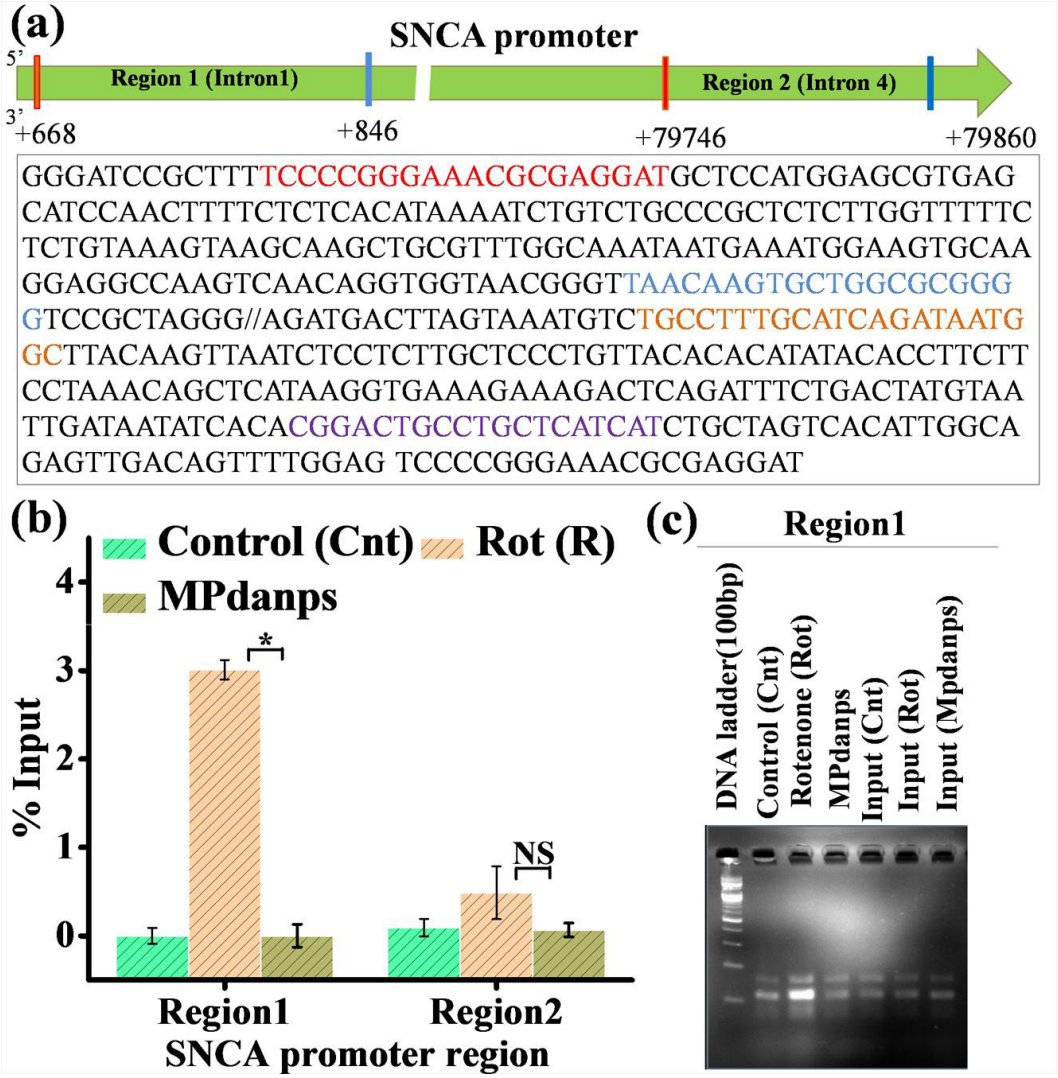


Fig.3.17 The SNCA gene promoter and epigenetic landscape of H3K27ac has been described (a). The ChIP results have divulged the SIRT1-mediated deacetylation of H3K27ac of the SNCA gene that leads to the reduction of synuclein.

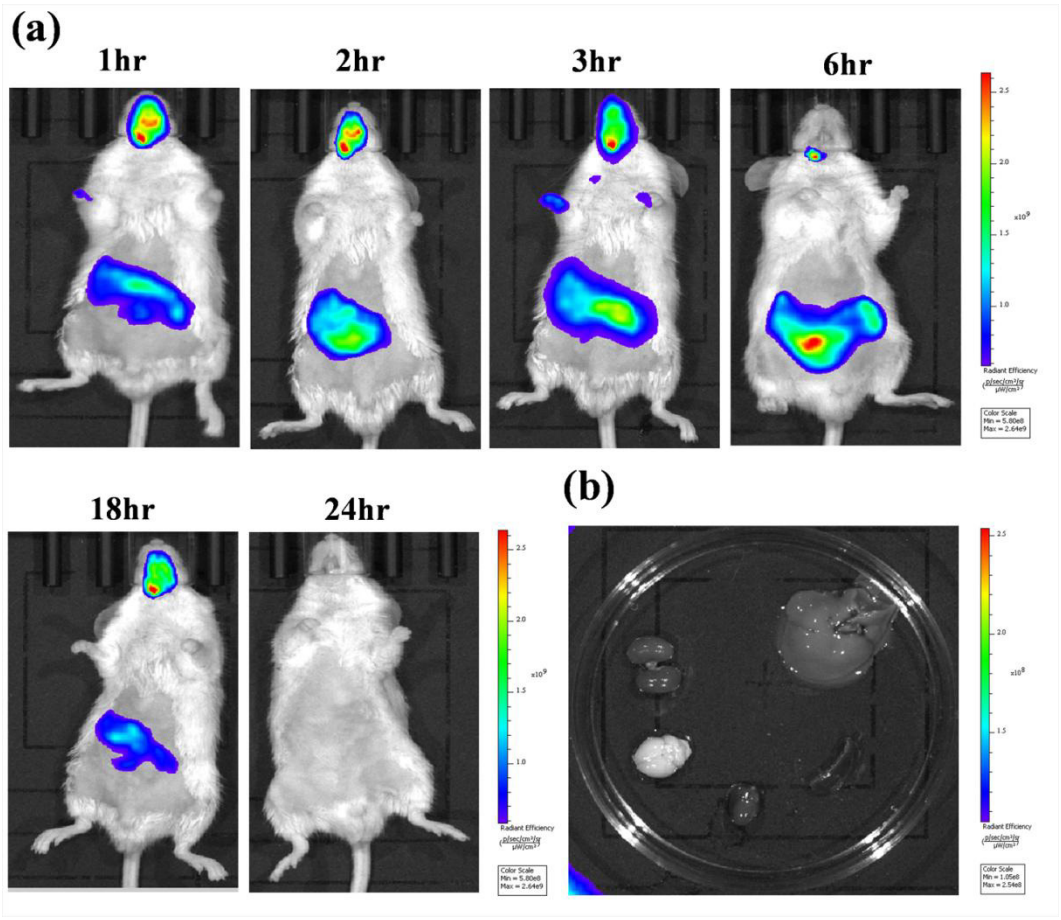


Fig.3.18. The *in vivo* (a) and *ex vivo* (b) biodistribution study indicates the clearance and good distribution profile of MPdanps.

3b.2.7. *In vivo* bio-distribution of Mpdanps reflects clearance of nanoformulation

*In vivo* biodistribution of ICG (Indocyanine Green) tagged MPdanps has been investigated to understand its clearance and distribution for 24 hours. The nanoformulation has shown a good biodistribution profile from oral to gut and brain, kidney. (Fig.3.18a) The initial hours till 6 hours, it has been passed to the brain which has been also supported by our previous report. (14)A high accumulation of particles in the kidney and gut indicates the clearance path of our oral nanoformulation. The 24-hour image of the animal is showing total clearance of the nanoformulation and confirmation of the *ex vivo* images of the organ 24 hours post-injection also proves the complete clearance of the nanoformulation. (Fig.3.18b) Herein, the plausible reason for our nanoformulation clearances is its biodegradable property that follows the degradation

pattern of melanosomes due to its nature-inspired features. (55) The results are also in accordance with our daily basis dosing of nanoformulation throughout the study that provides the rationale for the selection of dose duration due to its complete clearance from the body system. Thus, our nanoformulation has the potential to be a suitable nano-drug delivery system in the treatment of PD.

### 3b.3 Conclusion

In the overall finding of the presented work, we reported metformin-loaded polydopamine nanoparticles as an anti-PD agent by evaluating its neuroprtoective efficacy *in vivo* PD model. The key findings of the major studies like behavioural analysis exhibited immense protective potential by recovering the locomotor activity and cognitive behavior of animals against the rotenone-induced PD effect. In addition, therapeutic assessment of $TH^+$ neurons in SNpc region divulges the neuroprotective potential of presented nanoformulation in preclinical setup. The validation through the molecular expression of PD hallmarks also confirms the neuroprotective efficiency of our nanoformulation as major key finding. The significance and novelty of work is that the metformin nanoformulation neuroprotective action attributed to SIRT1 mediated deacetylation of H3k27 of the SNCA gene. In that, the evidence of immunoprecipitation and chromatin immunoprecipitation results has confirmed that our nanoformulation has the potential to reduce histone acetylation of SNCA as epigenetic regulation in PD treatment. Thus, the presented formulation has the immense potential that can epigenetically regulate the synuclein expression to pave the new dimension in PD therapy with multimodal approach of metformin nanoformulation. However, a detailed investigation of the SIRT1-induced SNCA gene repression is warranted in future studies. The presented nanoformulation has impressive result outcomes, however it lacking by safety study with long term effect and absence of commercial available PD drug as positive control in the study. As per our best knowledge no report is available in the public domain with metformin loaded nanoformulation in PD animal model study. The presented formulation may provide the solution to overcome side effect of levodopamine, a commercially available PD drug. In early stage of assessment, the finding of our nanoformulation is promising and comparable to behavioural data shown by levodopamine *in vivo* PD model. (56) All other reports of levodopamine are related to clinical study in PD patient that cannot be comparable to

presented preclinical data of animal study. In the translational application of the presented nanoformulation, bulk synthesis of unimodal nanoparticles and their long-term toxicity may be the challenges and limitations for the metformin nanoformulation. However, the results of the present study clearly divulge the neuroprotective caliber of our metformin nanoformulation as an epigenetic modulator that may be useful for the potential treatment of PD in a clinical setup.

3b.4 References


1. U. Muthane, M. Ragothaman, G. J. J. Gururaj, Epidemiology of Parkinson's disease and movement disorders in India: problems and possibilities. **55**, 719-724 (2007).
2. W. Poewe *et al.*, Parkinson's disease. **3**, 1-21 (2017).
3. I. J. Siddiqui, N. Pervaiz, A. A. Abbasi, The Parkinson Disease gene SNCA: Evolutionary and structural insights with pathological implication. *Scientific reports* **6**, 24475-24475 (2016).
4. L. Stefanis, α-Synuclein in Parkinson's disease. *Cold Spring Harb Perspect Med* **2**, a009399-a009399 (2012).
5. B. Thomas, M. F. Beal, Parkinson's disease. *Human molecular genetics* **16 Spec No. 2**, R183-194 (2007).
6. M. H. Polymeropoulos *et al.*, Mutation in the alpha-synuclein gene identified in families with Parkinson's disease. *Science* **276**, 2045-2047 (1997).
7. C. Labbé, O. Lorenzo-Betancor, O. A. Ross, Epigenetic regulation in Parkinson's disease. *Acta neuropathologica* **132**, 515-530 (2016).
8. M. Huang *et al.*, Mitochondrial dysfunction–induced H3K27 hyperacetylation perturbs enhancers in Parkinson's disease. *JCI Insight* **6** (2021).
9. S. Guhathakurta, E. Bok, B. A. Evangelista, Y.-S. Kim, Deregulation of α-synuclein in Parkinson's disease: Insight from epigenetic structure and transcriptional regulation of SNCA. *Prog Neurobiol* **154**, 21-36 (2017).
10. S. Guhathakurta *et al.*, Targeted attenuation of elevated histone marks at SNCA alleviates α-synuclein in Parkinson's disease. *EMBO Mol Med* **13**, e12188-e12188 (2021).
11. E. Sodersten *et al.*, others. 2014. Dopamine signaling leads to loss of Polycomb repression and aberrant gene activation in experimental parkinsonism. **10**, e1004574.

12. I. Wever, L. von Oerthel, C. M. R. J. Wagemans, M. P. Smidt, EZH2 Influences mdDA Neuronal Differentiation, Maintenance and Survival. **11** (2019).
13. B. S. Basavarajappa, S. Subbanna, Histone Methylation Regulation in Neurodegenerative Disorders. **22**, 4654 (2021).
14. M. N. Sardoiwala, A. K. Srivastava, B. Kaundal, S. Karmakar, S. R. Choudhury, Recuperative effect of metformin loaded polydopamine nanoformulation promoting EZH2 mediated proteasomal degradation of phospho-α-synuclein in Parkinson's disease model. *Nanomedicine: Nanotechnology, Biology and Medicine* **24**, 102088 (2020).
15. P. Hickey, M. J. D. d. Stacy, development, therapy, Available and emerging treatments for Parkinson's disease: a review. **5**, 241 (2011).
16. B. D. Li *et al.*, Adverse effects produced by different drugs used in the treatment of Parkinson's disease: a mixed treatment comparison. **23**, 827-842 (2017).
17. M. Foretz, B. J. N. R. E. Viollet, Metformin takes a new route to clinical efficacy. **11**, 390-392 (2015).
18. M. Clyne, Metformin—the new wonder drug? *Nature Reviews Urology* **11**, 366-366 (2014).
19. M. L. Wahlqvist *et al.*, Metformin-inclusive sulfonylurea therapy reduces the risk of Parkinson's disease occurring with Type 2 diabetes in a Taiwanese population cohort. **18**, 753-758 (2012).
20. Y. Liu *et al.*, Metformin attenuates blood-brain barrier disruption in mice following middle cerebral artery occlusion. *J Neuroinflammation* **11**, 177-177 (2014).
21. Y. Lin *et al.*, Evaluation of Metformin on Cognitive Improvement in Patients With Non-dementia Vascular Cognitive Impairment and Abnormal Glucose Metabolism. *Front Aging Neurosci* **10**, 227-227 (2018).
22. M. Lu *et al.*, Metformin prevents dopaminergic neuron death in MPTP/P-induced mouse model of Parkinson's disease via autophagy and mitochondrial ROS clearance. **19** (2016).
23. M. Kinaan, H. Ding, C. R. J. M. p. Triggle, practice, Metformin: an old drug for the treatment of diabetes but a new drug for the protection of the endothelium. **24**, 401-415 (2015).
24. E. Cuyàs *et al.*, Metformin Is a Direct SIRT1-Activating Compound: Computational Modeling and Experimental Validation. **9** (2018).

25. Y.-J. Guo *et al.*, Resveratrol alleviates MPTP-induced motor impairments and pathological changes by autophagic degradation of α-synuclein via SIRT1-deacetylated LC3. *Mol Nutr Food Res* **60**, 2161-2175 (2016).
26. P. Singh, P. S. Hanson, C. M. Morris, SIRT1 ameliorates oxidative stress induced neural cell death and is down-regulated in Parkinson's disease. *BMC Neuroscience* **18**, 46 (2017).
27. R. Manjula, K. Anuja, F. J. Alcain, SIRT1 and SIRT2 Activity Control in Neurodegenerative Diseases. **11** (2021).
28. A. Zhang, H. Wang, X. Qin, S. Pang, B. Yan, Genetic analysis of SIRT1 gene promoter in sporadic Parkinson's disease. *Biochemical and Biophysical Research Communications* **422**, 693-696 (2012).
29. L. Toker *et al.*, Genome-wide dysregulation of histone acetylation in the Parkinson's disease brain. *bioRxiv* 10.1101/785550, 785550 (2020).
30. L. Toker *et al.*, Genome-wide histone acetylation analysis reveals altered transcriptional regulation in the Parkinson's disease brain. *Molecular Neurodegeneration* **16**, 31 (2021).
31. B. Sampaio-Marques *et al.*, SNCA (α-synuclein)-induced toxicity in yeast cells is dependent on Sir2-mediated mitophagy. *Autophagy* **8**, 1494-1509 (2012).
32. A. Jangra, A. K. Datusalia, S. Khandwe, S. S. Sharma, Amelioration of diabetes-induced neurobehavioral and neurochemical changes by melatonin and nicotinamide: Implication of oxidative stress–PARP pathway. *Pharmacology Biochemistry and Behavior* **114-115**, 43-51 (2013).
33. P. Zhao *et al.*, Neuroprotective effects of fingolimod in mouse models of Parkinson's disease. *FASEB journal : official publication of the Federation of American Societies for Experimental Biology* **31**, 172-179 (2017).
34. S. P. Patil, P. D. Jain, P. J. Ghumatkar, R. Tambe, S. Sathaye, Neuroprotective effect of metformin in MPTP-induced Parkinson's disease in mice. *Neuroscience* **277**, 747-754 (2014).
35. S. H. El-Ghaiesh *et al.*, Metformin Protects From Rotenone–Induced Nigrostriatal Neuronal Death in Adult Mice by Activating AMPK-FOXO3 Signaling and Mitigation of Angiogenesis. **13** (2020).

36. L.-Y. Wang *et al.*, Catalpol Exerts a Neuroprotective Effect in the MPTP Mouse Model of Parkinson's Disease. **11** (2019).
37. M. L. Seibenhener, M. C. Wooten, Use of the Open Field Maze to measure locomotor and anxiety-like behavior in mice. *J Vis Exp* 10.3791/52434, e52434-e52434 (2015).
38. X. Zhao *et al.*, Baicalein alleviates depression-like behavior in rotenone- induced Parkinson's disease model in mice through activating the BDNF/TrkB/CREB pathway. *Biomedicine & Pharmacotherapy* **140**, 111556 (2021).
39. S. Ji, L. Wang, L. Li, Effect of Metformin on Short-Term High-Fat Diet-Induced Weight Gain and Anxiety-Like Behavior and the Gut Microbiota. **10** (2019).
40. I. O. Ishola *et al.*, Morin ameliorates rotenone-induced Parkinson disease in mice through antioxidation and anti-neuroinflammation: gut-brain axis involvement. *Brain Research* **1789**, 147958 (2022).
41. D. Zhang *et al.*, Microglial activation contributes to cognitive impairments in rotenone-induced mouse Parkinson's disease model. *Journal of neuroinflammation* **18**, 4-4 (2021).
42. G. Alam, J. R. Richardson, "Chapter 4 - Regulation of tyrosine hydroxylase: relevance to Parkinson's disease" in Genetics, Neurology, Behavior, and Diet in Parkinson's Disease, C. R. Martin, V. R. Preedy, Eds. (Academic Press, 2020), https://doi.org/10.1016/B978-0-12-815950-7.00004-7, pp. 51-66.
43. M. Gómez-Benito *et al.*, Modeling Parkinson's Disease With the Alpha-Synuclein Protein. *Frontiers in pharmacology* **11**, 356 (2020).
44. N. Katila *et al.*, Metformin lowers α-synuclein phosphorylation and upregulates neurotrophic factor in the MPTP mouse model of Parkinson's disease. *Neuropharmacology* **125**, 396-407 (2017).
45. G. Park *et al.*, Regulation of Histone Acetylation by Autophagy in Parkinson Disease. *J Biol Chem* **291**, 3531-3540 (2016).
46. R. Wang, H. Sun, G. Wang, H. Ren, Imbalance of Lysine Acetylation Contributes to the Pathogenesis of Parkinson's Disease. *Int J Mol Sci* **21** (2020).
47. P. Liu *et al.*, PAR2-mediated epigenetic upregulation of α-synuclein contributes to the pathogenesis of Parkinson′s disease. *Brain Res* **1565**, 82-89 (2014).

48. M. Markowicz-Piasecka *et al.*, Metformin - a Future Therapy for Neurodegenerative Diseases : Theme: Drug Discovery, Development and Delivery in Alzheimer's Disease Guest Editor: Davide Brambilla. *Pharm Res* **34**, 2614-2627 (2017).
49. Y. M. Song *et al.*, Metformin alleviates hepatosteatosis by restoring SIRT1-mediated autophagy induction via an AMP-activated protein kinase-independent pathway. *Autophagy* **11**, 46-59 (2015).
50. P. S. Pardo, A. M. Boriek, SIRT1 Regulation in Ageing and Obesity. *Mechanisms of Ageing and Development* **188**, 111249 (2020).
51. S. Gandhi *et al.*, Mitotic H3K9ac is controlled by phase-specific activity of HDAC2, HDAC3, and SIRT1. *Life Science Alliance* **5**, e202201433 (2022).
52. H. Gan *et al.*, B cell Sirt1 deacetylates histone and non-histone proteins for epigenetic modulation of AID expression and the antibody response. *Science advances* **6**, eaay2793 (2020).
53. I. H. Lee, Mechanisms and disease implications of sirtuin-mediated autophagic regulation. *Experimental & Molecular Medicine* **51**, 1-11 (2019).
54. E. Södersten *et al.*, Dopamine signaling leads to loss of Polycomb repression and aberrant gene activation in experimental parkinsonism. *PLoS Genet* **10**, e1004574-e1004574 (2014).
55. Y. Huang *et al.*, Mimicking Melanosomes: Polydopamine Nanoparticles as Artificial Microparasols. *ACS Central Science* **3**, 564-569 (2017).
56. P. Bagga, A. N. Chugani, K. S. Varadarajan, A. B. Patel, In vivo NMR studies of regional cerebral energetics in MPTP model of Parkinson's disease: recovery of cerebral metabolism with acute levodopa treatment. **127**, 365-377 (2013).

# Chapter 4a

---

# FTY720 loaded chitosan nanoformulations alleviate PD *in vitro* and *ex vivo* model

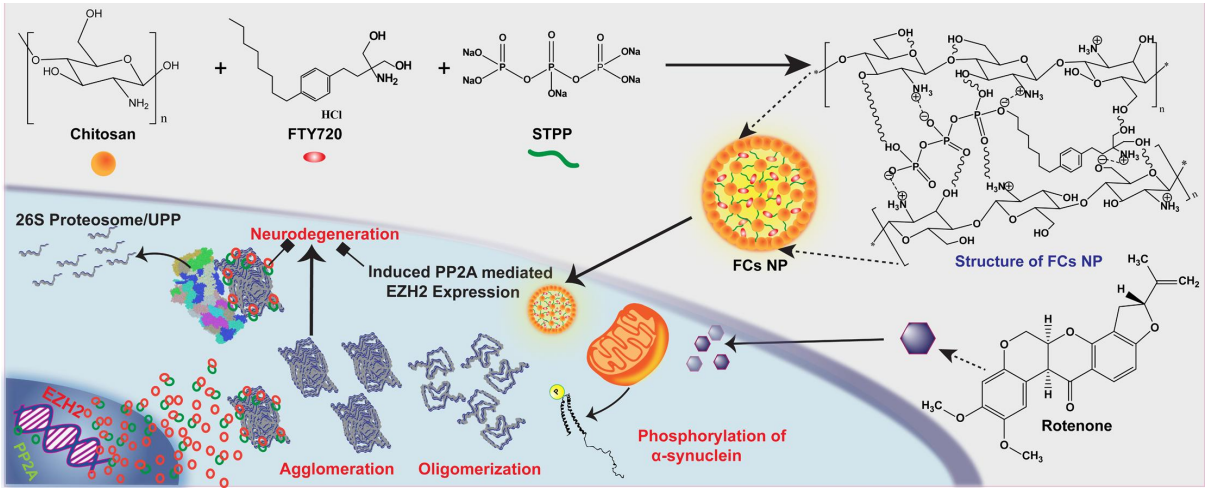

## 4a.1. Introduction

Parkinson's disease (PD) is a chronic neurodegenerative infirmity that progresses due to the degeneration of dopaminergic neurons as a cause of aggregated phospho-(ser 129) α-Syn. (1) The exact causes of the death of dopaminergic neurons are still unresolved. Mitochondrial dysfunction-inducing synucleinopathy leads to PD pathogenesis emphasizing the therapeutic targeting of phosphorylated α-Syn. (2) In the prevention of synucleinopathy associated with PD, pharmacological therapies and deep brain stimulation surgery has been found impressive. (3) Although, effective PD-controlling treatment is warranted because of the multiple side effects of existing treatments. (4) Recently, PP2A activator FTY720 has gained attention to prevent neurodegenerative and other nervous system-associated infirmities. (5, 6) FTY720 attenuates the PD progression by dephosphorylating α-Syn as an effective preventing mechanism. (2) The reported studies demonstrated the efficiency of FTY720 to cross the blood-brain barrier (BBB) (7), comprising anti-oxidative and anti-inflammatory properties(6) but the detailed neuroprotective activities of FTY720 are still unexplored. Besides having neurotherapeutic potential, FTY720 shows less bio-availability and a risk of severe infection. (8) Notably, free FTY720 has less stability in aqueous/buffer solutions of animal cell culture medium to study drug therapeutic effects. (9) The reports also have shown that it has very less solubility 0.2mg/ml in 1:1 ethanol: aqueous solution. Hence, a promising nano delivery approach has been considered to surpass the limitations of bare FTY720. (10) Therefore, we have demonstrated FTY720 loaded chitosan nanoparticles (FCsNPs) to improve their bioavailability and release kinetics in the present study. Herein, we aim to improve the drug release profile, and bio-availability of FTY720 through a neuroprotective nanocarrier, chitosan. Reports have rendered chitosan nanoparticles (CsNPs) as neuroprotective, anti-oxidant, and bio-compatible materials. (11, 12) Therefore, CsNPs were used to deliver FTY720 to combat PD.

Epigenetic regulation is a promising mechanism to explore PD regulation. Epigenetic regulators of polycomb repressor complexes 1 and 2 (PRC1/2) are gaining attention in PD maintenance. Enhancer of zeste homolog 2 (EzH2), a member of the PRC2 complex is vital for the maintenance of neuronal activities, and its deficiency leads to neurodegeneration including Parkinsonism. (13, 14) Similarly, B cell-specific Moloney murine leukemia virus integration site 1 (Bmi1), a member of PRC1 has been studied as a regulator of neuronal fate. (15) However, the

detailed mechanism of neuroprotection by PRC1/2 in PD has not been explored yet. A recent report has revealed that human polycomb protein 2, PRC1 member augments SUMOylation of α-Syn results in synucleinopathy. (16) Another report has enlightened the fact about SUMOylation and ubiquitination as reciprocal phenomena in the regulation of Synucleinopathy. (17) We recently reported the role of EzH2 in PD prevention via the reduction of α-synucleinopathy. (18) Herein, chitosan nanoformulation-mediated PP2A-EzH2 signaling for PD prevention has been investigated. As per current knowledge, this is the first report that has shown the interlinking of PP2A and EzH2 in the regulation of PD and demonstrated the synergistic neuroprotective effect of chitosan and FTY720 at a single platform.The project design of the chapter 3b represented for better understanding of hypothesis, rationale of chapter with justification of the selected compound aligned to expected outcomes of the aims as below.

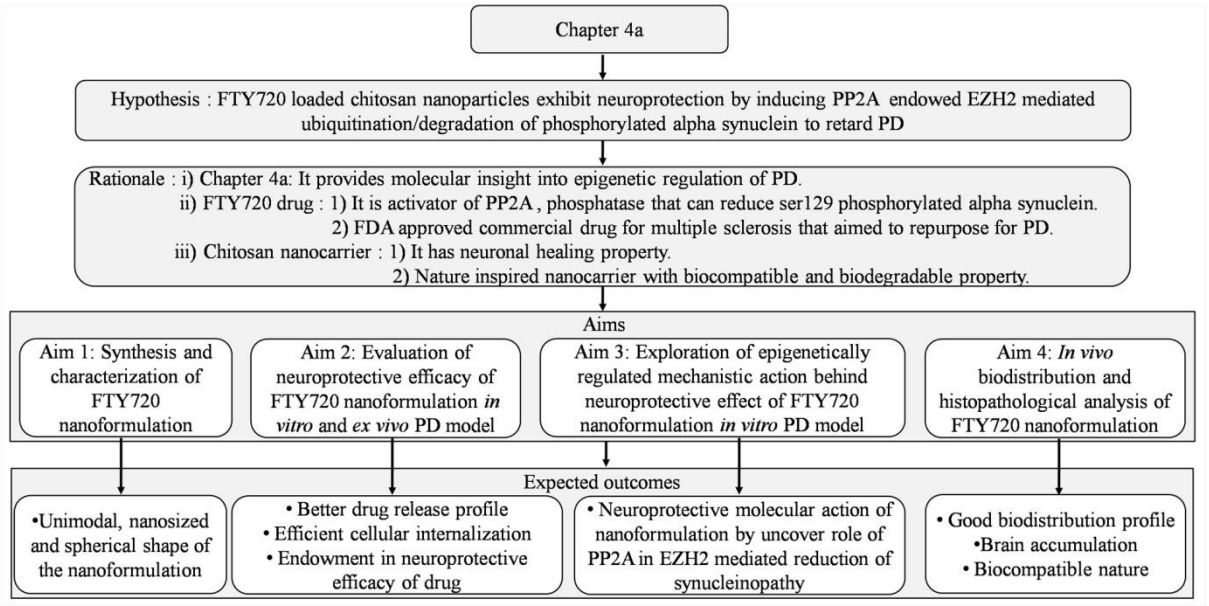


Scheme 5: The project design represents hypothesis, rationale, aims and it's aligned expected outcomes.

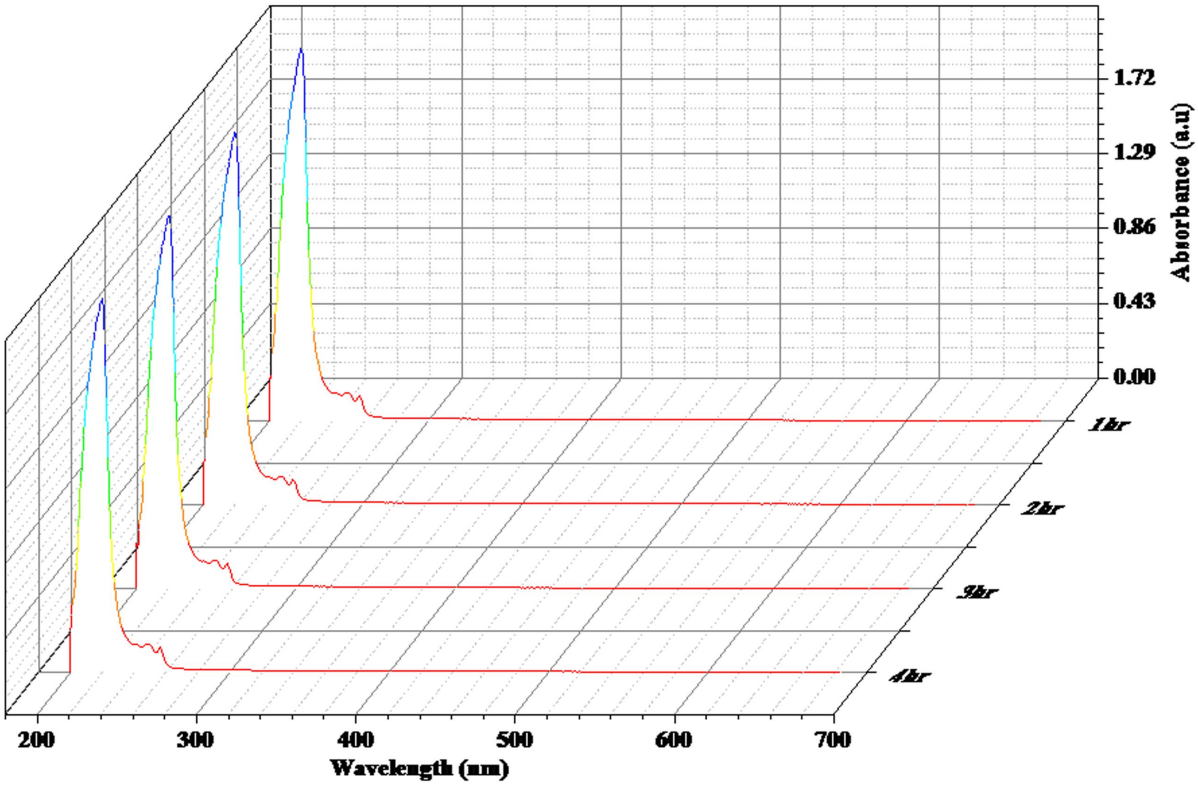


Fig.4.1 The Uv absorbance spectroscopy measurement shows the stability of FTY720 at pH 4 till 4 hours of exposure.

## 4a.2. Result and Discussion

### 4a.2.1. Synthesis and characterization of Chitosan-based FTY720 nanoformulation

CsNPs and FCsNPs were synthesized by the ion gelation method (19). Here, FCsNPs were synthesized at pH 4 for 1 hour before centrifugation and separation of nanoparticles. Hence, the stability of the FTY720 drug has been analyzed for four hours. The result shows that FTY720 is stable at acidic pH (fig.4.1) which is in agreement with the reported studies that have shown FTY720 drug release at pH 4.6. (20, 21) The formulated nanoparticles were evaluated through DLS measurements (Fig.4.2). Various ratios of chitosan: TPP were utilized for the formation of CsNPs. DLS measurement has shown CsNPs with the ratio of chitosan to TPP (2:1) have shown mean particle size 70±2 nm along with PDI 0.33±0.01, respectively. Chitosan nanoparticles with this ratio have shown good colloidal stability with 22±3 mV zeta potential. A 2:1 ratio was preferred for further study due to the smaller size of nanoparticles with better unimodality of

nanostructures in comparison to other ratios of chitosan to TPP. The obtained results are tabulated in table 4.1.

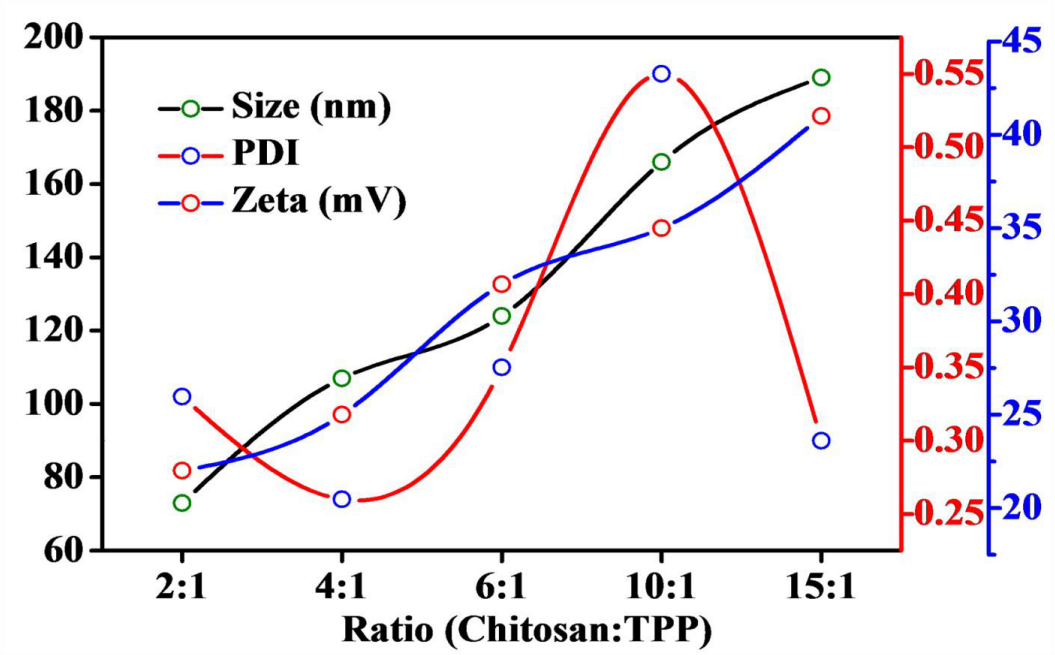


Fig.4.2. DLS measurements indicate that the 2:1 (Chitosan: TPP) ratio is providing a smaller size of chitosan nanoparticles with good colloidal stability.

The water-soluble polymeric nanoparticles, CsNPs were formed with the ratio of chitosan to TTP (2:1) of 59±4 nm hydrodynamic size with a polydispersity index (PDI) 0.33±0.05. FCsNPs were synthesized with a ratio of 5:1 (chitosan: FTY720) with a size increment to ~100 nm with 0.35±0.07 PDI (Fig.4.3a). This dispersed nanoformulation has represented considerable stability with a surface zeta potential of 22 ±3 mV and 18 ±4 mV for CsNPs and FCsNPs, respectively (Fig.4.3b). TEM images revealed the spherical morphology of nanosized particles with ~ 40 nm and ~100 nm size for CsNPs and FCsNPs, respectively (Fig.4.3c, d,). Further TEM and SEM images are described in Fig.4.4. SEM micrographs of CsNPs (Fig.4.4a) and FCsNPs (Fig.4.4b) have reflected the spherical shape and monodispersity of nanoformulations. TEM images have also shown the spherical shape of nanoparticles with an average size of CsNPs between 35-40 nm (Fig.4.4c) and 100-110 nm size of FCsNPs (Fig.4.4d). These microscopic images have confirmed and supported the DLS measurements to claim nanosized chitosan nanoparticles. Further, the stability of the nanoformulation has been analyzed with different time points for 10 days. The results have shown negligible changes in size, PDI, and zeta potential of

nanoformulation that indicates a good stability profile of nanoformulation (Fig.4.5). The results are also tabulated with obtained results in table 4.2.

Recently, the neuroprotective potential of chitosan nanoparticles has been demonstrated in the prevention of Alzheimer's disease and spinal cord injury (22-24). Therefore, chitosan nanoparticles were preferred to improve FTY720 availability at the disease site and also to provide combinational therapy at a single platform. Morphological evaluation of nanoparticles by DLS, SEM, and TEM reflects unimodal spherical-shaped nanoformulation with excellent stability. Chitosan: TTP (2:1) ratio was selected to form FTY720 loaded nanoparticles due to smaller size with better uniformity and possibility of intersecting BBB.

Physiochemical characterizations were performed to access the compatibility of drugs and nanocarriers. The results of XRD and FTIR were represented in Fig.4.6 which confirmed the amorphous nature of nanoparticles and the physicochemical interaction of the drug and nanocarrier, respectively. chitosan, CsNPs, and FCsNPs have shown a broad XRD peak at 20°, 29°, and 30°, respectively in lieu to report that has shown the amorphous structure of chitosan nanoparticles(25)(Fig.4.6a). Distinct XRD spectrums of FTY720 and TPP are due to their crystalline nature (26, 27). Here, the disappearance of FTY720, TPP, and chitosan XRD diffraction peaks could be because of overlapped amorphous carrier XRD peaks and cross-linking of chitosan and TPP(25, 28). FTIR spectra (Fig.4.6b) showed major transmittance bands at 3328 cm-1 (O-H and N-H stretching vibrations) and 1149 cm-1 (C-O-C bending vibrations) of chitosan supporting existing FTIR studies of chitosan (29, 30). Major transmittance bands of FTY720 acquired at 1513 cm-1 ( alkyl stretching vibrations), 1117 $cm^{-1}$ (aliphatic amine), 1066 cm-1( C-O presence), and 531 $cm^{-1}$ (C-Cl presence) are in lieu to reported study (20, 31). CsNPs synthesized after cross-linking of TPP and chitosan molecules may be recognized due to the formation of the C-O-P bond. FTIR spectrum of CsNPs has shown a broad peak at 1066 $cm^{-1}$ (C-O-P bond) and a broad band at 3328 $cm^{-1}$ (O-H and N-H stretching) confirming the involvement of hydrogen and noncovalent interaction in the formation of CsNPs(29, 32). Less broad peaks of 3328 $cm^{-1}$ and 1066 $cm^{-1}$ of CsNPs and 1117 $cm^{-1}$, 1513 $cm^{-1}$and 1066 $cm^{-1}$ of FTY720 confirm the formation of FCsNPs. Besides, less intense peaks of FTY720 and CsNPs in the spectrum of the physical mixture also support the physicochemical interaction of FTY720 and chitosan.

Hence, physiochemical analysis has characterized nanoparticles as amorphous and possessing major interaction of hydroxyl and aliphatic moiety of drug and nanocarrier.

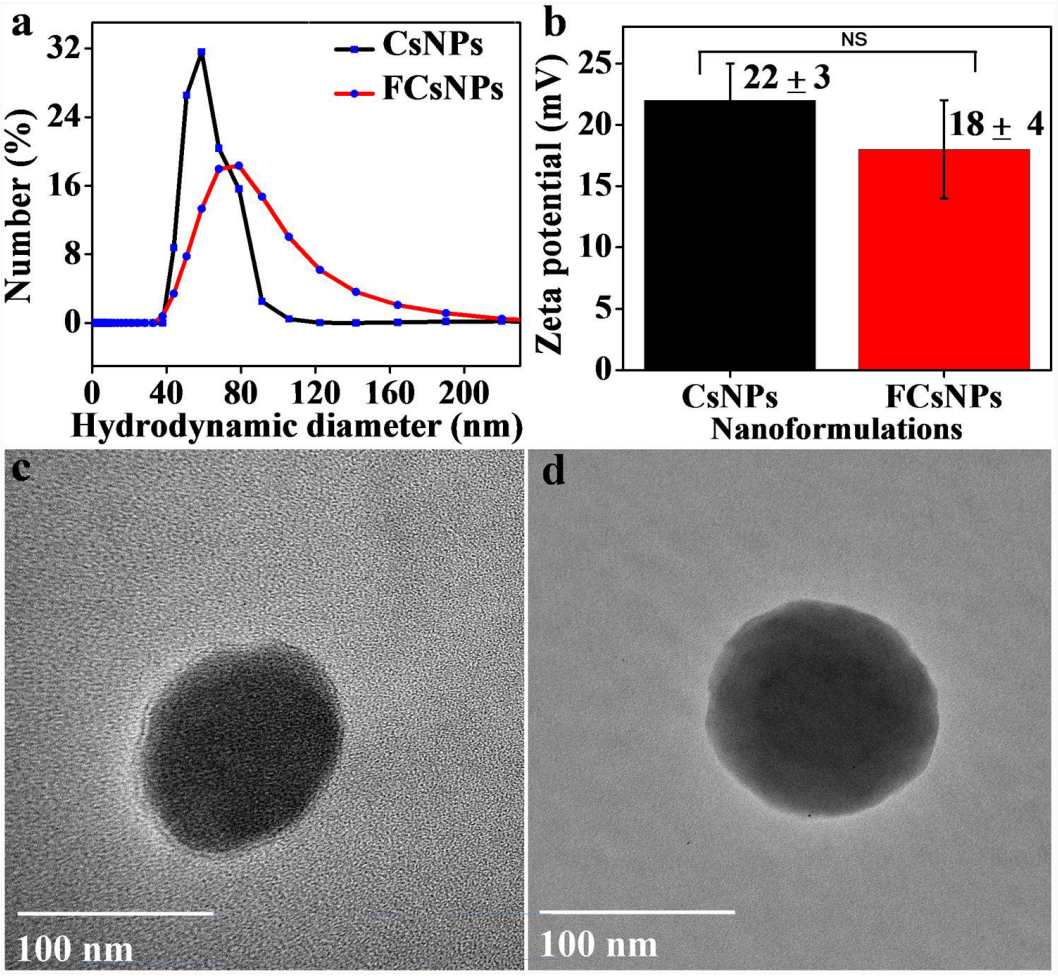


Figure 4.3. Morphological characterization of nanoformulations (a) The morphological evaluation of CsNPs and FCsNPs demonstrates the mean hydrodynamic size of nanoformulations; (b) zeta potential represents colloidal stability of nanoformulations (c) and (d) the TEM images are confirming spherical shape of placebo CsNPs and FCsNPs, respectively. TEM magnification: 60k X

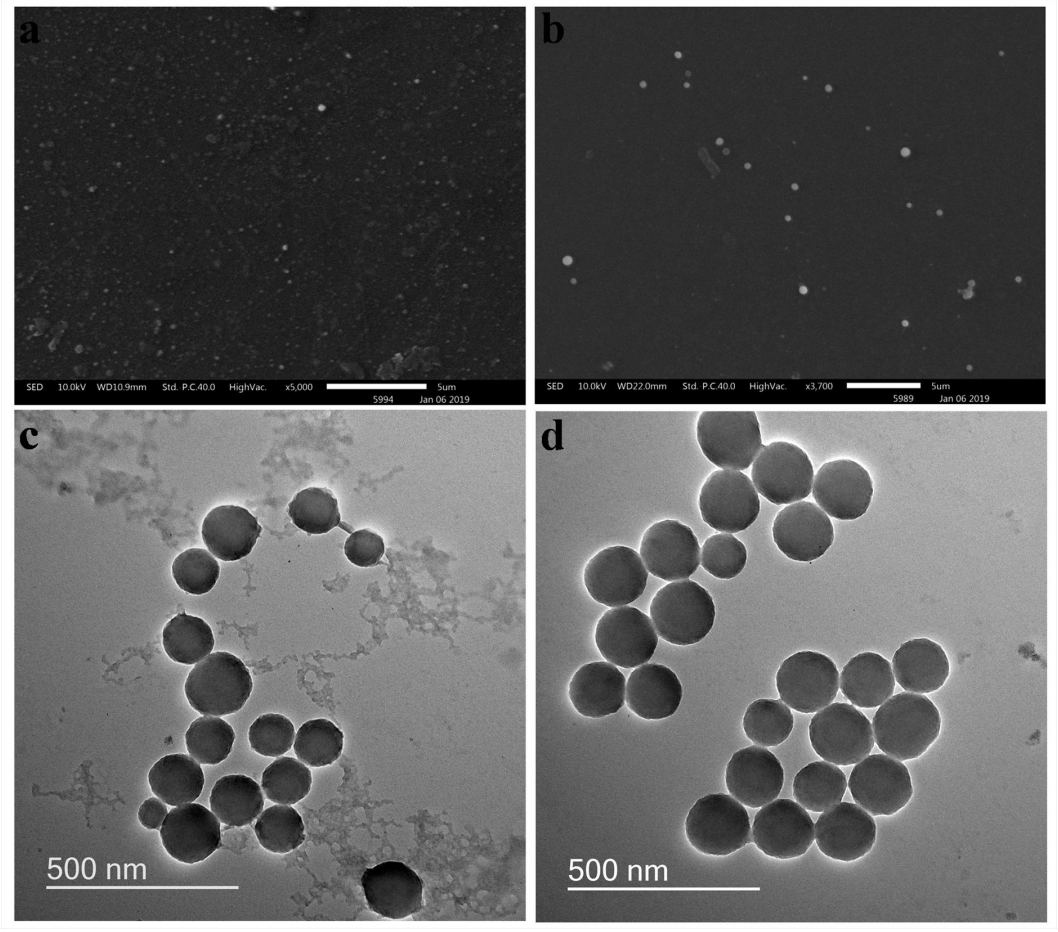


Fig.4.4 Electron microscopy of nanoparticles. SEM images of CsNPs (a) and FCsNPs (b) have shown spherical morphology and monodispersed nanoparticles. TEM images have confirmed nanosized spherical-shaped CsNPs (c) and FCsNPs (d). The TEM magnification: 20k X

Further, drug loading content and encapsulation efficiency of formulation were analyzed. The Bio-adhesiveness and permeabilization capacity of chitosan makes chitosan nanoparticle a more beneficiary nanocarrier system than other hydrophilic polymers. (33) Chitosan nanoparticles are reported as preferred nanocarrier systems to improve drug loading and encapsulation of the hydrophobic drugs due to their ability to entrap drugs within the layers formed by crosslinking of chitosan and STPP. (34, 35) Here also, the matrix of the core was prepared by ionic crosslinking of chitosan and STPP, and FTY720 as a cationic drug encapsulate within the layer of the matrix formed by electrostatic interactions. Entrapment of hydrophobic FTY720 drug within a matrix of chitosan polymeric nanoparticles enhances drug loading content and encapsulation efficiency. In support of the fact that chitosan nanoparticles provide a soluble matrix to load a higher

percentage of the drug (24), we achieved 17.52 ± 2 % and 87.6 ± 5 % drug loading and encapsulation capacity of nanoformulation.

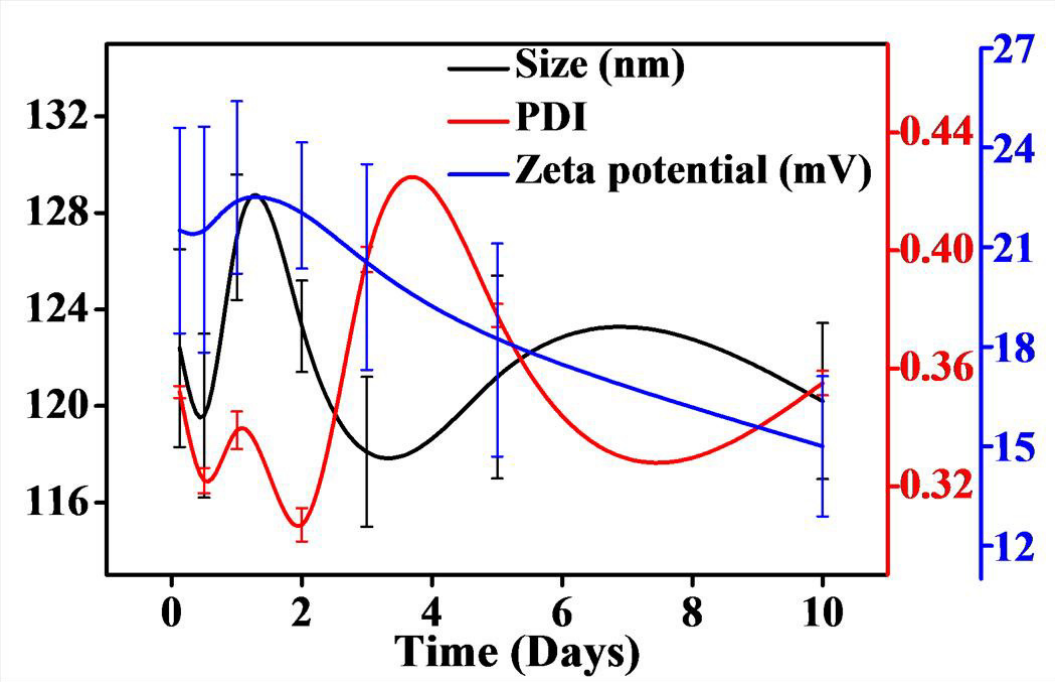


Fig.4.5. DLS measurements indicate the stability of nanoformulation at different periods.

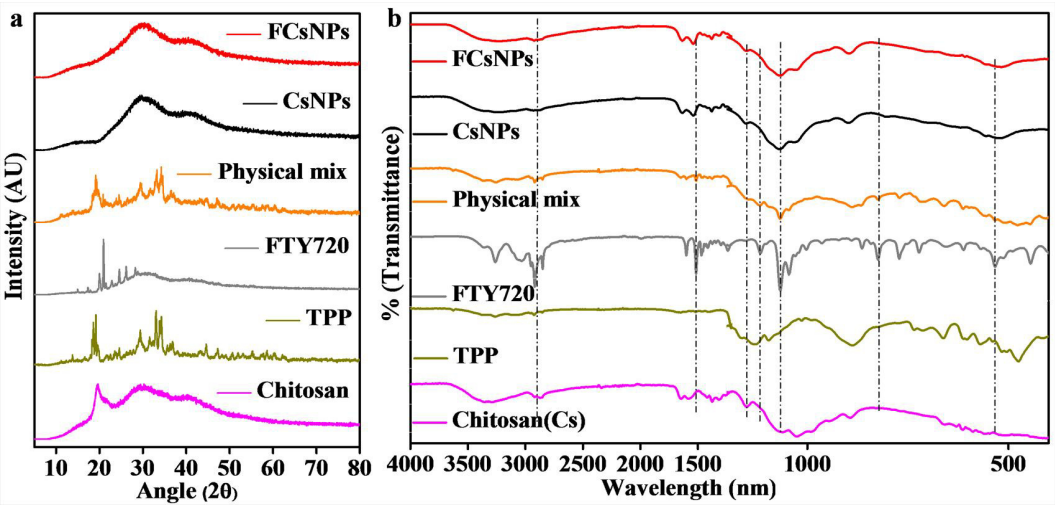


Fig. 4.6. Physicochemical characterization of nanoparticles. (a) XRD analysis revealed the amorphous nature of nanoparticles and (b) FTIR spectroscopy has confirmed non-covalent interaction between chitosan and FTY720 in the formation of FCsNPs.

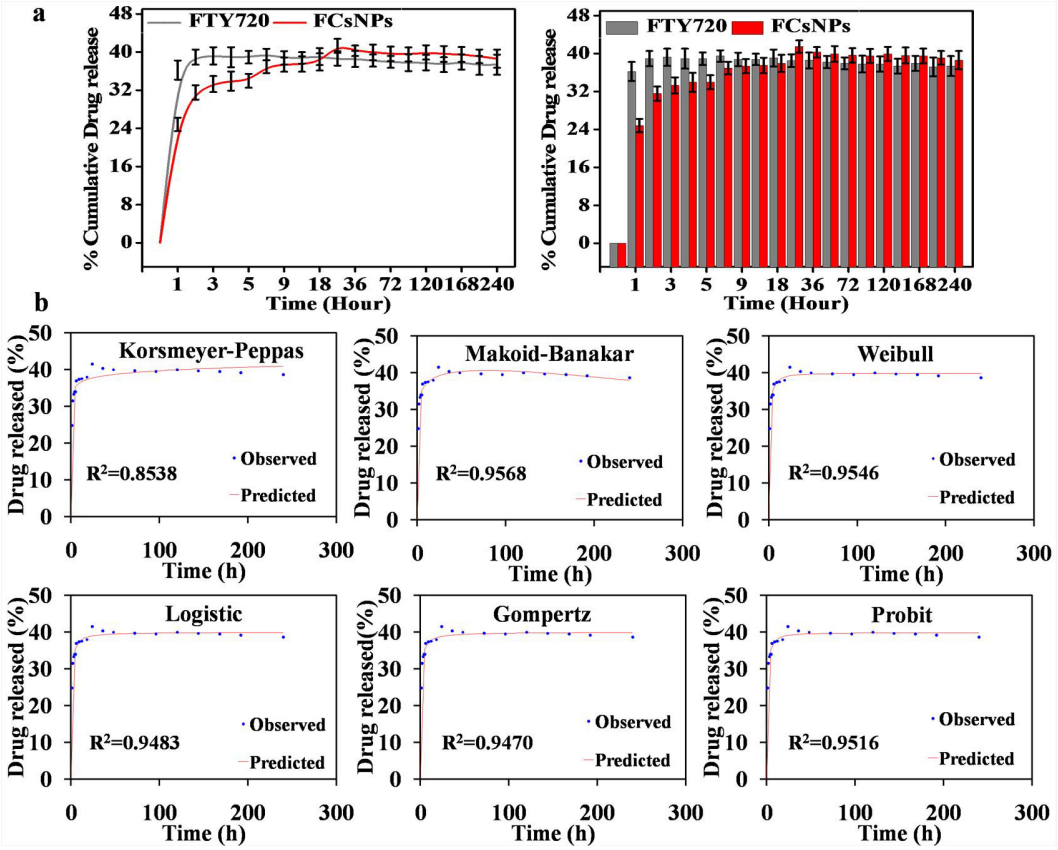


Fig.4.7 (a) *In vitro* drug release profile is indicating biphasic drug release kinetic of nanoformulation. (b) Best-fitted curves with respective mathematical models for release data of nanoformulation are represented.

4a.2.2. *In vitro* drug release analysis and mathematical modeling of release kinetic

Estimation of *In vitro* drug release was performed by mimicking *an in vivo* environment to understand the drug release profile. Equilibrium dialysis membrane methodology was followed to obtain drug release at mimicked physiological pH (Fig.4.7a). The results are represented in both the format curve and bar graph to understand the release profile with time with a comparison of FTY720 suspension and FCsNPs. Triplicate samples of FTY720 suspension and FCsNPs were analyzed to evaluate the drug-releasing pattern till 240 hours. FTY720 suspensions have shown a burst release pattern in the initial 2 hours with 39% ± 1.78% of drug release. At the other end, FCsNPs have demonstrated a biphasic release profile with an initial 25% ± 1.4% of burst release and then after a maximum of 41% ± 1.29% release after 24-36 hours and after

that, no gradual release was observed till 240 hours. The possible reason for the saturation is the lesser solubility of the FTY720-free drug or the lesser stability of the drug in an aqueous solution. (9) This result indicates the importance of drug-loaded chitosan nanoparticles in enhancing drug availability. Here, initial drug release is attributed to the diffusion and deposition of surface-lying molecules and more gradual release is due to the degradation of nanocarriers. This kind of drug release pattern is demonstrated beneficiary in the control and management of diseases (36). Our results are also in agreement with the study that showed the capability of chitosan nanocarriers in the improvement of drug bioavailability (19, 37). The controlled and slower drug release profile is believed to reduce drug cytotoxicity by limiting its premature release (38).

For a better understanding of drug release kinetics, drug release data were fitted with various kinetic models, and results are summarized in Table 4.3. The fitted model of the release kinetic is utilized for quantitative estimation of the drug delivery system. In the present study, the fittest model is selected based on three criteria: $R^2$, the AIC, and the MSC value by following the existing report, and fitted curves are presented in Fig.4.7b. (39) In that, they have shown the best model with a high coefficient of determination ($R^2$ ), a low Akaike information criterion (AIC), and a high model selection criterion (MSC) value. The mathematical modeling studies show six best-fitted models for FCsNPs concerning the value of $R^2$ = 0.8538, 0.9568, 0.9546, 0.9483, 0.9470, and 0.9516 for Korsmeyer-Peppas, Makoid-Banakar, Weibull, Logistic, Gompertz, and Probit, respectively. The release exponent, *n* value obtained from the Korsmeyer-Peppas and Makoid-Banakar model are 0.035 and 0.0722, respectively. These values of $n \leq 0.43$ for spherical shape nanoparticles are indicating the diffusion process as a possible release mechanism facilitated by Fickian transport. (40) Makoid-Banakar model is describing better release kinetics in comparison to other best-fitted models in consideration of AIC and MSC values. Modeling of FTY720 release from the chitosan-based nanocarrier system has been described as a well-fitted curve with a mathematical model (Korsmeyer-Peppas), empirical model (Makoid-Banakar, Weibull, and Gompertz), logistic and probit model. These models are indicating biphasic drug release patterns from the polymer-drug matrix. (41) Weibull model also describes scale (α) and shape (β) parameters. Scale parameter utilizes to estimate the necessary time for the release of loaded drugs in a formulation ($T_d$) and shape parameters for an understanding of the shape of the curve. (Costa & Sousa Lobo, 2001) $T_d$ was found to be 1.008 hours for FCsNPs and the shape of the curve is parabolic due to $\beta = 0.388<1$. Every fitted model

is indicating diffusion controlled biphasic release pattern, where encapsulated drug within the core of the polymeric matrix shows slower release and surface-bound drug residues show burst release. Hence, our particle system can be successfully modeled with a single model. Here, the Makoid-Banakar model has shown the best value for every parameter including the highest $R^2$ (0.9568), lowest AIC (56.2497), and highest MSC (2.7207). These parameters indicate that the release pattern of FTY720 from chitosan nanoparticles was biphasic and the diffusion process was controlled by the Fickian transport mechanism.

The release rate comparison of FTY720 between FTY720 suspension and FCsNPs has been also analyzed with DDSolver software. (42) The obtained release rate for FTY720 suspension and FCsNPs was 0.529 and 0.100, respectively. This represents a five-time slower release rate of FTY720 from chitosan nanoparticles. Hence, mathematical modeling of FTY720 release data confirms the importance of chitosan nanoparticles to improve the drug release profile.

4a.2.3. *In vitro* neurotherapeutic efficiency

Cell viability assays were carried out to analyze *in vitro* neurotherapeutic efficiency. The cytotoxic behavior of the drug and our nanoformulation was evaluated against SH-SY5Y, neuronal cells. MTT [3-(4, 5-dimethylthiazol-2-yl)-2, 5-diphenyltetrazolium bromide] assay has shown the biocompatible nature of FTY720 and our nanoformulations. FTY720, CsNPs, FCsNPs, and rotenone were treated in SH-SY5Y cells for 48 hours to estimate their cytotoxicity. Outcomes of the MTT reduction assay have indicated the bio-compatible nature of FTY720, CsNPs, and FCsNPs. FTY720 has shown cytotoxic effects at higher concentrations (2 μM). Dose-dependent cytotoxicity of rotenone was observed and a 2 μM dose was obtained as an IC50 dose of rotenone. A higher dose (2μM) of FTY720 has shown cytotoxicity (Fig.4.8a). Fig.4.8b is showing the biocompatibility of CsNPs and FCsNPs also at higher doses. This primary evaluation of nanoformulations has proved that bio-compatible nanoformulations possess the potency to be utilized for protection studies against chemical-induced neurotoxicity. Our previously established rotenone-induced *in vitro* PD model was followed (18) and an 800 nM dose of rotenone was considered as an acute dose in this study (Fig.4.8c). The acute dose of rotenone induces aggregation of phosphorylated α-Syn, a signature molecule of PD progression.

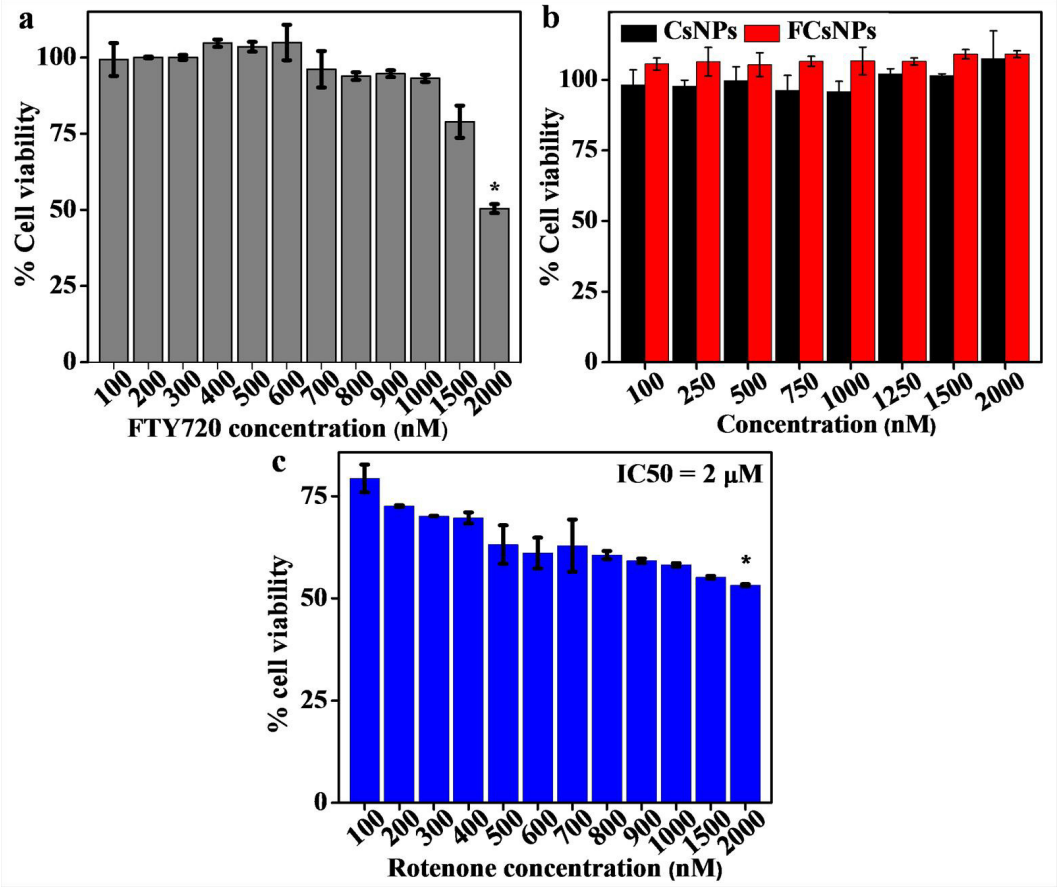


Fig.4.8 Cytotoxicity assessment of nanoformulations. (a) FTY720 has shown cytotoxicity at the higher dose (2 µM) and biocompatibility at lower doses. (b) Cytotoxicity assay of CsNPs and FCsNPs has revealed the biocompatible nature of both nanoformulations. (c) Dose-dependent cytotoxicity of rotenone has been obtained with IC50 at a 2 µM dose.

Neuroprotective efficiency of 0.5-1 µM bare FTY720, equivalent drug-containing concentration of CsNPs and FCsNPs were examined against 800 nM rotenone co-treated SH-SY5Y cells for 24 hours.1µM dose of formulation has shown higher neuroprotective efficiency. 1µM FCsNPs have provided a significantly higher percentage of cell protection in comparison to bare FTY720. (Fig.4.9a). A dose-dependent neuroprotective response has been analyzed that supports earlier reported similar observations (43, 44). Our nanoformulations have shown 1.3 folds increase in percentage cell survival against rotenone-induced neurotoxicity. FCsNPs had effectively minimized the protective dose of FTY720 (1µM) in comparison to existing reports that have shown 4 µM (43) and 40 µM (44) neuroprotective doses of free FTY720. Hence, our nanoformulation has demonstrated superior neuroprotective activity with dose minimization and

availing higher drugs at the site of action. The 1 μM dose of FTY720 and 1 μM dose of FTY720 carrying nanoparticles (1.96 mg) have been selected to utilize as a therapeutic dose for further study. Estimation of ROS generation was also performed to evaluate the anti-inflammatory and anti-oxidative response of nanoformulation. The Association of neurodegeneration with oxidative stress and inflammation is widely studied(45, 46). Fig.4.9b is showing the ROS scavenging potential of FCsNPs indicating the neuroprotective role of our nanoformulations. This property of nanoformulation is due to the ROS scavenging potential of chitosan nanoparticles in agreement with the existing report(47). Further, Jc1-based mitochondrial membrane potential analysis with flow cytometry was performed to evaluate the neuroprotective potential of nanoformulation. Fig.4.10 authenticates the neuroprotective effect of our nanoformulations against rotenone exposure. FCsNPs have shown better neuroprotective efficiency against rotenone-induced mitochondrial deficits in comparison to FTY720. CsNPs have also protected against mitochondrial oxidative stress. Results of the Jc1 dye-based assay are in good accordance with the MTT assay, where FCsNPs had represented a synergistic protective effect of FTY720 and CsNPs. Hence, results of the MTT assay, ROS estimation, and Jc1-based analysis have confirmed *in vitro* neurotherapeutic efficiency of FCsNPs. Herein, a dopaminergic neuronal model, SH-SY5Y cells are utilized to evaluate rotenone-induced neurotoxicity *in vitro* experimental PD model. A complex I inhibitor of the electron transport chain, rotenone hampers the 26S proteasomal pathway resulting to augment aggregated α-Syn, a signatory process of PD progression (48). Evaluation of *in vitro* therapeutic efficiency of nanoformulations against rotenone-induced neurotoxicity has confirmed the effective neuroprotective action of FCsNPs. Interpretation of cell viability assay, Jc1-based apoptosis assay, and ROS generation estimation support each other to divulge better neuroprotective efficacy of FCsNPs concerning placebo CsNPs and bare FTY720 drug.

Cellular uptake of nanoformulations is essential for enhancing drug availability and nanotherapeutic efficiency. Therefore, we have analyzed the cellular uptake of FCsNPs to dopaminergic neurons mimicking SH-SY5Y cells. Rhodamine B-tagged FCsNPs were visualized under confocal microscopy after 2, 4, and 8 hours of exposure to cells. CLSM micrographs indicate maximum cytoplasmic localization of nanoformulation after 4 hours of exposure to cells (Fig.4.9c). Cellular internalization analysis of our nanoformulations has clarified that particles were easily internalized to SH-SY5Y cells. Studies have demonstrated sphingosine-1-phosphate-

mediated uptake of FTY720 (5, 49) and clathrin-mediated endocytosis or phagocytosis as a possible mechanism of chitosan nanoparticle uptake in the neuronal cells (22, 24, 50). Muco-adhesiveness and paracellular accumulation of chitosan nanoparticles also facilitate higher drug availability to the disease site (24, 37). Hence, our FTY720 enriched chitosan nanoparticles are suitable to follow receptor-mediated endocytosis to cross BBB and paracellular transport to improve the bioavailability of the drug.

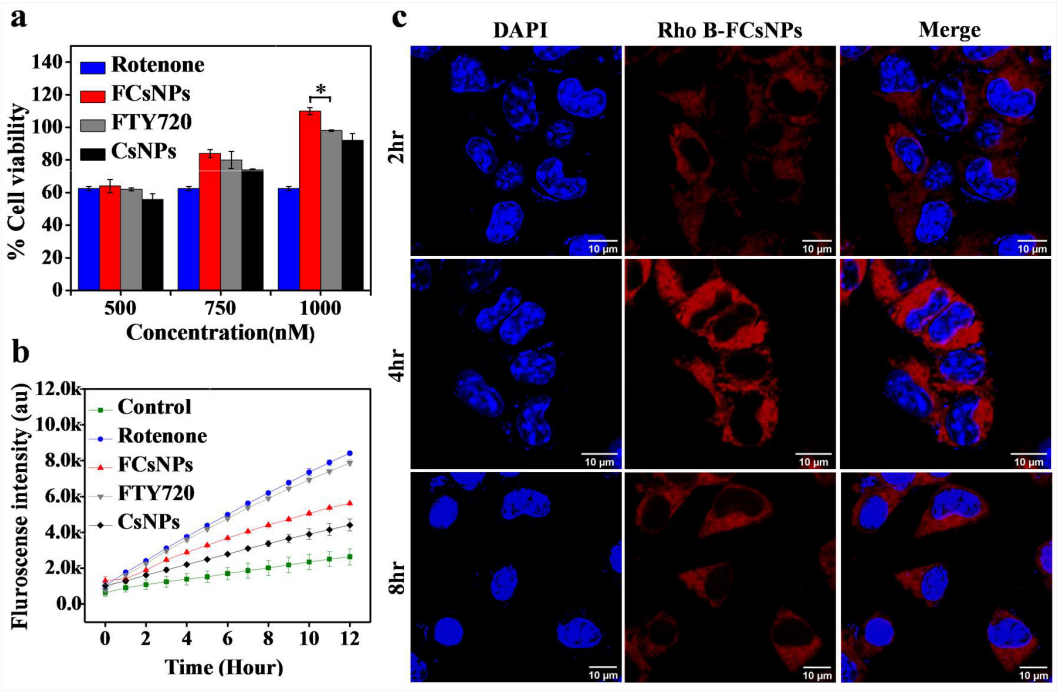


Figure 4.9. *In vitro* neurotherapeutic potentiality of nanoformulations (a) FCsNPs has shown neuroprotective effect against rotenone-induced cellular damage and PD effect (*$p<0.05$, one way ANOVA; Turkey and Bonferroni test). (b) ROS quenching with nanoformulations shows anti-inflammatory potential. (c) Cellular internalization of nanoformulation has represented major cytoplasmic uptake of nanoparticles after 4 hours of incubation. The scale bar-10 µm, magnification -63X

4a.2.4. Insight into the neuroprotective mechanism of FCsNPs

Gene expressions of BMI1, EZH2, PP2A, Mitogen-Activated Protein Kinase-Activated Protein Kinase 3 (MAPKAPK3/3Pk), and nuclear factor kappa-light-chain-enhancer of activated B cells

(NFkB) were analyzed (Fig.4.11a). The effect of the rotenone-treated group on gene expressions indicated significant downregulation of BMI1, EZH2, and PP2A with significant upregulated 3Pk and NFkB. Our nanoformulation has shown better regulation of rotenone-affected gene expression by upregulating the expression of BMI1, EZH2, and PP2A by lowering the expression level of 3Pk and NFkB. A significant reversal effect of our nanoformulation against rotenone-induced NFkB expression confirmed the anti-inflammatory potential of nanoformulation. The overall analysis demonstrates better neuroprotective efficiency of FCsNPs in comparison to bare drugs and nanocarrier alone.

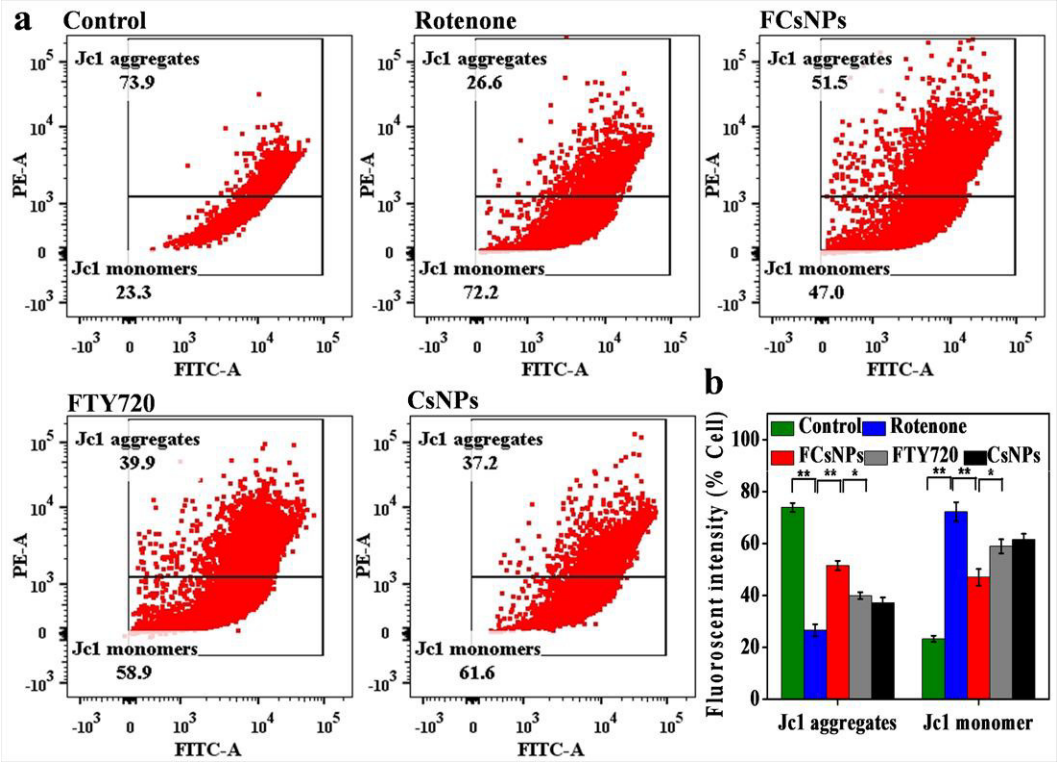


Figure 4.10. Mitochondrial membrane potential analysis (a) Flow cytometric analysis of Jc1 aggregates and monomers has clearly stated the neuroprotective effect of FCsNPs. (b) Quantitative representation of the number % of Jc1 aggregates (healthy cell) and Jc1 monomer (apoptotic cell) has shown (**p<0.01,*p<0.05; one way ANOVA; Turkey and Bonferroni test).

Further, expression profiles of PD target proteins were evaluated to confirm the neuroprotective mechanism of our nanoformulation. Epigenetic regulation-based neurotherapeutic strategies could potentially retard neurodegeneration(51). Hence, we investigated detailed protein expression analysis including polycomb based on our previous report on the epigenetic

regulation of Parkinsonism. Expression profiles of pSer129 α-Syn, EzH2, 3Pk, PP2A, and Caspase3 were analyzed (Fig.4.11b). Herein, nanoformulation caused significant downregulation of pSer129 α-Syn and Caspase3 as a reversal effect of rotenone-induced neurodegeneration. Further, we have assessed the expression of EzH2, PP2A, and 3Pk to confirm their association with PD progression. Results showed a significant reduction in EzH2, PP2A expression, and upregulation in 3Pk expression indicating the PD-inducing effect of rotenone. In contrast, nanoformulation has shown neuroprotection by significant upregulation of EzH2, PP2A, and downregulation of 3Pk. Quantification of protein expression was represented in Fig.4.11d. The promising results of PP2A and EzH2 expression led us to explore the interlink of these two markers. We also validated our findings in the presence or absence of PP2A inhibitor okadaic acid (OKA) and EzH2 inhibitor EPZ011989 (EPZ) (52).

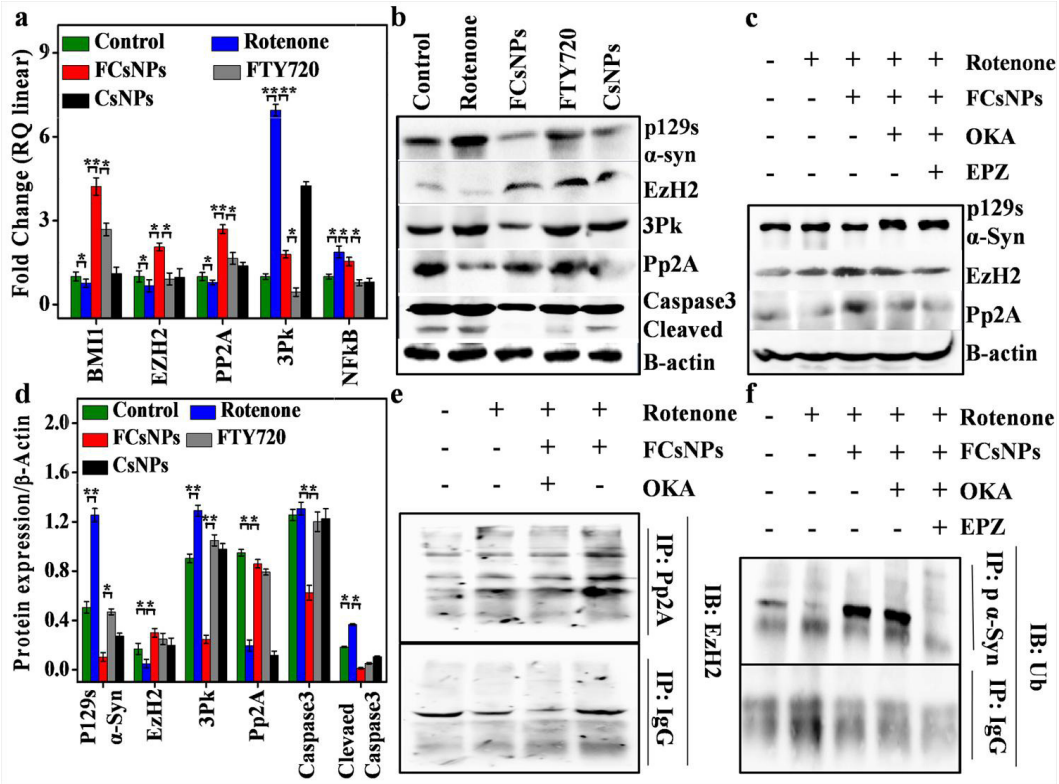


Figure 4.11. Insight into the neuroprotective mechanism of FCsNPs (a) Gene expression of BMI1, EZH2, 3pK, PP2A, and NFkB analyzed in regards to FCsNPs. Nanoformulations have represented significant induction of BMI1, EZH2, PP2A, and inhibition of 3pK and NFkB that shows the anti-inflammatory and neuroprotective effect (**p<0.01,*p<0.05; one-way ANOVA; Turkey and Bonferroni test). (b) Immunoblot images have shown and (d) quantitative

representation of protein expression was represented (*p<0.05; one-way ANOVA; Turkey and Bonferroni test). Significant elevation of EzH2, PP2A expression, and reduction of 3Pk, pSer129 α-Syn, and Caspase3 confirms neuroprotective potential. (c) The inverse relation of EzH2 and pSer129 α-Syn expression in the presence/absence of PP2A/EzH2 inhibitors confirms PP2A's influence on epigenetic neuroregulation. (e) IP results are confirming the novel direct physical interaction of PP2A and EzH2. (f) Immunoblots of IP analysis have shown PP2A-induced EzH2 mediated α-Syn degradation.

Interestingly, we found that OKA reduced the EzH2 expression and augmented phosphorylated α-Syn, a hallmark of PD. From our previous report, we know that EPZ suppresses the EzH2 expression and resulting in an enhancement in the level of phosphorylated α-Syn(18). Similarly, we found that the combined treatment of EPZ and OKA further attenuated the EzH2 expression and induces the expression of phosphorylated α-Syn in comparison to the OKA treatment (Fig.4.11c). Also, immunoprecipitation (IP) was performed to validate the interaction and therapeutic imprint of PP2A and EzH2 (Fig.4.11e). The quantification of the ratio of EzH2 with PP2A-IP/IgG-IP was represented in fig.4.12. Desirably, an IP result has shown novel direct physical interaction of PP2A and EzH2. Besides, an IP result has confirmed that inhibition of PP2A with OKA attenuated EzH2 expression and interaction. Our previous report and other similar reports demonstrated EzH2 as a promising regulatory target in α-synucleinopathy(18, 53). Hence, we have performed an IP experiment to show the ubiquitination of α-Syn, a regulatory target of PD. IP results have authenticated higher ubiquitination of α-Syn with the treatment of our nanoformulation. Also, it has been shown that the presence of OKA and EPZ hinders the ubiquitination process (Fig.4.11f). Overall gene and protein expression analysis has divulged the role of PP2A in EzH2-mediated ubiquitination and degradation of α-Syn. In the exploration of PP2A and EzH2 interaction, we have further examined PP2A interaction at different three promoter regions of EZH2. In this ChIP analysis, we found PP2A significantly binding at -436 to the +48 region of the EZH2 promoter (Fig.4.13). PP2A has shown nonsignificant binding at other regions (-1107 to -1002) and (-862 to -678). In the future, an insight into the mechanism of transcription regulation is warranted. Herein, we proved the novel physical interaction of PP2A and EZH2 in the regulation of PD prevention. Death of dopaminergic neurons, a signature event of Parkinsonism is the outcome of elevated levels of aggregated pSer129 α-Syn and Caspase3-mediated apoptosis (54). In our study, the downregulation of pSer129 α-Syn and Caspase3

protein expression is confirming the neuroprotective action of nanoformulation against rotenone-induced neurodegeneration. Hence, effective inhibition of PD hallmark, pSer129 alpha-synuclein is reflecting the superior neuroprotective efficacy of our nanoformulation.

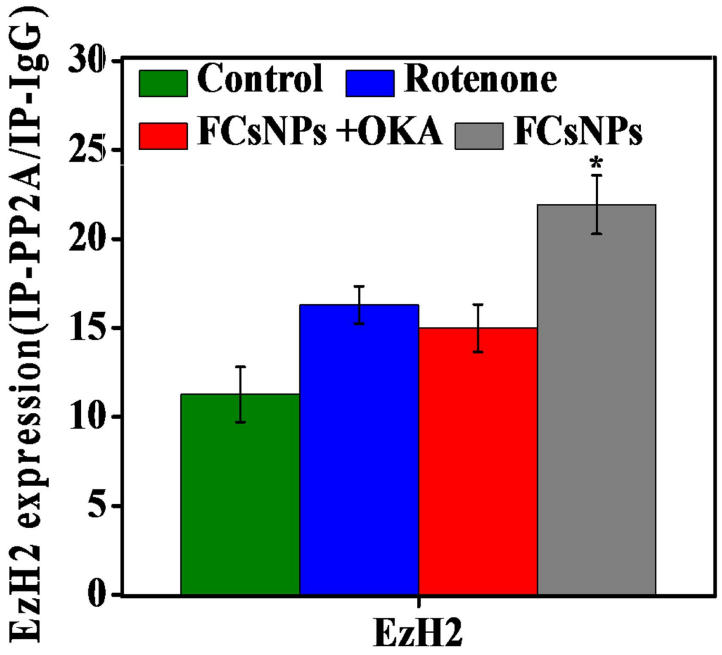


Fig.4.12. Quantification of the ratio of EzH2 presence after pull down with PP2A and IgG ($p \leq 0.5$)

Further, reduced expression of 3Pk and upregulation of PP2A, EzH2 protein expression also validated the reversal action of our nanoformulations against rotenone-induced neurodegeneration. In further exploration of the neuroprotective mechanism, it has been noted that PP2A has influenced EzH2-mediated epigenetic regulation of α-Synucleinopathy. Protein expression of EzH2 and p129s α-Syn in the presence of potent PP2A inhibitor okadaic acid and EzH2 inhibitor EPZ011989 has confirmed PP2A influence on EzH2 mediated PD regulation. Our previous report and other reports have shown inhibition or deficiency of EzH2 resulting in neurodegeneration and PD progression (13, 14, 18). Report of dephosphorylation of α-Syn due to upregulated PP2A demonstrating PP2A as a therapeutic target for PD prevention (2, 54). Therefore, we are keen to explore the novel physical interaction of PP2A and EzH2 to know its regulatory effect on PD. In observation, we found novel direct physical interaction of PP2A and EzH2.

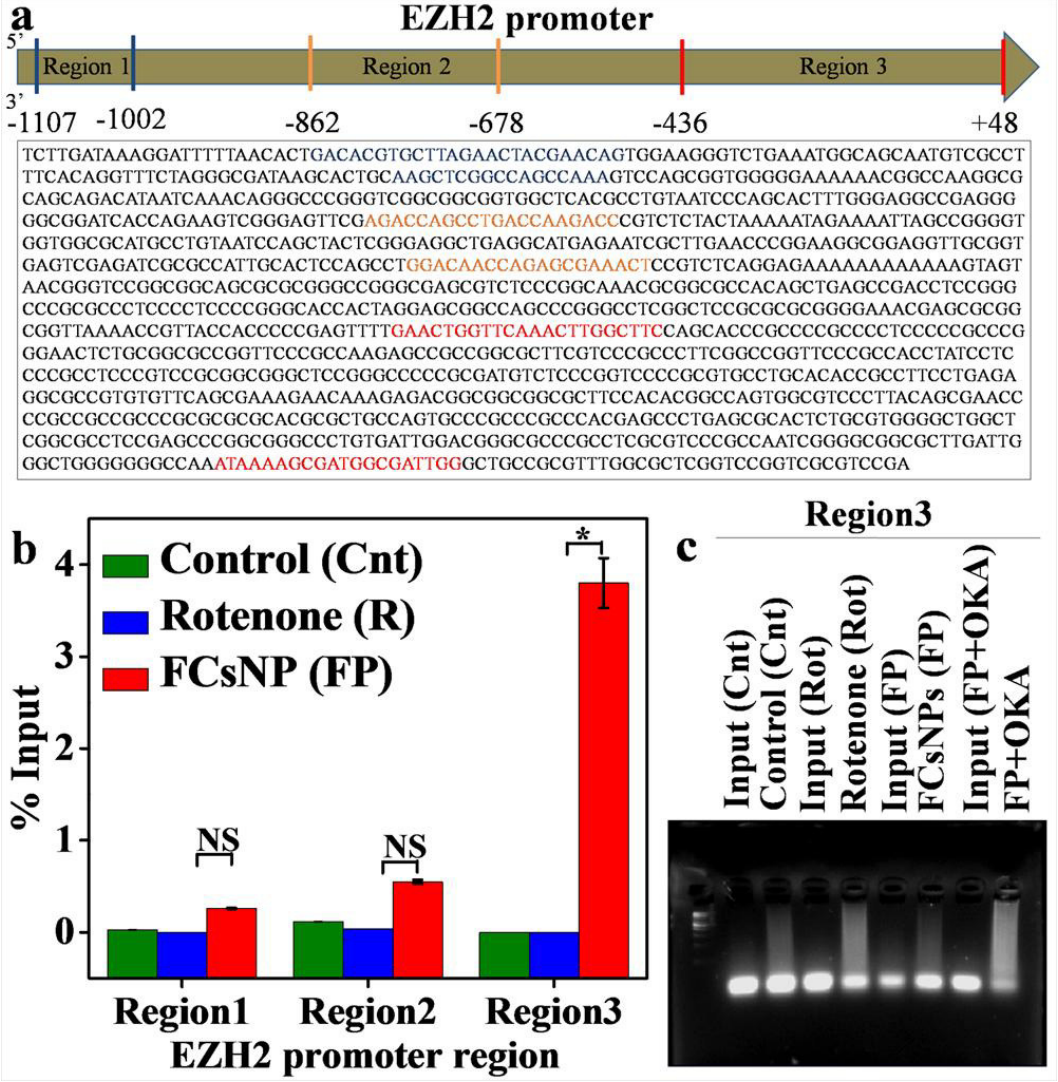


Figure 4.13. ChIP analysis (a) Nucleotide sequence of EZH2 promoter regions with primer sets illustrated. (b) The percentage input analysis method has shown significant qPCR amplification of the EZH2 promoter region (-436 to +48) with control, rotenone, and FCsNPs from anti-PP2A ChIPs. (c) Agarose gel micrograph of qPCR amplicons of the EZH2 promoter region (-436 to +48) confirms the neurotherapeutic efficiency of FCsNPs against rotenone-induced effect by binding alteration of PP2A to EZH2 (-436 to +48) promoter region.

The inhibitory effect of okadaic acid has proved inhibition of PP2A resulted in the depletion of EzH2. In further elucidation, upregulated ubiquitin expression as a neuroprotective effect of FCsNPs and downregulated ubiquitin expression in the presence of okadaic acid and EPZ011989 clearly stated PP2A stimulated EzH2 mediated α-Syn ubiquitination and degradation. Hence, we

proved the PP2A-induced EzH2 mediated α-Syn ubiquitination and degeneration as a neuroprotective mechanism of our nanoformulation. Further, ChIP-based EZH2 expression analysis has validated the camouflaged role of PP2A in EZH2-mediated PD prevention. Besides, It has revealed novel binding of PP2A at the EZH2 promoter region (-436 to +48). Recently, the report of acute treatment of rotenone has demonstrated a reduction in ubiquitylated proteins by showing the importance of E1A activity for the efficient functioning of the ubiquitin-mediated proteasomal degradation pathway (UPP) (55). In the UPP, the binding of ubiquitin to the aggregated or dysfunctional proteins directs them to the UPP machinery. Therefore, our study has divulged the neuroprotective mechanism of nanoformulation by attenuating the rotenone effect and PP2A-stimulated EzH2-mediated ubiquitination and degradation of α-Syn. Earlier reports about the involvement of human polycomb protein 2, a member of PRC1 in SUMOylation mediated α-Syn aggregation and the inverse relationship of SUMOylation and ubiquitination have shown epigenetic regulatory mechanisms in PD management (16, 17). Our recent investigation about EzH2 mediated proteasomal degradation of α-Syn in PD regulation has also demonstrated the importance of epigenetic regulation in PD pathogenesis (18). In this study, we have updated our knowledge about the neuroprotective mechanism of EzH2-mediated epigenetic regulation of α-Syn degradation by demonstrating PP2A as an upstream regulator. To the best of our knowledge, this study has first time reported the regulatory role of PP2A in EzH2-mediated regulation of PD-associated α-Synucleinopathy.

Immunohistochemistry (IHC) analysis for primary therapeutic targets (EzH2, PP2A, and pSer129 α-Syn) was performed in mice brain slice culture (Fig.4.14). The primary aim to conduct this experiment is to evaluate the neuroprotective effect of nanoformulations at the tissue level after observation of *in vitro* neurotherapeutic potential. Surface plots are analyzed by Image J software. Herein, IHC analysis has shown supportive results in the agreement of protein expression analysis. Elevated expression of EzH2, PP2A, and reduction in pSer129 α-Syn expression has confirmed the neuroprotective behavior of our nanoformulation against the inverse action of rotenone. These results are also in lieu to immunoblot expression interpretation that showed higher neuroprotection efficiency of FCsNPs in comparison to placebo nanoparticles and bare drugs. Here, Pser129 α-Syn inhibition by our nanoformulation is in the agreement with the neuroprotective study of arctigenin against rotenone-induced toxicity (56). Upregulation of EzH2 expression by FCsNPs is comparable with EzH2 induction with our previously reported

metformin-loaded Polydopamine nanoformulation against the rotenone effect (18). As per our knowledge, no study has reported PP2A expression as a function of the neuroprotective role of nanoformulation in the rotenone-induced PD model. The present study is the first report that studied the camouflaged role of PP2A in the epigenetic regulation of PD prevention.

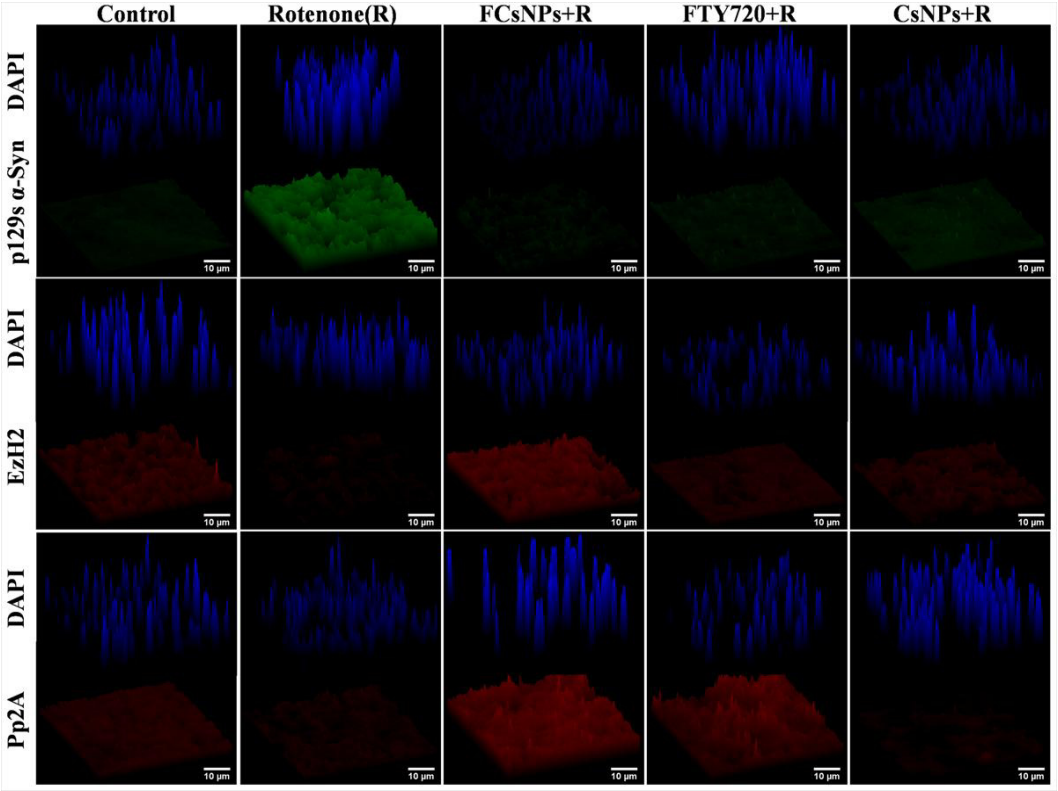


Figure 4.14. Immunohistochemical analysis in brain slice culture. CLSM micrographs as a reflection of IHC analysis of protein expression are suggesting nanoparticle-mediated neurotherapeutic intervention of PD by showing upregulated EzH2, PP2A, and inhibited pSer129 α-Syn against rotenone simulated neuropathy. For better visualization of results, the surface plot of images is represented by using image j software. Scale bar-10µm, magnification-10X.

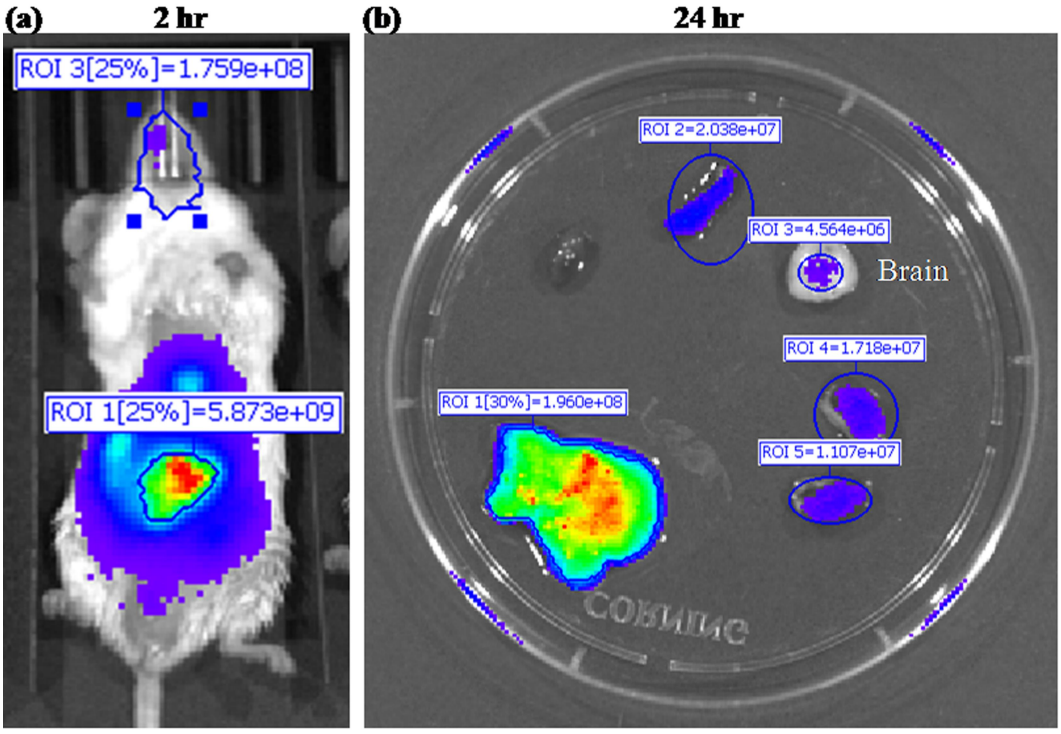


Figure 4.15. Retention of nanoparticles in the brain (a) Quantified radiant efficiency of in vivo bio-distribution image shows brain accumulation of nanoparticles after 2 hours. (b) Retention of nanoparticles in the brain has been revealed by analysis of ex vivo radiant efficiency after 24 hours.

4a.2.5. *In vivo* bio-distribution

*In vivo* bio-distribution of ICG (Indocyanine Green) bound FCsNPs was examined to understand the bio-distribution profile of our nanoformulation (Fig.4.16a). A pattern has shown a good distribution profile with major distribution to the liver, kidney, spleen, and brain. In the initial hours of post-injection, nanoformulation has shown accumulation in the heart and then the brain. $1.759 \times 10^8$ radiant efficiencies have been analyzed with a quantified image of *in vivo* bio-distribution after 2 hours of injection (Fig.4.15a). This result confirms that our nanoparticles have BBB crossing efficiency. After 4 hours, significant accumulation has been observed in the liver and kidney. The clearance of nanoparticles has been observed after 24 hours. The mice were sacrificed after 24 hours and organs were isolated for *ex-vivo* imaging. *Ex vivo* imaging has confirmed the retention of nanoparticles in the brain and also shown significant accumulation in

the liver and kidney (Fig.4.16b,c). In fig.4.15b, 4.564 × $10^6$ radiant efficiencies have been observed in the brain after 24 hours with an ex vivo study, which is 2.57% of the amount reached to the brain after 2 hours. The results show a better retention ability of our formulation compared to existing reports that have demonstrated less than 24-hour retention of their nano delivery system in the brain. (57-60) Here, higher accumulation into the liver and kidney indicates a clearance mechanism of nanoformulation in agreement with existing reports that have shown the first-pass metabolism as a clearance path (61). The presence of sphingosine-1-phosphate receptors of FTY720(49) and clathrin-mediated endocytosis of chitosan nanoparticles (50, 62) in the brain may facilitate the brain targeting of FCsNPs. Hence, *in vivo* and *ex vivo* bio-distribution analysis has confirmed the efficiency of our nanoformulation to cross BBB. The histological analysis has been performed to observe the biocompatibility of nanoformulation. In fig.4.17, results have shown no toxicological demarcation and deterioration in the tissue sections of vital organs (brain, heart, kidney, liver, and spleen). Considering this fact, CsNPs could be a new promising nanocarrier system for FTY720 in the treatment of chronic and acute neuronal infirmities.

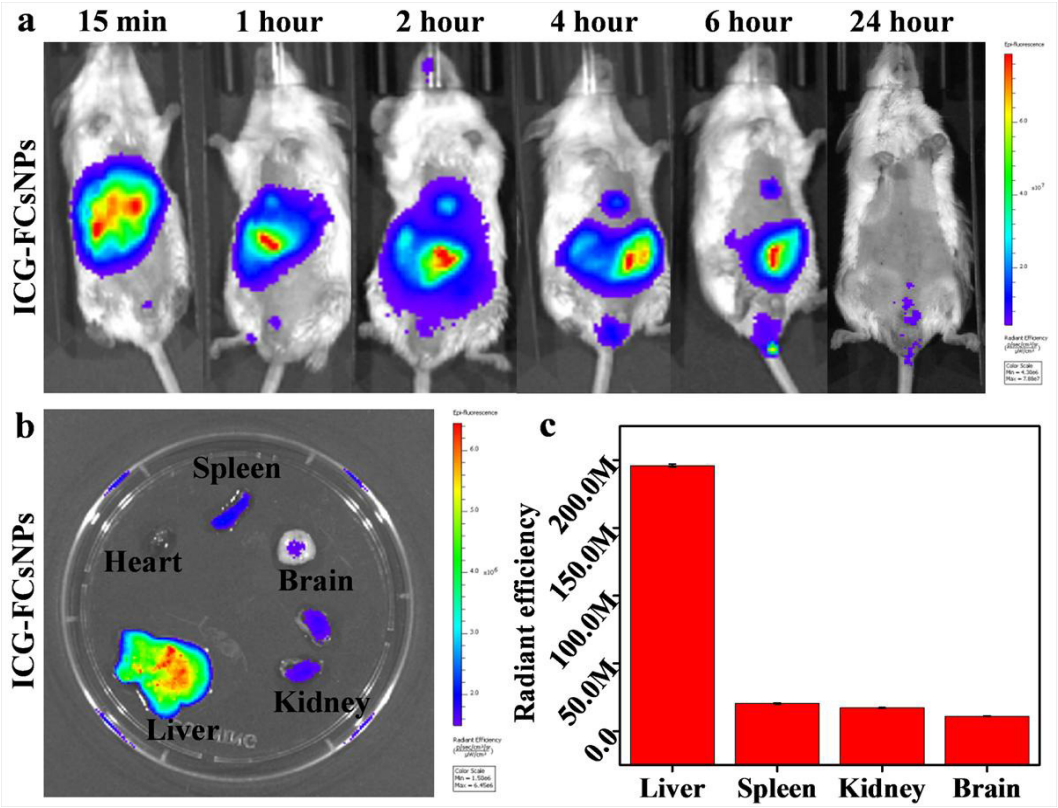

Figure 4.16. *In vivo/ex vivo* bio-distribution analysis (a) *In vivo* bio-distribution analysis reflects the higher intake of nanoformulation to the heart, brain, liver, spleen, and kidney as distribution profile. (b) *Ex vivo* organ reflectance imaging has shown higher retention in the liver, kidney, spleen, and brain 24 hours of post-injection. (c) Quantification of particles was presented as a function of radiant efficiency.

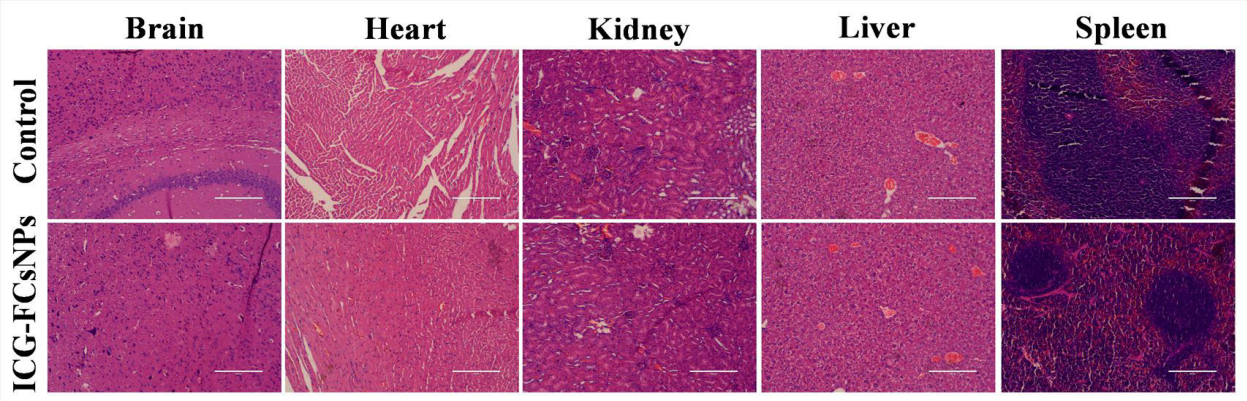


Figure 4.17. Histological analysis reveals the bio-compatible nature of nanoparticles without any deformation in tissues of vital organs. (The scale bar- is 200 µm, magnification-20X)

Table 4.1. Chitosan: TPP ratio and results of DLS measurement parameters are tabulated.

| Chitosan:TPP | Parameters | | |
|---|---|---|---|
| | Size (nm) | PDI | Zeta potential (mV) |
| **2:1** | 73 ± 1.23 | 0.33± 0.0059 | 22 ± 2.3 |
| **4:1** | 107 ± 1.54 | 0.26 ± 0.0072 | 25 ± 4.01 |
| **6:1** | 124 ± 1.96 | 0.35 ± 0.0035 | 32 ± 3.66 |
| **10:1** | 166 ± 2.7 | 0.55 ± 0.0061 | 35 ± 3.25 |
| **15:1** | 189 ± 1.81 | 0.3 ± 0.0013 | 41 ± 4.58 |

Table 4.2. Results of DLS measurement parameters are tabulated with different periods.

| Time period | Parameters | | |
|---|---|---|---|
| | Size (nm) | PDI | Zeta potential (mV) |
| **0.125** | 122.4 ± 4.1 | 0.352 ± 0.0021 | 21.5 ± 3.1 |
| **0.5** | 119.6 ± 4.1 | 0.322 ± 0.0043 | 21.23 ± 3.4 |
| **1** | 127 ± 2.6 | 0.339 ± 0.0064 | 22.8 ± 2.6 |
| **2** | 123.3 ± 1.9 | 0.307 ± 0.0056 | 22.25 ± 1.9 |
| **3** | 118.1 ± 3.1 | 0.397 ± 0.0043 | 20.4 ± 3.1 |
| **5** | 121.2 ± 4.21 | 0.378 ± 0.00388 | 17.9 ± 3.21 |
| **10** | 120.2 ± 3.23 | 0.355 ± 0.00411 | 15 ± 2.11 |

Table 4.3. Comparison of the FTY720 release data obtained after fitting the release profile of FTY720-loaded chitosan nanoparticles. (Bold font represents good fitting parameters)

| Model | FTY720 loaded Chitosan nanoparticles | | | |
|---|---|---|---|---|
| | Parameters | $R^2$ | AIC | MSC |
| **Zero order** | $k_0$ = 0.266 | -46.4135 | 183.2626 | -3.9642 |
| **First order** | $k_1$ = 0.004 | -41.1859 | 181.0430 | -3.8473 |
| **Higuchi** | $k_H$ = 3.978 | -24.3882 | 171.3947 | -3.3395 |
| **Korsmeyer-Peppas** | **$k_{KP}$ = 33.73<br>n = 0.035** | **0.8538** | **77.4043** | **1.6071** |
| **Hixson-Crowell** | $k_{HC}$ = 0.001 | -42.9784 | 181.8336 | -3.8890 |
| **Hopfenberg** | $k_{HB}$ = 0.000 | -41.2058 | 183.0519 | -3.9531 |
| **Baker-Lonsdale** | $k_{BL}$ = 0.000 | -21.6089 | 169.1918 | -3.2236 |
| **Makoid-Banakar** | **$k_{MB}$ = 31.866<br>n = 0.072<br>k = 0.001** | **0.9568** | **56.2497** | **2.7207** |
| **Peppas-Sahlin** | $k_1$ = 34.169<br>$k_2$ = -2.607 | 0.6410 | 94.4812 | 0.7085 |
| **Weibull** | **α = 0.807<br>β = 0.388<br>Ti = 0.433<br>Fmax = 39.689** | **0.9546** | **57.2094** | **2.6702** |
| **Quadratic** | $k_1$ = 0.000<br>$k_2$ = 0.008 | -31.2538 | 177.9424 | -3.6842 |
| **Logistic** | **α = 0.509<br>β = 2.278<br>Fmax = 39.92** | **0.9483** | **57.6473** | **2.6472** |
| **Gompertz** | **α = 0.479<br>β = 2.011<br>Fmax = 40.019** | **0.9470** | **58.1310** | **2.6217** |
| **Probit** | **α = 0.338<br>β = 1.299<br>Fmax = 39.722** | **0.9516** | **56.3947** | **2.7131** |

## 4a.3 Conclusion

Oveall finding indicate the immense neurotherapeutic potentiality of FTY720-enriched chitosan nanoparticles as combinatorial therapy. The major key findings include attenuation of rotenone-stimulated mitochondrial insults; neuronal and cellular damages by decreasing pSer129 α-Syn. The improved drug release profile and higher cellular internalization of nanoparticles is the addition key finding exhibits significance of nanoformulation in compare to bare drug. The major breakthrough finding of this study also is the epigenetic regulatory mechanism describing the camouflaged role of PP2A in the EzH2 mediated α-Syn regulation. Although, the precise role of PP2A involving other epigenetic regulators for PD prevention is yet to be investigated. Nevertheless, several lines of evidence from the molecular study indicate that our

nanoformulation-induced PP2A is likely to attenuate α-Synucleinopathy and may represent a promising neurotherapeutic strategy. The benefit of the presented nanoformulation is to overcome the limitation of FTY720, insoluble drug by providing neuroprotective nanocarrier. The major significance and novelty of presented work is FTY720 has been first time conjugated in the nanoparticles with aim to treat PD. As per our best knowledge, no other FTY720 loaded nanoformulation is reported. As FTY720 is FDA approved and safe drug so far and chitosan naoparticle is also widely reported biocompatible nanoparticles therefore presented formulation has better chance to get translated in clinical application. However, the limitations of the presented work are the lack of positive control (levodopamine, a commercial PD drug) and lack of animal study. Indeed, the bulk synthesis and long term toxicity of nanoformulation may hinder the translational potential of presented work in further clinical investigation. However, our study elucidates the neuroprotective efficiency of chitosan-based FTY720 nanoformulation in the retardation of rotenone-induced PD deficits by inducing PP2A-EzH2 mediated pSer129 α-Syn ubiquitination/ degradation in PD prevention. In the future perspective of the research, the study might be useful to treat neurological disorders including Parkinson's disease by using chitosan-based novel nano delivery of FTY720 at preclinical and clinical setup.

## 4a.4 References


1. A. Oueslati, Implication of Alpha-Synuclein Phosphorylation at S129 in Synucleinopathies: What Have We Learned in the Last Decade? *J Parkinsons Dis* 6, 39-51 (2016).
2. G. Vidal-Martinez *et al.*, FTY720 Improves Behavior, Increases Brain-Derived Neurotrophic Factor Levels and Reduces α-Synuclein Pathology in Parkinsonian GM2+/− Mice. *Neuroscience* 411, 1-10 (2019).
3. A. H. V. Schapira, Treatment Options in the Modern Management of Parkinson Disease. *Archives of Neurology* 64, 1083-1088 (2007).
4. B. D. Li *et al.*, Adverse effects produced by different drugs used in the treatment of Parkinson's disease: A mixed treatment comparison. *CNS neuroscience & therapeutics* 23, 827-842 (2017).

5. P. Zhao *et al.*, Neuroprotective effects of fingolimod in mouse models of Parkinson's disease. 31, 172-179 (2017).
6. R. Cipriani, J. C. Chara, A. Rodríguez-Antigüedad, C. Matute, FTY720 attenuates excitotoxicity and neuroinflammation. *Journal of Neuroinflammation* 12, 86 (2015).
7. S. F. Hunter, J. D. Bowen, A. T. Reder, The Direct Effects of Fingolimod in the Central Nervous System: Implications for Relapsing Multiple Sclerosis. *CNS Drugs* 30, 135-147 (2016).
8. T. Takasaki, K. Hagihara, R. Satoh, R. Sugiura, More than Just an Immunosuppressant: The Emerging Role of FTY720 as a Novel Inducer of ROS and Apoptosis. *Oxid Med Cell Longev* 2018, 4397159 (2018).
9. Y. Mao *et al.*, A novel liposomal formulation of FTY720 (fingolimod) for promising enhanced targeted delivery. *Nanomedicine: nanotechnology, biology, and medicine* 10, 393-400 (2014).
10. J. K. Patra *et al.*, Nano based drug delivery systems: recent developments and future prospects. *Journal of Nanobiotechnology* 16, 71 (2018).
11. B. Chen, J. Li, R. B. Borgens, Neuroprotection by chitosan nanoparticles in oxidative stress-mediated injury. *BMC Research Notes* 11, 49 (2018).
12. K. Divya, V. Smitha, M. S. Jisha, Antifungal, antioxidant and cytotoxic activities of chitosan nanoparticles and its use as an edible coating on vegetables. *Int J Biol Macromol* 114, 572-577 (2018).
13. M. von Schimmelmann *et al.*, Polycomb repressive complex 2 (PRC2) silences genes responsible for neurodegeneration. *Nature neuroscience* 19, 1321-1330 (2016).
14. E. Sodersten *et al.*, Dopamine signaling leads to loss of Polycomb repression and aberrant gene activation in experimental parkinsonism. *PLoS genetics* 10, e1004574 (2014).
15. M. Abdouh *et al.*, Bmi1 is down-regulated in the aging brain and displays antioxidant and protective activities in neurons. *PloS one* 7, e31870 (2012).
16. Y. Oh, Y. M. Kim, M. M. Mouradian, K. C. Chung, Human Polycomb protein 2 promotes alpha-synuclein aggregate formation through covalent SUMOylation. *Brain research* 1381, 78-89 (2011).

17. R. Rott *et al.*, SUMOylation and ubiquitination reciprocally regulate alpha-synuclein degradation and pathological aggregation. *Proceedings of the National Academy of Sciences of the United States of America* 114, 13176-13181 (2017).
18. M. N. Sardoiwala, A. K. Srivastava, B. Kaundal, S. Karmakar, S. R. Choudhury, Recuperative effect of metformin loaded polydopamine nanoformulation promoting EZH2 mediated proteasomal degradation of phospho-alpha-synuclein in Parkinson's disease model. *Nanomedicine* 24, 102088 (2019).
19. S. H. Hussein-Al-Ali, A. Kura, M. Z. Hussein, S. Fakurazi, Preparation of chitosan nanoparticles as a drug delivery system for perindopril erbumine. 39, 544-552 (2018).
20. E. Masoudipour, S. Kashanian, N. Maleki, A. Karamyan, K. Omidfar, A novel intracellular pH-responsive formulation for FTY720 based on PEGylated graphene oxide nano-sheets. *Drug Development and Industrial Pharmacy* 44, 99-108 (2018).
21. H. Alshaker *et al.*, New FTY720-docetaxel nanoparticle therapy overcomes FTY720-induced lymphopenia and inhibits metastatic breast tumour growth. *Breast Cancer Research and Treatment* 165, 531-543 (2017).
22. Y. Cho, R. Shi, R. B. Borgens, Chitosan produces potent neuroprotection and physiological recovery following traumatic spinal cord injury. *The Journal of Experimental Biology* 213, 1513 (2010).
23. G. Kerch, The potential of chitosan and its derivatives in prevention and treatment of age-related diseases. *Mar Drugs* 13, 2158-2182 (2015).
24. J. Sarvaiya, Y. K. Agrawal, Chitosan as a suitable nanocarrier material for anti-Alzheimer drug delivery. *Int J Biol Macromol* 72, 454-465 (2015).
25. T. Lam *et al.*, SYNTHESIS AND CHARACTERIZATION OF CHITOSAN NANOPARTICLES USED AS DRUG CARRIER. *J. Chem.* 44 (2006).
26. F. Sadeghi, A. Fayazi, Analysis of Crystalline Structure of Sodium Tripolyphosphate: Effect of pH of Solution and Calcination Conditions. *Industrial & Engineering Chemistry Research* 51, 1093-1098 (2012).
27. J.-R. Wang, S. Li, B. Zhu, X. Mei, Insight into the conformational polymorph transformation of a block-buster multiple sclerosis drug fingolimod hydrochloride (FTY 720). *Journal of Pharmaceutical and Biomedical Analysis* 109, 45-51 (2015).

28. D. R. Naik, J. P. Raval, *Amorphous polymeric binary blend pH-responsive nanoparticles for dissolution enhancement of antiviral drug* (2012), vol. 68.
29. A. Geçer, N. Yildiz, A. Çalımlı, B. Turan, Trimethyl chitosan nanoparticles enhances dissolution of the poorly water soluble drug Candesartan-Cilexetil. *Macromolecular Research* 18, 986-991 (2010).
30. C. Lustriane, F. Dwivany, V. Suendo, M. Reza, Effect of chitosan and chitosan-nanoparticles on post harvest quality of banana fruits. *Journal of Plant Biotechnology* 45, 36-44 (2018).
31. L. Rezaie shirmard *et al.*, Nanoparticulate fingolimod delivery system based on biodegradable poly (3-hydroxybutyrate-co-3-hydroxyvalerate) (PHBV): design, optimization, characterization and in-vitro evaluation. *Pharmaceutical development and technology* 22, 1-11 (2015).
32. S. Gokila, T. Gomathi, S. P.N, A. Sukumaran, Removal of the heavy metal ion chromiuim(VI) using Chitosan and Alginate nanocomposites. *International Journal of Biological Macromolecules* 10.1016/j.ijbiomac.2017.05.117 (2017).
33. S. A. Özkan, A. Dedeoğlu, N. Karadaş Bakirhan, Y. Özkan, Nanocarriers Used Most in Drug Delivery and Drug Release: Nanohydrogel, Chitosan, Graphene, and Solid Lipid. *Turkish journal of pharmaceutical sciences* 16, 481-492 (2019).
34. A. Rajan, G. S T, P. P.K, Chitosan Nanoparticle for Drug Delivery – A Mini Review. 8, 4181-4190 (2017).
35. J. Li *et al.*, Chitosan-Based Nanomaterials for Drug Delivery. *Molecules* 23, 2661 (2018).
36. P. Jose, K. Sundar, C. H. Anjali, A. Ravindran, Metformin-loaded BSA nanoparticles in cancer therapy: a new perspective for an old antidiabetic drug. *Cell biochemistry and biophysics* 71, 627-636 (2015).
37. D. Patel, S. Naik, A. Misra, Improved transnasal transport and brain uptake of tizanidine HCl-loaded thiolated chitosan nanoparticles for alleviation of pain. *J Pharm Sci* 101, 690-706 (2012).
38. J. H. Lee, Y. Yeo, Controlled Drug Release from Pharmaceutical Nanocarriers. *Chemical engineering science* 125, 75-84 (2015).

39. R. M. Shah, D. S. Eldridge, E. A. Palombo, I. H. Harding, Microwave-assisted formulation of solid lipid nanoparticles loaded with non-steroidal anti-inflammatory drugs. *International Journal of Pharmaceutics* 515, 543-554 (2016).
40. P. Costa, J. M. Sousa Lobo, Modeling and comparison of dissolution profiles. *European Journal of Pharmaceutical Sciences* 13, 123-133 (2001).
41. S. Dash, P. N. Murthy, L. Nath, P. Chowdhury, Kinetic modeling on drug release from controlled drug delivery systems. *Acta Pol Pharm* 67, 217-223 (2010).
42. Y. Zhang, M. Huo, J. Zhou, S. Xie, PKSolver: An add-in program for pharmacokinetic and pharmacodynamic data analysis in Microsoft Excel. *Computer Methods and Programs in Biomedicine* 99, 306-314 (2010).
43. M. Ren *et al.*, FTY720 Attenuates 6-OHDA-Associated Dopaminergic Degeneration in Cellular and Mouse Parkinsonian Models. *Neurochem Res* 42, 686-696 (2017).
44. M. H. Moon, J. K. Jeong, Y. J. Lee, S. Y. Park, FTY720 protects neuronal cells from damage induced by human prion protein by inactivating the JNK pathway. *Int J Mol Med* 32, 1387-1393 (2013).
45. S. A. Correa, K. L. Eales, The Role of p38 MAPK and Its Substrates in Neuronal Plasticity and Neurodegenerative Disease. *Journal of signal transduction* 2012, 649079 (2012).
46. H. J. Lee, C. Kim, S. J. Lee, Alpha-synuclein stimulation of astrocytes: Potential role for neuroinflammation and neuroprotection. *Oxidative medicine and cellular longevity* 3, 283-287 (2010).
47. S. Sarangapani *et al.*, Chitosan nanoparticles' functionality as redox active drugs through cytotoxicity, radical scavenging and cellular behaviour. *Integr Biol (Camb)* 10, 313-324 (2018).
48. M. Shamoto-Nagai *et al.*, An inhibitor of mitochondrial complex I, rotenone, inactivates proteasome by oxidative modification and induces aggregation of oxidized proteins in SH-SY5Y cells. *Journal of neuroscience research* 74, 589-597 (2003).
49. K. K. Dev *et al.*, Brain sphingosine-1-phosphate receptors: implication for FTY720 in the treatment of multiple sclerosis. *Pharmacol Ther* 117, 77-93 (2008).

50. L. Q. Jiang *et al.*, Intracellular disposition of chitosan nanoparticles in macrophages: intracellular uptake, exocytosis, and intercellular transport. *Int J Nanomedicine* 12, 6383-6398 (2017).
51. J. B. Kwok, Role of epigenetics in Alzheimer's and Parkinson's disease. *Epigenomics* 2, 671-682 (2010).
52. J. E. Campbell *et al.*, EPZ011989, A Potent, Orally-Available EZH2 Inhibitor with Robust in Vivo Activity. *ACS medicinal chemistry letters* 6, 491-495 (2015).
53. Y. Wang *et al.*, HIV-1 Vpr disrupts mitochondria axonal transport and accelerates neuronal aging. *Neuropharmacology* 117, 364-375 (2017).
54. B. I. Perez-Revuelta *et al.*, Metformin lowers Ser-129 phosphorylated alpha-synuclein levels via mTOR-dependent protein phosphatase 2A activation. *Cell death & disease* 5, e1209 (2014).
55. Q. Huang, H. Wang, S. W. Perry, M. E. Figueiredo-Pereira, Negative regulation of 26S proteasome stability via calpain-mediated cleavage of Rpn10 subunit upon mitochondrial dysfunction in neurons. *J Biol Chem* 288, 12161-12174 (2013).
56. N. Zhang, D. Dou, X. Ran, T. Kang, Neuroprotective effect of arctigenin against neuroinflammation and oxidative stress induced by rotenone. *RSC Advances* 8, 2280-2292 (2018).
57. A. P. Mann *et al.*, A peptide for targeted, systemic delivery of imaging and therapeutic compounds into acute brain injuries. *Nature communications* 7, 11980 (2016).
58. B. R. Bitner *et al.*, Antioxidant carbon particles improve cerebrovascular dysfunction following traumatic brain injury. *ACS nano* 6, 8007-8014 (2012).
59. J. Xu *et al.*, Theranostic Oxygen Reactive Polymers for Treatment of Traumatic Brain Injury. 26, 4124-4133 (2016).
60. D. Yoo *et al.*, Core-Cross-Linked Nanoparticles Reduce Neuroinflammation and Improve Outcome in a Mouse Model of Traumatic Brain Injury. *ACS nano* 11, 8600-8611 (2017).
61. L. J. McCreight, C. J. Bailey, E. R. Pearson, Metformin and the gastrointestinal tract. *Diabetologia* 59, 426-435 (2016).
62. R. Villaseñor, J. Lampe, M. Schwaninger, L. J. C. Collin, M. L. Sciences, Intracellular transport and regulation of transcytosis across the blood–brain barrier. 76, 1081-1092 (2019).

# Chapter 4b

---

# Neuroprotective effect of FTY720 loaded chitosan nanoformulations retard PD *in vivo* model

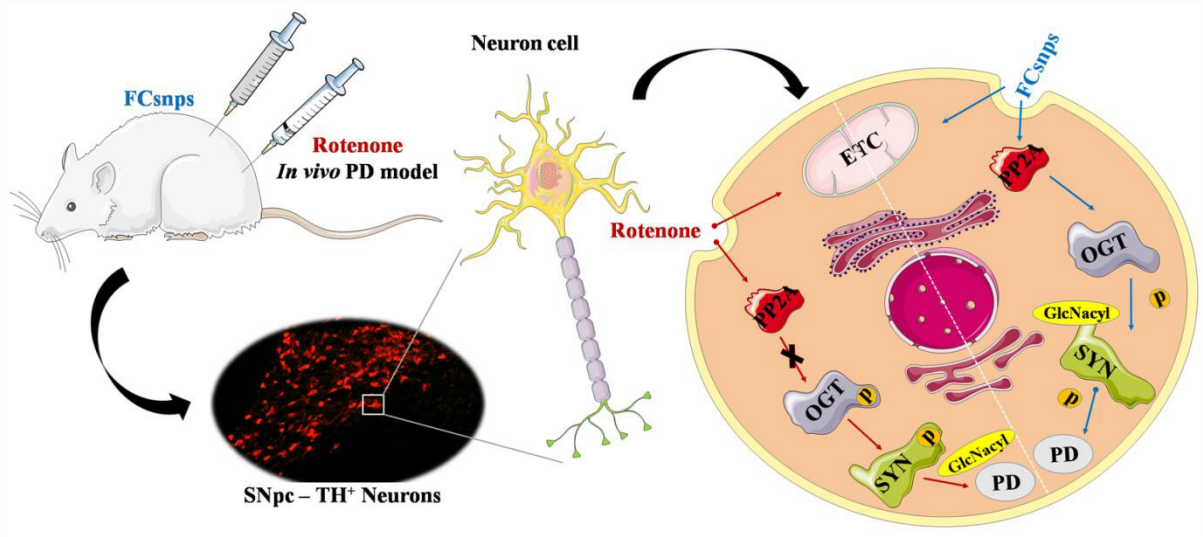

## 4b.1. Introduction

Parkinson's disease (PD) burden is increasing with time at globe including in developing countries like India. (1) The formation of Lewy bodies and death of dopaminergic neurons is the major factor behind PD etiology. (2) The aggregated synuclein is the major contributor to Lewy bodies and the pathological condition that arises from the aggregated synuclein is called synucleinopathy. (3) Existing treatment regimes effectively slow down the PD progression, but the associated multiple side effects including dementia, tremor, fatigue, etc. limit their therapeutic efficacy. (4) Hence, there is a need for a new therapeutic candidate that can manage PD conditions more efficiently by controlling synuclein aggregation, a major player in PD progression. In recent times, FTY720, a PP2A activator has emerged as a promising neurotherapeutic candidate in the treatment of neurodegenerative infirmities. (5-7) The blood-brain barrier crossing efficiency of FTY720 is also reported with its anti-inflammatory and anti-oxidative potential. (8),(9) However, the therapeutic efficiency of FTY720 has been compromised due to its hydrophobic nature, insolubility, less bio-availability, and associated risk of severe infection. (10) We have previously reported the FTY720 loaded chitosan nanoparticles to overcome the limitation of the FTY720 drug by considering the promising advantages of nanotechnology in the drug delivery system. (11) In that, we have demonstrated an improved drug release profile of FTY720 with release kinetics, minimization of therapeutic dose, and neuroprotective caliber in vitro and ex vivo PD model. Herein in the present study, we have explored the therapeutic action and neuroprotective mechanism of FTY720 loaded chitosan nanoparticles in vivo PD model.

The Association of post-translational modification of synuclein in PD etiology has a great influence on PD management. (12) In that, the phosphorylation and nitration of synuclein have a bad impact that leads to synuclein aggregation and PD progression, while O-GlcNacylation of synuclein reduces synucleinopathy which has been well demonstrated. Indeed, the enzyme, O-GlcNacyl transferase (OGT) responsible for O-GlcNacylation of synuclein is also reported to be reduced during the PD conditions. (13) Thus, the strategy to endow O-GlcNacylation paves the way for the development of PD treatment. Recently, the literature has demonstrated that phosphorylation of OGT leads to loss of activity and expression. (14) However, the detailed molecular mechanism and OGT regulation have not been explored, yet. Therefore, we have investigated whether our FTY720 nanoformulation can restore OGT level and activity by

activating PP2A as therapeutic action. In the present study, we have demonstrated the neurotherapeutic potential of FTY720 nanoformulation that has been confirmed by the restoration of TH, a signature therapeutic target of PD. As per current knowledge, the present study first time revealed the camouflage role of PP2A in OGT restoration and endowment of O-GlcNacylation of synuclein to reduce synucleinopathy. Thus, the study divulges the FTY720 nanoformulation mediated PP2A activation and its direct physical interaction with OGT leads to OGT activation and O-GlcNacylation of synuclein to alleviate the synucleinopathy. The project design of the chapter 3b represented for better understanding of hypothesis, rationale of chapter with justification of the selected compound aligned to expected outcomes of the aims as below.

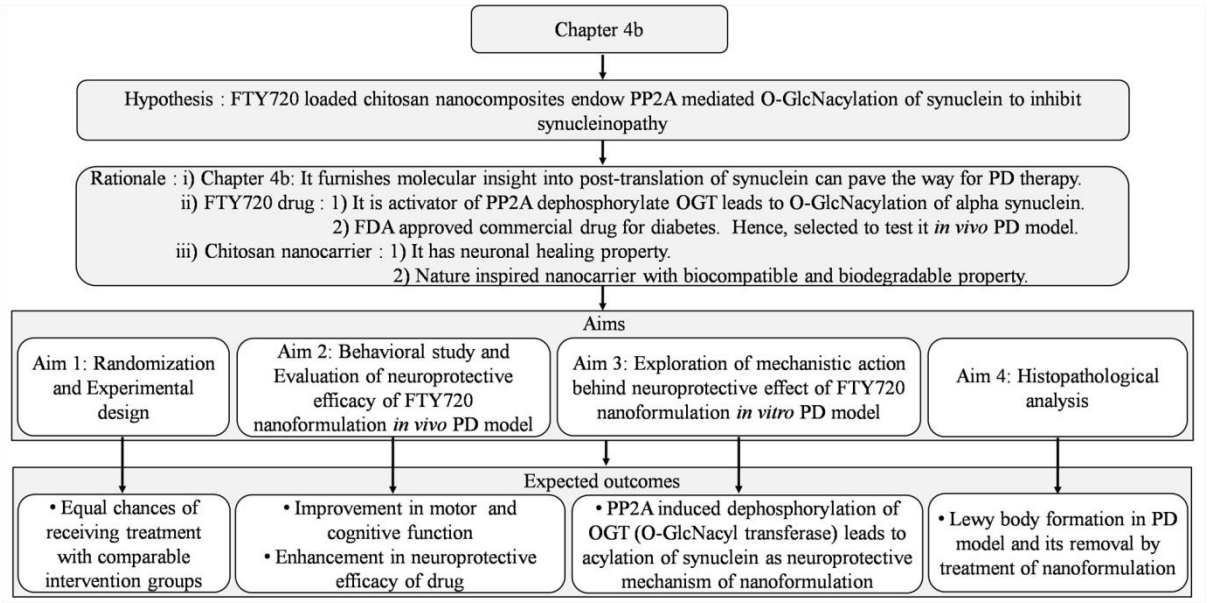


Scheme 6: The project design represents hypothesis, rationale, aims and it's aligned expected outcomes.

## 4b.2. Result and Discussion

### 4b.2.1. FCsnps alleviate the behavioral changes against the rotenone effect

The experimental design of the rotenone model and treatment has been shown in fig.4.18a. The therapeutic effect of FCsnps has been evaluated through the behavioral study against rotenone-induced deficits. The reduction in the grip strength by ~ 2 folds observed with the rotenone effect and ~ 3 folds elevation in the decent latency was also observed as the rotenone effect. (Fig.4.18b, 1c) The ~ 2 folds recovery in the grip strength and decent latency by FCsnps has

been observed against rotenone-induced insults. The spontaneous alteration assay has been performed to evaluate the improvement in cognitive impairment by our nanoformulation. The report has shown rotenone's impact on the impairment of cognitive function in PD progression. (15, 16) In the result, the rotenone exhibited ~30% reduction in the alteration movement from the A-B-C arm and FCsnps has shown improvement in the cognitive function by restoring ~25% alteration movement. (Fig.4.18d) Herein, the FCsnps has shown a similar pattern of improvement in the behavioral activity that has been reported by existing literature on FTY720 formulation. (17) Thus, the FCsnps has exhibited neuroprotective potential by restoring behavioral changes to normal activity that improves cognitive impairment and motor dysfunction.

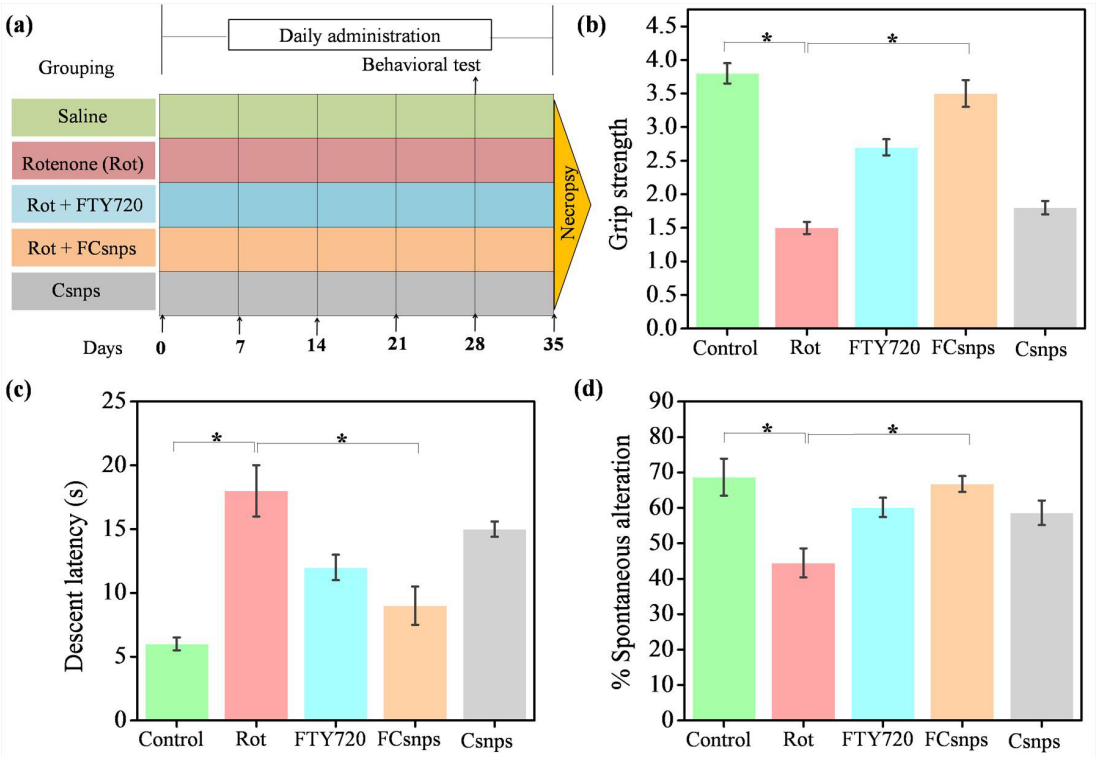


Figure.4.18 Experimental design has been shown (a), The behavioral study has exhibited improvement in grip strength (b), decent latency (c), and cognitive impairment (d) against rotenone-induced deficits.

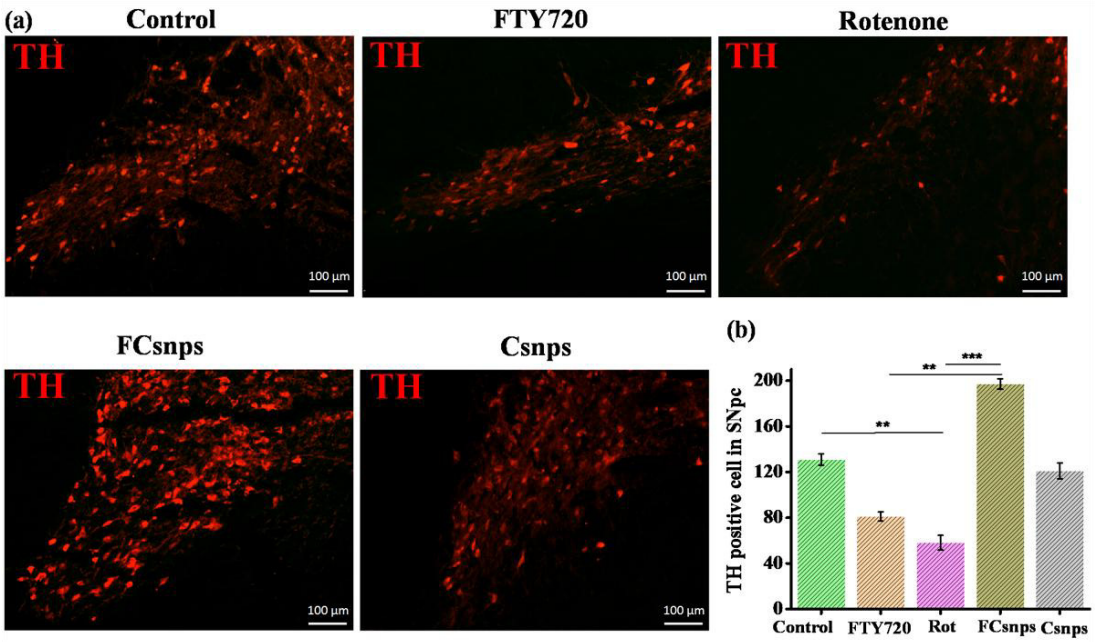


Figure.4.19. The neurotherapeutic potential of FCsnps has been verified by examining TH expression in SNpc (a) and the quantification of TH-positive neurons has been also illustrated (b).

4b.2.2. TH+ neurons restoration indicates the neuroprotective effect of FCsnps

TH is the hallmark of dopaminergic neurons that resides in the substantial nigra. Therefore, the immunofluorescence imaging of substantial nigra has been conducted to confirm the rotenone-induced model and verify the neuroprotective efficacy of FCsnps. The presence of TH+ neurons has been quantified and presented with the images. (Fig.4.19) Herein, the reduction in the TH+ and dopamine-producing neurons results in PD pathogenesis. The results have shown a higher number of loss of TH+ neurons with a rotenone effect that signifies the establishment of a rotenone-induced PD model. At the other end, FCsnps has exhibited restoration of TH+ neurons that confirmed the neuroprotective effect of FCsnps. Herein, the FCsnps has shown better restoration of TH+ neurons in comparison to FTY720 and Csnps. The neuroprotective effect of our nanoformulation in vivo is also supported by our previously reported report of the neuroprotective effect of FTY720-loaded chitosan nanoparticles in vitro and ex vivo PD models. (11) The results have shown ~2.4 folds decrease in TH+ neurons and ~4 folds restoration after FCsnps treatment which has shown a better therapeutic effect in comparison to the existing report of FTY720 formulation shown ~1.33 folds restoration after ~1.44 folds reduction in the dopaminergic neurons in the PD treatment. (18) The possible reason behind the neurotherapeutic

effect of FCsnps could be the improved drug kinetics property of nanoformulations that endows FTY720 efficacy shown in the previously reported literature. (11)

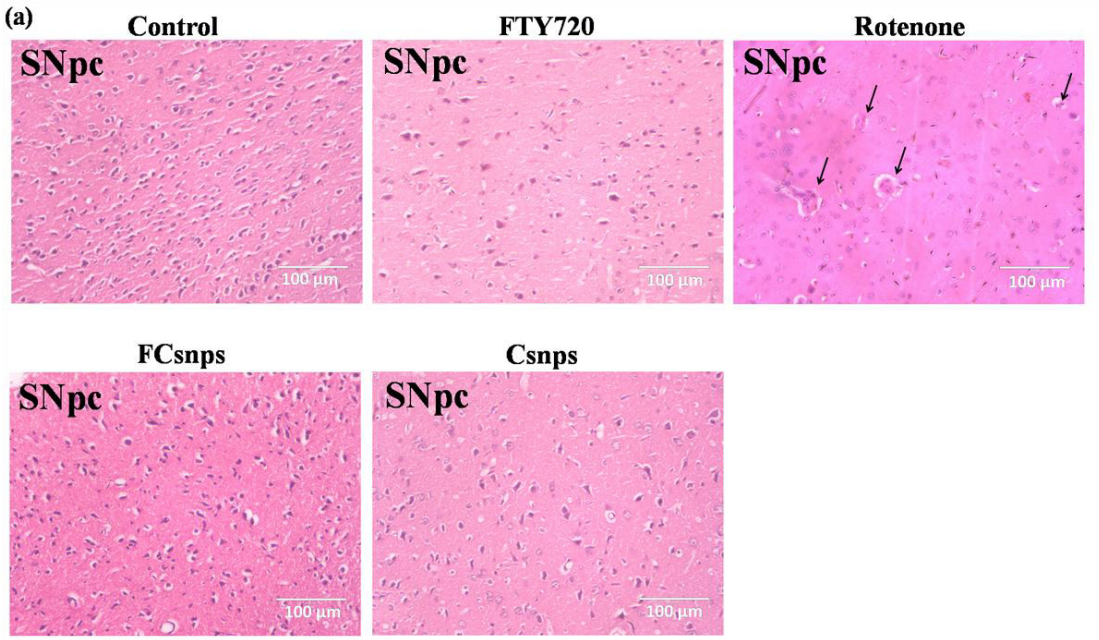


Figure.4.20. The histopathological analysis of SNpc has shown rotenone-induced Lewy body formation and restoration of healthy condition with FCsnps treatment.

4b.2.3. FCsnps improves histopathological demarcation signifies the neuroprotective effect

The histopathological examination has been conducted to verify rotenone-induced effects and restoration of healthy conditions by FCsnps. The images of Substantial nigra (SNpc) have confirmed the neurodegeneration due to rotenone and the recovery has been observed with the treatment of FCsnps. The black arrow has highlighted Lewy body structures in SNpc (Fig.4.20) and degeneration of neurons in the hippocampus (Fig.4.21). The similar kind of Lewy body structures and pathological demarcation supports the finding of our results that signifies the establishment of rotenone-induced PD models. Herein, the restoration of healthy neuronal conditions and recovery of neuronal cells with the treatment of FCsnps has confirmed the neuroprotective effect of FCsnps. (19) (20) The results of the histopathological analysis are in line with the existing reports that have shown the neuroprotective effect of another neuroprotective candidate by histopathological examination. (20) Herein, FCsnps exhibited better neuroprotective potential in comparison to FTY720 and Csnps, and the results of

behavioral activity, TH+ neurons assessment, and histopathological analysis support each other that divulges neuroprotective effect of FCsnps.

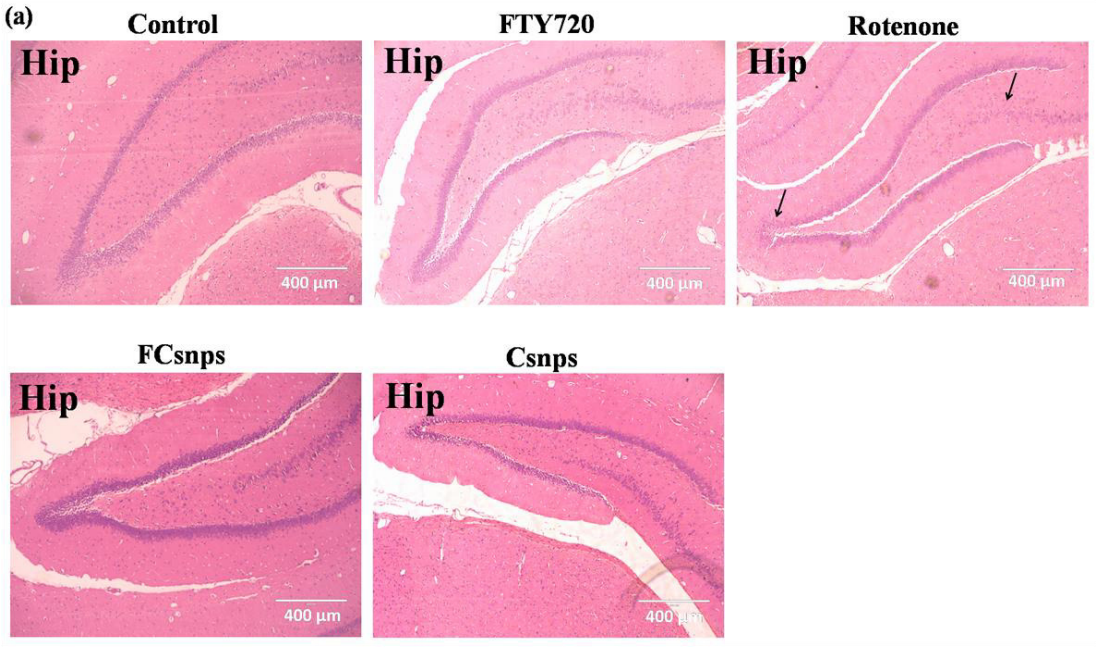


Figure.4.21. Neurodegeneration has been noted in the rotenone group and FCsnps exhibited recovery of the neurons.

4b.2.4. FCsnps endow O-GlcNacylation of synuclein to prevent Parkinson's disease

The rotenone-induced PD model has been verified through investigation of TH and p-alpha synuclein, a hallmark of PD. The loss of TH and synuclein accumulation has been reported as a major cause of PD progression and TH recovery and synuclein inhibition pave the way for PD treatment. (21, 22) The result has shown ~ 10 folds reduction in the TH expression and the FCsnps exhibited ~20 folds improvement in the TH expression. (Fig.4.22a) FCsnps has shown a better therapeutic effect by recovery of ~20 folds TH expression in comparison to the reported literature that has demonstrated ~ 2.5 folds restoration of TH. (23) Similarly, Syn oligomerization was also significantly upregulated by ~9 folds and reduced by ~4 folds with the treatment of FCsnps. The results have confirmed the superior neuroprotective efficacy of FCsnps in comparison to the existing report of FTY720 formulation in alpha-synuclein reduction. (24) Hence, the protein expression of PD signature molecules has confirmed the establishment of the PD model and verified the neuroprotective effect of FCsnps. Herein, MPdanps have shown better

protection against rotenone in comparison to Met and Pdanps also in line with the results of the behavioral study and IHC study.

In the exploration of the neuroprotective action of the FCsnps, the FTY720 has the potential to enhance PP2A expression that can able to restore the level of its therapeutic target in the PD treatment. (11) Herein, the reports have demonstrated that phosphorylation of OGT leads to hampering the OGT activity. (13) OGT is widely reported to perform O-GlcNacylation of synuclein to inhibit its accumulation. (14, 25) Therefore, the present study has explored the effect of FCsnps by activating PP2A on the expression of OGT and O-GlcNacylation of synuclein. The ~3 folds inhibition of PP2A and ~ 12 folds reduction of OGT has been noted as rotenone-induced effects and FCsnps has shown significant ~ 4 folds upregulation of PP2A and ~10 folds recovery of OGT. (Fig.4.22a) The quantitative representation of protein expression analysis has been shown in fig.4.22b. The protein expression analysis and immunoprecipitation study results have confirmed the PP2A-mediated OGT upregulation and first time revealed PP2A and OGT direct physical protein-protein interaction in the PD treatment. (Fig.4.22c) To validate the effect of FCsnps on the synuclein O-GlcNacylation, the immunoprecipitation study has confirmed that O-GlcNacylation of synuclein has been endowed by FCsnps against rotenone-induced insults. (Fig.4.22c)

### 4b.3 Conclusion

The study can be concluded by observing the several key findings that FCsnps have the potential to induce the PP2A-mediated OGT upregulation and O-GlcNacylation of synuclein in the inhibition of synuclein accumulation. In the major key finding, the improvement in motor neuron function and cognitive function of nanoformulation received animals against rotenone induced insults are included. In addition, the recovery of $TH^+$ neuronal cells present in the SNpc region shows the therapeutic efficiency of nanoformulation. The removal of lewy body formation from the SNpc and hippocampus region divulges the neuroprotective calibre of presented nanoformulation. The finding of neuroprotective effect of FCsnps arbitrated through the results of behavioral study, IHC, and protein expression analysis. In the protein expression analysis, we have first time explored the role of PP2A in endowment of O-GlcNacylation of synuclein to reduce synucleinopathy. As per our best knowledge, no report is available to showcase FTY720

based nanooformulation in context of PD treatment that also provide significance to the presented work. Due to presence of FDA approved drug and highly biocompatible nanocarrier, our nanoofrmulation has immense potential to translate its efficacy at further clinical studies. However, bulk synthesis, long term toxicity and off targeting of nanoparticles may be the future challenges to the presented nanoformulation. However, the study divulges the anti-parkinsonian action of FCsnps by endowing the PP2A-mediated O-GlcNacylation of synuclein to treat synucleinopathy which may provide the solution after further exploration in the clinical setup.

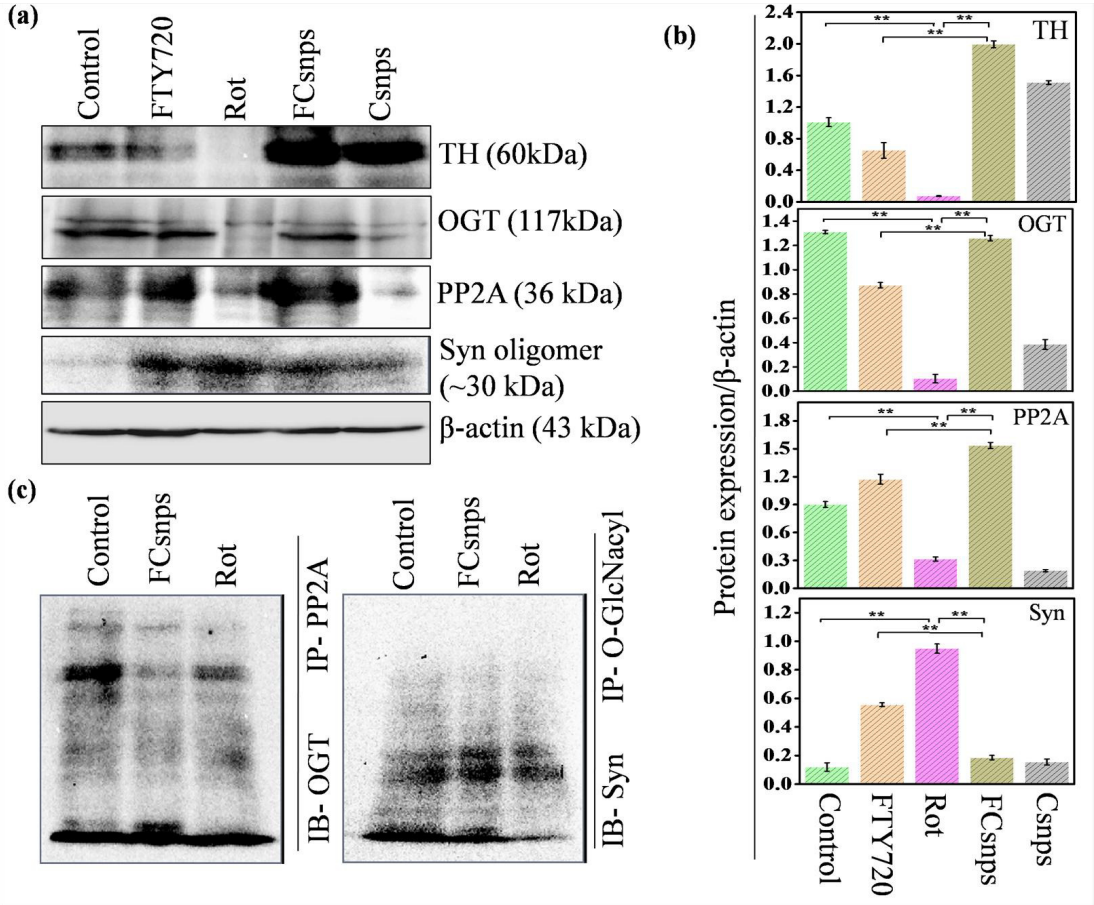


Figure.4.22. Protein expression analysis has validated the neurotherapeutic efficacy of FCsnps (a) and the quantified protein expression has been represented (b). The immunoprecipitation study is also showing the effect of FCsnps that induced PP2A-mediated O-GlcNacylation of synuclein in the PD treatment (c).

4b.4 References


1. D. M. Radhakrishnan, V. Goyal, Parkinson's disease: A review. *Neurol India* **66**, S26-S35 (2018).
2. A. Galvan, T. Wichmann, Pathophysiology of parkinsonism. *Clin Neurophysiol* **119**, 1459-1474 (2008).
3. S. Mullin, A. Schapira, alpha-Synuclein and mitochondrial dysfunction in Parkinson's disease. *Mol Neurobiol* **47**, 587-597 (2013).
4. B. D. Li *et al.*, Adverse effects produced by different drugs used in the treatment of Parkinson's disease: A mixed treatment comparison. *CNS neuroscience & therapeutics* **23**, 827-842 (2017).
5. P. Zhao *et al.*, Neuroprotective effects of fingolimod in mouse models of Parkinson's disease. **31**, 172-179 (2017).
6. G. Vidal-Martinez *et al.*, FTY720/Fingolimod Reduces Synucleinopathy and Improves Gut Motility in A53T Mice: contributions of pro-brain-derived neurotrophic factor (pro-bdnf) and mature bdnf. *J Biol Chem* **291**, 20811-20821 (2016).
7. P. Joshi *et al.*, Fingolimod Limits Acute Aβ Neurotoxicity and Promotes Synaptic Versus Extrasynaptic NMDA Receptor Functionality in Hippocampal Neurons. *Scientific Reports* **7**, 41734 (2017).
8. S. F. Hunter, J. D. Bowen, A. T. Reder, The Direct Effects of Fingolimod in the Central Nervous System: Implications for Relapsing Multiple Sclerosis. *CNS Drugs* **30**, 135-147 (2016).
9. R. Cipriani, J. C. Chara, A. Rodríguez-Antigüedad, C. Matute, FTY720 attenuates excitotoxicity and neuroinflammation. *Journal of Neuroinflammation* **12**, 86 (2015).
10. T. Takasaki, K. Hagihara, R. Satoh, R. Sugiura, More than Just an Immunosuppressant: The Emerging Role of FTY720 as a Novel Inducer of ROS and Apoptosis. *Oxid Med Cell Longev* **2018**, 4397159 (2018).
11. M. N. Sardoiwala, S. Karmakar, S. R. Choudhury, Chitosan nanocarrier for FTY720 enhanced delivery retards Parkinson's disease via PP2A-EzH2 signaling in vitro and ex vivo. *Carbohydrate Polymers* **254**, 117435 (2021).
12. J. Zhang, X. Li, J. D. Li, The Roles of Post-translational Modifications on α-Synuclein in the Pathogenesis of Parkinson's Diseases. *Frontiers in neuroscience* **13**, 381 (2019).

13. B. E. Lee *et al.*, O-GlcNAcylation regulates dopamine neuron function, survival and degeneration in Parkinson disease. *Brain* **143**, 3699-3716 (2020).
14. R. Gélinas *et al.*, AMP-Activated Protein Kinase and O-GlcNAcylation, Two Partners Tightly Connected to Regulate Key Cellular Processes. *Frontiers in endocrinology* **9**, 519 (2018).
15. I. O. Ishola *et al.*, Morin ameliorates rotenone-induced Parkinson disease in mice through antioxidation and anti-neuroinflammation: gut-brain axis involvement. *Brain Research* **1789**, 147958 (2022).
16. D. Zhang *et al.*, Microglial activation contributes to cognitive impairments in rotenone-induced mouse Parkinson's disease model. *Journal of neuroinflammation* **18**, 4-4 (2021).
17. G. Vidal-Martinez *et al.*, FTY720 Improves Behavior, Increases Brain Derived Neurotrophic Factor Levels and Reduces α-Synuclein Pathology in Parkinsonian GM2+/− Mice. *Neuroscience* **411**, 1-10 (2019).
18. É. Pépin, T. Jalinier, G. L. Lemieux, G. Massicotte, M. Cyr, Sphingosine-1-Phosphate Receptors Modulators Decrease Signs of Neuroinflammation and Prevent Parkinson's Disease Symptoms in the 1-Methyl-4-Phenyl-1,2,3,6-Tetrahydropyridine Mouse Model. *Frontiers in pharmacology* **11**, 77 (2020).
19. R. Taipa, J. Pinho, M. Melo-Pires, Clinico-Pathological Correlations of the Most Common Neurodegenerative Dementias. *Frontiers in neurology* **3**, 68 (2012).
20. M. Kujawska *et al.*, Neuroprotective Effects of Pomegranate Juice against Parkinson's Disease and Presence of Ellagitannins-Derived Metabolite—Urolithin A—In the Brain. **21**, 202 (2020).
21. G. Alam, J. R. Richardson, "Chapter 4 - Regulation of tyrosine hydroxylase: relevance to Parkinson's disease" in Genetics, Neurology, Behavior, and Diet in Parkinson's Disease, C. R. Martin, V. R. Preedy, Eds. (Academic Press, 2020), https://doi.org/10.1016/B978-0-12-815950-7.00004-7, pp. 51-66.
22. M. Gómez-Benito *et al.*, Modeling Parkinson's Disease With the Alpha-Synuclein Protein. *Frontiers in pharmacology* **11**, 356 (2020).
23. J. Motyl, Ł. Przykaza, P. M. Boguszewski, P. Kosson, J. B. Strosznajder, Pramipexole and Fingolimod exert neuroprotection in a mouse model of Parkinson's disease by

activation of sphingosine kinase 1 and Akt kinase. *Neuropharmacology* **135**, 139-150 (2018).

24. I. Segura-Ulate, B. Yang, J. Vargas-Medrano, R. G. Perez, FTY720 (Fingolimod) reverses α-synuclein-induced downregulation of brain-derived neurotrophic factor mRNA in OLN-93 oligodendroglial cells. *Neuropharmacology* **117**, 149-157 (2017).

25. P. Levine *et al.*, α-Synuclein O-GlcNAcylation alters aggregation and toxicity, revealing certain residues as potential inhibitors of Parkinson's disease. *Proceedings of the National Academy of Sciences* **116**, 201808845 (2019).

# Chapter 5a

---

# Hytrin-loaded nanohybrid inhibit PD *in vitro* and *ex vivo* model

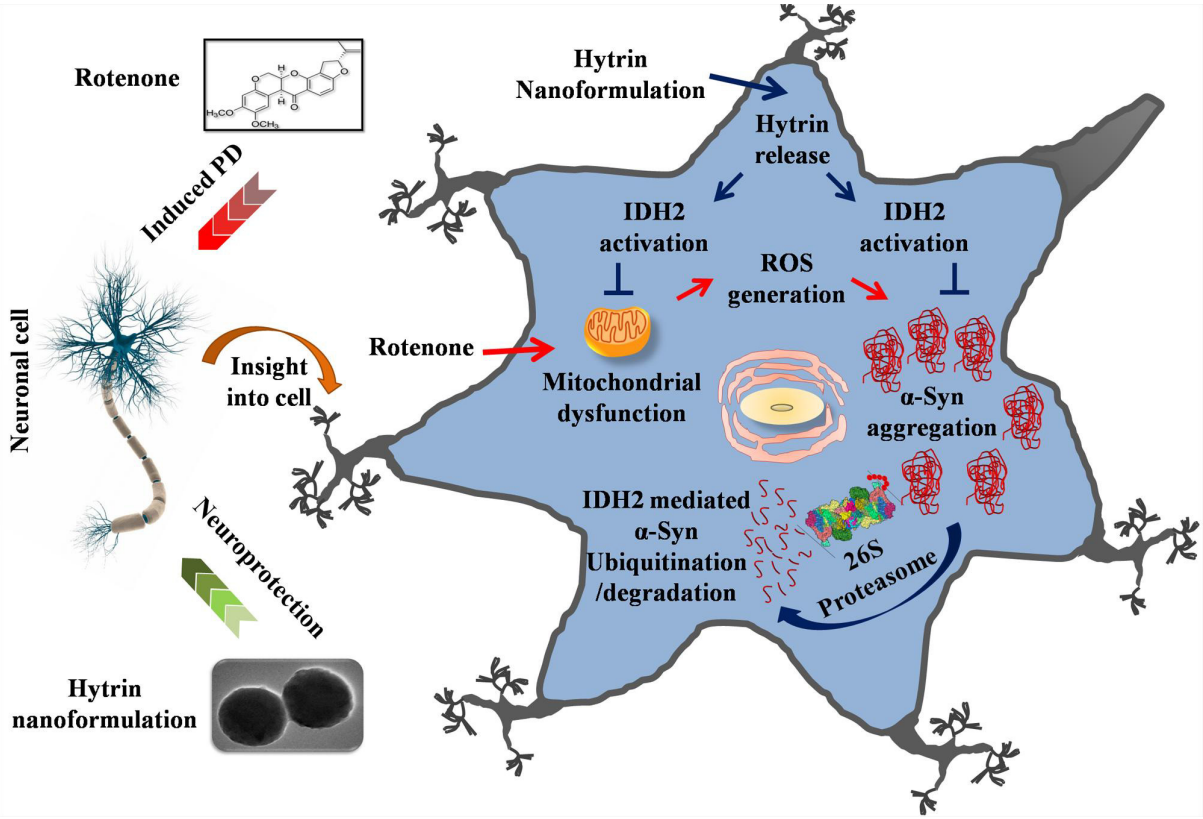

5a.1. Introduction

Parkinson's disease (PD) progresses due to the degeneration of dopaminergic neurons as a cause of aggregated alpha-synuclein. (1) According to the PD foundation, more than 10 million peoples worldwide live with PD. It is expected that 1.3 million people will be suffering from PD by 2030 in the US only and 90% of PD cases are sporadic. In PD pathogenesis, the exact causes behind the death of dopaminergic neurons are still unresolved. Mitochondrial dysfunction and its association with synucleinopathy lead to PD progression and pathogenesis accentuating therapeutic targeting of phosphorylated α-Syn. (2)In the treatment of synucleinopathy-associated PD, recent therapies like deep brain stimulation, and pharmacological and non-pharmacological therapies have been found to have a better response. (3) However, effective PD therapy is still warranted due to the multiple side effects of available treatment regimens. (4) Recently, Hytrin has gained interest as a potent neuroprotective agent. Hytrin has been demonstrated to readily cross the blood-brain barrier, and efficiently slow down neuronal death in parkinsonism. (5)Indeed, a study has also demonstrated that Hytrin enhances adenosine triphosphate (ATP), Pyruvate, and nicotinamide adenine dinucleotide phosphate(NADP+) generations that are important in the maintenance of mitochondrial energy homeostasis.NADP+-dependent isocitrate dehydrogenase 2(IDH2)inductions, a key regulatory process of mitochondrial redox homeostasis have been shown for curtailing oxidative stress-induced cell damage. (6, 7)Furthermore, deficiency of this mitochondrial redox regulator, IDH2 has been demonstrated to exacerbate 1-methyl-4-phenyl-1,2,3,6-tetrahydropyridine (MPTP) -induced PD pathogenesis.(8) Indeed, α-Synuclein accumulation reported to cause mitochondrial dysfunction and affect cellular respiration in PD pathogenesis. (9)Recently, IDH2 has been reported as a novel suppressor of α-synuclein mediated toxicity, a hallmark of PD.(10)Therefore, we are keen to understand IDH2-mediated Hytrin neurotherapeutic effect in the reduction of synucleinopathy and PD treatment.

Despite potential therapeutic effects, an FDA-approved drug, Hytrin has some limitations like burst drug release kinetics with rapid absorption leads to premature release that restricts neurotherapeutic potential due to higher dose requirements. (11, 12) Thus, a strategy is warranted to improve drug release kinetics with the minimization of the required neurotherapeutic dose of Hytrin. The dose-dependent side-effect of Hytrin is well studied (13) and minimization of the dose is the better way to endow neurotherapeutic potential. In the context of that, a promising nano-drug delivery approach has been applied to surpass the limitations of bare Hytrin(14). Here,

we have demonstrated for the first time Hytrin-loaded polydopamine-serotonin nanohybrid (H@PSNPs) that improves drug release kinetics, mitochondrial function, and IDH2 activation mediated reduction of synucleinopathy resulting in a potential neurotherapeutic effect. The present study aimed to provide combinatorial treatment of three neuroprotective agents; Hytrin, dopamine, and serotonin by encapsulating Hytrin in the matrix of polydopamine-serotonin hybrid nanoparticles. The recent update in PD etiology has rendered the loss of both dopaminergic and serotonergic neurons as the common mechanisms in PD pathogenesis. (15) In the previous report, we demonstrated the neuroprotective and anti-inflammatory potential of polydopamine nanoparticles. (16, 17)Hence, the strategy behind considering Hytrin-loaded polydopamine-serotonin nanoparticles is to replenish dopamine and serotonin by providing three neuroprotective agents at a single platform.

In the mechanism of alpha-synuclein degradation, ubiquitination and proteasomal-mediated degradation are major pathways. However, the rotenone-induced insults have been reported to reduce the level of ubiquitinylated proteins and E1A activity required for the functioning of ubiquitination and proteasomal-mediated degradation pathway. (18)Therefore, it is important to enhance the ubiquitination of alpha-synuclein to drag it to proteasomal machinery. In the molecular aspect, IDH2 has been demonstrated to reduce alpha-synuclein toxicity in the yeast system, but a detailed mechanism has not been explored yet. (10)Thus, we explored the Hytrin and H@PSNPs effect on IDH2 activation against rotenone-induced toxicity and IDH2-mediated degradation of alpha-synuclein. As per current knowledge, no report has shown IDH2 mediated mechanistic pathway in the degradation of alpha-synuclein in PD regulation.

Herein, a potent Hytrin nanoformulation has been evaluated to examine its neurotherapeutic effect against PD that can overcome the present limitation of bare Hytrin. The molecular mechanistic action of H@PSNPs attributed to IDH2 mediated endowment of alpha-synuclein degradation. In the present study for the first time, we have demonstrated the neurotherapeutic potential of Hytrin-loaded polydopamine-serotonin nanohybrid that regulates IDH2 endowed alpha-synuclein degradation by the ubiquitin/proteasome pathway having significant importance in neuronal survival and PD prevention. The project design of the chapter 3b represented for better understanding of hypothesis, rationale of chapter with justification of the selected compound aligned to expected outcomes of the aims as below.

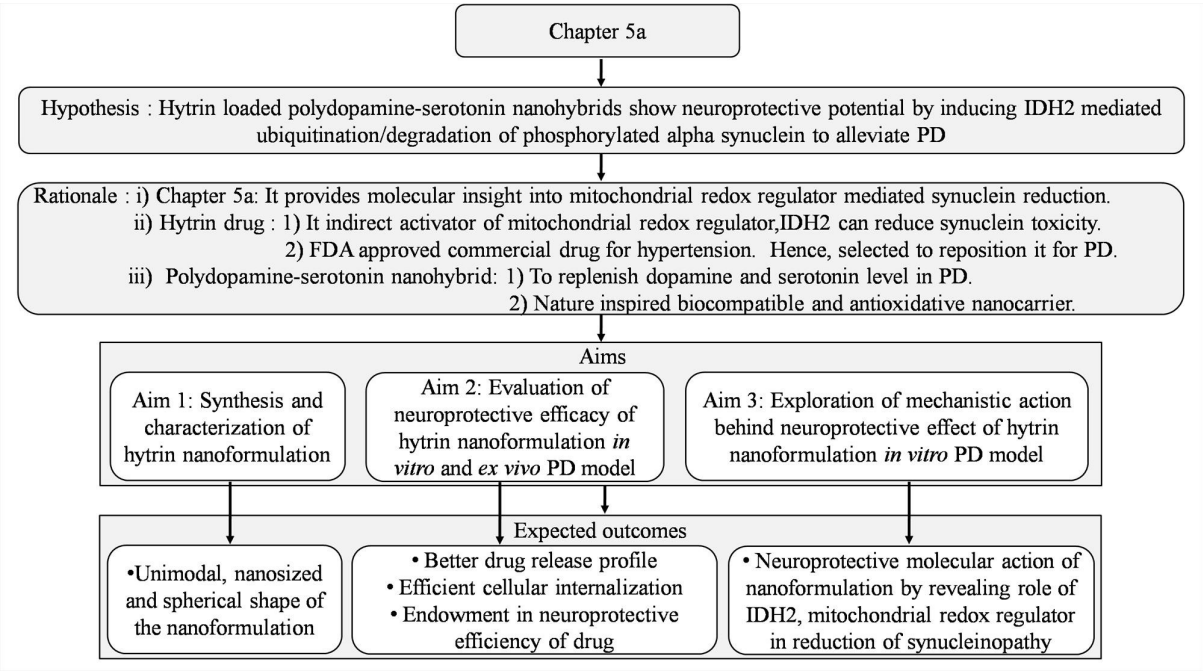


Scheme 7: The project design represents hypothesis, rationale, aims and it's aligned expected outcomes

5a.2. Results and discussion

The new neurotherapeutic agent is warranted in the development of PD curative therapy due to the ineffectiveness of present therapy. In recent times, Hytrin has been proposed as a promising neurotherapeutic candidate in PD treatment due to its ability to restore energy production. (5)Hytrin induces ATP, Pyruvate, and NADP+ productions that lead to activate NADP+ dependent IDH2, a regulator of mitochondrial redox status (5, 19) However, the effect of Hytrin on IDH2 expression has not been well understood, yet. Moreover, a deficiency of mitochondrial redox regulator, IDH2 has been shown as a cause of PD progression. (8) Indeed, synucleinopathy-induced mitochondrial dysfunction impairs cellular respiration in PD pathogenesis. (9)Recently, IDH2 has been reported as a novel suppressor of α-synuclein mediated toxicity, a hallmark of PD in the yeast system.(10) Therefore, we are keen to understand the IDH2-mediated neurotherapeutic effect of Hytrin in the reduction of synucleinopathy-induced PD. Although, the burst release profile, rapid absorption, and higher therapeutic dose requirement of Hytrin restrict its therapeutic potential. (11, 12)Thus, we have applied a strategy by formulating Hytrin in polydopamine-serotonin nanocarrier to improve the drug release profile with minimization of the therapeutic required dose. The deficiency of

dopamine and serotonin is reported as a cause of Parkinsonism. (15) In the previous report, we demonstrated the blood-brain barrier (BBB) crossing potential, anti-inflammatory, and protective effects of polydopamine nanoparticles in PD models. (16) Hence, polydopamine-serotonin nanoparticles have been preferred to improve the Hytrin release profile and aim to provide combinatorial therapy at a single platform. H@PSNPs has exhibited promising neuroprotective effect by showing recuperative action against rotenone-induced neuronal deficits *in vitro* and *ex vivo* experimental PD models.

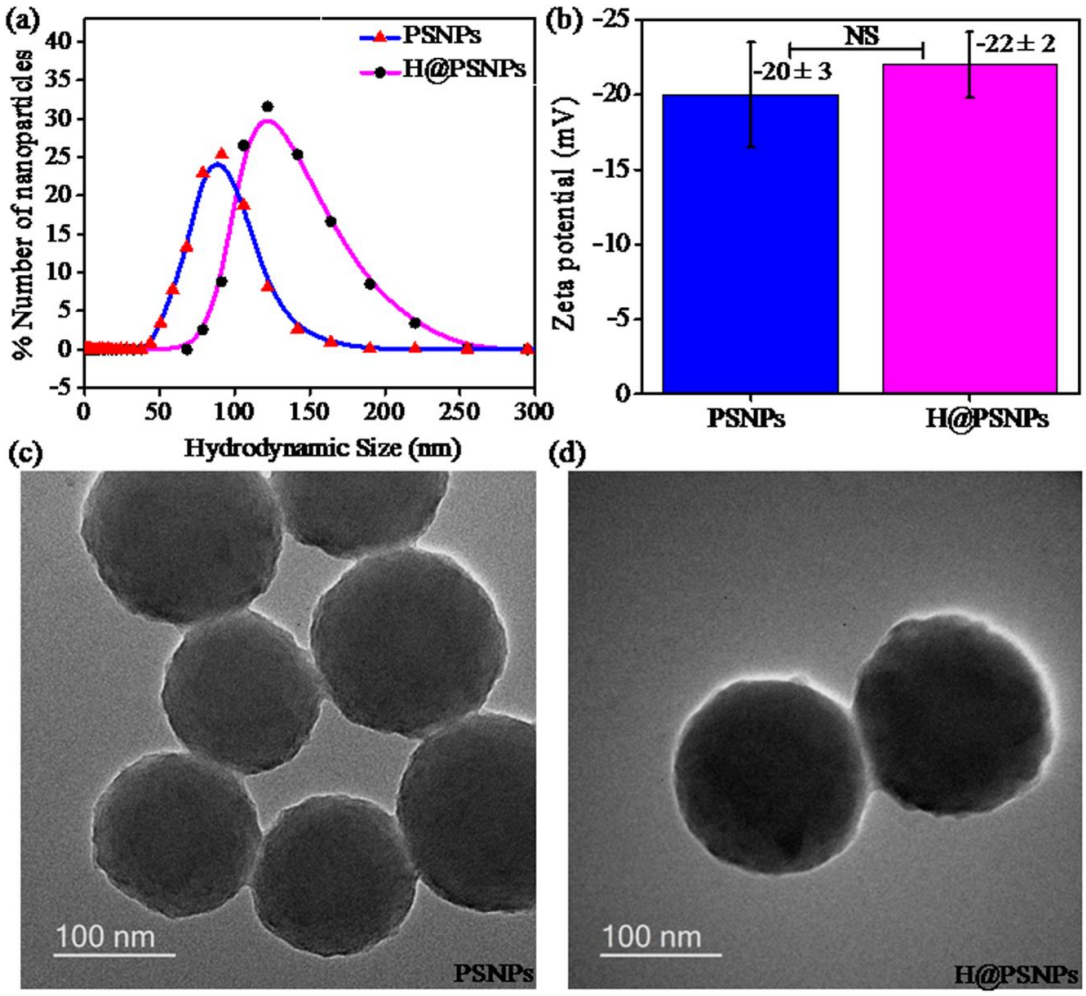


Figure 5.1. Morphological analysis of nanoparticles. (a) The mean hydrodynamic size of PSNPs and H@PSNPs have shown nanosized and monodispersity ; (b) zeta potential elucidates colloidal stability of (c,d) TEM micrographic images have confirmed spherical shape of PSNPs and H@PSNPs, respectively.

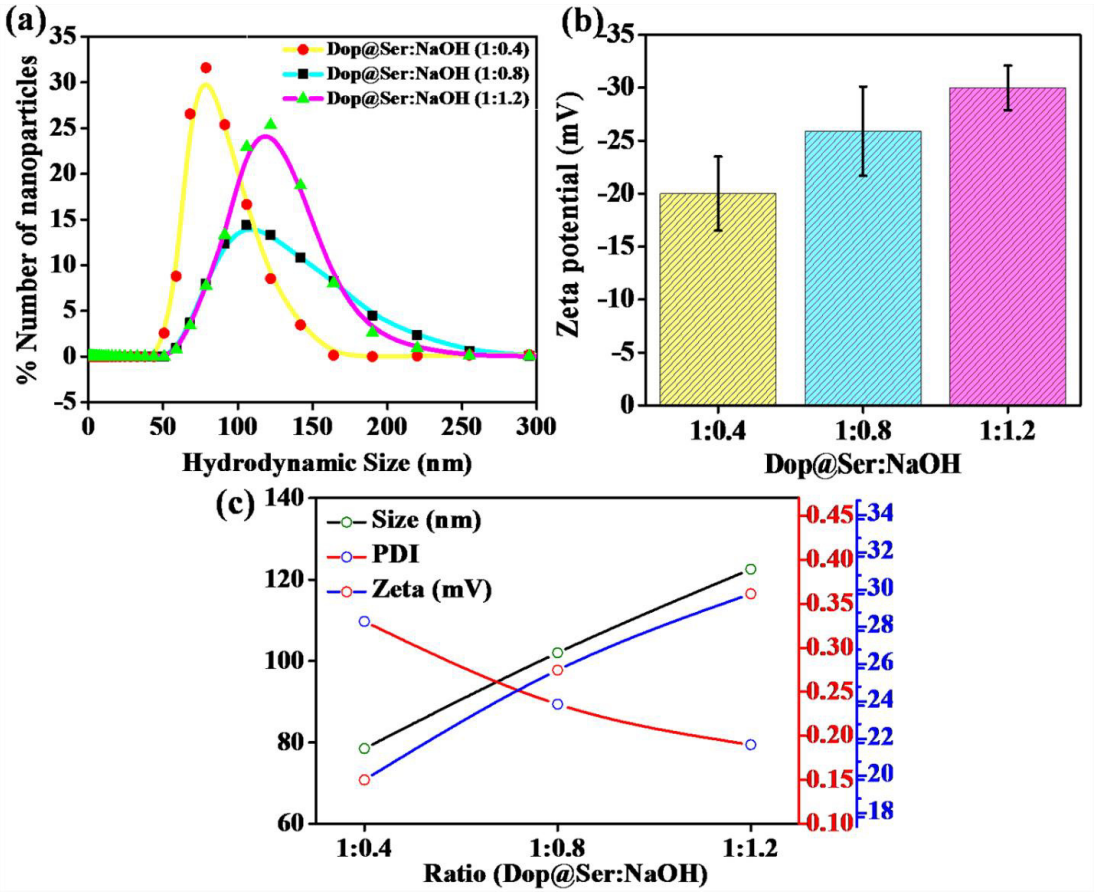


Figure 5.2. Optimization of nanoparticles; (a) Hydrodynamic size have been presented with different ratio of precursors and oxidizing agent, (b) surface zeta potential of nanoparticles suggesting stability of nanohybrids, and (c) the optimization curve shows an increment of the nanohybrid size with increasing concentration of the oxidizing agent.

5a.2.1. Characterizations of nanoformulations

PSNPs and H@PSNPs have been synthesized by following the solution oxidation method. (16)Characterization of nanoformulation has been executed to validate the synthesis of PSNPs and H@PSNPs.The DLS analysis has shown mean hydrodynamic size, polydispersity index (PDI), and surface zeta potential of nanoformulations as follows; 90 ± 2 nm, 0.09 ± 0.005, and -20 ± 3 mV, respectively for PSNPs and 120 ± 3 nm, 0.210 ± 0.63 and -22 ± 2 mV, respectively for H@PSNPs (Fig.5.1a and b). The size, PDI, and zeta potential analysis indicate colloidal stability and monodispersed nanosized particles.TEM micrographic images have also revealed a

spherical shape with ~ 90 nm size of PSNPs and ~ 120 nm size of H@PSNPs that is comparable with our previous study. (16)(Fig.5.1c and 1d)

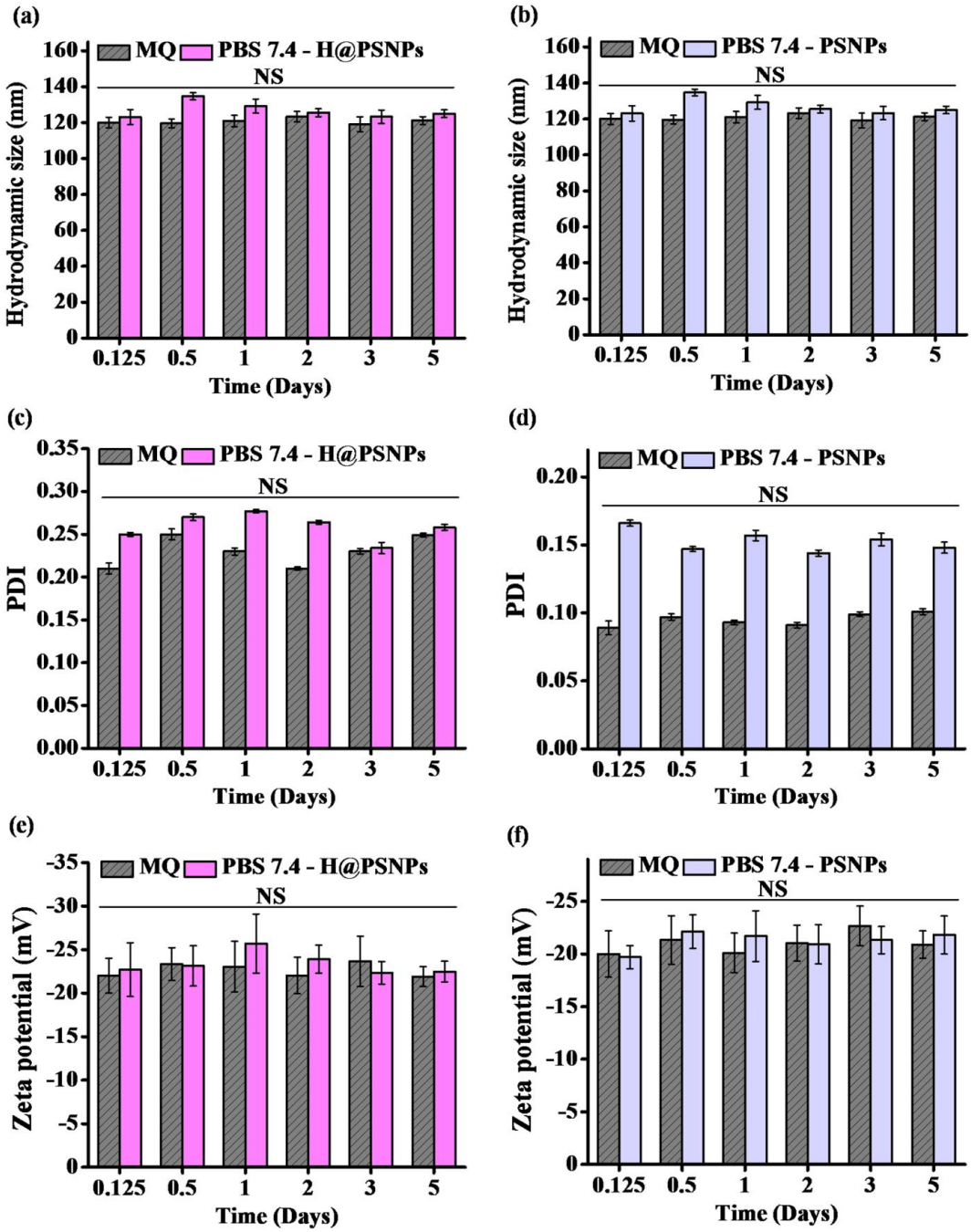


Fig.5.3. *In vitro* solution stability of nanoparticles; (a,b,) Hydrodynamic size measurements, (c,d) polydispersity index and (e,f) surface zeta potential kinetic shows better stability of nanoformulations at Milli-Q water and physiological pH condition.

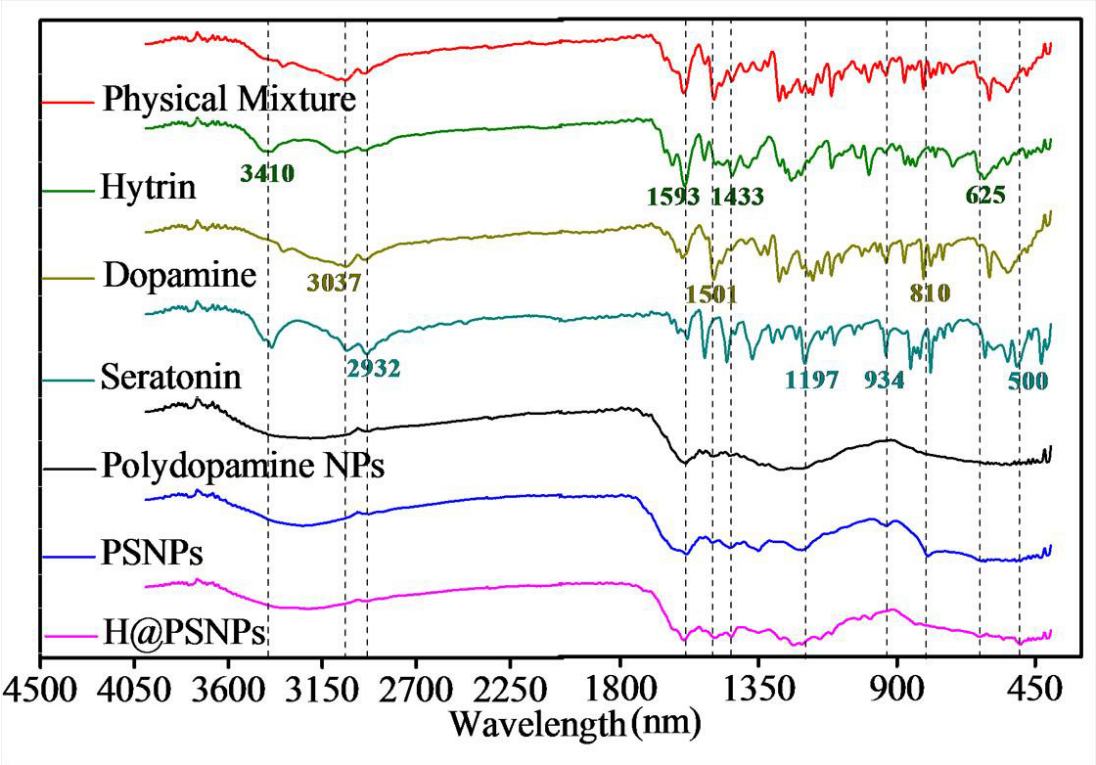


Figure 5.4. Physicochemical characterization of nanoparticles. FTIR spectroscopy has confirmed the non-covalent interaction between dopamine, serotonin, and Hytrin in the formation of H@PSNPs.

The data for the synthesis of PSNPs with various ratios have been shown in fig.5.2 which indicates the smallest size of nanoparticles with a 1:0.4 ratio of dopamine/serotonin to NaOH. Further, time-dependent stability of H@PSNPs and PSNPs has shown a good stability profile of nanoformulations in Milli-Q and physiological condition (pH 7.4) (Fig.5.3). Morphological evaluation of nanoformulation by DLS and TEM represents monodispersed colloidal stable and spherical shaped nanoparticles.

The FTIR spectrum (Fig.5.4) has shown the respective peaks to indicate the plausible interactions of the drug and nanocarrier. The involvement of the –OH group and pi-pi interactions have been found major non-covalent interactions in the formation of H@PSNPs. Further, encapsulation efficiency and drug loading content of nanoformulation were determined. Hytrin, dopamine, and serotonin, all precursors are water-soluble. Therefore, H@PSNPs are also obtained as water-soluble after non-covalent polymerization. The higher aqueous solubility of precursors is the possible reason for the higher drug loading and encapsulation capacity of

nanoformulation. In accordance with the previous report that polydopamine serves as a multivalent matrix for higher drug loading (20), we obtained 70.4 ± 6% encapsulation efficiency and 14.8 ± 2%drug loading content respectively. The physicochemical characterization by FTIR has revealed interactions of hydroxyl, amine, and aliphatic functional groups as major interactions in the formation of H@PSNPs.

5a.2.2 *In vitro* drug release analysis and mathematical modeling of release kinetics

Determination of *In vitro* drug release was executed via mimicking *in-vivo* conditions to reveal the drug release profile. The equilibrium dialysis membrane method has been applied to estimate drug release profiles at mimicked physiological pH. Hytrin suspension and H@PSNPs were analyzed to examine drug release till 96 hours. The obtained results are represented in a curve and bar graph to compare the release profile of H@PSNPs with Hytrin suspension. (Fig.5.5a)Hytrin suspension has exhibited more than 40% release in the initial 8 hours. In contrast, H@PSNPs have shown a sustained release profile with ~10% release in an initial 8 hours and ~ 70% release after 96 hours. It suggests the importance of H@PSNPs in improving drug availability at a disease site. The controlled and slower drug release profile is attributed to reducing drug cytotoxicity by limiting its premature release. (21) Mathematical modeling has shown fitted models like first order and Korsmeyer-Peppas (mathematical model), Makoid-Banakar, Weibull, Gompertz (empirical model), and probit model that have explained slower and sustained release of Hytrin from H@PSNPs.The best six fitted models; first-order kinetic, Korsmeyer-Peppas, Makoid-Banakar, Weibull, Gompertz, and Probit have been selected by considering the obtained values of $R^2$ = 0.9938, 0.9927, 0.9951, 0.9961, 0.9973, and 0.9960, respectively. (Fig.5.5b) Gompertz has represented the best-fitted model indicates slower drug disposition at the initial and end of the drug release curve that is controlled by the Fickian transport mechanism. For a better understanding of drug release kinetics, the fitted data and results of the drug release kinetic model are displayed and explained in Table 5.1. In the further assessment of solubility, H@PSNPs have shown a 17% improvement in the solubility of the Hytrin. (Fig.5.6a)

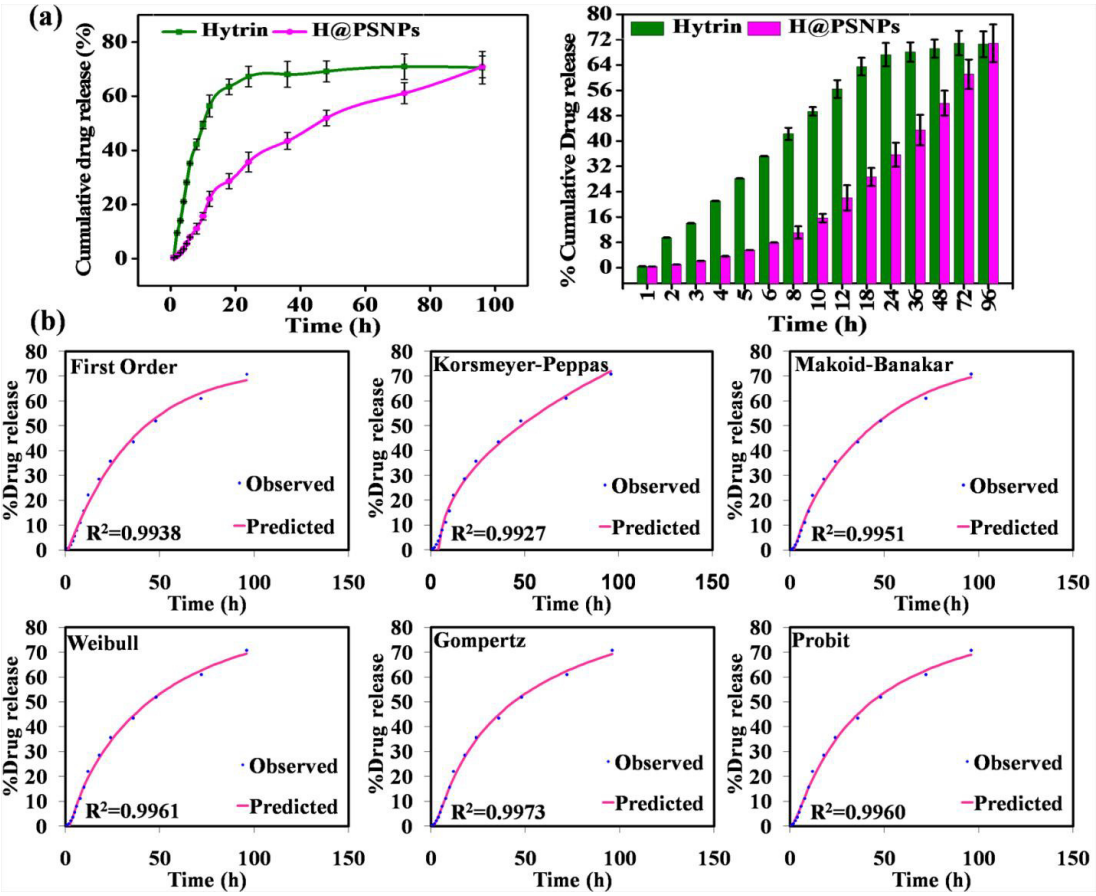


Figure 5.5. (a) *In vitro, the* drug release profile is reflecting slower and more sustainable drug release kinetic of nanoformulation. (b) Best-fitted curves with respective mathematical models for release data of nanoformulation are demonstrated.

Herein, *in vitro* drug release determination revealed a slower and sustained release profile of H@PSNPs. The time-dependent and continuous release of the drug could be helpful to improve required drug availability at the site of action. Our results are in support the fact that polydopamine and polyserotonin nanocarriers have promising potential in the development of a better nano-drug delivery system. (20, 22)The slower and sustained drug release profile is considered to minimize drug cytotoxicity by limiting its premature release and reducing the required therapeutic dose(21).

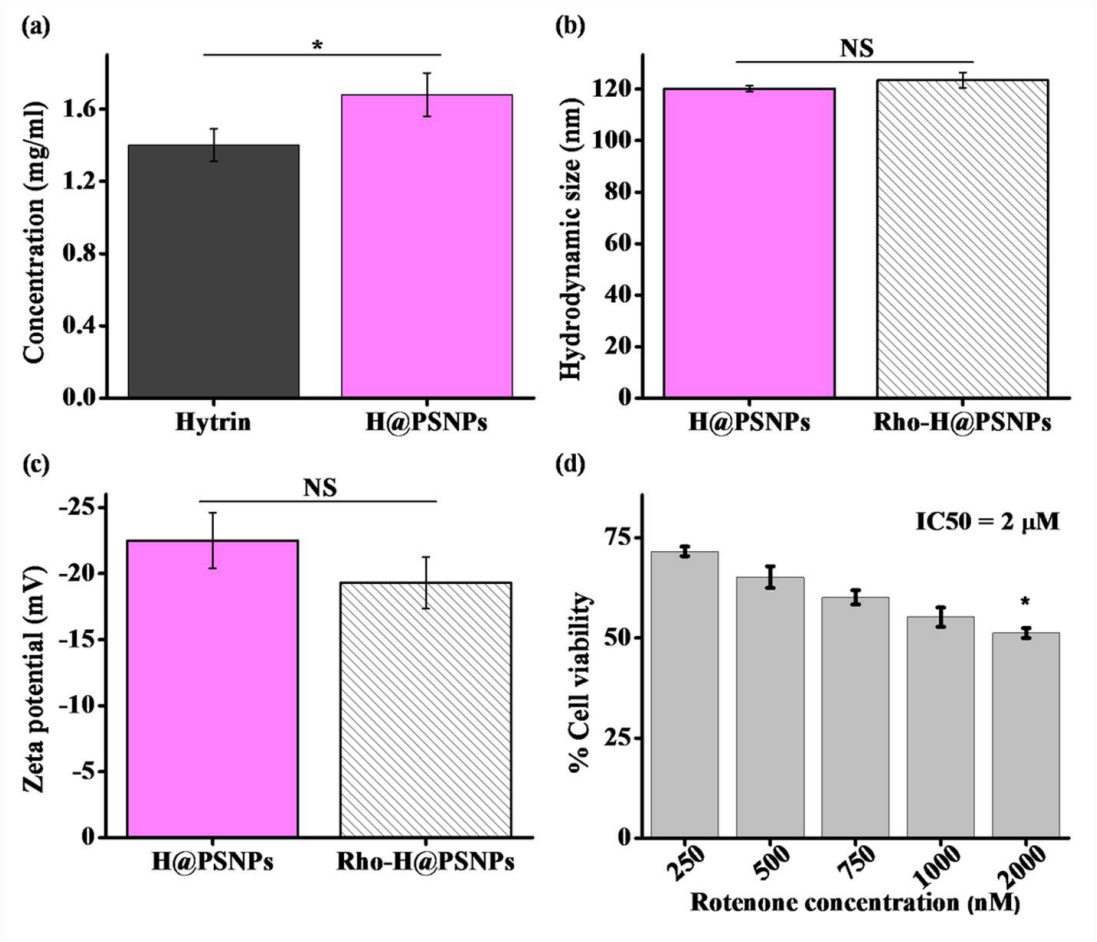


Fig.5.6. (a) Solubility analysis has revealed the efficiency of nanoparticle to boost the drug solubility, (b) Size measurements and (c) zeta potential analysis suggest a good stability profile of our nanoformulation, (d) rotenone-induced cytotoxicity and dose effect has been presented.

5a.2.3. Cellular internalization of nanoformulation in SH-SY5Y and 3D raft.

The cellular internalization potential of nanoparticles is essential to understand before assessing the therapeutic effect. Therefore, we have conducted the cellular uptake study of PSNPs to SH-SY5Y cells, the model of dopaminergic neuron cells. Cellular internalization of rhodamine B-tagged H@PSNPs was examined under confocal microscopy after 4 hours of exposure to SH-SY5Y cells. Confocal Laser Scanning Microscopy (CLSM) micrographic images are indicating higher cytoplasmic uptake of nanoparticles. (Fig.5.7a) Herein, the hydrodynamic size measurement and surface zeta potential of rhodamine B tagged H@PSNPs have been performed to understand the effect of rhodamine B on the size and surface charge of the nanoformulation. In

fig.5.6b and 5.6c, rhodamine B has imposed a nonsignificant effect on the size and zeta potential of the H@PSNPs. The flow cytometry assay for cellular internalization of rho-H@PSNPs has been performed to quantify the percentage uptake. Fig.5.8 has shown the 87.4 % majority of the cells have uptaken the nanoformulation.

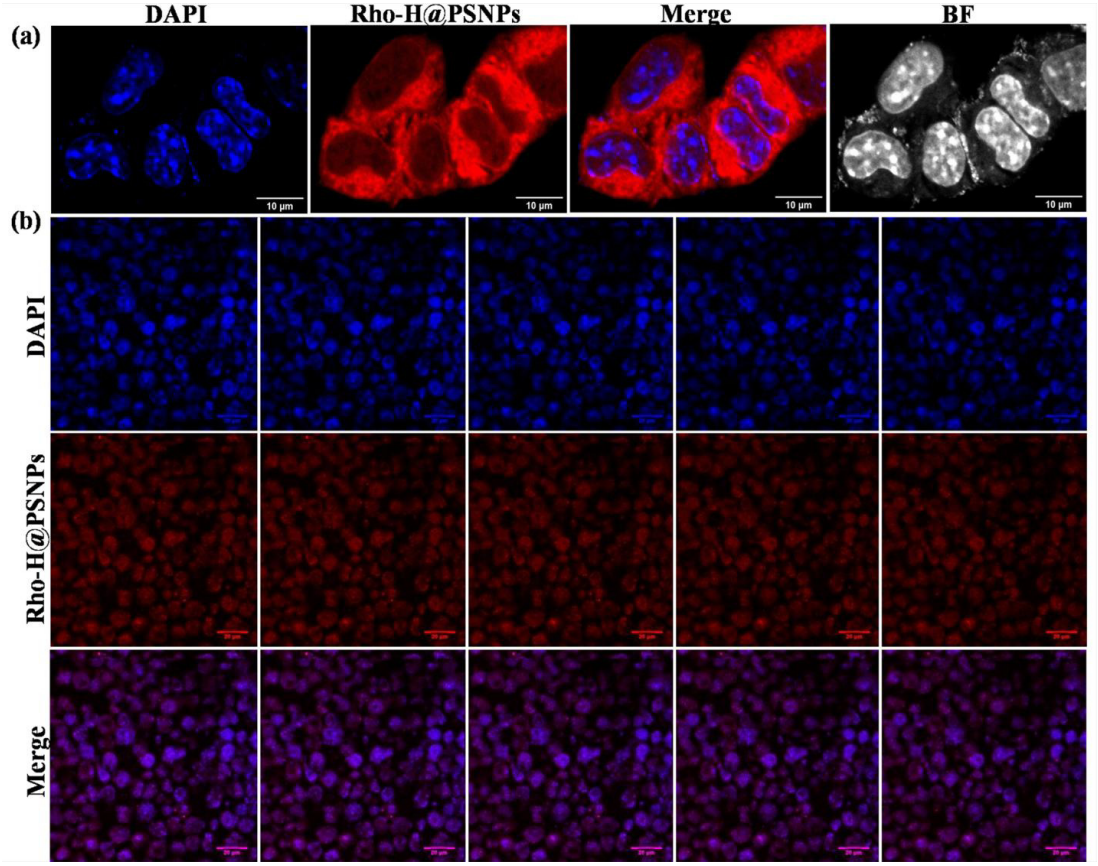


Figure 5.7. (a) Cellular uptake of nanoformulation has represented major cytoplasmic uptake of nanoformulation. (b) The internalization of nanoformulation into a 3D raft of SH-SY5Y has shown the potential of nanoparticles to penetrate complex tissue-mimicking structures.

3D multilayer culturing of SH-SY5Y has been performed to observe nanoparticle internalization potential at the tissue-mimicking model. The CLSM images are also reflecting the good penetrating ability of nanoparticles into the compact multilayer structure of cells that mimics tissue structures. (Fig.5.7b)

Cellular uptake study and internalization to the raft of SH-SY5Ycells have revealed the potential of nanoparticles to be penetrated the neuronal cells and tissue-mimicking structures. Abundant

expression of dopamine and serotonin receptors in the brain may facilitate the entry of dopamine and serotonin-based nanostructures. (23, 24) Hytrin is known to bind with the alpha-adrenergic receptor that facilitates its ready internalization. (25) Therefore, the plausible mechanism of H@PSNPs uptake could be receptor-mediated endocytosis and making it highly potent in the crossing of BBB.

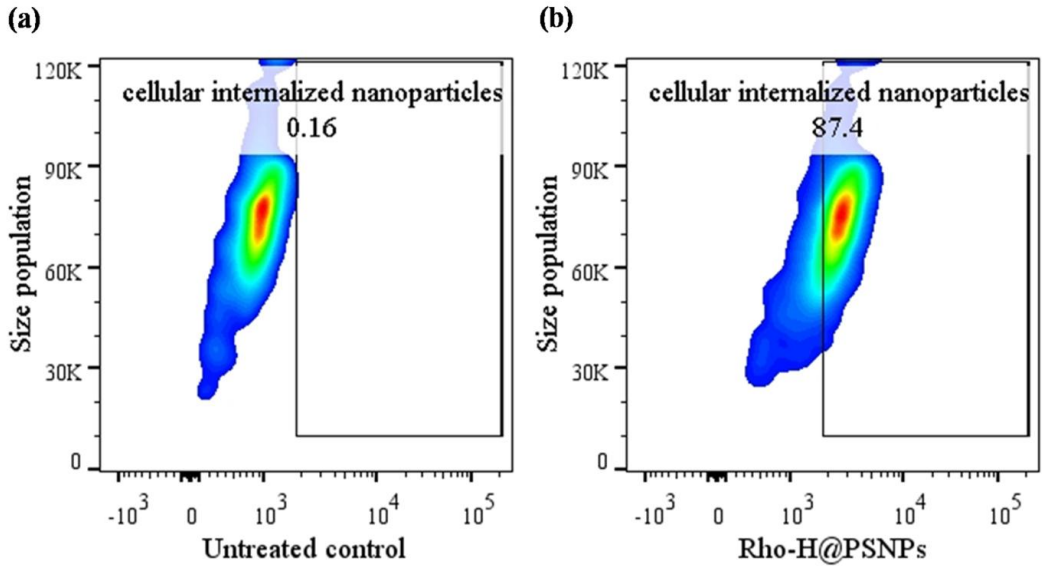


Fig.5.8. Cellular internalization of Rho-H@PSNPs reflects cellular uptake in the majority of the cells.

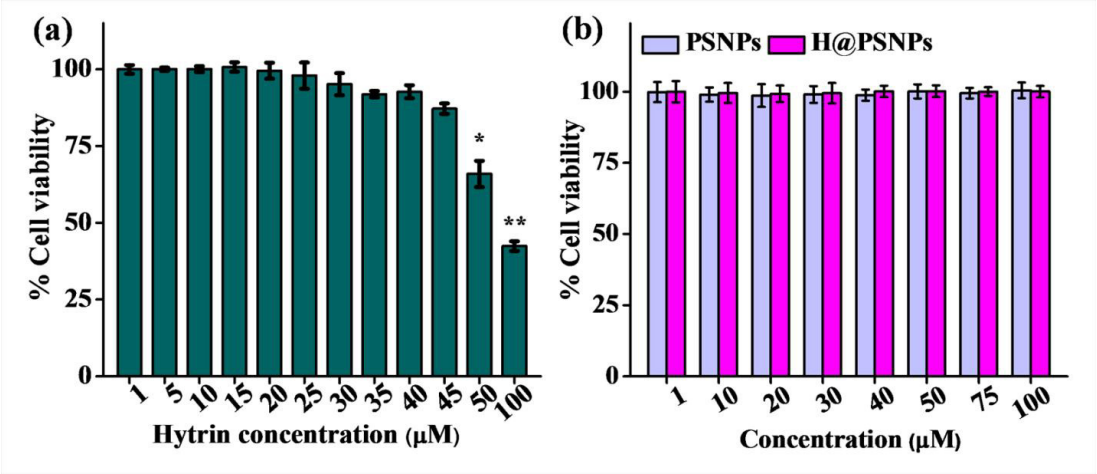


Figure 5.9. Cytotoxicity assessment of Hytrin (a), blank PSNPs, and Hytrin-loaded PSNPs was presented (b). Hytrin, blank PSNPs, and Hytrin-loaded PSNPs have shown bio-compatible

behavior and Hytrin has shown toxicity at higher concentrations (**p<0.01,*p<0.5, one way ANOVA; Tukey and Bonferroni test).

5a.2.4. *In vitro* neurotherapeutic efficiency

Cellular viability analysis has been performed to estimate *in vitro* neurotherapeutic efficiency. The MTT reduction assay has shown the biocompatible nature of our drug and nanoformulation. A higher dose (50μM) of Hytrin has shown a toxic effect (Fig.5.9a). Fig.5.9b is representing a biocompatible characteristic of PSNPs and H@PSNPs also at higher doses. Hence, we have primary results to apply these nanoformulations for protection studies against chemical-induced toxic effects. Rotenone-induced *in vitro* PD model has been followed from our previously reported study. (16, 26)Acute rotenone induces aggregation of alpha-synuclein, a hallmark of PD. The protective effect of 0.75 – 2.5 μM of bare Hytrin, equivalent Hytrin carrying concentration of PSNPs and PSNPs was analyzed against co-treated 750nM rotenone in SH-SY5Y cells for 48 hours. (Fig.5.10a)2.5 μM H@PSNPs have exhibited significantly better protection with respect to bare Hytrin after 48 hours of treatment duration. The dose-dependent protective effect of Hytrin has been obtained in support of the reports that have shown similar analysis. (5, 19)Our nanoformulations have exhibited 3 folds recovery in percentage cell survival against 48 hours of treatment of rotenone (Fig.5.10a)H@PSNPs have minimized the neuroprotective dose of Hytrin (2.5 μM) in comparison to the existing report that has demonstrated 10 μM(5) protective dose of bare Hytrin. Thus, Hytrin nanoformulation has expressed a superior neuroprotective effect with a reduction in therapeutic dose and enhanced drug availability.

Comprehensive studies have shown that neuroinflammation is associated with neuroprotection. (27, 28) We have also performed a ROS generation study to observe the ROS scavenging property of our nanoformulation in the prevention of rotenone-induced effects.Fig.5.10b is representing the ROS scavenging effect of H@PSNPs confirming the anti-neuroinflammatory potential of our nanoformulations. The plausible reason behind the higher anti-inflammatory activity of H@PSNPs is due to the renowned ROS scavenging potential of polydopamine nanoparticles. (16)Inhibition of the mitochondrial complex I of the electron transfer chain (ETC) has been widely studied as a cause of higher ROS production. Rotenone, a potent inhibitor of

complex I of ETC is known to cause mitochondrial dysfunction and elevated ROS generation. Herein, our nanoformulation reverts rotenone-induced insults by scavenging the ROS.

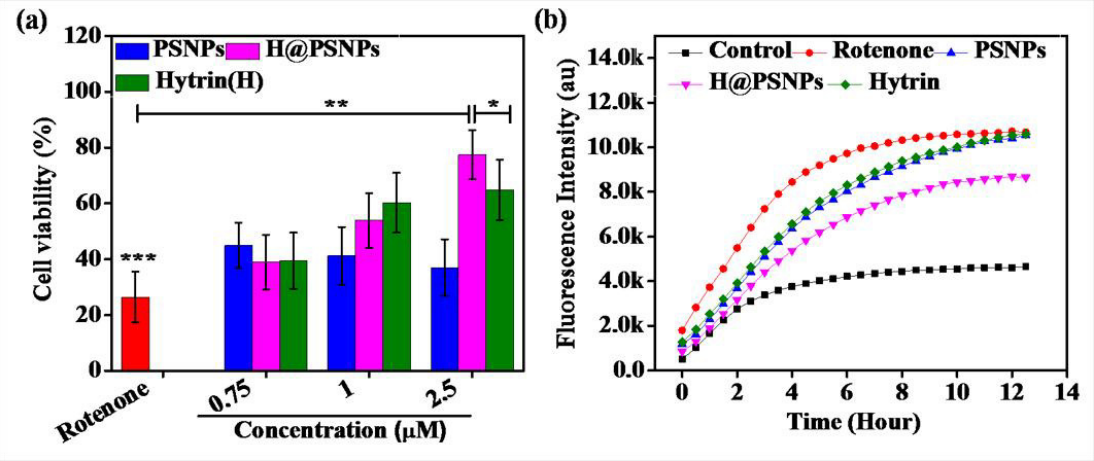


Figure 5.10. *In vitro* neurotherapeutic efficiency of nanoformulation(a) H@PSNPs has exhibited a neuroprotective effect against rotenone-induced cellular damage and PD effect (*p<0.05, **p<0.01,***p<0.001). (b) ROS scavenging potential of nanoformulations is confirming the anti-inflammatory activity.

Moreover, Jc1-based mitochondrial potential analysis has been conducted to examine the neuroprotective effect of our nanoformulation. Jc1 dye has been utilized to observe mitochondrial membrane potential. (Fig.5.11a) Healthy mitochondria with hyperpolarized membrane potential have been monitored by red fluorescence of Jc1 aggregation inside mitochondria. In apoptotic cells, mitochondria have depolarized membrane potential identified by the green fluorescence of free Jc1 molecules in the cytoplasm. Rotenone, a potential mitochondrial inhibitor has been applied to induce mitochondrial insults. In the results, 65.4% and 34.6 % of cells were representing green and red fluorescence, respectively on the challenge with rotenone indicating mitochondrial insults. In contrast, H@PSNPs have exhibited significant recovery of mitochondrial membrane potential by reflecting 39.3% Jc1 monomer and 60.7% Jc1 aggregates cell population respectively. (Fig.5.11b)Our Hytrin nanoformulation has shown a better protective effect in comparison to bare drugs and PSNPs. Results of Jc1 based assay are in support of the results with MTT reduction assay and ROS estimation assay, where H@PSNPs have exhibited a cumulative effect of Hytrin and PSNPs. Thus, outcomes of MTT reduction, ROS estimation, and Jc1-based analysis have confirmed *in vitro* neurotherapeutic potential of H@PSNPs.

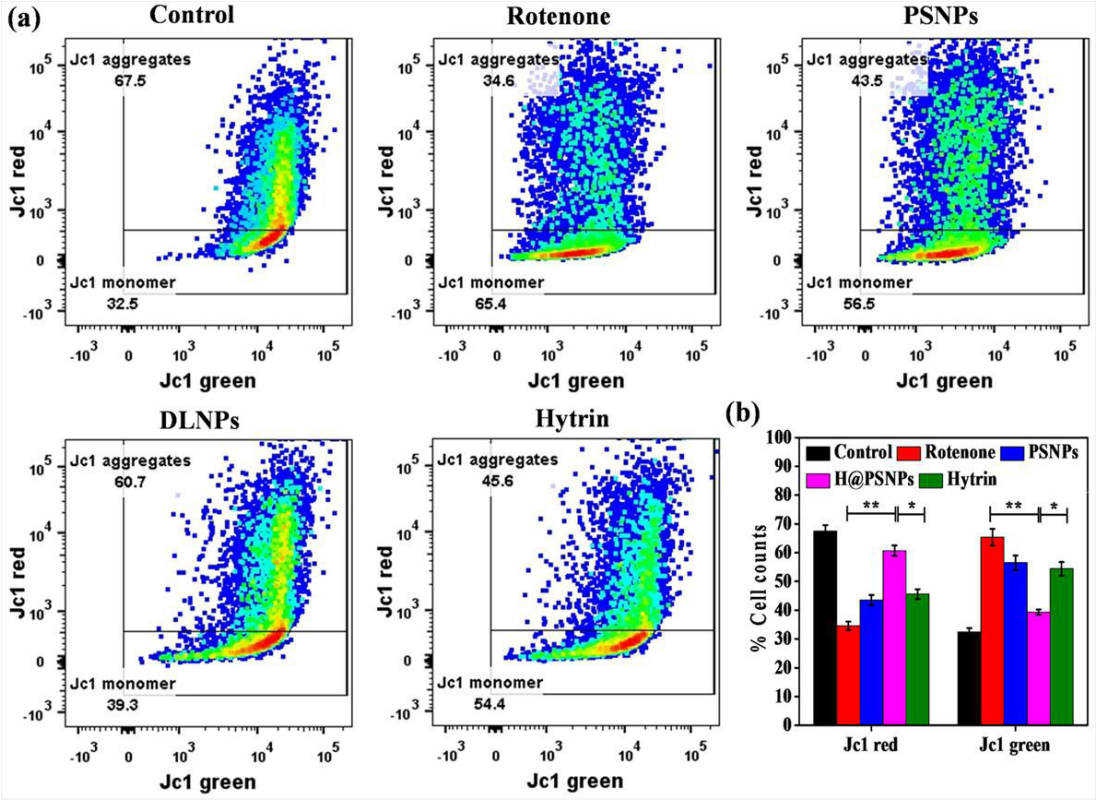


Figure 5.11. Mitochondrial membrane potential analysis (a) Flow cytometry examination of Jc1 assay indicating a restorative effect of H@PSNPs. (b) Quantitative representation of % of Jc1 red (healthy mitochondrial cells) and Jc1 green (dysfunctional mitochondrial cells) have been displayed (*p<0.05,**p<0.01).

Herein, the dopaminergic neuronal model, SH-SY5Y cells are used to determine the neuroprotective effect against rotenone-induced neurotoxicity *in vitro* PD model. Rotenone is known to inhibit the complex I of the electron transport chain and the 26S proteasomal pathway leads to PD pathogenesis and progression (29). Rotenone-induced PD in vitro model (SH-SY5Y) and ex vivo model (mouse brain slice) have been employed in the present study. Effective neuroprotective efficiency of H@PSNPs has been confirmed against rotenone-induced neuronal deficits. Outcomes of critical examination of cellular protection assay, Jc1 mitochondrial membrane potential assay, and ROS generation study are in agreement with each other to divulge higher neuroprotective potential than blank PSNPs and bare Hytrin. Hytrin is demonstrated as a potential neurotherapeutic candidate due to its ready brain accumulation and ability to endow mitochondrial and cell energy against chemical-induced insults. (5)However, an effective higher dose of Hytrin has been found susceptible to pathological conditions like low

blood pressure and postural hypotension. (13) Therefore, it is warranted to develop a delivery platform for the minimization of therapeutic doses by targeting and enriching the drug release at the disease site. Herein, our nanoformulation has exhibited an effective strategy to improve the drug release profile with minimization of the therapeutic dose of Hytrin by enriching it into polydopamine-serotonin nanoparticles. Our nanoparticles system has shown a drastic reduction in the neurotherapeutic dose of Hytrin (2.5 μM) in comparison to the reported dose of bare Hytrin (10 μM). (5)Results showing ROS scavenging properties of our nanoformulations agree with the reports that demonstrated polydopamine nanoparticles as a neurotherapeutic agent due to their biocompatibility and ROS scavenging potentials. (16) Similarly, Studies about polyserotonin nanoparticles are also in lieu to our results that recently reported it as biocompatible and proposed as a multifunctional material for biomedical applications. (22)Results of Jc1-based mitochondrial membrane potential are also in support of the existing reports that have demonstrated the neuroprotective effects of nanoformulations by restoring the mitochondrial membrane potentials. (26)Thus, our hytrin nanoformulation has exhibited neuroprotective potential by reversing the rotenone-induced mitochondrial ETC complex I inhibition, ROS generation, and mitochondrial dysfunction.

5a.2.5. Molecular insight into the neuroprotective mechanism of H@PSNPs

Protein expression analysis has been performed to explore the H@PSNPs effect on IDH2 and alpha-synuclein degradation against rotenone-induced aberration. Results of the expression study of IDH2 and pSer129 α-Syn were represented in fig.5.12a indicating validation of the rotenone *in vitro* PD model. The expression analysis of IDH2, pSer129 α-Syn, and CASPASE3 has shown the neuroprotective effect of H@PSNPs by upregulating IDH2 and reducing the expression of pSer129 α-Syn and cleaved CASPASE3 against rotenone effect. (Fig.5.12c) The quantification of protein expression by image J has been represented in fig.5.12d which also confirms the significant neuroprotective action of H@PSNPs.

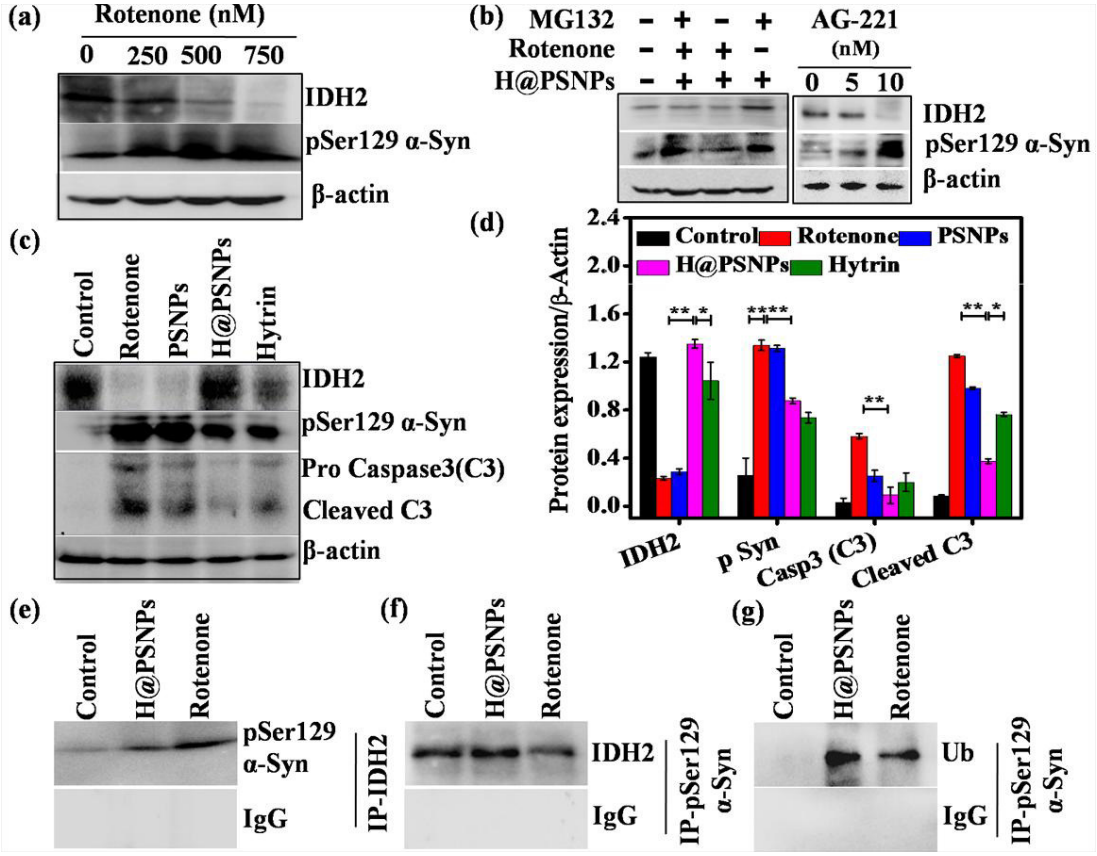


Figure 5.12. Molecular insights into the neuroprotective actions of H@PSNPs (a) Rotenone treatment has shown a reciprocal relation of IDH2 and pSer129 alpha-synuclein expression. (b) The neuroprotective action of H@PSNPs has been examined in presence of AG-221 and MG132 reflects H@PSNPs follow proteasomal degradation pathway in retardation of synucleinopathy (c) Immunoblot analysis has shown the reduction of cleaved CASPASE3, pSer129 alpha-synuclein, and upregulation of IDH2 (d) quantitative representation of protein expression was described (*p<0.05, **p<0.01) (e,f) IP and reverse IP results are revealing novel direct physical interaction of IDH2 and alpha-synuclein. (g) Immunoblots of IP analysis have confirmed nanoformulation-induced IDH2-mediated alpha-synuclein ubiquitination and proteasomal degradation.

An exploration of the pathway of synuclein degradation, a potent inhibitor of the 26S proteasomal pathway (MG132) has been applied by following our previous report. (16) The results have confirmed that H@PSNPs follow proteasomal degradation pathways in the reduction of synucleinopathy as a neurotherapeutic mechanism. (Fig.5.12b)The results confirmed the reciprocal relation of IDH2 and pSer129 α-Syn expression which provide us the lead to explore their relationship further in detail. Indeed, IDH2 has been projected as a novel suppressor

of synuclein toxicity. (10) Hence, we have employed a potent IDH2 inhibitor (AG-221) to confirm the reciprocal relation of IDH2 and pSer129 α-Syn expression. (Fig.5.12b) The validated results allowed us to explore the direct physical interaction of IDH2 and pSer129 α-Syn. In confirmation of these findings, the novel physical interaction of IDH2 and pSer129 α-Syn has been observed through immunoprecipitation (IP) and reversed IP studies. (Fig.5.12e and f) Fig.5.12g has confirmed that H@PSNPs regulate IDH2-mediated ubiquitination and proteasomal degradation of α-Syn.

Our results of elevated expression of P-alpha-synuclein are confirming the rotenone-induced PD *in vitro* model. A deficiency of dopamine and serotonin leads to PD generation and the death of neurons. (15)Elevated pSer129 alpha-synuclein expression and CASPASE3-mediated apoptosis are the major reasons for neuronal death in PD pathogenesis. (30) Herein, attenuation of pSer129 α-Syn and CASPASE3 expression is confirming the neuroprotective action of our nanoformulation against rotenone-induced insults. H@PSNPs have exhibited a significant reduction in pSer129 alpha-synuclein (double fold) and cleaved CASPASE3 (six-fold) expression to rotenone stimulation. The results are in agreement with the existing reports that have shown pSer129 alpha-synuclein reduction as a neurotherapeutic approach in PD prevention. (30)Thus, significant inhibition of pSer129 alpha-synuclein, PD signatory molecule is divulging a better neuroprotective effect of our nanoformulation.

Further, reduced expression of IDH2, a key regulator of mitochondrial redox status has been obtained. The deficiency of IDH2 has been recognized as one of the causes of PD progression. (8)Indeed, IDH2 has been shown to suppress alpha-synuclein toxicity. (10) Herein, the reciprocal relation of the IDH2 and pSer129 alpha-synuclein has led us to explore IDH2 mediated neuroprotective mechanistic action of our hytrin nanoformulation. Hytrin mediated IDH2 upregulation has been confirmed. In further exploration, it has been found that our nanoformulation follows the proteasomal degradation pathway in the prevention of synucleinopathy. MG132, a potent inhibitor of the proteasomal pathway has been employed to block the 26Sproteasomal machinery by following our previous report. (16) This study divulges that the neuroprotective mechanistic action of H@PSNPs is working through the proteasomal degradation pathway. Therefore, we are keen to know the involvement of IDH2 in synuclein degradation and PD regulation. Herein, the immunoprecipitation study has revealed the camouflage role of IDH2 in the reduction of synucleinopathy and confirmed the novel physical

interaction of IDH2 and alpha-synuclein. In further insights into molecular mechanisms, upregulated ubiquitination of alpha-synuclein has been confirmed with an immunoprecipitation study. Recently, the report has shown the vital role of E1A activity in the efficient working of ubiquitin-mediated proteasomal degradation pathway (UPP) and it has been hampered by the rotenone effect. (18) Herein, the immunoprecipitation outcome of IDH2 and Synuclein with respective immunoblotting of synuclein and ubiquitin by protein expression results in presence of MG132 has proved that IDH2 has been involved in synuclein ubiquitination and proteasomal mediated degradation. Therefore, the present study has divulged the neuroprotective mechanism of H@PSNPs by reducing the rotenone effect and IDH2-mediated ubiquitination and degradation of alpha-synuclein. This study has upgraded knowledge about the neuroprotective mechanism of IDH2-mediated alpha-synuclein degradation in PD prevention. To the best of our knowledge, the present study has first time demonstrated a combinatorial nano-drug delivery system by involving three neuroprotective drugs; dopamine, serotonin, and Hytrin at a single platform. Indeed, the IDH2-mediated alpha-synuclein ubiquitination and proteasomal degradation in PD regulation have also been studied and reported for the first time.

5a.2.6. IHC analysis in *ex vivo* PD model

The neurotherapeutic efficiency of H@PSNPs has been evaluated in an *ex vivo* PD model after obtaining eminent therapeutic potential *in vitro* PD model. To investigate the response, the immunohistochemistry (IHC) of potential therapeutic targets has been conducted in mice brain slice cultures. Results of IDH2 and pSer129 α-Syn expressions have confirmed the neurotherapeutic efficiency of H@PSNPs by upregulating the IDH2 level and reducing pSer129 α-Syn expression at the tissue level. (Fig.5.13) Hence, the successful therapeutic efficiency of H@PSNPs *in vitro and ex vivo* indicates the promising neuroprotective caliber of our nanoformulation in the development of PD treatment.

Herein, IHC results of upregulated IDH2 and reduced pSer129 α-Syn also confirmed the neuroprotective action of H@PSNPs against the rotenone-induced *ex vivo* PD model. The results are supporting the outcome of protein expression analysis and indicate the higher neuroprotective potential of H@PSNPs in comparison to bare drug and placebo PSNPs in mice brain slice culture. To summarize, the above-mentioned results have represented H@PSNPs' neurotherapeutic

efficiency that suggests promising and immense neurotherapeutic caliber of H@PSNPs in preclinical setup in PD prevention.

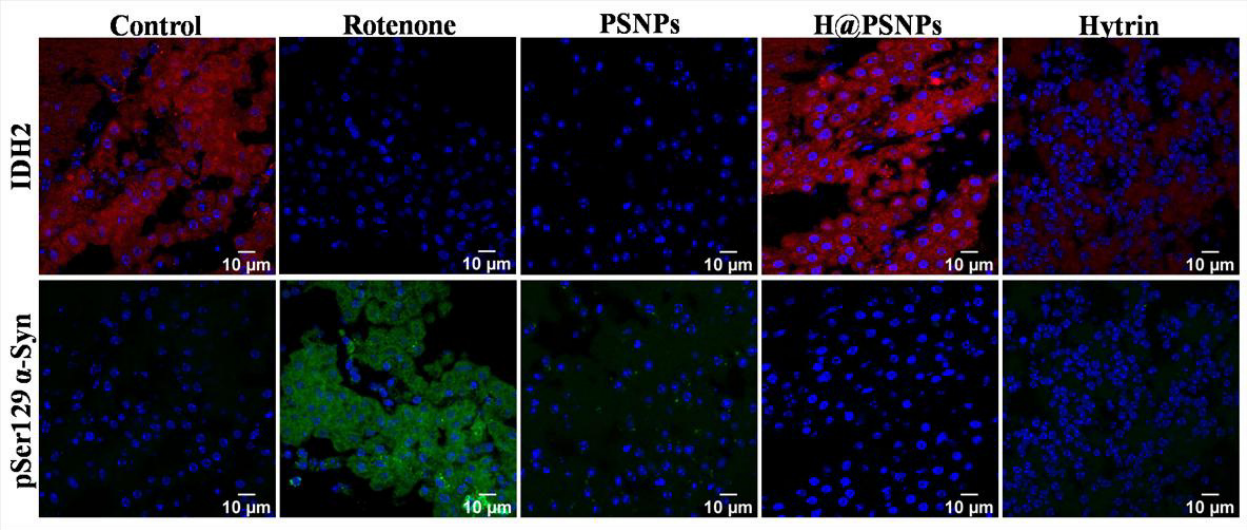


Figure 5.13. Immunohistological analysis in *ex vivo* PD experimental model. Confocal images of IHC analysis are reflecting the neurotherapeutic potential of nanoformulation by showing upregulated IDH2 and reduced pSer129 alpha-synuclein against rotenone-induced neurotoxicity *ex vivo*.

## 5a.3 Conclusion

The overall finding of the study elucidates the remarkable neurotherapeutic potency of Hytrin-loaded polydopamine-serotonin nanohybrids as a combinatorial drug delivery system for PD prevention. The key finding of major studies includes nanosized, unimodal and spherical naoparticles. In addition, the improved drug's release kinetics of hytrin by preventing its burst drug release and recovery of mitochondria against rotenone induced damage. Thus, the attenuation of rotenone-induced mitochondrial dysfunctions and neuronal death with reduction of pSer129 α-Syn divulges the immense neurotherapeutic efficiency of our hytrin nanoformulation.

Table 5.1. The results of mathematic models of Hytrin release kinetics from H@PSNPs have been summarized.

| Model | H@ PSNPs | | | |
|---|---|---|---|---|
| | Parameters | $R^2$ | AIC | MSC |
| **Zero order** | $k_0$ = 0.893 | 0.87 | 105.6415 | 1.9069 |
| **First order** | **$k_1$ = 0.027** | **0.9938** | **61.6827** | **4.8375** |
| **Higuchi** | $k_H$ = 6.759 | 0.9165 | 98.9965 | 2.3499 |
| **Korsmeyer-Peppas** | **$k_{KP}$ = 7.976**<br>**n = 0.487** | **0.9927** | **64.1569** | **4.6725** |
| **Hixson-Crowell** | $k_{HC}$ = 0.004 | 0.9597 | 88.9444 | 3.0200 |
| **Hopfenberg** | $k_{HB}$ = 0.000 | 0.9753 | 82.4417 | 3.4535 |
| **Baker-Lonsdale** | $k_{BL}$ = 0.001 | 0.9908 | 66.7331 | 4.5008 |
| **Makoid-Banakar** | **$k_{MB}$ = 4.034**<br>**n = 0.733**<br>**k = 0.005** | **0.9951** | **58.7406** | **5.3306** |
| **Peppas-Sahlin** | $k_1$ = 7.825<br>$k_2$ = 1.315 | 0.9898 | 69.8172 | 4.2952 |
| **Weibull** | **α = 23.005**<br>**β = 0.814**<br>**Ti = 2.820**<br>**Fmax = 84.294** | **0.9961** | **55.5204** | **5.2483** |
| **Quadratic** | $k_1$ = 0.000<br>$k_2$ = 0.016 | 0.9834 | 76.4728 | 3.8515 |
| **Gompertz** | **α = 7.173**<br>**β = 1.232**<br>**Fmax = 129.329** | **0.9973** | **48.9858** | **5.6839** |
| **Probit** | **α = -2.634**<br>**β = 1.696**<br>**Fmax = 89.986** | **0.9960** | **55.1539** | **5.2727** |

The significance and novel finding of the study reveals the camouflaged role of Hytrin nanoformulation-mediated IDH2 activation in the regulation of synucleinopathy. Thus, our study divulges the neurotherapeutic potential of Hytrin-loaded polydopamine-serotonin in the restoration of rotenone-stimulated PD deficits by endowing IDH2-mediated pSer129 alpha-synuclein ubiquitination and proteasomal degradation in the PD treatment. Indeed, the molecular studies suggest that our nanoformulation potentiated IDH2 expression to attenuate synucleinopathy and paves the promising therapeutic way. The hytrin is FDA approved drug and nature inspired polydopamine-serotonin nanohybrid have the potential to act in synergistic way to develop combinatorial PD treatment. The translational potential of the presented nanoformulation may provide the solution of PD treatment by overcoming the existing limitation of commercial PD drug in the clinical set-up. The limitations of the present study comprise lack of commercial drug group as positive control and animal study. The long term toxicity, safety analysis, bulk nanoparticle synthesis and off targeting could be the possible challenges associated with the presented nanoformulation. However, the presented nanoformulation has first time exhibited hytrin loaded polydopamine-serotonin nanohybrid. There is no other hytrin

encapsulated nanoparticles report in the public domain to compare the presented nanoformulation, only bare FTY720 report in PD are available. However, our nanoformulation has shown improved neuroprotective efficacy in compare to bare FTY720. Hence, FTY720 loaded nanohybrid has immense potential to be new PD therapeutic candidate if studied further in clinical set-up.

## 5a.4 References


1. A. Oueslati, Implication of Alpha-Synuclein Phosphorylation at S129 in Synucleinopathies: What Have We Learned in the Last Decade? *J Parkinsons Dis* 6, 39-51 (2016).
2. S. Mullin, A. Schapira, alpha-Synuclein and mitochondrial dysfunction in Parkinson's disease. *Mol Neurobiol* 47, 587-597 (2013).
3. A. H. V. Schapira, Treatment Options in the Modern Management of Parkinson Disease. *Archives of Neurology* 64, 1083-1088 (2007).
4. B. D. Li *et al.*, Adverse effects produced by different drugs used in the treatment of Parkinson's disease: A mixed treatment comparison. *CNS neuroscience & therapeutics* 23, 827-842 (2017).
5. R. Cai *et al.*, Enhancing glycolysis attenuates Parkinson's disease progression in models and clinical databases. *The Journal of clinical investigation* 129, 4539-4549 (2019).
6. S. Y. Park, S. M. Lee, S. W. Shin, J. W. Park, Inactivation of mitochondrial NADP+-dependent isocitrate dehydrogenase by hypochlorous acid. *Free Radic Res* 42, 467-473 (2008).
7. K. Smolková, P. Ježek, The Role of Mitochondrial NADPH-Dependent Isocitrate Dehydrogenase in Cancer Cells. *International Journal of Cell Biology* 2012, 273947 (2012).
8. H. Kim *et al.*, IDH2 deficiency promotes mitochondrial dysfunction and dopaminergic neurotoxicity: implications for Parkinson’s disease. *Free Radical Research* 50, 853-860 (2016).

9. X. Wang *et al.*, Pathogenic alpha-synuclein aggregates preferentially bind to mitochondria and affect cellular respiration. *Acta Neuropathologica Communications* 7, 41 (2019).
10. J. Liang *et al.*, Novel suppressors of alpha-synuclein toxicity identified using yeast. *Human molecular genetics* 17, 3784-3795 (2008).
11. M. K. Kumar, K. Nagaraju, S. Bhanja, M. J. I. J. o. P. S. Sudhakar, Research, Formulation and evaluation of sublingual tablets of terazosin hydro-chloride. 5, 417 (2014).
12. S. Bhattacharjee, Understanding the burst release phenomenon: toward designing effective nanoparticulate drug-delivery systems. 12, 21-36 (2021).
13. Z. Dong *et al.*, Tamsulosin versus terazosin for benign prostatic hyperplasia: a systematic review. *Systems biology in reproductive medicine* 55, 129-136 (2009).
14. J. K. Patra *et al.*, Nano based drug delivery systems: recent developments and future prospects. *Journal of Nanobiotechnology* 16, 71 (2018).
15. J. Grosch, J. Winkler, Z. Kohl, Early Degeneration of Both Dopaminergic and Serotonergic Axons – A Common Mechanism in Parkinson's Disease. 10 (2016).
16. M. N. Sardoiwala, A. K. Srivastava, B. Kaundal, S. Karmakar, S. R. Choudhury, Recuperative effect of metformin loaded polydopamine nanoformulation promoting EZH2 mediated proteasomal degradation of phospho-α-synuclein in Parkinson's disease model. *Nanomedicine: Nanotechnology, Biology and Medicine* 24, 102088 (2020).
17. A. K. Srivastava, S. Roy Choudhury, S. Karmakar, Melatonin/polydopamine nanostructures for collective neuroprotection-based Parkinson's disease therapy. *Biomaterials Science* 8, 1345-1363 (2020).
18. Q. Huang, H. Wang, S. W. Perry, M. E. Figueiredo-Pereira, Negative regulation of 26S proteasome stability via calpain-mediated cleavage of Rpn10 subunit upon mitochondrial dysfunction in neurons. *J Biol Chem* 288, 12161-12174 (2013).
19. X. Chen *et al.*, Terazosin activates Pgk1 and Hsp90 to promote stress resistance. *Nature chemical biology* 11, 19-25 (2015).
20. J. Hou *et al.*, A novel high drug loading mussel-inspired polydopamine hybrid nanoparticle as a pH-sensitive vehicle for drug delivery. *Int J Pharm* 533, 73-83 (2017).

21. J. H. Lee, Y. Yeo, Controlled Drug Release from Pharmaceutical Nanocarriers. *Chemical engineering science* 125, 75-84 (2015).
22. N. Nakatsuka *et al.*, Polyserotonin Nanoparticles as Multifunctional Materials for Biomedical Applications. *ACS Nano* 12, 4761-4774 (2018).
23. A. Mishra, S. Singh, S. Shukla, Physiological and Functional Basis of Dopamine Receptors and Their Role in Neurogenesis: Possible Implication for Parkinson's disease. *J Exp Neurosci* 12, 1179069518779829-1179069518779829 (2018).
24. L. C. Berumen, A. Rodríguez, R. Miledi, G. García-Alcocer, Serotonin Receptors in Hippocampus. *The Scientific World Journal* 2012, 823493 (2012).
25. H. Lepor, M. Baumann, E. Shapiro, The alpha adrenergic binding properties of terazosin in the human prostate adenoma and canine brain. *The Journal of urology* 140, 664-667 (1988).
26. M. N. Sardoiwala, S. Karmakar, S. R. Choudhury, Chitosan nanocarrier for FTY720 enhanced delivery retards Parkinson's disease via PP2A-EzH2 signaling in vitro and ex vivo. *Carbohydrate Polymers* 254, 117435 (2021).
27. S. A. Correa, K. L. Eales, The Role of p38 MAPK and Its Substrates in Neuronal Plasticity and Neurodegenerative Disease. *Journal of signal transduction* 2012, 649079 (2012).
28. H. J. Lee, C. Kim, S. J. Lee, Alpha-synuclein stimulation of astrocytes: Potential role for neuroinflammation and neuroprotection. *Oxidative medicine and cellular longevity* 3, 283-287 (2010).
29. M. Shamoto-Nagai *et al.*, An inhibitor of mitochondrial complex I, rotenone, inactivates proteasome by oxidative modification and induces aggregation of oxidized proteins in SH-SY5Y cells. *Journal of neuroscience research* 74, 589-597 (2003).
30. B. I. Perez-Revuelta *et al.*, Metformin lowers Ser-129 phosphorylated alpha-synuclein levels via mTOR-dependent protein phosphatase 2A activation. *Cell Death Dis* 5, e1209 (2014).

# Chapter 5b

---

# Neuroprotective effect of Hytrin-loaded polydopamine-serotonin nanoformulations reduce PD condition *in vivo* model

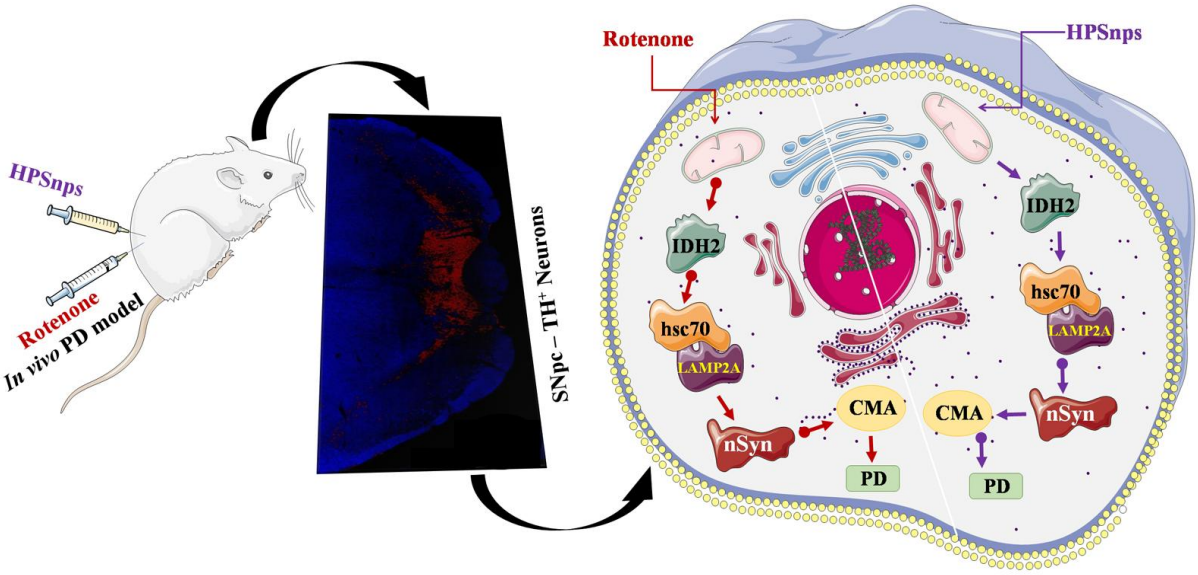

## 5b.1. Introduction

Parkinson's disease (PD) is a progressive disease that majorly occurs due to post-translational modifications of alpha-synuclein. (1, 2) The core cause of neuronal death is still not well understood. Mitochondrial dysfunction is one of the major factors involved in synuclein accumulation. (3) recent therapies like deep brain stimulation and non-pharmacological and pharmacological therapies exhibit better responses. (4) However, multiple side-effects of existing therapies hinder therapeutic efficacy. (5) In recent decades, Hytrin emerged as a neuroprotective candidate that can penetrate the blood-brain barrier in the treatment of Parkinson's disease. (6) Hytrin has the limitation of burst drug release and rapid absorption that restricts its therapeutic efficacy. Therefore, we have developed and previously reported the nano-drug delivery system by formulating Hytrin-loaded polydopamine-serotonin nanoparticles that exhibited improved drug release kinetics, mitochondrial function, and reduction of synucleinopathy. (2)

The present study has been focused to understand the camouflaged role of IDH2 in the reduction of post-translated alpha-synuclein by utilizing our reported Hytrin nanohybrids. Our previous study has explored the IDH2 role in the reduction of phosphorylated alpha-synuclein, while the present study aimed to understand the IDH2 role in the reduction of nitrated alpha-synuclein. Recently, the nitrated alpha-synuclein forms due to reactive nitrogen or oxygen species also have been reported as one of the causes of alpha-synuclein aggregation. (7) Indeed, IDH2 is the known therapeutic marker in the reduction of reactive oxygen/nitrogen species leading to maintaining the redox balance of the mitochondria. (8) In this regard, Hytrin induces IDH2, a mitochondrial redox regulator whose reduction leads to PD progression. (9) Mitochondrial dysfunction leads to loss of heat shock protein 70 (hsc70) which is also supported by the literature demonstrated reduction of heat shock protein 70 in the rotenone-induced condition. (10, 11) Here, hsc70 is a major player in chaperone-mediated autophagy (CMA) and works along with Lamp2a (lysosome-associated membrane protein) in the reduction of misfolded or mutated proteins from the cells. (12) Accumulating several shreds of evidence, the study directed to explore the role of IDH2 in the activation of chaperone-mediated autophagy by inducing the hsc70/lamp2a signaling *in vivo* PD model. The project design of the chapter 3b represented for better understanding of hypothesis, rationale of chapter with justification of the selected compound aligned to expected outcomes of the aims as below.

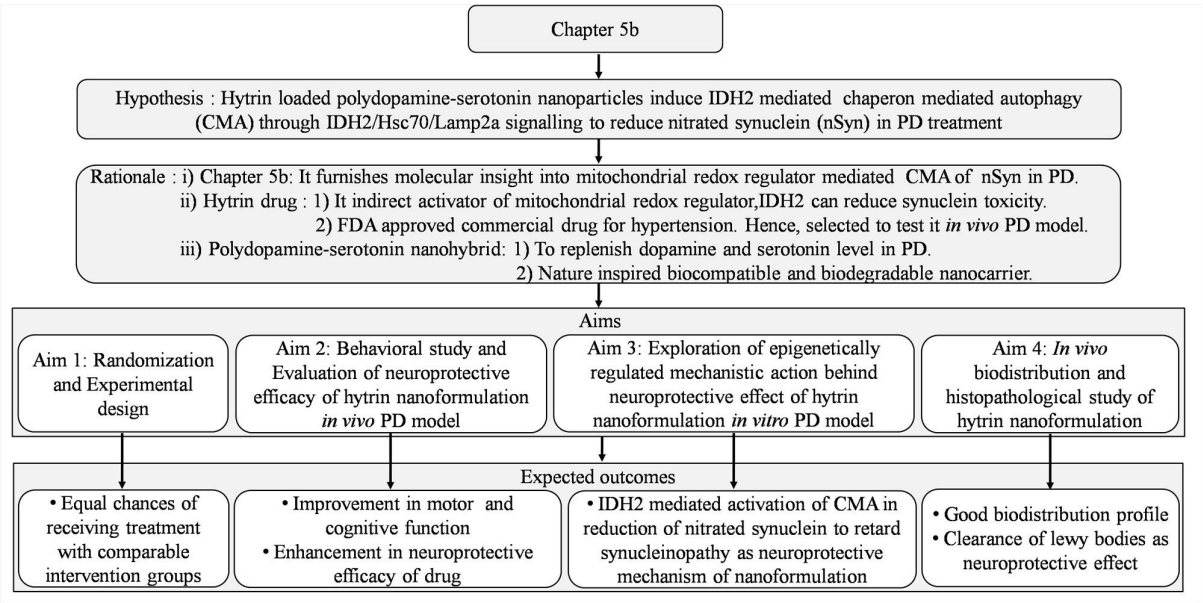


Scheme 8: The project design represents hypothesis, rationale, aims and it's aligned expected outcomes.

The present study has evaluated the neurotherapeutic effect of the hytrin nanohybrid *in vivo* PD model. The results have elucidated the neurotherapeutic efficacy of Hytrin nanohybrid by improving behavioral activity and restoring dopaminergic neuron cells against rotenone-induced insults. In the mechanism of alpha-synuclein degradation, CMA also plays a major role as one of the protein degradation pathways. (13) However, rotenone has been reported to reduce CMA activity. (10, 11) Therefore, it is imperative to enhance the CMA process for PD treatment. In that aspect, a study has shown the induction of IDH2 by our FTY720 nanohybrid which upregulated hsc70/lamp2a expression in the lysosomal degradation of nitrated synuclein. As per our knowledge, the study first time revealed the camouflaged role of IDH2 on induction of CMA activity in the reduction of alpha synucleinopathy. Thus, the study divulges the Hytrin nanohybrid induced IDH2/hsc70/lamp2a signaling in the reduction of synucleinopathy.

## 5b.2. Result and Discussion

### 5b.2.1. *In vivo* bio-distribution of HPSnps reflects clearance and accumulation in the brain

*In vivo* bio-distribution study has been performed to understand the BBB crossing potential with the administration route with dose duration for the therapeutic application. For that, ICG tagged HPSnps has been administrated by two routes, i.v. (Fig.5.14a) and

i.p. (Fig.5.14c) for 24 hours. The nanoformulation has shown a good biodistribution profile by showing accumulation in the brain.

In fig.5d, the intraperitoneal route has shown better accumulation of HPSnps in the brain after 24 hours in comparison to the intravenous administration. (Fig.5.14b) In the initial 3 hours, i.v. injected HPSnps has shown deposition in the brain, while i.p. injected HPSnps exhibited brain deposition till 6 hours in the live animal imaging. (Fig.5.14a and 5.14c) Thus, the results are supporting the notion that HPSnps are biocompatible and the i.p administration route is showing better retention of HPSnps in the brain than the i.v. route. Hence, the i.p administration is preferred for *in vivo* therapeutic studies. The results are in line with our previous report in which the study has shown brain retention of polydopamine nanoparticles. (14) The major clearance of the HPSnps has been observed after 24 hours of administration. Therefore, daily dose administration has been preferred to give the animals during the study. Hence, the HPSnps is a suitable candidate for the delivery of drugs to the brain and herein for Parkinson's disease.

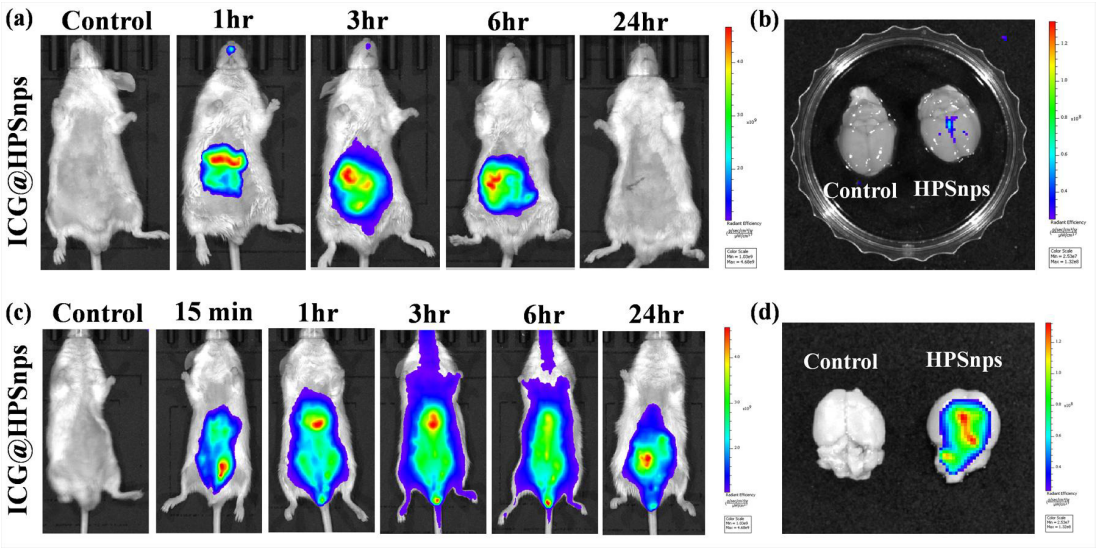


Fig.5.14 (a) In vivo biodistribution profile of i.v. injected HPSnps and (b) ex vivo imaging showing brain retention after 24 hours. (c) In vivo biodistribution images showing i.p. administered HPSnps and (d) its retention in the brain after 24 hours

5b.2.2. Histopathological analysis shows the neuroprotective effect of HPSnps

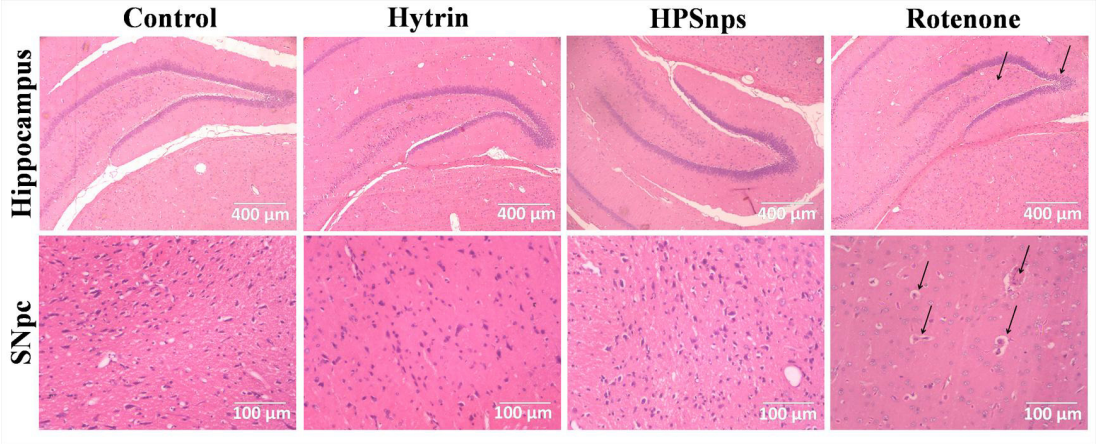


Fig.5.15 Histological images reflect the neuroprotective effect of HPSnps.

The excised and processed brain sections have been stained with Hematoxylin and Eosin to observe the rotenone effect and neuroprotection by the presented neuroprotective candidate, HPsnps. (Fig.5.15) The black arrow has been an introduction to indicate the presence of a Lewy body in the Substantial nigra (SNpc) and degenerated neurons in the hippocampus region due to the rotenone effect. The H&E images of HPSnps have not shown any Lewy body and loss of neurons that indicates the neuroprotective effect of the nanoformulation. The formation of the Lewy body in the SNpc has in supports our finding that validates our rotenone-induced PD models. (15, 16) Herein, the reduction of Lewy bodies and protection of the neurons from degeneration is in line with the existing reports that have shown the neuroprotection efficiency of the neuroprotective candidate has been shown through histological study. (17) (18) Herein, HPSnps has shown enhanced neuroprotective efficiency in comparison to the bare drug by improving drug protection caliber through nanocarrier-mediated delivery. The study has presented results of behavioral study, TH positive neuron cells examination in SNpc, protein expression analysis with details of mechanistic action of neuroprotective HPSnps, and histological analysis are in support of each other to divulge the neuroprotective potential of HPsnps.

5b.2.3. HPSnps improves behavioral defects to reverse the rotenone effect

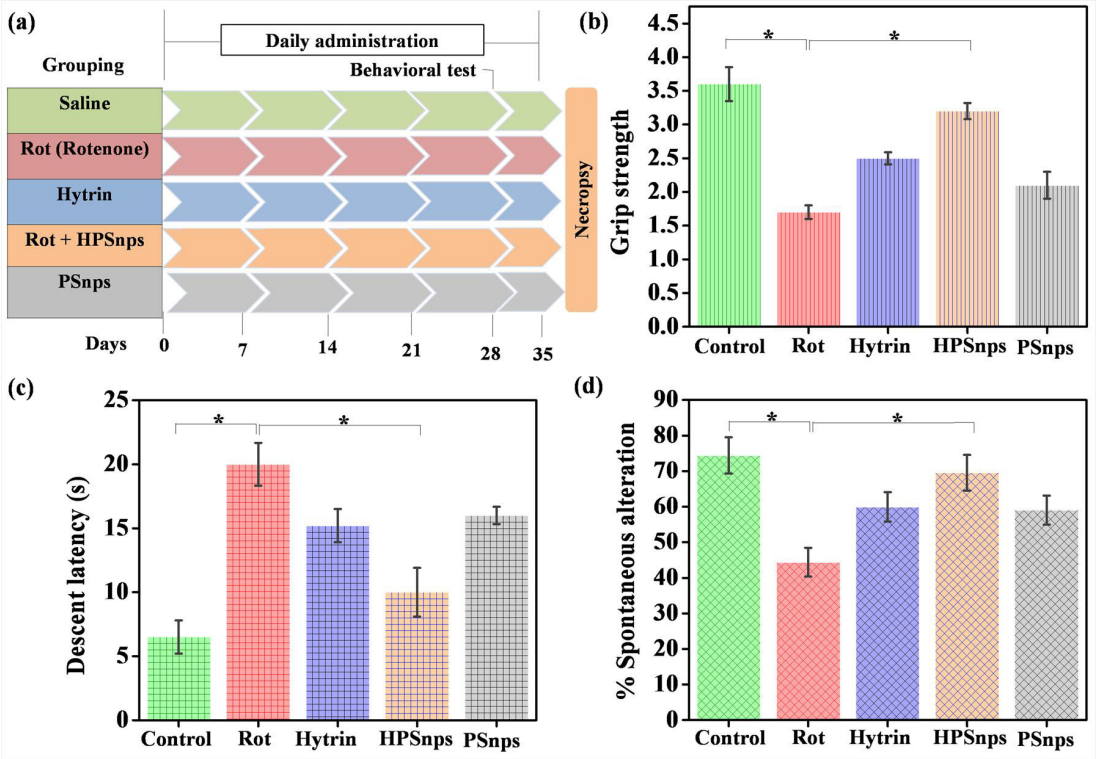


Fig.5.16 Experimental design and behavioral testing indicate the protective caliber of HPSnps.

The rotenone-induced PD model and its experimental design have been illustrated in fig.5.16a. A behavioral study has been performed to observe the protective effect of HPSnps against rotenone-induced insults. The rotenone has shown ~2 folds reduction of grip strength and ~3 folds induction in decent latency. (Fig.5.16b, 1c) HPSnps has exhibited ~2 folds improvements in the grip strength and decent latency against rotenone-induced damages. The cognitive impairment by rotenone and protection by HPSnps has also been assessed through the spontaneous alteration assay. The results are in support of the existing literature that has demonstrated rotenone-induced cognitive impairment in PD conditions. (19, 20) The result has shown ~1.66 folds cognitive impairment as means of percentage spontaneous alteration. HPSnps has exhibited ~1.5 folds recovery in the cognitive impairment caused by rotenone. (Fig.5.16d) Herein, the behavioral test results are in line with the existing report of Hytrin formulation with similar folds recovery from the PD condition. (6) HPSnps has shown a better neuroprotective effect in comparison to the blank PSnps and Hytrin by attenuating the rotenone-induced effect.

5b.2.4. HPSnps restores $TH^+$ neurons

TH is a therapeutic target of PD that is majorly expressed in the substantial nigra of the midbrain. Therefore, the expression analysis of the $TH^+$ neurons has been performed to examine the neuroprotective efficiency of the HPSnps. In fig.5.17 and 5.18, the images have shown a remarkable loss of $TH^+$ neurons due to the rotenone effect and the noticeable recovery of neurons has been observed with the treatment of HPSnps. Herein, the loss of dopaminergic neurons signifies the PD effect induced by rotenone and its recovery indicates the neuroprotective potential of HPSnps. The results support the finding of our previous reports that have shown the neuroprotective caliber of Hytrin-loaded polydopamine-serotonin nanoparticles *in vitro* and *ex vivo* PD models. (2) The results of $TH^+$ neuron recovery is in lieu to the existing reports of Hytrin formulation that has shown ~2 folds recovery of dopaminergic neuron in SNpc.(6) Herein, the expression analysis of other two important PD markers, PD hallmark nitrated synuclein and Chaperone mediated autophagy marker Lamp2a have also been monitored. The nitrated synuclein elevated expression in the SNpc has been noted within the rotenone group and its reversal neuroprotective action has been observed by HPSnps treatment. (Fig.5.17) Similarly, a reduced level of Lamp2a has been noticed in the TH+ neurons cells population due to rotenone-induced damages and its restoration has been obtained through the neuroprotective effect of HPSnps.(Fig.5.18) The synuclein and lamp2a results support the clinical fact that has demonstrated Hytrin facilitates the reduction of the synuclein accumulation and chaperone-mediated anti-apoptosis. (6)

5b.2.5. HPSnps induces CMA activity as a neuroprotective effect

The TH and nitrated synuclein, hallmarks of PD have been investigated to confirm rotenone-induced damages and the recuperative effect of HPSnps. It is well reported that posttranslational modification of synuclein, nitrated synuclein leads to synuclein aggregation, and the reduction of TH results in PD progression. (7, 21-24) The ~5 folds reduced TH expression has confirmed the establishment of a rotenone-induced PD model and ~ 6 folds restoration through treatment of HPSnps indicates a neuroprotective effect. (Fig.5.19a) Further, ~ 3 folds elevated nitrated synuclein expression signifies the rotenone-induced PD effect and HPSnps has shown ~3 folds reduction in the nitrated

synuclein expression. Herein, HSPnps has exhibited ~3 folds higher restoration of TH expression in comparison to the existing literature that shows the anti-PD effect of Hytrin. (6) In continuous with our previous report, the IDH2 expression has been examined in vivo PD model and results are in line with our previous study that validates the neuroprotective effect of HPSnps.(2)

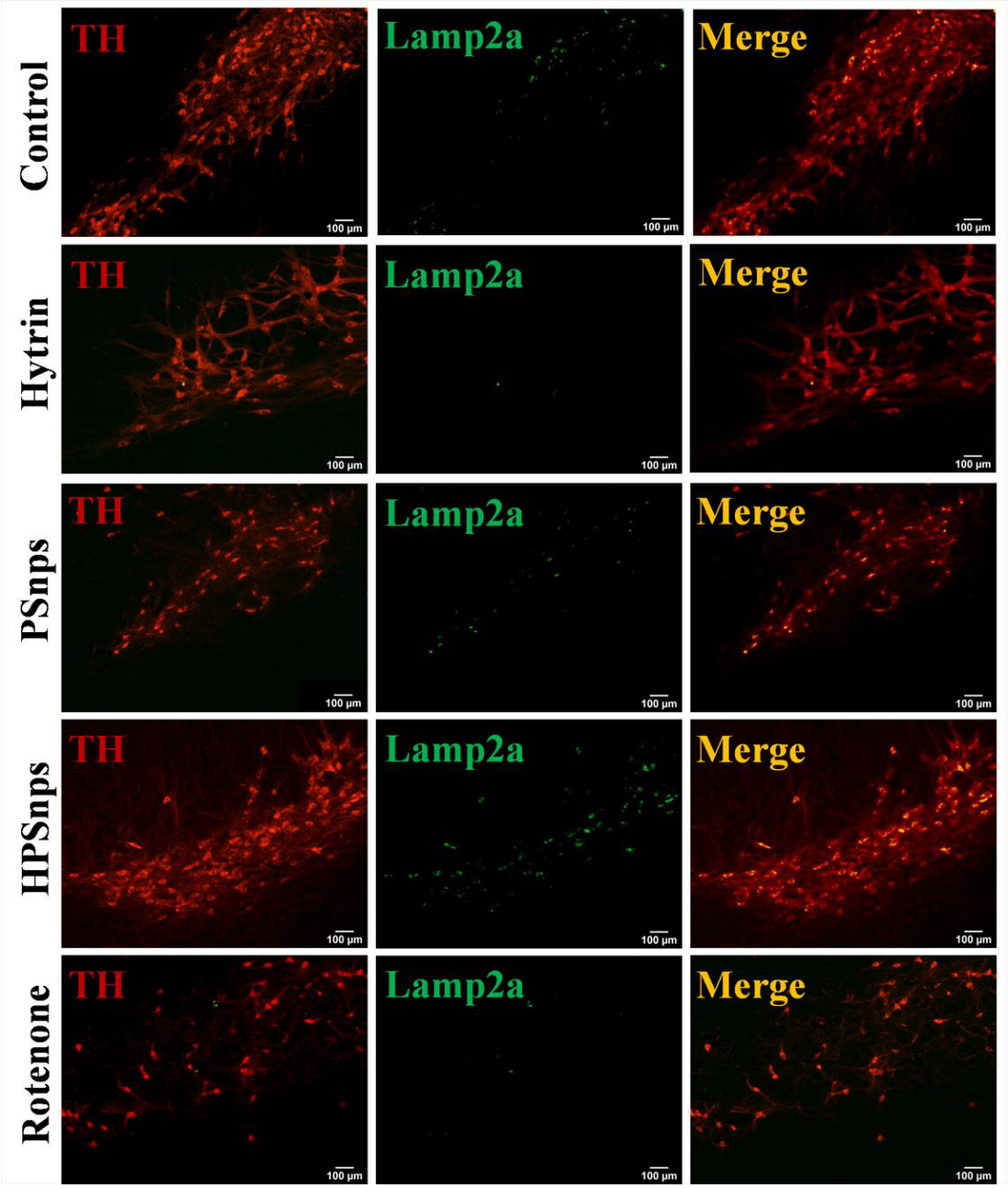

Fig.5.17 Immunofluorescence images of TH and Lamp2a in the SNpc regions show higher neurodegeneration in rotenone-induced conditions and the protective effect of HPSnps against rotenone-induced insults.

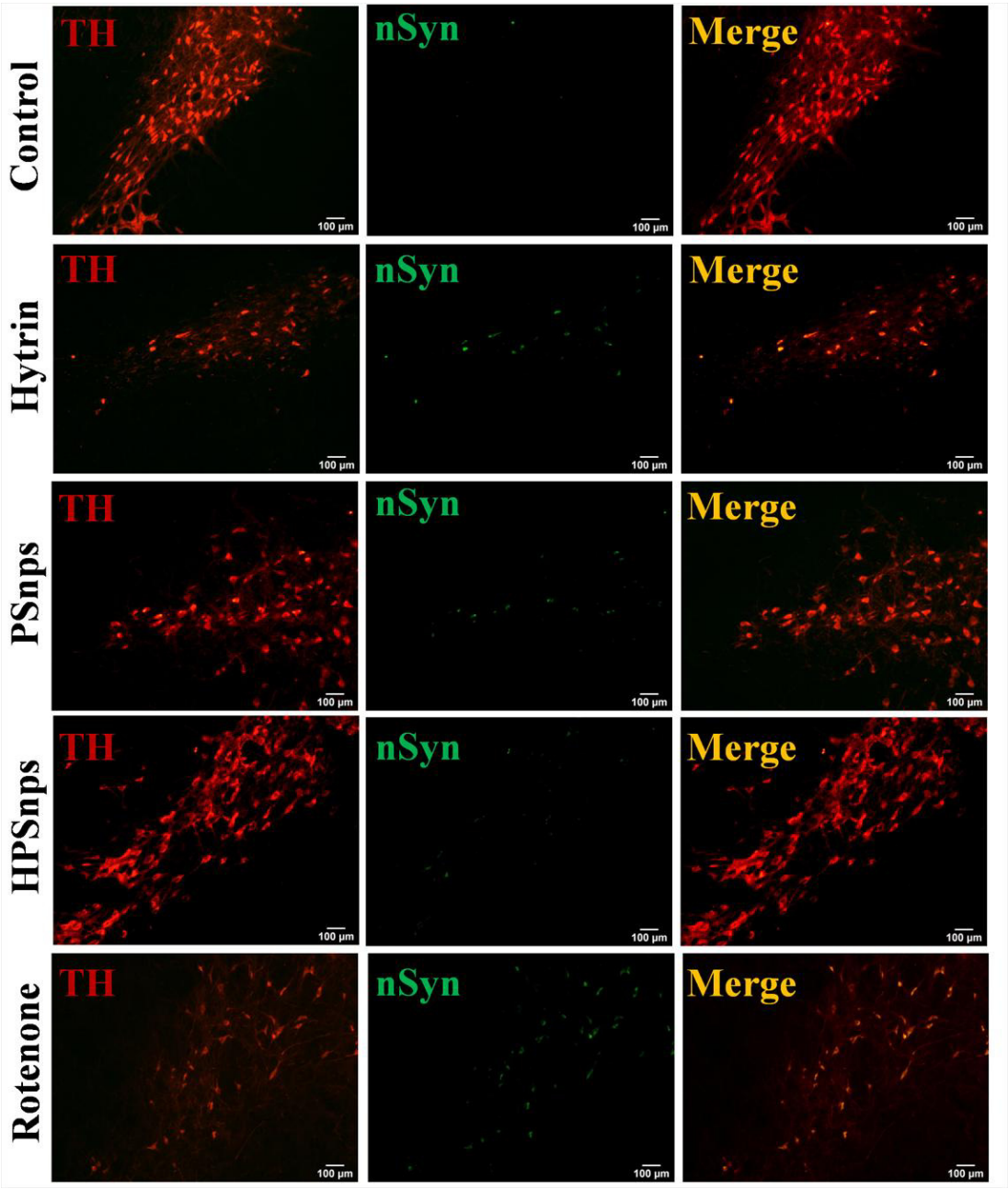


Fig.5.18 TH and nSyn colocalization images suggest the neuroprotective caliber of HPSnps

Recently, IDH2 is the mitochondrial redox regulator, and its role in the attenuation of synuclein toxicity is known and the fact is also supported by our previous report. Indeed, the heat shock protein and Lamp2a, both CMA signature molecules reduce in the PD conditions and the IDH2-mediated mitochondrial redox regulation endows the CMA activity. (25, 26) Therefore, we also explored the IDH2, Hsc70, and Lamp2a expression in rotenone-induced conditions and the protective effect of HPSnps. In the results, ~ 6 folds, ~ 4 folds, and ~ 10 folds inhibition of IDH2, Hsc70, and Lamp2a have been found, and that restored ~ 4.5 folds, ~ 10 folds, and ~ 4 folds with the treatment of HPSnps, respectively. (Fig.5.19a, b) The results are indicating the reduction in CMA signature molecular markers with a reduction of IDH2.

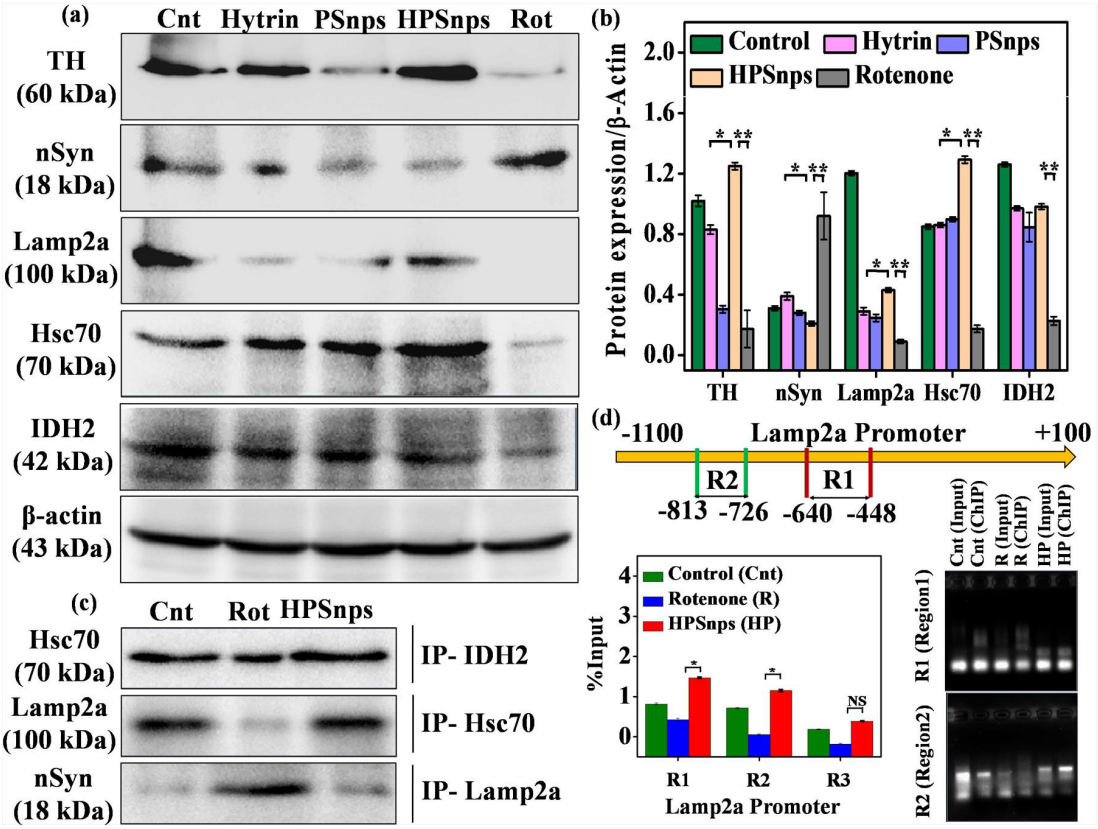


Fig.5.19 Molecular insights into the neuroprotective potential of HPSnps reveals IDH2 role in the endowment of CMA activity.

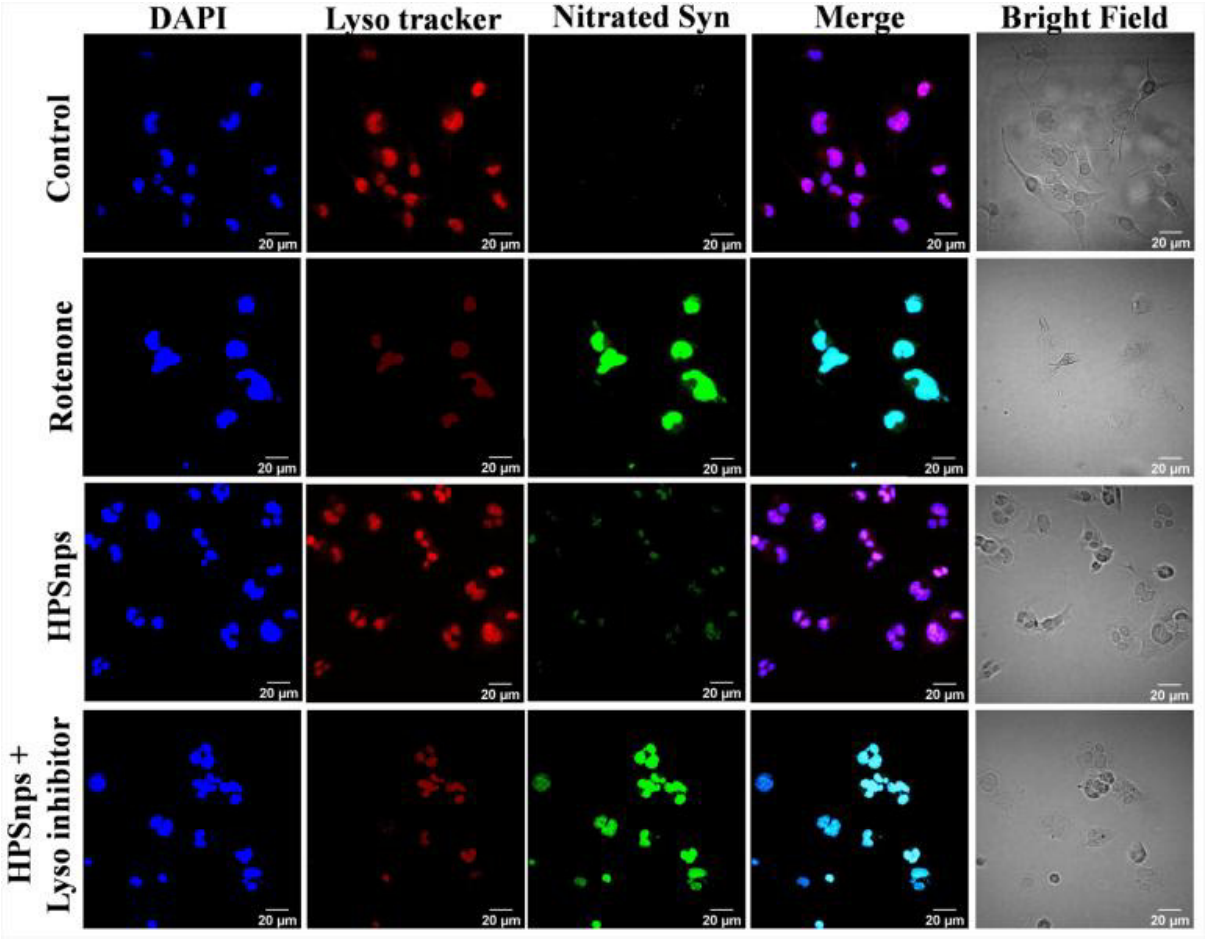


Fig.5.20 The lysosomal inhibitor confirms that HPSnps follows a lysosomal-mediated degradation pathway for nitrated synuclein.

Hence, the immunoprecipitation study has been performed to reveal IDH2-mediated regulation of CMA activity. (Fig.5.19c) Results have shown direct physical interaction of IDH2 with Hsc70 that interacts with Lamp2a and nSyn. Herein, the present study has first time uncovered the camouflaged role of IDH2 in the endowment of CMA activity. Indeed, the existing report demonstrated that Hsc70 is involved in the regulation of Lamp2a expression. (25, 27) Thus, the chromatin immunoprecipitation (ChIP) assay has been conducted to explore the Hsc70-mediated regulation of Lamp2a expression and interestingly results have shown Hsc70 binding to the promoter site of the Lamp2a contributing to Lamp2a expression. (Fig.5.19d) In that, ChIP-qPCR and agarose gel images of qPCR products have shown reduced Hsc70 binding to Lamp2a promoter region 1 (-448 to -640) and region 2 (-726 to -813). The results indicate that Hsc70

may require for the transcriptional activation of Lamp2a.In fig.5.20, the lysosomal inhibitor has been introduced to confirm the lysosomal-mediated degradation of nitrated synuclein. The confocal micrograph has shown clear evidence that in the presence of a lysosomal inhibitor our nanoformulation has not been efficient to reduce the nitrated synuclein level. It means that our nanoformulation works through the lysosomal-mediated degradation pathway of nitrated synuclein. Thus, several pieces of evidence divulge the neuroprotective potential of HPSnps that induces IDH2-mediated CMA activity for the clearance of the nitrated synuclein. Hence, the HPSnps may be utilized as one of the neuroprotective agents for PD treatment at the clinical stage.

### 5b.3 Conclusion

The overall finding of the study demonstrated Hytrin-loaded polydopamine-serotonin nanohybrids as promising anti-Parkinsonian candidate. The major key findings suggest the recovery of locomotor activity, cognitive impairment, and recovery $TH^+$ neurons against rotenone induced damage in SNpc of mice brain indicate the neuroprotective potential of HPSnps. In addition, the co-localization of Lamp2a and nSyn with $TH^+$ neurons and protein expression analysis confirms the neuroprotective efficiency of HPSnps. The significance of the present study is that it explained the molecular pathway by which IDH2 reduces the synuclein toxicity. The protein expression study explored the IDH2 role in the endowment of the CMA activity in the clearance of nSyn leading to reduce PD condition. The pieces of evidence from the results of immunoprecipitation and chromatin immunoprecipitation confirmed HPSnps-induced IDH2/Hsc70/Lamp2a signalling in the reduction of nitrated synuclein. Hence, the present study first time has shown the IDH2/Hsc70/Lamp2a signalling in degradation of nitrated synuclein by enhancing CMA activity. As per our best knowledge, there is no report that has demonstrated hytrin loaded nanoformulation in PD treatment to compare our nanoformulation. But, our nanoformulation has shown superior neuroprotection efficacy in comparison to bare hytrin drug. The hytrin is FDA approved drug and polydopamine-serotonin nanohybrid is biocompatible, stable plus biodegradable which make our nanoformulation as a promising candidate to translate into clinical application. However,

the therapeutic comparison with commercial drug in preclinical model is major lacking point of the presented work with translational challenges like bulk nanoparticle synthesis, off targeting and long term toxicity may hinder the translational potential of our nanoformulation. However, a detailed investigation of the IDH2-induced Lamp2a gene repression is warranted in future studies. Thus, HPSnps may be promising candidates to be used and explored at the clinical stage for PD treatment.

5b.4 References


1. A. Oueslati, Implication of Alpha-Synuclein Phosphorylation at S129 in Synucleinopathies: What Have We Learned in the Last Decade? *J Parkinsons Dis* 6, 39-51 (2016).
2. M. N. Sardoiwala, S. J. Mohanbhai, S. Karmakar, S. R. Choudhury, Hytrin loaded polydopamine-serotonin nanohybrid induces IDH2 mediated neuroprotective effect to alleviate Parkinson's disease. *Materials Science and Engineering: C* https://doi.org/10.1016/j.msec.2021.112602, 112602 (2021).
3. S. Mullin, A. Schapira, alpha-Synuclein and mitochondrial dysfunction in Parkinson's disease. *Mol Neurobiol* 47, 587-597 (2013).
4. A. H. V. Schapira, Treatment Options in the Modern Management of Parkinson Disease. *Archives of Neurology* 64, 1083-1088 (2007).
5. B. D. Li *et al.*, Adverse effects produced by different drugs used in the treatment of Parkinson's disease: A mixed treatment comparison. *CNS neuroscience & therapeutics* 23, 827-842 (2017).
6. R. Cai *et al.*, Enhancing glycolysis attenuates Parkinson's disease progression in models and clinical databases. *The Journal of clinical investigation* 129, 4539-4549 (2019).
7. Y. He, Z. Yu, S. Chen, Alpha-Synuclein Nitration and Its Implications in Parkinson's Disease. *ACS Chemical Neuroscience* 10, 777-782 (2019).
8. R. Cairns, I. Harris, S. McCracken, T. Mak, Cancer Cell Metabolism. *Cold Spring Harbor symposia on quantitative biology* 76, 299-311 (2011).

9. H. Kim *et al.*, IDH2 deficiency promotes mitochondrial dysfunction and dopaminergic neurotoxicity: implications for Parkinson's disease. *Free Radical Research* 50, 853-860 (2016).
10. H. J. Jang *et al.*, Glutamine induces heat-shock protein-70 and glutathione expression and attenuates ischemic damage in rat islets. *Transplantation proceedings* 40, 2581-2584 (2008).
11. G. Sala *et al.*, Rotenone down-regulates HSPA8/hsc70 chaperone protein in vitro: A new possible toxic mechanism contributing to Parkinson's disease. *Neurotoxicology* 54, 161-169 (2016).
12. K. A. Malkus, H. Ischiropoulos, Regional deficiencies in chaperone-mediated autophagy underlie α-synuclein aggregation and neurodegeneration. *Neurobiology of disease* 46, 732-744 (2012).
13. T. Vogiatzi, M. Xilouri, K. Vekrellis, L. Stefanis, Wild type alpha-synuclein is degraded by chaperone-mediated autophagy and macroautophagy in neuronal cells. *J Biol Chem* 283, 23542-23556 (2008).
14. M. N. Sardoiwala, A. K. Srivastava, B. Kaundal, S. Karmakar, S. R. Choudhury, Recuperative effect of metformin loaded polydopamine nanoformulation promoting EZH2 mediated proteasomal degradation of phospho-α-synuclein in Parkinson's disease model. *Nanomedicine: Nanotechnology, Biology and Medicine* 24, 102088 (2020).
15. V. Bogaerts *et al.*, A novel locus for dementia with Lewy bodies: A clinically and genetically heterogeneous disorder. *Brain : a journal of neurology* 130, 2277-2291 (2007).
16. S. R. Bonam, C. Tranchant, S. Muller, Autophagy-Lysosomal Pathway as Potential Therapeutic Target in Parkinson’s Disease. 10, 3547 (2021).
17. R. Taipa, J. Pinho, M. Melo-Pires, Clinico-Pathological Correlations of the Most Common Neurodegenerative Dementias. *Frontiers in neurology* 3, 68 (2012).
18. M. Kujawska *et al.*, Neuroprotective Effects of Pomegranate Juice against Parkinson's Disease and Presence of Ellagitannins-Derived Metabolite—Urolithin A—In the Brain. 21, 202 (2020).

19. I. O. Ishola *et al.*, Morin ameliorates rotenone-induced Parkinson disease in mice through antioxidation and anti-neuroinflammation: gut-brain axis involvement. *Brain Research* 1789, 147958 (2022).
20. D. Zhang *et al.*, Microglial activation contributes to cognitive impairments in rotenone-induced mouse Parkinson's disease model. *Journal of neuroinflammation* 18, 4-4 (2021).
21. R. Burai, N. Ait-Bouziad, A. Chiki, H. A. Lashuel, Elucidating the Role of Site-Specific Nitration of α-Synuclein in the Pathogenesis of Parkinson's Disease via Protein Semisynthesis and Mutagenesis. *J Am Chem Soc* 137, 5041-5052 (2015).
22. Y. Liu, M. Qiang, Y. Wei, R. He, A novel molecular mechanism for nitrated α-synuclein-induced cell death. *Journal of Molecular Cell Biology* 3, 239-249 (2011).
23. G. Alam, J. R. Richardson, "Chapter 4 - Regulation of tyrosine hydroxylase: relevance to Parkinson's disease" in Genetics, Neurology, Behavior, and Diet in Parkinson's Disease, C. R. Martin, V. R. Preedy, Eds. (Academic Press, 2020), https://doi.org/10.1016/B978-0-12-815950-7.00004-7, pp. 51-66.
24. M. Gómez-Benito *et al.*, Modeling Parkinson's Disease With the Alpha-Synuclein Protein. *Frontiers in pharmacology* 11, 356 (2020).
25. L. Alvarez-Erviti *et al.*, Influence of microRNA deregulation on chaperone-mediated autophagy and α-synuclein pathology in Parkinson's disease. *Cell Death Dis* 4, e545-e545 (2013).
26. G. Sala, D. Marinig, A. Arosio, C. Ferrarese, Role of Chaperone-Mediated Autophagy Dysfunctions in the Pathogenesis of Parkinson's Disease. 9 (2016).
27. P. Maiti, J. Rossignol, G. Dunbar, Curcumin Modulates Molecular Chaperones and Autophagy-Lysosomal Pathways In Vitro after Exposure to Aβ42. *Journal of Alzheimer's Disease & Parkinsonism* 07 (2017).

# Conclusion and Future Prospects

The aim of this thesis was to develop a new nanodrug delivery platform to overcome the limitations of anti-parkinsonian drugs like metformin, FTY720 and Hytrin. The metformin and Hytrin has the burst release, and rapid adsorption constrain, while FTY720 is has the hydophobicity issue. Therefore, the study specifically interested to provide solution by introducing well-defined, stable, biocompatible, nature-inspired and reproducible nanoformulations that might be utilized as PD therapeutic agents. To achieve the goals, the selections have been made on the basis of necessity of the PD treatments and requirements of the nanoformulations. The neuroprotective potential carrying nanaocarriers have been chosen with aim to furnish synergistic approach at a single platform. Three different nanoparticles have been prepared; polydopamine nanoparticles, chitosan nanoparticles and polydopamine-serotonin nanoparticles. Herein, Polydopamine nanoparticles and polydopamine-serotonin nanohybrids have been employed with aim to replenish the dopamine level which generally reduced during the PD progression. The chitosan nanoparticles have been considered as the neurotherapeutic agent having neuronal healing property. Hence, the chitosan nanoparticles also applied to provide the benefits in the PD therapy as a synergistic approach. The utilized drugs metformin, FTY720 and Hytrin have known for their neuroprotective potential and they are repurposed drugs for the neurodegenerative disease. Dopamine, serotonin are the neurohormones and chitosan are coming from the chitin. All selected precursors are the nature inspired. Hence, we aimed to develop the nanoformulation might be scale up for the clinical setup due to their feasibility and known beneficial characteristics. In the developed nanoformulations, metformin loaded polydopamine nanoparticles considered to deliver metformin. Metformin is the wonder molecules having efficiency to reduce ser129 phosporylated alpha synuclein level, a hallmark of PD. Metformin also having the epigenetic modulation ability to regulate epigenetic mechanism by activating SIRT1, histone deacetylase level. Similarly, FTY720 loaded chitosan nanoparticles employed to deliver FTY720 in PD treatment. FTY720 is the activator of PP2A, a phosphatase which usually dephosphorylates the synuclein molecule, a signature marker of PD. The hytrin loaded polydopamine-sertonin nanohybrids applied to deliver hytrin, an activator of IDH2, redox regulator of mitochondria which reduces the synucleinopathy. Hence, the nanoscale ~100 nm colloidal nanosystems have been projected which successfully cross the blood-brain barrier and exhibited accumulation in the brain. These biocompatible nanoformulations have shown improved drug release profiles by enhancing solubility of drugs and providing slower drug

release kinetics. Thus, the combinations of these drugs and nanocarriers proved to be promising therapeutic candidate for PD. The projected nanoformulation have been challenged to evaluate the neuroprotective potential of them with rotenone, PD causing known pesticides *in vitro*, *ex vivo* and *in vivo* models. The promising neuroprotective effects of nanoformulations have been observed with improvement of behavioral deficits, molecular expression of PD signature molecules like tyrosine hydroxylase and by reducing phosphorylated apha-synuclein.

In the PD management, the epigenetic regulations are gaining interest due to ~90 % cases of idiopathic PD. Hence, the major cause is any of the environmental factors that ultimately modulating epigenetic machinery in the PD progression. The polycomb repressor groups of proteins, EZH2 and BMI1 have been well studied and their depletion leads to PD. Similarly, the rotenone induces hyper histone acetylation of SNCA; a synuclein gene leads to synucleinopathy. Indeed, the shutdown of proteasomal degradation machinery and post-translational modifications of synuclein leads to PD pathogenesis. Hence, it is warranted to understand the epigenetic regulation in PD to demonstrate the therapeutic candidates work on the epigenetic pathways. Hence, the present thesis has emphasized to explore the effects of nanoformulation on epigenetic machinery and uncover the epigenetic regulation in the PD treatment. In the exploration of nanoprotective mechanism, the metformin loaded polydopamine nanoformulation has shown EZH2 mediated alpha-synuclein ubiquitination/ proteasomal degradation. The metformin loaded polydopamine naoparticle neuroprotective effect also confirmed by induction of SIRT1, histone deacetylase to deacetyl H3K27 to repress the SNCA gene expression. The PP2A also have the regulatory role on alpha-synuclein reduction and the phosphorylation of EZH2 leads to EZH2 degradation. Hence, the FTY720 loaded chitosan naoparticles have uncovered the PP2A-EZH2 signaling that endows EZH2 mediated alpha-synuclein ubiquitination/ proteasomal degradation. The role of PP2A through exploration of FTY720 loaded chitosan nanoparticles protective mechanism has also been revealed to stabilize the OGT, an acyl transferase to synuclein. The Glc-N-acylation of synuclein provides stability to synuclein monomers and prevents the synuclein aggregation in treatment of synucleinopathy. The hytrin loaded polydopamine-serotonin nanoparticles have been projected to explore how IDH2 reducing the synuclein toxicity. In exploration, the IDH2 mediated ubiquitination/proteasomal degradation of synuclein has been found as the neuroprotective mechanism. Besides the ubiquitination and proteasomal degradation, the study also found that the nanoformulations also follow the chaperone mediated autophagy

pathways to reduce alpha-synuclein. Thus, the present thesis has proved the neuroprotective efficiency of presented nanoformulations in preclinical models. The nanoformulations have shown promising therapeutic potential to be utilized in clinical setup to explore it therapeutic efficacy that might be emerged as better therapeutic agent in future. Herein, the nanoformulation of metformin, FTY720 and Hytrin has been reported for the first time in treatment of PD as per our best knowledge. To showcase benefits and significance of our nanoformulations, the comparison of neuroprotective effect of presented nanoformulations with other nanocarriers or nano based systems in PD has been discussed herewith. The triphenylphosphonium functionalized mito-metformin encapsulated polyanhydride nanoparticle (1) in PD treatment has shown higher neuroprotective dose 3 μM in compare to our nanoformulation and it neuroprotective efficacy has not been tested vigorously as we tested with different experimental set. Hence, our nanoformulations has performed superior than reported mito-meformin nanoformulation in PD treatment. Besides discussed report of metformin based nanoformulation, no other metformin, FTY720 and hytrin based nanoformulation reported yet. Hence, we compared our nanoformulations with other reported potent drug based nano based systems to understand comparative status of our nanoformulations. In that, Oral apomorphine loaded solid lipid nanoparticles (2), angiopep functionalized human GDNF loaded dendrigraft poly L-lysine – polyethylenegycol nanosystem (3) and resveratrol loaded poly sorbate 80 coated poly lactide nanoparticles (4) have shown comparable drug release profile with effective targeting and the neuroprotective effects by mean of behavioural study and $TH^+$ neuaronal cells results are also comparable with finding of our nanoformulation. However, our nanoformulations may provide more beneficiary profile in the long term toxicity analysis with translational application of discussed nanocarrier systems due to presence of FDA approved drugs with nature inspired nanocarriers in our nanossytems. Our nanoformulations have shown superior nanotherpaeutic potential in compare to other reported nanocarriers in PD treatment like bromocriptine loaded solid lipid nanoparticles (5), ropinirole loaded solid lipid nanoparticles, dopamine loaded PLGA nanoparticles (6), schisantherin A loaded PEG-PLGA nanoparticles (7), deferexamine loaded PEG-PLGA nanoparticles (8) and black phosphorus nanosheets (9). The major factors of the superiority of our nanoformulations are slower and biphasic drug release profile, minimization of therapeutic dose and biocompatible nature of nanoparticle system. The future study of clinical safety parameters and long term utilization of these projected nanoformulations might answer

about the future utility of the nanoformulations. However, the nature inspired nanocarriers and FDA approved drugs provides somewhat confidence that projected nanoformulations will exhibit good safety profile in clinical study due to presence of highly biocompatible and safe drugs. The exploration of epigenetic regulation in the PD treatment also paves the way to understand the events of early onset PD like hyper histoneacetylation of SNCA and role of epiegenetic regulators like EZH2 in PD pathogenesis. Hence, the knowledge about epigenetic involvement in PD regulation paves the way to find the therapeutic agents having ability to modulate the epigenetic machinery working in PD progression and treatment.

References


1. B. W. Schlichtmann *et al.*, Functionalized polyanhydride nanoparticles for improved treatment of mitochondrial dysfunction. **110**, 450-459 (2022).
2. M. J. Tsai *et al.*, Oral apomorphine delivery from solid lipid nanoparticles with different monostearate emulsifiers: pharmacokinetic and behavioral evaluations. *J Pharm Sci* **100**, 547-557 (2011).
3. R. Huang *et al.*, Angiopep-conjugated nanoparticles for targeted long-term gene therapy of Parkinson's disease. *Pharm Res* **30**, 2549-2559 (2013).
4. G. d. R. Lindner *et al.*, Improved neuroprotective effects of resveratrol-loaded polysorbate 80-coated poly(lactide) nanoparticles in MPTP-induced Parkinsonism. **10**, 1127-1138 (2015).
5. E. Esposito *et al.*, Solid lipid nanoparticles as delivery systems for bromocriptine. *Pharm Res* **25**, 1521-1530 (2008).
6. R. Pahuja *et al.*, Trans-blood brain barrier delivery of dopamine-loaded nanoparticles reverses functional deficits in parkinsonian rats. *ACS Nano* **9**, 4850-4871 (2015).
7. T. Chen *et al.*, Small-Sized mPEG–PLGA Nanoparticles of Schisantherin A with Sustained Release for Enhanced Brain Uptake and Anti-Parkinsonian Activity. *ACS Applied Materials & Interfaces* **9**, 9516-9527 (2017).
8. L. You *et al.*, Targeted Brain Delivery of Rabies Virus Glycoprotein 29-Modified Deferoxamine-Loaded Nanoparticles Reverses Functional Deficits in Parkinsonian Mice. *ACS Nano* **12**, 4123-4139 (2018).

9. W. Chen *et al.*, Black Phosphorus Nanosheets as a Neuroprotective Nanomedicine for Neurodegenerative Disorder Therapy. **30**, 1703458 (2018).

# List of Publications

**List of Publications of thesis**

1. **M.N. Sardoiwala**, A.K. Srivastava, B. Kaundal, S. Karmakar, S.R. Choudhury, Recuperative effect of metformin loaded polydopamine nanoformulation promoting EZH2 mediated proteasomal degradation of phospho-α-synuclein in Parkinson's disease model, **Nanomedicine: Nanotechnology, Biology and Medicine** 24 (2020) 102088.
2. **M.N. Sardoiwala**, S. Karmakar, S.R. Choudhury, Chitosan nanocarrier for FTY720 enhanced delivery retards Parkinson's disease via PP2A-EzH2 signaling in vitro and ex vivo, **Carbohydrate Polymers** (2020) 117435.
3. **M.N. Sardoiwala**, S.J. Mohanbhai, S. Karmakar, S.R. Choudhury, Hytrin loaded polydopamine-serotonin nanohybrid induces IDH2 mediated neuroprotective effect to alleviate Parkinson's disease, **Materials Science and Engineering: C** (2021) 112602.
4. **M.N. Sardoiwala,**B. Vaidya, L. Biswal,S.S. Sharma,S. Karmakar,S.R. Choudhury, Metformin nanoformulation epigenetically regulate SIRT1 mediated histone deacetylation of SNCA gene to retard Parkinson's disease, in communication
5. **M.N. Sardoiwala,**L. Biswal,B. Mrunalini, S. Karmakar, S.R.Choudhury, FTY720 nanoformulation induces O-GlcNacylation of synuclein to alleviate synucleinopathy, in communication
6. **M.N. Sardoiwala,**L. Biswal, B. Mrunalini, S. Karmakar, S.R. Choudhury, Hytrin nanoformulation induced chaperon mediated autophagy in reduction of nitrated synuclein in PD treatment, in communication

**List of Other Publications**

**Research Articles**

7. **M.N. Sardoiwala,** A.C. Kushwaha, A. Dev, N. Shrimali, P. Guchhait, S. Karmakar, S.R. Choudhury, Hypericin-Loaded Transferrin Nanoparticles Induce PP2A-

Regulated BMI1 Degradation in Colorectal Cancer-Specific Chemo-Photodynamic Therapy. **ACS Biomaterials Science & Engineering,** 6 (5) (2020), 3139-3153.

8. **M.N. Sardoiwala,** S.J. Mohanbhai, A.C. Kushwaha, A. Dev, L. Biswal, S.S. Sharma, S.R.Choudhury,S. Karmakar, Melatonin mediated inhibition of EZH2-NOS2 crosstalk attenuates inflammatory bowel disease in preclinical in vitro and in vivo models. **Life Science** 302 (2022), 120655.
9. **M.N. Sardoiwala,** S.Nagpal, B. Bhatt, S.R.Choudhury**,** S.Karmakar, Size controlled improved delivery of melatonin-polydopamine nanocomposites attenuate preclinical diabetic retinopathy through inhibition of VEGF-PKCδ pathway, under revision **ACS Molecular Pharmaceutics**.
10. **M.N. Sardoiwala,** L.Biswal, B. Mrunalini, S.R.Choudhury,S.Karmakar, Melatonin-loaded Polydopamine nanocomposites prevent retinal neurodegeneration in the diabetic retinopathy preclinical model, in communication.
11. **M.N. Sardoiwala,** A.Sood, L.Biswal, S.R. Choudhury, S.Karmakar, Reconstituted super paramagnetic protein "magnetotransferrin" for brain targeting to attenuate Parkinsonism, **ACS Applied Materials Interface** 15,10 (2023), 12708-12718 .
12. **M.N. Sardoiwala,** L.Biswal, S. Karmakar, S.R.Choudhury, FTY720 nanoparticles induced PP2A/EZH2/FOXP3 signaling endows Treg action to alleviate Parkinsonism, in communication.
13. A.C. Kushwaha, S.J. Mohanbhai, **M.N. Sardoiwala**, M. Jaganathan, S. Karmakar, S.R.Choudhury, Nanoemulsified Genistein, and Vitamin D Mediated Epigenetic Regulation to Inhibit Osteoporosis **ACS Biomat. Sci. Eng.**8 (9) (2022), 3810.
14. A. Dev, **M.N. Sardoiwala**, A. Sharma, J.M. Soni, S.R. Choudhury, S. Karmakar, Nanoacetylated *N*-(4-Hydroxyphenyl) Retinamide Modulates Histone Acetylation–Methylation Epigenetic Disparity to RestrictEpithelial–Mesenchymal Transition in Neuroblastoma **ACS Med. Chem. Lett.** 2022, 13 (7) (2022) 1109.
15. A. Dev, **M.N. Sardoiwala**, M. Boddu, J.M. Soni, S.R. Choudhury, S.Karmakar, 4-Oxo-fenretinide-Loaded Human Serum Albumin Nanoparticles for the Inhibition of Epithelial–Mesenchymal Transition in Neuroblastoma Xenografts **ACS Appl. Nano Mater.**5 (5) (2022) 7540.
16. J.M. Soni, **M.N. Sardoiwala**, S. Gupta, N. Shrimali, S.R. Choudhury, S.S. Sharma, P. Guchhait, S. Karmakar, Colon targeted chitosan-melatonin monotherapy for preclinical Inflammatory Bowel Disease. **Biomaterials Advances**136 (2022) 212796.

17. A. Dev, **M.N. Sardoiwala**, A.C. Kushwaha, S. Karmakar, S.R. Choudhury, Genistein nanoformulation promotes selective apoptosis in oral squamous cell carcinoma through repression of a 3PK-EZH2 signaling pathway. **Phytomedicine** 80 (2021) 153386.
18. A. Sood, A. Dev, **M.N. Sardoiwala**, S.R. Choudhury, S. Chaturvedi, A.K. Mishra, S.Karmakar, Alpha-ketoglutarate decorated iron oxide-gold core-shell nanoparticles for active mitochondrial targeting and radiosensitization enhancement in hepatocellular carcinoma. **Material Science and Engineering C**80 (2021) 153386.
19. A.K. Srivastava, **M.N. Sardoiwala**, S.R. Choudhury, S. Karmakar, Coupled catalytic dephosphorylation and complex phosphate ion-exchange in networked hierarchical lanthanum carbonate grafted asymmetric bio-composite membrane **Journal of colloid and Interface** 80 (2021) 153386.
20. J.M. Soni, **M.N. Sardoiwala**, S.R. Choudhury, S.S. Sharma, S. Karmakar, Melatonin-loaded chitosan nanoparticles endow nitric oxide synthase 2 mediated anti-inflammatory activity in an inflammatory bowel disease model. **Materials Science and Engineering: C**124 (2021) 112038.
21. A.C. Kushwaha, S.J. Mohanbhai, **M.N. Sardoiwala**, A. Sood, S. Karmakar, S.R. Choudhury, Epigenetic Regulation of Bmi1 by Ubiquitination and Proteasomal Degradation Inhibit Bcl-2 in Acute Myeloid Leukemia. **ACS Applied Materials & Interfaces** 12 (23) (2020), 25633-25644.
22. A. Dev, S.J. Mohanbhai, A.C. Kushwaha, A. Sood, **M.N. Sardoiwala**, S.R. Choudhury, S. Karmakar, κ-carrageenan-C-phycocyanin based smart injectable hydrogels for accelerated wound recovery and real-time monitoring. **Acta Biomaterialia** 109 (2020), 121-131.
23. B. Kaundal, A.K. Srivastava, **M.N. Sardoiwala**, S. Karmakar, S.R. Choudhury, A NIR-responsive indocyanine green-genistein nanoformulation to control the polycomb epigenetic machinery for the efficient combinatorial photo/chemotherapy of glioblastoma. **Nanoscale Advances**1 (6) (2019), 2188-2207.

**Review Articles**

24. **M.N. Sardoiwala,** A.K. Srivastava, S. Karmakar, S.R. Choudhury, Nanostructure Endows Neurotherapeutic Potential in Optogenetics: Current Development and Future Prospects. **ACS Chemical Neuroscience**10 (8) (2019), 3375-3385.

25. **M.N. Sardoiwala,** B.Kaundal, S.R. Choudhury, Toxic impact of nanomaterials on microbes, plants, and animals. **Environmental Chemistry Letters** 16 (1) (2018), 147-160.

**Conference Paper**

26. A.K. Srivastava, **M.N. Sardoiwala,**B. Kaundal, S.R. Choudhury, S.Karmakar, Tailoring Biomolecular Interactions of Hybrid Nanostructures for their Diagnostic and Therapeutic Applications in Neurodegenerative Diseases. **Biophysical Journal**116 (3) (2019), 315a.

**Book Chapters**

27. **M.N. Sardoiwala,** B. Kaundal, S.R. Choudhury, Chapter 37 - Development of Engineered Nanoparticles Expediting Diagnostic and Therapeutic Applications AcrossBlood–Brain Barrier. In *Handbook of Nanomaterials for Industrial Applications*, Mustansar Hussain, C., Ed. **Elsevier**: **2018**; pp 696-709.
28. **M.N. Sardoiwala,** A.K. Srivastava, S.R. Choudhury, S.Karmakar, Nanobiosensors and Its Application in Agriculture and Food. In *21st Century Nanoscience–A Handbook*, **CRC Press**: **2020**; pp 21-1-21-14.
29. A. Dev, **M.N. Sardoiwala,** S. Karmakar, Silica Nanoparticles: Methods of Fabrications and Multidisciplinary Applications. In Functionalized Nanomaterials II: Applications, **CRC Press**: **2021**; pp 189.

# Workshop, Conferences Attended and Awarded

1. Oral presentation on "Neurotherapeutic nanocomposite endows epigenetic regulation mediated Parkinson's disease treatment", *2nd Research Scholar Day*, 31th March– 1st April, 2022, Institute of Nano Science and Technology, Mohali Punjab, India.
2. Poster presentation on "Nature-Inspired Nanocomposites Endow Epigenetic Mediated Neurotherapeutic Potential of antiparkinsonian" Nanomaterials & Nanoengineering: APA NANOFORUM – 2022, CSIR, National Physical Laboratory, New Delhi, India.
3. Poster presentation on "Nature-Inspired Nanocomposites Endow Epigenetic Mediated Neurotherapeutic Potential of Neuroprotetive Agents in PD Prevention" 2020 Virtual MRS Spring/Fall Meeting, Warrendale, PA, 15086, USA.
4. Poster Participated "Epigenetic Regulation by Metformin Nanoformulation Alleviate Parkinson's Disease" in Annual Meeting Chemical Biology Unit 2022, Institute of Nano Science and Technology, Mohali Punjab, India
5. CSIR junior research fellowship and senior research fellowship awarded during the PhD tenure.
6. Awarded first prize in the poster presentation Annual Meeting Chemical Biology Unit 2022, Institute of Nano Science and Technology, Mohali Punjab, India

# Permissions from Journals for reuse of content in Thesis

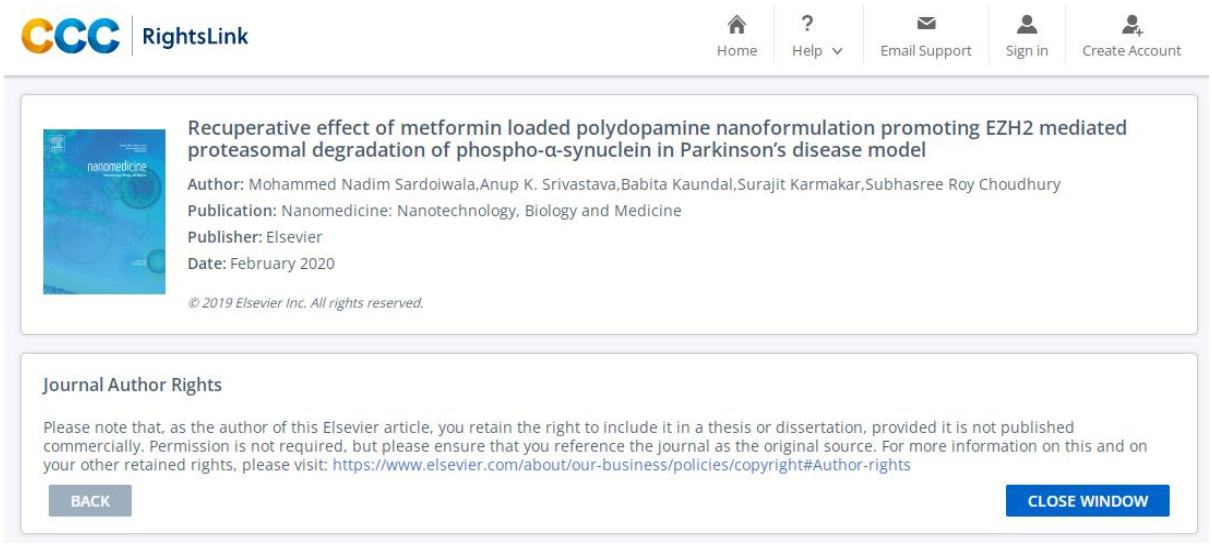

RightsLink

Home | Help | Email Support | Sign in | Create Account

Recuperative effect of metformin loaded polydopamine nanoformulation promoting EZH2 mediated proteasomal degradation of phospho-α-synuclein in Parkinson's disease model

**Author:** Mohammed Nadim Sardoiwala,Anup K. Srivastava,Babita Kaundal,Surajit Karmakar,Subhasree Roy Choudhury

**Publication:** Nanomedicine: Nanotechnology, Biology and Medicine

**Publisher:** Elsevier

**Date:** February 2020

*© 2019 Elsevier Inc. All rights reserved.*

Journal Author Rights

Please note that, as the author of this Elsevier article, you retain the right to include it in a thesis or dissertation, provided it is not published commercially. Permission is not required, but please ensure that you reference the journal as the original source. For more information on this and on your other retained rights, please visit: https://www.elsevier.com/about/our-business/policies/copyright#Author-rights

BACK CLOSE WINDOW

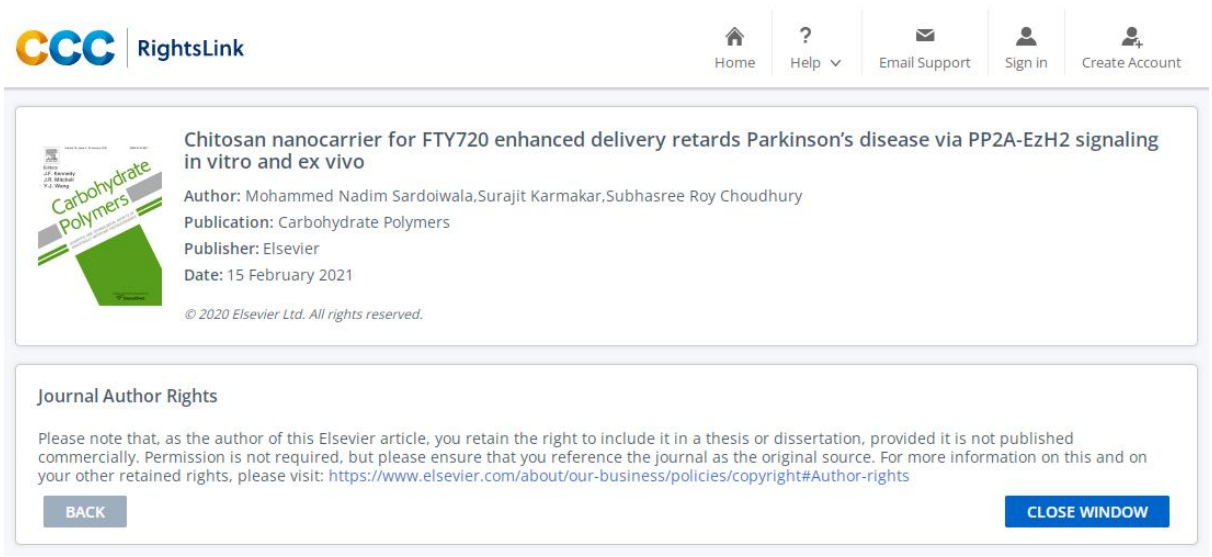

RightsLink

Home | Help | Email Support | Sign in | Create Account

Chitosan nanocarrier for FTY720 enhanced delivery retards Parkinson's disease via PP2A-EzH2 signaling in vitro and ex vivo

**Author:** Mohammed Nadim Sardoiwala,Surajit Karmakar,Subhasree Roy Choudhury

**Publication:** Carbohydrate Polymers

**Publisher:** Elsevier

**Date:** 15 February 2021

*© 2020 Elsevier Ltd. All rights reserved.*

Journal Author Rights

Please note that, as the author of this Elsevier article, you retain the right to include it in a thesis or dissertation, provided it is not published commercially. Permission is not required, but please ensure that you reference the journal as the original source. For more information on this and on your other retained rights, please visit: https://www.elsevier.com/about/our-business/policies/copyright#Author-rights

BACK CLOSE WINDOW

MOHAMMED NADIM <nadim.ph16240@inst.ac.in>

## Re: Obtain permission request - Journal (1327518) [221208-020446]

**Rights and Permissions (ELS)** <Permissions@elsevier.com> Fri, Dec 9, 2022 at 9:33 AM
Reply-To: "Rights and Permissions (ELS)" <Permissions@elsevier.com>
To: nadim.ph16240@inst.ac.in

Dear Mr. Mohammed Nadim Sardoiwala,

Thank you for contacting us.

As an Elsevier journal author, you retain the right to Include the article in a thesis or dissertation (provided that this is not to be published commercially) whether in full or in part, subject to proper acknowledgment; see https://www.elsevier.com/about/policies/copyright for more information. As this is a retained right, no written permission from Elsevier is necessary.

As outlined in our permissions licenses, this extends to the posting to your university's digital repository of the thesis provided that if you include the published journal article (PJA) version, it is embedded in your thesis only and not separately downloadable.

Thank you.

Kind regards,

**Thomas Rexson Yesudoss**
Copyrights Coordinator
**ELSEVIER** | HCM - Health Content Management

Visit Elsevier Permissions

---

**From:** Administrator
**Date:** Thursday, December 08, 2022 12:15 PM GMT

Dear ,

Thank you for contacting the Permissions Granting Team.

We acknowledge the receipt of your request and we aim to respond within seven business days. Your unique reference number is 221208-020446.

Please avoid changing the subject line of this email when replying to avoid delay with your query.

Regards,

Permission Granting Team

---

**From:**
**Date:** Thursday, December 08, 2022 12:15 PM GMT
[Quoted text hidden]
[Quoted text hidden]